



**EUROPEAN FORUM
for RECIPROCATING
COMPRESSORS**

5th EFRC Conference



March 21-23, 2007, Prague, Czech Republic

Contents

DESIGN & ENGINEERING

Improved Method for Job Specific Crankshaft Stress Calculation - 17 -
Willem van der Toom; THOMASSEN COMPRESSION SYSTEMS

**Design of Horizontal Opposed Reciprocating Compressor for Hydrogen Provided
by Stepless Capacity Control** -23 -
Jaroslav Kraml; CKD NOVE ENERGO

**The Role of Improved Valve Technology in the Utilization of Natural
Gas Resources** - 28 -
Bernhard Spiegl, G. Machu, P. Steinrueck; HOERBIGER

FUNDAMENTALS

**Advances in Fundamental Understanding of the Dynamic Sealing
Action in packing Systems** - 40 -
Tino Lindner-Silwester; HOERBIGER

**Dry-Running Sealing Systems in Practice New –Challenges
by New Materials** - 51 -
Norbert Feistel; BURCKHARDT COMPRESSION

VALVES

**Evaluation of the Coefficients used for Simulation for Cylinder
Valves for Reciprocating Compressors** - 65 -
Fabione Manfrone, Massimo Schiavone, Enzo Giacomilli; COZZANI

Semi-Active Compressor Valve Development and Testing - 76 -
*Klaus Brun, John P. Platt, Ryan Gernentz, Mitchel Smolik; SOUTHWEST RESEARCH
INSTITUTE, BP EXPLORATION & PRODUCTION TECHNOLOGY*

**The Application of Elastomeric Materials to Reciprocating
Compressor Valves** - 84 -
Kevin Durham; COOK MANLEY

PULSATIONS & VIBRATIONS

- Further Improvement of Pulsation and Vibration Studies
for Reciprocating Compressors** - 95 -
Georg Samland, Nicole Retz; BURCKHARDT COMPRESSION
- Dynamic Analysis of Large Intercoolers and Tubular Reactors Installed
in LDPE Plants with a Hyper Compressor** - 103 -
Marco Passeri, Matteo Romiti, Stefano Generozi; GE OIL & GAS
- Mitigation of High-Frequency Pulsations Using Multi
Bore Restriction Orifices** - 114 -
Harry Korst, Leonard van Lier; TNO SCIENCE AND INDUSTRY

OPERATING & MAINTENANCE

- Practice Report – Design und Putting into Operation of
New Compressor Units** - 125 -
Claus pollok; E.ON HANSE
- Reciprocating Compressor Foundations – They do not last forever** - 132 -
Robert van Lienen, Harry Lankeau; NEAC COMPRESSOR SERVICE

DESIGN & ENGINEERING

- Extensive Optimisation Analyses of the Piping of Two Large
Underground Gas Storage Compressors** - 145 -
*André Eijk, Harry Korst; TNO SCIENCE AND INDUSTRY,
Gert Ploumen; ESSENT, Dirk Heyer; HGC*
- Minimisation of Gas Loss During Condensate Drains** - 157 -
*Thomas Heumesser, Ernst Huttar, Rainer Scheifinger;
LEOBERSDORFER MASCHINENFABRIK*
- Dynamic Design of the Foundation of Reciprocating Machines
of Offshore-Installations – Case Study** - 162 -
Jan Steinhausen; KÖTTER CONSULTING ENGINEERS

EFRC RESEARCH

- Modelling Fluid Dynamics, Heat Transfer and Valve Dynamics
in a Reciprocating Compressor** - 171 -
Roland Aigner, H. Steinrück; TU VIENNA
- Model Based Diagnostics of Reciprocating Compressors** - 181 -
Matthias Huschenbett, Gotthard Will; TU DRESDEN
- Identification of Noise Sources in Reciprocating Compressors** - 188 -
Leonard van Lier; TNO SCIENCE AND INDUSTRY

SPECIAL TOPIC: LNG

- Overhaul of a 8-Cylinder Ingersoll Rand Compressor for a
Liquefaction Process** - 201 -
Burkhard Katzenbach; RWE ENERGY
- Online Condition Monitoring of LNG Boil Gas Compressors** - 204 -
*Josu Elorza Etxebarria; BAHIA BISCAYA GAS
Thorsten Bickmann; PROGNOST SYSTEMS*

SPECIAL TOPIC: FPSO

- Dynamic Analysis of Reciprocating Compressors on FPSO Topside Modules** - 217 -
Kelly Eberle, Chris Harper; BETA MACHINERY ANALYSIS
- Large Reciprocating Compressor Packages on FPSOs** - 228 -
Graham Gilkison, Stephen Rowntree; INDEPENDENT TECHNOLOGY

OPERATIONS & MAINTENANCE

- Optimized MTBM with Model Based Online Diagnostics** - 238 -
Christian Koers; PROGNOST SYSTEMS
- Ethylene Boil Off Gas Compressor in Petrochemical Plant Availability Enhancement** - 245 -
Syed Fuad Abbas, Mousa A. Al-Haijan; SABIC
Klaus Hoff; NEUMAN & ESSER
- Increased Availability and Reliability by OEM Maintenance Agreements** - 254 -
Hans Bongers, Rob Crena de Jongh; THOMASSEN COMPRESSION SYSTEMS and NAM

DRIVE TRAIN

- Pros and Cons of Various Coupling Types for Reciprocating Compressor Installations** - 263 -
Gerhard Knop; Klaus H. Hoff; NEUMAN & ESSER
- Torsional Design Considerations for Reciprocating Compressors** - 273 -
Thomas J. Stephens; ARIEL CORPORATION

DRIVE TRAIN

- Optimisation of Reciprocating Compressor Plants by Using Flexible Couplings Supported by Advanced Engineering Methods** - 286 -
Andreas Laschet, Michael Matzkeit; ARLA MASCHINENTECHNIK, VULKAN KUPPLUNGS- UND GETRIEBBEBAU B. HACKFORTH
- Utilization of Soft-Starter VDF in Reciprocating Compressor Applications** - 295 -
Carsten Ritter, Heinz Kobi, Peter Morf; ABB SWITZERLAND



5th Conference of the EFRC March 21 - 23, 2007 Prague, Czech Republic

DESIGN & ENGINEERING

- Improved Method for Job Specific Crankshaft Stress Calculation** - 17 -
Willem van der Toom; THOMASSEN COMPRESSION SYSTEMS
- Design of Horizontal Opposed Reciprocating Compressor for Hydrogen Provided by Stepless Capacity Control** - 23 -
Jaroslav Kraml; CKD NOVE ENERGO
- The Role of Improved Valve Technology in the Utilization of Natural Gas Resources** - 28 -
Bernhard Spiegl, G. Machu, P. Steinrueck; HOERBIGER





Improved method for job specific crankshaft stress calculation

by:

Willem van der Toom

Technology Division

THOMASSEN COMPRESSION SYSTEMS

Rheden

The Netherlands

**5th Conference of the EFRC
March 21-23, 2007
Prague, Czech Republic**

Abstract:

The load on a compressor crankshaft varies with the crank angle and differs with every machine and load condition. Finite Element calculations to check every crankshaft and load case would result in an enormous amount analysis.

Traditional crankshaft design rules such as those based on research performed by Lloyd's Register of Shipping, and used by CIMAC, were developed for internal combustion engines. The stresses calculated using these rules are only really valid for crankshafts loaded in or around Top Dead Centre (TDC). In contrast, the maximum load on a crankshaft of a reciprocating compressor is not necessarily around TDC.

Thomassen has extended the CIMAC design rules for the application to reciprocating compressors. The method as described in the rules is maintained. The so called stress concentration factors, used for the determination of the bending and torsion stresses, have been determined for all web angles. All frame type crankshafts have been modelled in Finite Elements. From these, additions and corrections to the existing polynomials of the SCF's have been extracted, for an easy to use but accurate calculation. With the modified analytical model it is now easy to check every Thomassen crankshaft for any possible cylinder and load configuration.

1 Introduction

During operation a crankshaft is subjected to fluctuating bending moments and torques due to gas and mass forces. The load of a compressor is dependent on many variables, such as the number of cylinders, type of cylinders, pressure ratios, compressor speed, unloading conditions etc. The shape and loading of a crankshaft make it a complex stress analysis problem.

The maximum rod load of a crank varies, depending on the duty and load of a cylinder. For example for the first picture the maximum load is at 133°, 65% tension and 324°, 59% compressive and for the second picture at 81°, 39% tension and at 273°, 74% compressive. During one crank revolution the load variation characteristic is different for every compressor.

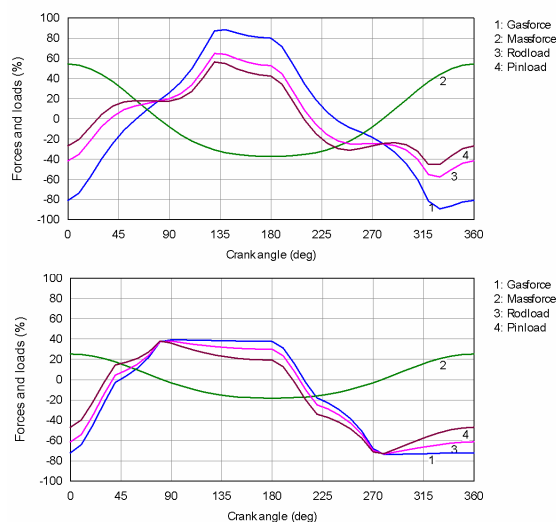


Figure 1 : Rod load diagrams

Multiple cylinder compressors especially show great variations in the combination of loads on different cranks and different unloading conditions per cylinder. For example: eight cylinders with two cylinders per stage already have sixteen possible load configurations for the 75% load case when only HE are unloaded. It is virtually impossible to design a crankshaft for the worst case condition. A piston rod for example is designed to withstand the rated rod load but designing a crankshaft for the rated rod load is not sufficient. Compressors with heavily loaded cylinders need not necessarily yield the highest load for the crankshaft. The crankshaft loading is dependent on the combination of loading on different cranks. This means that a crankshaft should be checked for every specific compressor and load condition. This results in numerous

calculations per compressor, which is time consuming, especially when Finite Element models are used

An easy to use analytical calculation method for calculating crankshaft stresses therefore becomes an attractive option.

2 Experimental work

Much research has been performed on crankshafts in the past. Most of this was based on crankshafts for internal combustion engines. One of the most extensive of these efforts was performed by Lloyd's Register of Shipping, ref: ["The Calculation of Crankshaft Stress" commonly known as "The Silver Book"]. These experiments gave insight in the influence of geometric parameters such as crankpin diameter, web width, web thickness, fillet radii etc. on the stress and deformation in a crankshaft.

For these experiments a series of single throw crankshafts were manufactured. Different types of loads were applied in such a way that the effect of each individual type of load on the overall stress level could be identified. Stresses were obtained by strain gauge measurements in the fillet between crankpin and webs.

Measurements were carried out for the following load conditions :

1. Uniform bending in the plane of the throw
2. Three point bending in the plane of the throw
3. Torsion without any transverse restraint of the journal
4. Shear loading

The following illustrations give a schematic overview of the cases that were measured. Measurements were performed with different crankshaft geometries with the crankshafts at TDC only.

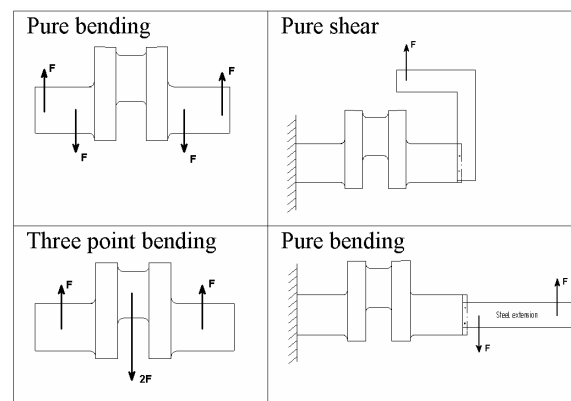


Figure 2 : Testing arrangements

3 CIMAC method

CIMAC developed crankshaft design rules for internal combustion engines using the results of the research from Lloyd's Register of Shipping. The CIMAC method considers the crankshaft as a straight continuous beam of constant diameter supported at the main bearings and loaded at the crank positions. Stress concentration factors are subsequently used to account for the actual crankshaft geometry whereby:-

$$s = SCF \cdot s_{nominal}$$

Separate and different factors, dependent on crankshaft geometry, are used for torsion and bending. The CIMAC method is in practice an easy to use method for calculating stresses in a crankshaft.

Thomassen has in the past used the CIMAC method to calculate stresses in crankshafts. Verification of these calculations with strain gauge measurements has shown however, that the CIMAC method is conservative. The measured stresses can be considerably lower than the stresses calculated with the CIMAC method for the aforementioned reasons.

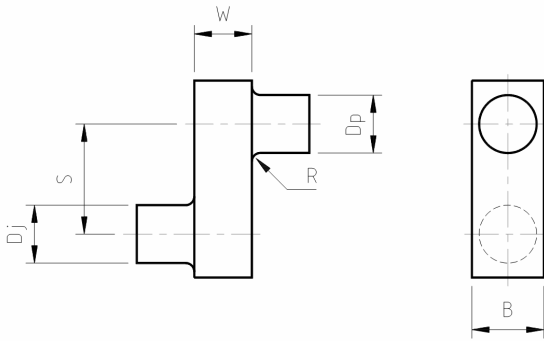


Figure 3 : Single crank element

Stress concentration factor for torsion

Stress concentration factors for torsion can be determined with following CIMAC equation

$$SCF_T = [0.9 \cdot r^{(-0.3+0.1(1-r))}] \cdot [7.9 - 10.7 \cdot b + 5.3 \cdot b^2 - 0.86 \cdot b^3] \cdot [w^{-0.15}]$$

$$s = \frac{(D_p + D_j)}{2} \cdot S, \quad r = \frac{R}{D_p}, \quad w = \frac{W}{D_p}, \quad b = \frac{B}{D_p}$$

Stress concentration factor for bending

Stress concentration factors for bending can be determined with the following CIMAC equations

$$SCF_b = 2.69 \cdot f(s, w) \cdot f(w) \cdot f(b) \cdot f(r) \cdot f(d_j) \cdot f(d_p)$$

$$f(s, w) = -4.9 + 29.2w - 77.6w^2 + 91.94w^3 - 40.04w^4$$

$$+ (1-s)(9.5 - 58.4w + 159.3w^2 - 192.6w^3 + 85.3w^4)$$

$$+ (1-s)^2(-8.8 + 25.0w - 70.6w^2 + 87.03w^3 - 39.2w^4)$$

$$f(w) = 2.1790w^{0.7171}$$

$$f(b) = 0.6840 - 0.0077b + 0.1473b^2$$

$$f(r) = 0.2081r^{0.5231}$$

$$f(d_j) = 0.9993 + 0.27d_j - 1.0211d_j^2 + 0.5306d_j^3$$

$$f(d_p) = 0.9978 + 0.3145d_p - 1.5241d_p^2 + 2.4147d_p^3$$

3.1 Stress calculation with the CIMAC method

Measurements and FE calculations both show that the location of the highest stress is in the radius between the crank pin and the web, location b in the picture below. Here it is assumed that the maximum torsional stress and maximum bending stress occur at the same location. This is a conservative approach as in practice the maximum bending stress and torsional stress occur at different locations on the crankpin. The error introduced by this assumption is however, not large.

The crankshaft is modelled for a two cylinder configuration. Four, six or eight cylinders can be seen as multiple two cylinders as every crank pair is separated by main bearings. To take into account additional cranks, an additional torque from previous cranks is added to the two cylinder model.

Stresses are calculated as if the crankshaft is a straight shaft. These stresses are then multiplied with the previously discussed SCFs to account for the crankshaft geometry.

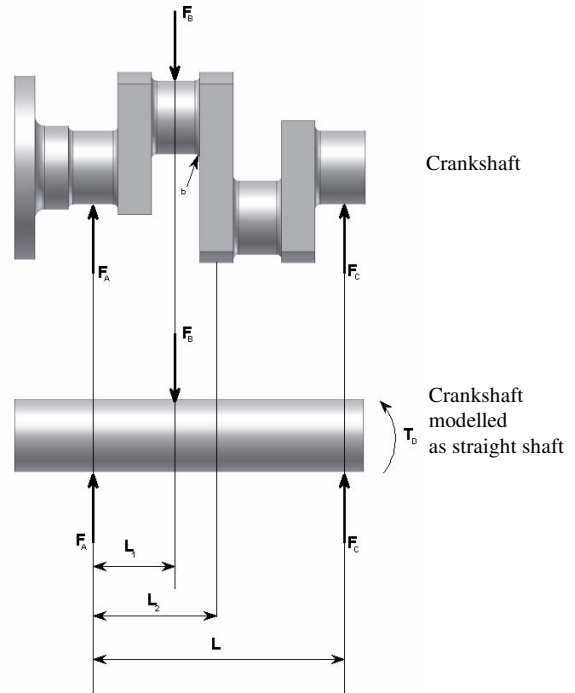


Figure 4 : Crankshaft model

3.1.1 Bending stress

The bending stress in the long web at location b calculated with cylinder B loaded:

$$F_A = F_B \left(1 - \frac{L_1}{L}\right) \quad \Sigma M_c = 0$$

$$F_c = F_B - F_A \quad \Sigma F = 0$$

$$M_{Long\ web} = F_c \cdot (L - L_2)$$

$$\sigma_B = \frac{M_{long\ web}}{W_b} \cdot SCF_{bending}$$

Crankpin section modulus in bending: $W_b = \frac{I}{6} \cdot B \cdot W^2$

3.1.2 Torsional stress

Torsional stress calculated with cylinder B loaded

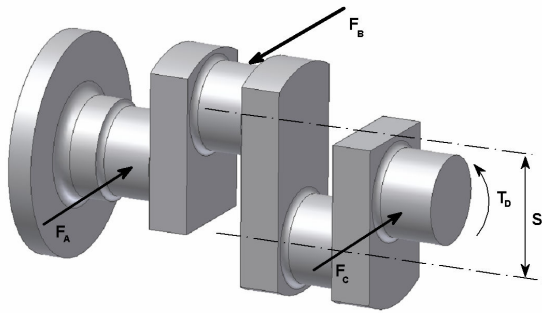


Figure 5: crankshaft

$$T_b = T_d - F_c \cdot \frac{s}{2}$$

$$\tau = \frac{T_b \cdot SCF_{torsion}}{W_t}$$

Crankpin section modulus in Torsion: $W_t = \frac{\pi}{16} \cdot D^3$

3.2 Stress evaluation

The assessment of stresses is with the Gough quarter ellipse model. In the Gough Criterion the allowable equivalent bending stress and torsional stress are combined. This method has the feature that any combination of bending and torsion can be reduced to a single value which should be less than unity.

The Gough criterion can be determined with following equation:

$$Gough_criterion = \sqrt{\left(\frac{\sigma_B}{\sigma_{allowable}}\right)^2 + \left(\frac{\tau}{\tau_{allowable}}\right)^2}$$

If this outcome is less than unity, the stresses in the crankshaft are an allowable combination within the Gough Criterion. Allowable stresses for three different materials are shown in Figure 6.

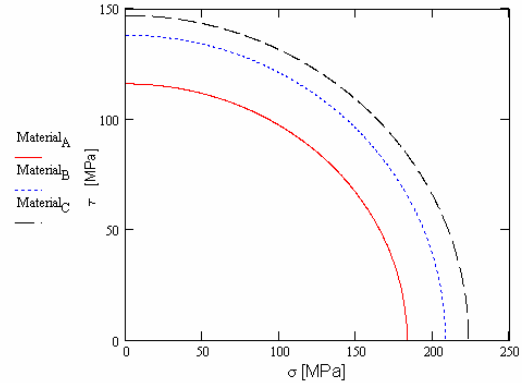


Figure 6: Gough quarter ellipse

4 CIMAC method compared with FE

To enable comparison between the CIMAC method and FE analysis, two FE models were made. The first with a force parallel to the crank web in the TDC position, the second with the force at 90° to this position.

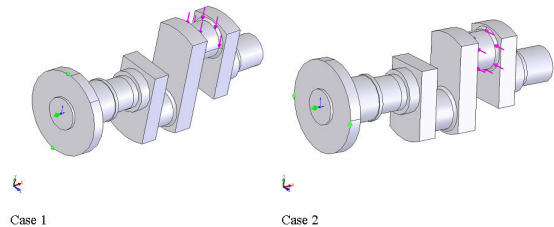


Figure 7: Crankshaft FE models

Boundary conditions:

In the FE model, the crankshaft is supported at the edge of each bearing. The required restraint implemented at the driving flange is rotational fixation and translational freedom.

Results

Below are the CIMAC results compared with the FE results.

		Difference
Case 1	0 degr.	- 19 %
Case 2	90 degr.	- 42 %

As can be seen from the results, the stresses calculated with FE are lower than the stresses calculated with the CIMAC method. Notable is case

2 where the applied force is perpendicular to the plane of the crank.

The large difference in case 2 can be explained by the fact that the stress concentration factors from CIMAC are based on experiments where crankshafts were only loaded in the plane of the crank.

5 Determination of new SCF's

As every crankshaft requires checking for all load conditions an easy to use calculation method is of great advantage. The CIMAC method can be useful but has certain drawbacks. One is that the CIMAC stress concentration factors were not valid for some compressor crankshaft geometries, as the pin/web proportion was not always within the range examined by Lloyd's Register of Shipping. FE calculations for the stress concentration factors confirm that the CIMAC values are only valid in and around TDC, but not necessarily at the maximum crankshaft load.

As the SCF for torsion is not dependent on the crank angle, only the to be used SCF's for bending require recalculation at changing crank angles. For every compressor type a FE model of the crankshaft with a variable stroke was made. For different crank angles the Von Mises stress in the fillet between the pin and the long web is calculated. With following equation, the SCF for bending can than be derived.

$$\sigma_{VonMises} = \sqrt{\sigma_b^2 + 3 \cdot \tau_{torsie}^2} \rightarrow$$

$$\sigma_{VonMises} = \sqrt{(SCF_{bending} \cdot \sigma_b)^2 + 3 \cdot (SCF_{torsion} \cdot \tau_{torsie})^2}$$

With for $SCF_{torsion}$ the SCF according CIMAC

$$SCF_{bending} = \sqrt{\frac{\sigma_{VonMises}^2 - 3 \cdot (SCF_{torsion} \cdot \tau_{torsie})^2}{\sigma_b^2}}$$

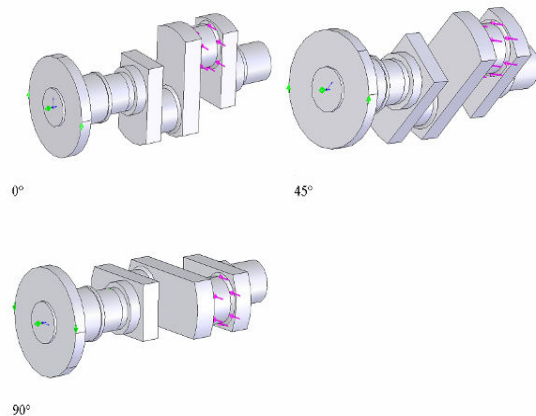


Figure 9 : Crankshaft FE models

The stress concentration factors have been derived with the rod load at different strokes and three different angles per compressor type, 90°, 45° and 0°.

Based on the data from these FE calculations new SCF's are derived as a function of the crank angle and stroke. The newly defined SCF's (at TDC) give differences of 20% to 30% for smaller frames when compared to the CIMAC values, while for the larger frames there is almost no difference. This confirms that the CIMAC SCF's are not valid for all pin/web proportions. The CIMAC stress concentration factors are valid for following geometry parameters:

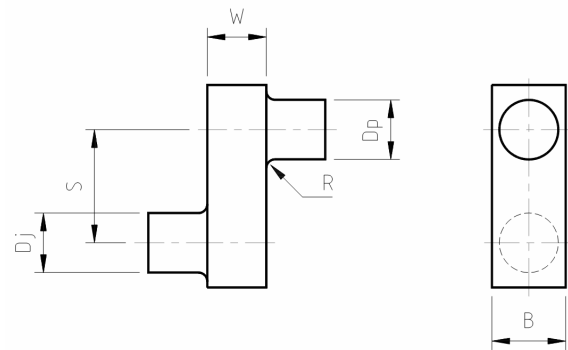


Figure 8: Single crank element

$$1.077 \leq b \leq 1.77 \quad b = \frac{B}{Dp}$$

$$0.173 \leq w \leq 0.74 \quad w = \frac{W}{Dp}$$

$$-0.25 \leq s \leq 0.45 \quad s = \frac{S - \frac{(Dp+Dc)}{2}}{Dp}$$

In Figure 10 and Figure 11 the SCF's for two different crankshafts are shown. The CIMAC SCF has been added for comparison,. The largest difference is to be found in the SCF as a function of crank angle.

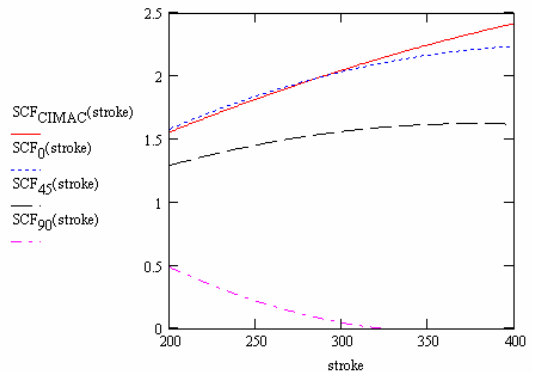


Figure 10: SCF large frame (b=1.4, w=0.5, s=0.5 / 0)

It is evident from *Figure 10* that for a crankshaft having geometry similar to that of an internal combustion engines crankshaft, the CIMAC SCF for TDC is almost equal to the FE derived SCF.

Conversely, *Figure 11* illustrates that for crankshafts that do not correspond closely to engine crankshafts, that SCF's diverge.

The newly established SCF's, as a function of stroke and crank angle have now been incorporated in software in which the actual rod loading of the

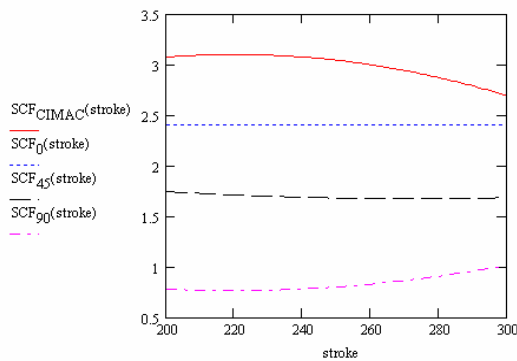


Figure 11: SCF small frame (b=1.3, w=0.53, s=-0.25/-0.9)

compressor is also calculated. With the actual rod load for every crank angle and crank, and incorporating new SCF's it is straightforward to accurately calculate the stress in every Thomassen crankshaft for all load conditions and cylinder combinations.

6 Conclusion

Thomassen has extended the CIMAC design rules for stress calculation in crankshafts for the application in reciprocating compressors. The method as described in the CIMAC rules is retained. The so called stress concentration factors, used for the determination of the bending stresses have been determined for all web angles. With the modified analytical model it is easy to check every Thomassen crankshaft with any possible cylinder configuration. This has resulted in an easy to use but accurate calculation method that results in a reliable and economical crankshaft.

7 Symbols

Symbol	Description	unit
B	Web width	[mm]
b	CIMAC geometry parameter	[-]
D _j	Journal diameter	[mm]
D _p	Pin diameter	[mm]
F	Force	[N]
L	Length	[mm]
M	Moment	[Nm]
R	Radius	[mm]
r	CIMAC geometry parameter	[-]
S	Stroke	[mm]
s	CIMAC geometry parameter	[-]
SCF	Stress concentration factor	
T	Torque	[Nm]
W	Web thickness	[mm]
w	CIMAC geometry parameter	[-]
W _b	Section modulus in bending	[m ³]
W _t	Section modulus in torsion	[m ³]
σ	Stress	[MPa]



ČKD NOVÉ ENERGO

MEMBER OF ČKD PRAGUE GROUP

Design of Horizontal Opposed Reciprocating Compressor for Hydrogen Provided by Stepless Capacity Control

By:

Jaroslav KRAML
ČKD Nové Energo
Klecakova 1947
Prague
Czech Republic
jaroslav.kraml@ckdenergo.cz

5th Conference of the EFRC
March 21-23, 2007
Prague, Czech Republic

Abstract:

This paper presents a description of design of horizontal-opposed two-stage oil-free four-cylinder piston compressor ČKD model 4 DBK 430B for hydrogen.

It particularly deals with a design of compressor cylinders including FEM analysis, a capacity control of compressor and with a torsional vibration analysis of compressor unit.

Cylinders are modeled using parametric CAD system and resulting 3D model is analyzed by FEM for a stress.

The system of capacity control used in this unit is stepless capacity control system. The system consists of actuators that are installed on each suction valve of individual cylinders providing stepless capacity control from 0 to 100%, compressor interface unit and hydraulic unit.

The torsional vibrations of system consisting of reciprocating compressor and electric motor are simulated in a process of compressor unit design. The results of TVA will be practically verified after manufacturing of the unit during a test operation.

1 Introduction

The objective of this paper is to describe some aspects of design of horizontal-opposed, two-stage, oil-free piston compressor for a compression of hydrogen gas.

Namely I am going to mention a design of new cylinders, a torsional vibration analysis (TVA) and a stepless capacity control system of unloaders on each suction valve that is able to control capacity during each revolution.

2 Selection and Sizing

This compressor is designed to the specific capacity, suction and discharge pressures required by the User. We selected one of our company standard crankshaft mechanisms 4bkm40. That means four-cylinder, horizontal-opposed compressor with the maximum connecting rod force of 450 000 N.

It is one of following horizontal-opposed crankshaft mechanisms that are in our company's inventory:

Horizontal-opposed crankshaft model	No. of cylinders	Maximum connecting rod force (kN)
2bkm10	2	110
4bkm10	4	110
6bkm10	6	110
4bkm16	4	175
6bkm16	6	175
8bkm16	8	175
4bkm25	4	275
6bkm25	6	275
8bkm25	8	275
4bkm40	4	450

Resulting compressor assembly layout is shown in following Fig.1.

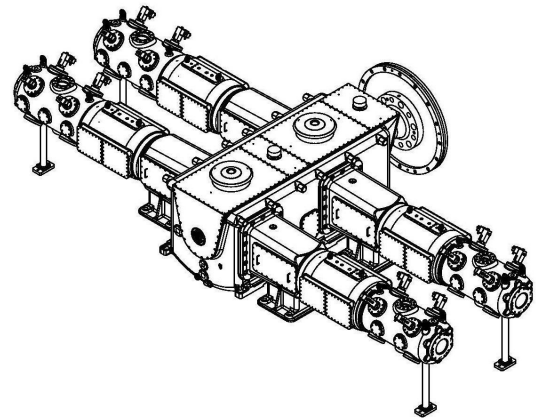


Figure 1: Compressor Layout

All input data were used in a thermodynamic analysis and sizing that gave a result of two-stage compressor with two first stage cylinders of diameter of 430 mm and two second stage cylinders of diameter of 320 mm.

We named the compressor 4 DBK 430 B. The figure 4 for four cylinders, D for two-stage, B for horizontal-opposed compressor, K for compressor, 430 for the first stage cylinder diameter and finally B for oil-free type. All these figures and characters are a part of official CKD compressor terminology.

The compressor is of oil-free type, i.e. pistons are fitted by PTFE piston and rider rings. Pressure packings of both stages are also provided by PTFE sealing elements.

Packing cases are vented and purged by nitrogen. Distance pieces are of Type C, long two-compartment ones according to API 618, latest edition.

The compressor is driven by our company asynchronous electric motor model 5V 323-20HW giving 4200 kW at 298 rpm via rigid coupling. The electric motor is installed in one bearing pillow block.

The suction and discharge piping lines are provided by suction and discharge pulsation dampers that are sized again according to API 618, latest edition.

The auxiliaries includes a lubricating system provided by two electric motor driven oil pumps, double oil filters and necessary piping, fittings and frame.

The unit is provided by PLC based control system that enables safe and reliable control, automatic start and stop of the unit and also a system of warning and shutdowns in case of exceeding any of controlled parameters. This system also includes some elements of condition monitoring, namely rod-drop monitoring.

This project of two compressors (one operating and one standby), drivers and auxiliaries as the whole was directed in Project Data Management (PDM) system software that enabled a control during parallel design, stress analysis and manufacturing.

3 Cylinders

The new cylinders of both stages had to be designed and we designed them using high end CAD/CAM/CAE system. This CAD system enabled fully parametric 3D model to be created that was furthermore used for assembly of these cylinders on standard parts of compressor crankshaft mechanism and distance piece.

3D model included valve nests, water space and gas space all bolt holes, liners and covers.

A simplified version of 3D model “as simple as possible and as complex as necessary” was used for Finite-Elements-Method of stress calculation of both cylinders.



Figure 2: 3D model of cylinder

The FEM calculations of cylinders were made using advanced FEM system enabling stress analysis with contact. The cylinders were calculated in all possible static load modes from gas pressure, water pressure, bolts loading and contact during insertion of liner.

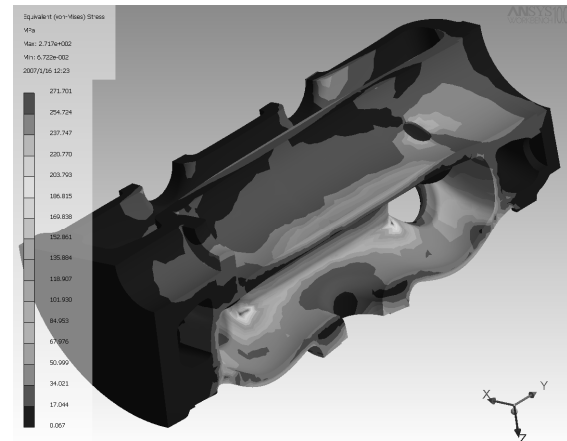


Figure 3: Distribution of stress at cylinder

Correct boundary conditions, calculating model net with nodes and elements had to be carefully applied.

The calculations resulted in stress distribution at cylinders with maximum load in particular areas. 3D models were modified according these results to bring the stress down.

4 Torsional Vibration Analysis

The analysis of torsional vibrations in unit with large reciprocating compressor driven by electric motor is one of major task. It is necessary to analyze torsional vibrations before the compressor train had been built. We used advanced simulation tool but at first we had to create a simulation model of moments of inertia connected by stiffness elements. These elements and moments were derived from 3D models and drawings of individual elements of the unit. All excitation data came from loads of compressor. We performed an analysis of excitability of possible resonance domains.

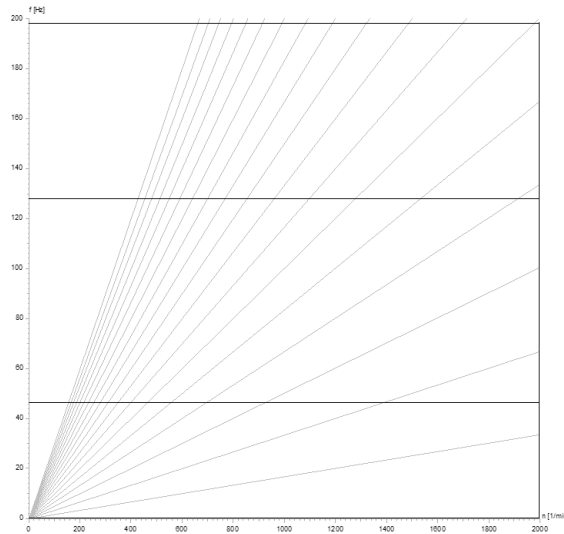


Figure 4: Campbell diagram

Torsional natural frequencies of compressor-electric motor system including coupling and flywheel shall lay out of operating speed within 10% and within 5% of any multiple speeds up to and including tenth multiple. We calculate actual torques including the maximum torsional stresses for the operating speed and provide stress analysis of crankshaft to show safety factors are within mentioned acceptable margins.

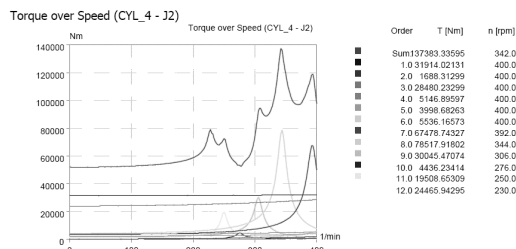


Figure 5: Compressor excitation

The results of TVA will be practically verified after manufacturing of the unit during a test operation.

5 Capacity Control

5.1 Generally

The User required stepless capacity control system. We offered the hydraulically actuated computerized compressor control system that enables a capacity control within the range of (0) 10% to 100% of capacity.

The system is reliable, efficient, flexible compressor control system for optimal use of resources.

The capacity control method is based on the so called reverse flow control principle. A portion of the gas which was taken into the cylinder during the suction cycle is pushed back into the suction line during the compression cycle.

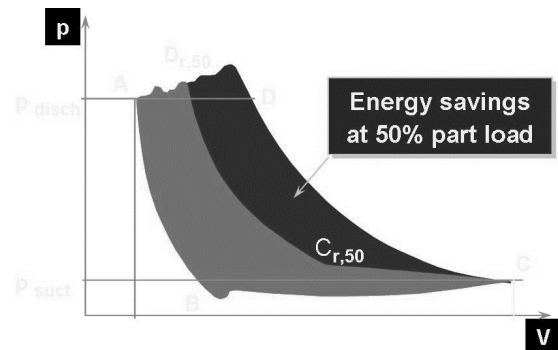


Figure 6: p-v diagram

The minimum continuous load depends on gas composition, operating conditions and compressor design parameters. The system is based on components of the injection technology for large diesel engines, enhanced by state of the art digital computing and control technology.

Hydraulically actuated unloaders keep the suction valves open during part of the compression cycle.

Thus part of the gas taken into the cylinder during the suction cycle is pushed back into the suction space. In this way the gas volume per working stroke can be controlled.

This system saves compression power at part load, since the energy consumption of a compressor is proportional to the quantity of gas compressed per compression cycle.

The capacity closed loop control is done by the DCS / PLC.

The system provides in addition to control as a standard feature suction valve nest temperature measurement.

Temperature sensors are integrated in each actuator. The last version of this system is as control as monitoring platform.

Fast-TIMs feature decentralized data acquisition and bus communication. They are designed to be installed at or close to the compressor and save field wiring and installation costs.

This system also offers increased reliability, reduces operating costs and provides some condition monitoring information as suction and discharge gas temperature.

Another data acquired from control system as gas discharge pressure and temperature, individual valve temperatures, rod displacement and position indicating wear of rider rings, vibration of compressor frame and many more are monitored in the control system of unit.

5.2 Description of Parts

Each suction valve of all cylinders was fitted by unloader and actuator. They perform the actual control task – delaying the closing of the suction valves at part load.

Hydraulic unit (HU) and hydraulic piping supply the mechanical energy to the actuators.

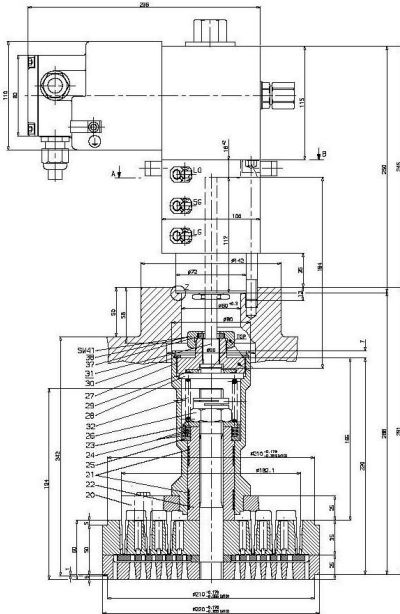


Figure 7: Actuator Assembly Drawing

The actuators are also supplied by 48 V DC by the External Power Supply (EPS).

These actuators are supplied by the Compressor Interface Unit (CIU) via data lines (BUS) with information when individual suction valves should be opened or closed. The actuators are connected by the bus to the Compressor Interface Unit (CIU).

The CIU is synchronized with the compressor speed via a TDC-sensor and an Isolation Amplifier IA. The CIU is informed of the capacity required from each compressor stage by the Distributed Control System (DCS) by 4-20 mA signals. The CIU feeds back the valve nest temperatures of each valve, again by 4-20 mA signals. Signals can be exchanged using the Modbus interface.

The CIU provides the electronic control of the actuators and serves as interface between the system and DCS / PLC where closed loop control is performed.

The communication between DCS, PLC or loop controller and the system is based on analog and binary signals.

The system features data acquisition of fast signals and can be upgraded into a monitoring platform.

The measurements can be read via the digital Monitoring Interface (Modbus).

The TDC-sensor synchronizes CIU with compressor speed and gives reference of the crank shaft position.

The CIU performs the real time calculation of suction valve opening and closing time and sends the commands to the actuators. Thus compressor output becomes a simple analog control variable for the plant operator.

By using digital control technology the system can react within 3 revolutions to change compressor output. Therefore the system is the ideal choice for those applications where fast and precise control is required.

6 Conclusion

A computer simulation is a useful tool to analyse torsional vibrations in reciprocating compressor unit. I can recommend using this method in the first stages of project to be still able to change design.

FEM analysis of heavily loaded parts is a necessity and high-end CAD/CAM/CAE system is very powerful tool that enables such analysis.

The stepless capacity control system used in this project is reliable and efficient compressor control system for optimal use of resources.

7 Acknowledgements

The author wishes to thank Dipl.Ing. Milan Šafr for his kind support concerning this project and his assistance doing the calculations and detailed analyses.



The role of improved valve technology in the utilization of natural gas resources

by:

B. Spiegl, G. Machu, P. Steinrueck

**Innovation & Technology
HOERBIGER KT Holding**

Vienna

Austria

bernhard.spiegl@hoerbiger.com

**5th Conference of the EFRC
March 21-23, 2007
Prague, Czech Republic**

Abstract:

To safeguard the future supply with natural gas considerable investments into compression equipment in gas gathering, gas processing, gas storage and gas transportation is required. In order to keep cost of investment low, compressors are rated at higher speed asking for substantially increased valve performance and valve reliability.

In this paper an approach to overcome the physical limits of standard valve technologies is outlined. It is demonstrated how recent results in mathematical modeling of valve dynamics, material science and manufacturing technology lead to innovative solutions to cope with said challenges.

Numerous successful field installations and performance measurement all over the world demonstrate impressive power saving potentials and reliability gains for the compressor user.

1 Introduction

Natural gas is becoming more and more important to satisfy the increasing energy consumption of the world. The demand for compression equipment for gas gathering, gas transport and gas storage is increasing rapidly.

Most of the existing gas field suffer of decreasing gas pressure and thereby further increase the need for efficient gas compression to boost the gas pressure to the needed pressure levels of the pipelines.

In order to keep investment cost down, gas field and pipeline operators press for increased compressor speed. Very often increased compressor speed goes hand in hand with reduced compressor efficiency and reliability. Standard plate valve technologies reach their physical limits.

In recent years valves employing multiple sealing elements such as ring valves or (mini) poppet valves have emerged. Although these valve types may have merits with regard to performance and robustness, also applications with rather poor performance have been reported. The comprehensive investigation and field measurement of such valve failures have encountered unexpected problems in regard to valve dynamics and subsequent damages.

Significant changes in efficiency and reliability of compressor valves for high speed compressors require the simultaneous improvement of:

- Valve design
- Valve dynamic simulation
- Material technology
- Valve spring technology

2 Ring valves and design inherent ring dynamics phenomena

Ring valve become more and more popular in the compressor industry. The tapered seat lands do not cause the high flow deflection like in standard plate type valves. But the argument of having better efficiency compared to plate type valves due to better flow characteristics is only true if the spacing between the seat lands is in the same range. Most ring valves in use today to not have significantly higher efficiency due to the usage of broad and robust valve rings and thereby do not utilize the theoretical efficiency potential of ring valves.

Of course valve efficiency is also a question of valve lift. In demanding high speed applications the valve lift is often limited by the maximum allowable valve opening impact speed of the sealing element and the valve spring. So the only way to significantly improve the efficiency of the valve is by increasing the number of rings in a given valve dimension – meaning to reduce the ring width. The parallel optimization of the seat land angle to the target lift further improves the effective valve flow area.

HOERBIGER has two ring type valves (CX, CE) with different ring widths in use (CX: 16 mm, CE: 10 mm). A ring width of 16 mm in combination with standard lifts in the range of 1 to 2.5 mm does not lead to high valve efficiency – these valves are designed for high robustness in light weight gas applications like hydrogen. But still a ring width of 10 mm with standard lifts does not lead to outstanding valve efficiency.



Figure 1: HOERBIGER CX and CE ring type valves

Figure 2 demonstrates the achievable valve efficiency depending on the lift. Poppet valves require very high lifts to provide efficiency. Plate type valves reach their physical limits at a alpha value of ~ 18%. The alpha value defines the relation between the given valve port area and effective flow area of the valve. Due to the better flow characteristics of tapered ring type valves the maximum theoretical efficiency of ring type valves is higher. But most of today's ring valves do not allow the utilization of the high efficiency due to the need of high valve lifts caused by the high ring widths.

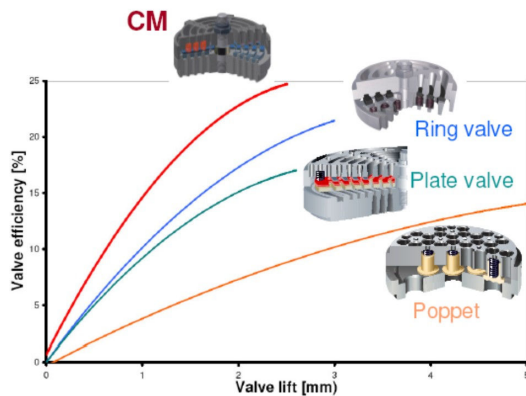


Figure 2: Alpha valves for different valve concepts depending on valve lift

Obviously the only way to significantly improve valve efficiency in high speed compressors is to increase allowable valve lifts or further increase the number of valve rings in a given valve dimension.

In figure 3 the valve efficiency of a new high efficiency valve (CM valve) is outlined. Beside a high maximum the valve already provides high flow area at moderate lifts. This was achieved by reducing the valve ring width down to 7.75 mm.

Within the CM valve development and by analysing some failed CE valves in demanding applications we had to observe unexpected valve motion and valve problems.

2.1 Unexpected field problems

The failed valves returned for reconditioning almost always exhibited the same problems: broken rings and springs which were either broken or had lost on overall uncompressed length, hinting at plastic deformation in the spring wire.

That was a very strange and initially unexplainable situation: on the one hand, there was the CX valve which proved to be a very robust design, having a very good lifetime. On the other hand, there was the scaled down, smaller brother which used the same concept and exhibited occasionally unacceptable run times.

Furthermore, a close look at the CX and CE field applications revealed no significant difference

As a next step, two possible root causes were identified:

- Oil sticktion of the sealing elements
- Poor dynamic spring performance

2.2 Problem analysis, conclusions

Oil sticktion would lead to a huge overshoot of pressure at the moment where the valve is supposed to open. A close look into continuous condition monitoring data of a customer actually revealed exactly that failure mechanism, as can be seen in figure 3:



Figure 3: p-t traces at two different times laid onto each other reveal a sharp pressure rise (grey curve) at the discharge valve opening hinting at oil sticktion

An in-depth analysis of the second failure mode, including dynamic Finite Element analysis to cross check with standard engineering limits, ended with a big disappointment: neither engineering limits of dynamic stresses in the springs were violated nor could anything be found with regard to the material quality of the spring wire.

These findings led to three conclusions:

1. As a plastic deformation is occurring in the spring wire the only possible conclusion is that impact speeds of the sealing elements (causing dynamic stresses in the wire) are of the same order of magnitude or higher as the wave propagation speed inside the spring.
2. Simulated impact speeds of the sealing elements calculated with industry standard valve dynamics calculation methods would never ever predict speeds even coming close to the wave propagation speed inside the spring.
3. To understand the failure root cause oil sticktion effects of the sealing elements have to be accounted for.

2.3 Activities to resolve the problems

The findings in section resulted in a couple of parallel activities. In order to prove conclusion 1 of section 2.1, a dynamic spring tester was developed which was capable of producing the high impact speeds required to reproduce the observed spring setting (i.e. a continuous loss of uncompressed length). The spring tester is described section 2.4.

Deep thought was put into analyzing the industry standard valve dynamics calculation. Here, a fundamental breakthrough was achieved by identifying pressure waves inside the compressor's cylinder and the interaction of multiple, individual rings together with oil sticktion as the leading mechanism to explain the occurrence of high impact speeds.

Hence, a completely new simulation model was written which is capable of mapping the instantaneous flow inside a cylinder of a reciprocating compressor and the interaction with multiple, individual sealing elements in conjunction with oil sticktion. The simulation model is described in section 2.5.

As oil sticktion emerged as a root cause of failure, an oil sticktion tester enabling testing of different ring / seat geometries was developed. By the help of this tester, a ring and seat combination was identified which reduces oil sticktion effects to a minimum.

Calculation results obtained by the new model using the knowledge generated with the oil sticktion tester explain the observed failures and helped to define countermeasures which led to an improved valve design, exhibiting no failures so far at the time of writing!

2.4 Dynamic spring testing

In order to get a better understanding of the mechanism of spring setting, dynamic FEM calculations were performed and a spring tester for spring shock loading was designed. The high speed shock loading device allows to induce impact loads on prestressed springs under similar conditions as in compressor valves with speeds up to 30 m/sec. Beside the effect of one single impact the influence of high impact numbers ($>10E4$) can be investigated.

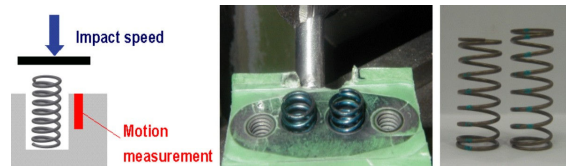


Figure 4: Concept of the spring tester

The results clearly show a certain impact speed level at which spring setting (a residual plastic deformation reducing the uncompressed spring length, see the rightmost picture in figure 4) caused by impact loading occurs. Below this level no spring setting can be detected - even with high numbers of impacts. This value is only slightly affected by the spring design but strongly defined by the spring wire material itself.

The threshold values obtained give clear evidence of plastic deformation in spring wires. The most important finding was that the impact speeds required to give rise to spring setting are more than three times higher than the calculated opening impact speeds of the compressor valve. Obviously unknown dynamic effects must be the reason for this discrepancy.

2.5 Simulation model

E. Machu (1) was the first to identify the unsteady flow inside the cylinder as the key to explaining phenomena associated with abnormal high indicator pressures during discharge and valve losses.

G. Machu (3) managed to show that the inclusion of pressure waves inside the cylinder leads to a realistic prediction of valve sealing element impact speeds. Hence, the model described in (3) was extended to cope with multiple, individually sprung sealing elements.

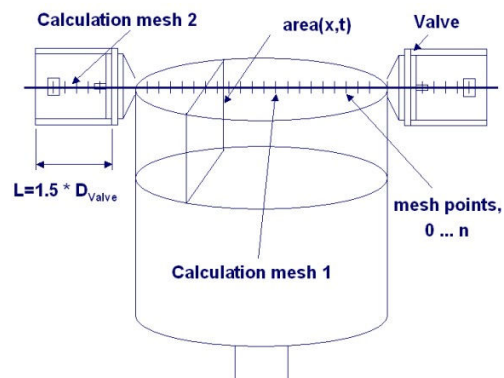


Figure 5: Simulation model

Figure 5 exhibits the model used in the calculations. There are three interconnected calculation domains, the suction and discharge chambers, and the cylinder.

In the course of the calculation, the piston will increasingly diminish the valve passage area. This effect is included in the simulations.

The governing system of equations was already discussed in G. Machu (3), hence only the basic system is described here. The state of the gas in the cylinder is determined by two factors: on the one hand from the kinematics of the drive, which determines the volume inside the cylinder (= area(x,t) at each node point) and therefore the isentropic change of state of the gas. On the other hand from the in- and outflow into the nodes from neighboring nodes, or the flow through the suction or discharge valve at the boundary.

In order to calculate the velocity $u(x,t)$ and the pressure $p(x,t)$ at every node point at time t [s], one has to solve the unsteady Euler equations of fluid dynamics (one dimensional, inviscid, in conservative form, please review Anderson (2)):

Equation of continuity:

$$\frac{\partial(\rho A)}{\partial t} + \frac{\partial(\rho A u)}{\partial x} = 0 \quad \text{and}$$

Euler equation:

$$\frac{\partial(\rho A u)}{\partial t} + \frac{\partial(\rho A u^2 + p A)}{\partial x} = p \frac{\partial A}{\partial x} \quad (1)$$

In equation 1, $\rho(x,t)$ [kg/m³] denotes the density with respect to space and time, $u(x,t)$ [m/s] and $p(x,t)$ [bara] the velocity and pressure, respectively, and $A(x,t)$ [m²] is the area at the position x . As the change of state of the gas is assumed to be isentropic, no additional energy equation has to be solved.

In order to solve equation 1, there are a lot of first and second order methods available in the literature. Here, a variant of the Lax – Wendroff method, namely the method of MacCormack is used (2. order with respect to space and time).

With the calculated pressure, a differential equation of each of the valve's individual sealing elements is solved:

$$m_{SE} \ddot{Y} = \eta \Delta p F O - F_{Springs} \quad (2),$$

where Y denotes the lift [m], η [l] is the lift-dependent drag coefficient, Δp the differential pressure across the sealing element and FO [m²] is

the pressurized area. $F_{Springs}$ [N] denotes the closing spring force acting on the individual sealing element, and m_{SE} [kg] the mass of the sealing element.

Oil sticktion is incorporated into the model mainly as a pressure which reduces the actual pressure differential across the individual sealing element until an (arbitrary) lift of 0.05 [mm] is reached.

If one of the valve's sealing elements is in the open position, the velocity in the gap is calculated according to the pressure ratio across the sealing element. The corresponding massflow [kg/s] is calculated by:

$$\dot{m} = A_{eff} \rho_K u \quad (3)$$

A_{eff} [m²] denotes the effective flow area of the individual sealing element at time t [s] and is a function of the lift.

The sum of each individual massflow is used as the boundary condition for the flow dynamics calculation (meshes (1) and (2), or (1) and (3) in figure 4), and is positive or negative depending on the pressure ratio. The pressure is extrapolated from the neighboring nodes.

If the valves are closed, then the massflow is zero, and the pressure is mirrored.

2.6 The oil sticktion tester

The primary requirement to be met by the sticktion tester was to provide a quantitative measure for the oil sticktion effect under conditions resembling those in a compressor as close as possible. This consideration has led to the development of an oil sticktion tester as sketched in figure 6.

Basically, the tester consists of a ring valve (2 valve rings) subjected to a constant counter pressure $p_2=7\text{bar}$ and a time-varying prechamber pressure p_1 . The latter pressure is controlled by three high speed solenoid valves with large cross section (HOERBIGER SV26) that feed the prechamber with pressurized air (p_{supply} up to 30bar). With this configuration, prechamber pressure-rise rates up to 11000 bar/s are achievable.

The prechamber pressure and the motion of the sealing element were measured by means of a pressure transducer and two capacitive distance transducers, respectively.

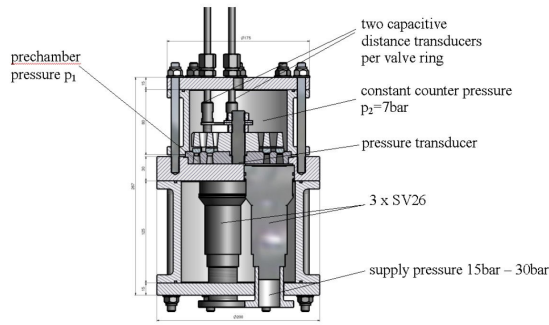


Figure 6: Oil sticktion tester

The time delay of ring opening $\Delta t_{stick} = t_{oil} - t_{dry}$ due to the presence of oil (oil type VDL 150 was used) turned out as a repeatable quantitative measure of the oil sticktion effect (cf. figure 7: the y-axis is showing volts due to the nature of the pressure and distance transducers – internally that signal is transferred into [bara] and lift [m]). Here, t_{oil} and t_{dry} denote the elapsed time between pressure equalization over the ring (prechamber pressure p_1 equal to counter pressure p_2 plus equivalent spring load p_{spring}) and ring opening (for the sake of a repeatable examination of the experimental data taken as the moment when the ring lift exceeds 0.02mm) in the presence respectively absence of oil.

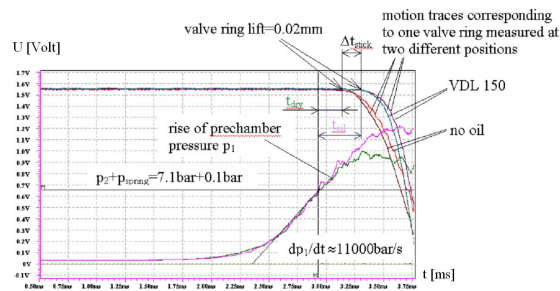


Fig. 7: Results from the oil sticktion test

2.7 Calculation results incorporating the finding from the oil sticktion tester

Looking at one of the failed applications, figure 8 (a) exhibits a simulation of a suction valve (4 rings) in the absence of oil (nondimensional lift and pressure). What can be seen is the fact that due to the different spring forces on each of the individual rings also a different lift curve and therefore impact speed (at a nondimensional lift of 1) of the individual sealing element is obtained.

This observation is due to the fact that the pressure differential across the valve (namely cylinder pressure minus line pressure) immediately breaks down the more the rings open, and the remaining differential is of the order of magnitude of the spring pressure (please refer to G. Machu (3) for further details on valve impact speed phenomena).

Figure 8 (b) shows the effect on valve dynamics in the presence of oil sticktion, equal for all rings. The impact speed dramatically increases (an average factor of 2.8 when compared to the oil free case (a)), because of the hugely increased initial pressure differential across the valve due to oil sticking the ring to the seat. The effect of individual spring pressure on the speed becomes hardly noticeable. The impact speed (not shown in the graphs) of each ring is derived by the time derivative of the lift curve.

Still, the calculated speeds are not high enough to come close to the speeds where spring setting sets in (conclusion 1 of section 1.3)!

Now, the degree of freedom of each individual ring comes into play: most likely, each ring will experience a different sticktion situation. If we now think of a situation where all rings are wetted with oil, but the smallest ring is not so immersed it could happen that it breaks off earlier than the other rings – that is just an arbitrary assumption made in order to demonstrate the effect this may have on the valve dynamics.

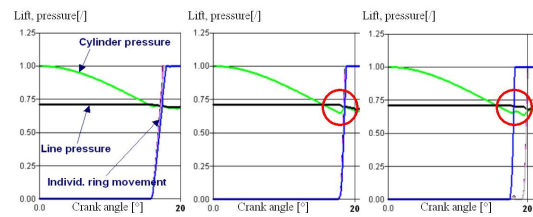


Fig. 8: (a) suction valve ring dynamics without oil, (b) with equal oil sticktion (2.5 bar) for each ring, (c) oil sticktion for all rings, but smallest one breaks loose at 80% sticktion pressure (a little earlier than the other rings)

What then happens is that the full pressure differential acts only on this single ring. As it is the smallest ring, it doesn't contribute much effective flow area to reduce the pressure differential. Hence, it gets dramatically accelerated during the full opening event, leading to an impact speed which corresponds to the wave propagation speed inside the springs!

The other rings now get seriously delayed because the fully open smallest ring decreases the pressure differential to such an extent that it falls below the one required for overcoming the oil sticktion. Hence, only when sufficient pressure differential is built up again, the other rings open as well.

Now, one could ask why that phenomena did not occur with the CX valve – the answer is simple: the CX valve has a much wider ring width, leading to the fact that if one ring would open early, it would contribute (relatively) so much effective flow area that the pressure differential is immediately reduced and the acceleration breaks down of that individual ring, leading to only moderate impact speeds.

2.8 Motion measurements with multi-ring valve on a high speed compressors

To check the simulation results with real measurements a 192 mm valve with 7 (!) individual rings was equipped with motion sensors. On the larger rings two positions are measured to get information about tilting motion (Fig.9).

Measurements were made in a broad range of speeds, compression ratios and pressures. The measured motions and velocities were very close to the estimated and calculated values.

But under a certain operating conditions (not at maximum condition) a unexplainable and chaotic movement of the outermost ring (fig.10) could be observed. Under this condition a closing impact speed 10 times higher than normal could be found. Closing speeds in that range immediately lead to ring breakage and valve failure.

Based on that findings it became obvious that a reliable valve concept with a high number of individual rings is not possible for high speed compressors.



Fig. 9: Test valve with 7 individual rings equipped with motion sensors

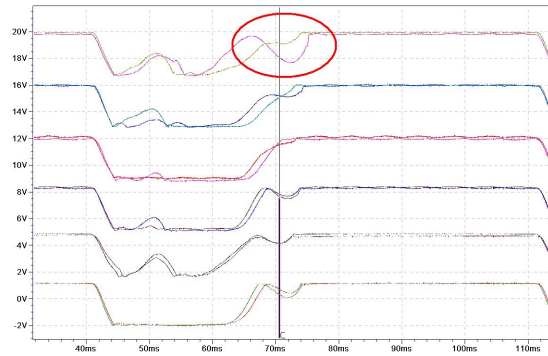


Fig. 10: Traces show valve ring motion of 5 different rings. Measurements taken on two opposite positions. Marked area shows the chaotic ring motion of outermost ring during closing

2.9 Advanced design concept based on fundamental findings

The findings demonstrate that a valve concept with a high number of individual rings can lead to uncontrollable chaotic valve ring motion and thereby premature valve failures.

The need for higher valve efficiency with standard lifts can only be fulfilled with reduced narrow spaced rings.

The new HOERBIGER CM valve synchronizes the ring motion and provides outstanding valve efficiency. The usage of new valve ring material and advanced spring technologies further supports the high robustness and reliability.

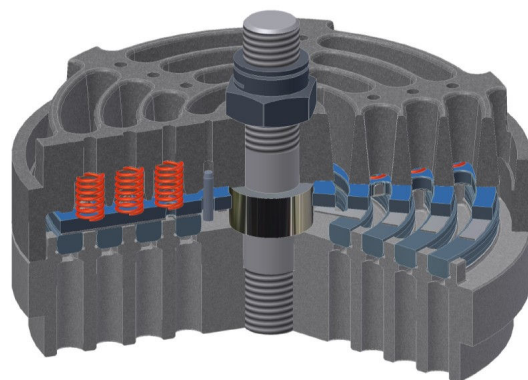


Fig. 11: CM valve with synchronizing plate

3 Material technology

Since the introduction of nonmetallic materials to the compressor market decades ago the valve suppliers constantly have tried to increase the reliability and lifetime of valve sealing elements. Nevertheless the improvement potential soon gets to the limitations of commercially available materials and production processes installed. All valve materials in use today were developed for general applications like automotive, consumer products,... and are not designed to match the needed properties in compressor. The load on valve sealing elements is quite unique due to the combination of dynamic impact loads, high temperature and gas exposure and the more or less static load by the differential pressures. The specific overall load combination requires purpose designed material.

The basis to generate guidelines for new materials is the fundamental understanding of the loads occurring during operation and the micro mechanics involved during crack initiation and advancement.

The stress situation in valve material was modeled by taking the full orthotropic viscoelastic material characteristic into account. Together with the investigation of the residual stress state and the micromechanic failure mode a new valve material can be designed for compressor applications.

The new HOERBIGER HP is the first purpose build compressor valve material with outstanding properties like absolute fatigue resistance.

The most common reason for premature valve failure is material fatigue or fatigue crack growth. Small cracks in the material or on the surface, for example caused by impact on sharp seat lands, increase in size by high load frequency and are supported by residual stresses in the material. The crack propagates through the reinforced material mainly by surrounding the short fiber reinforcement. Crack advancement is thereby also supported by the coalescence of material flaws preferably at the fiber ends of the short fiber reinforced material. Even if fibers themselves have high fatigue strength, the fatigue behavior of standard short fiber reinforced materials at high load cycles it is still determined by the nonmetallic surrounding matrix.

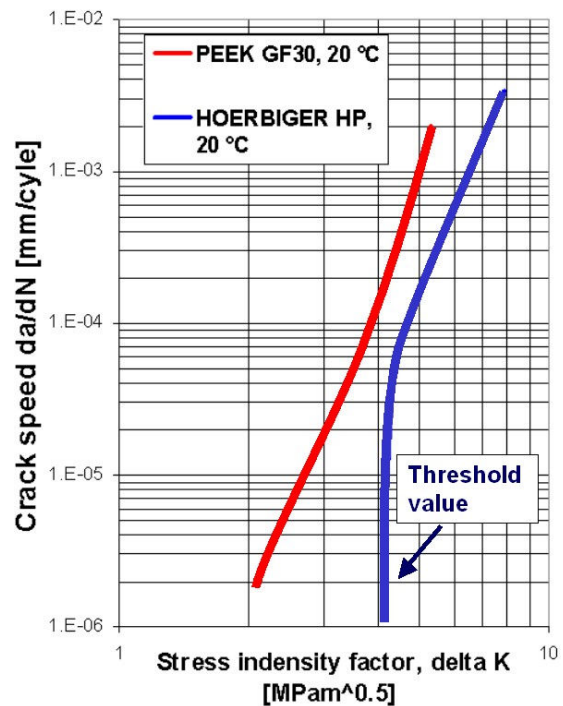


Fig. 12: Fatigue crack resistance of PEEK GF30 and HOERBIGER HP

In order to overcome the limitations of commonly used short fiber reinforced materials, for the new HP material a very special type of reinforcement is used. A special planar long carbon fiber reinforcement prevents a potential crack from going around the fiber reinforcement. To improve the crack resistance the bonding levels between the carbon fibers and the polymer matrix is adjusted in that way that a certain amount of sliding on the fiber surface is allowed. This spreads the stress concentration near the crack tip and thus preventing crack advancement up to high load levels – creating a “threshold” value below which no crack advancement can be found. This exceptional crack stop ability was proven by fatigue test probes (Fig.11). The HP material does not show crack advancement up to very high cyclic stress levels – at these stress levels standard short fiber reinforced material would fail after short operation time. This feature works like a shock absorber and forms the basis for HP’s unique crack stopping ability. Due to this HP specific property no more fatigue crack growth in valve plates can be found any more.

The outstanding properties of HP was already proven in more than 6000 successful field installations.

4 Spring technology

Having improved materials in hand the springs become the weakest link in compressor valves. The demand for higher efficiency in high speed compressors force the valve producer to extend the application envelope of the valve springs.

The load on valve springs in high impact speed applications is completely different from low speed compressors. Where at low speed the dynamic shock loading plays a minor role, at high speed the stress rise by dynamic shock loading is the major load factor. All the calculation methods have to take the dynamic effects into account. Beside the effect of stress rising due to shock loading also the effect of reducing the minimum prestressing level by expansion waves has to be considered.

Standard spring technology soon reaches its limits. Advanced spring wire materials, spring designs and spring after treatment techniques are needed to significantly improve the spring life time. Many of the known standard spring wire treatment methods like shot peening are not applicable to the typical spring sizes and the negative effects on spring corrosion resistance.

To overcome this limitation HOERBIGER is developing a tailored surface treatment method for new valve springs. Therefore the first test rig for testing compressor valve type springs in different corrosive gases has been designed and installed. Based on first results a 5 to 10 times higher spring lifetime will be possible.

A high number of valves with these new spring technologies and calculation method are already running in demanding applications without any problems.

5 Proven valve efficiency

Due to the high valve efficiency and the high allowable impact speeds, this generation of valves can run in high speed compressors with standard valve lifts and thereby significantly reduce the valve losses compared to standard valve equipment without reducing reliability.

The new valve type is already installed in different field installations in gas gathering, gas storage and gas transport. Emphasis was given to select demanding high speed applications.

In some installation the calculated valve motion was verified by motion measurements and performance improvements were measured.

In a variable speed gas storage compressor (Neumann&Esser) CM valves have been installed since 3 years. PROGNOST monitoring system calculated 7 to 8 % energy savings compared to standard plate valves.

In a 900 rpm large high speed pipeline compressor a CM type valve has proven 8 % energy savings. The operator calculated more than 120 000 \$ annual saving per compressor by changing to this valve type.

6 Conclusions

To safeguard the future supply with natural gas considerable investments into compression equipment in gas gathering, gas processing, gas storage and gas transportation is required. In order to keep cost of investment low, compressors are rated at higher speed asking for substantially increased valve performance and valve reliability.

Very often standard cylinders are used and run at higher compressor speed. In this case higher valve efficiency is needed in order not to cause additional power consumption. The only way to increase valve flow area for a given valve size is to go for tapered seat lands and ring valves with high number of rings leading to maximum flow area.

With simulations and measurements it was shown, that oil sticktion in valves with high number of individual rings can cause chaotic valve motion and multiple impact speeds during opening and closing. The found impact speeds are in a range to cause spring deformation and ring breakage. To achieve the targeted reliability goals in high speed compressors ring valves the motion of the rings needs to be synchronized.

But it is not only a question of design. Also improvement in the are of sealing element materials are needed together with improve spring technologies. In both areas new knowledge was gained what will lead to increased reliability in future.

Numerous successful field installations and performance measurement all over the world demonstrate impressive power saving potentials and reliability gains for the compressor user.

7 References

- (1) E. Machu: Problems with modern high speed short stroke reciprocating compressors: Increased power requirement due to pocket losses, piston masking and gas inertia, eccentric gas load on the piston. *Gas machinery conference Denver / USA* (1998)
- (2) J.D.Anderson: *Computational Fluid Dynamics* (1995), McGrawHill
- (3) G. Machu: Pulsationen im Verdichtungsraum – eine potentielle Schadensursache?, *Industriepumpen + Kompressoren 2* (2005), pp. 70 - 73



Advances in fundamental understanding of the dynamic sealing action in packing systems

by:

Dr. Tino Lindner-Silwester
Research & Development
HOERBIGER Ventilwerke GmbH & Co KG
Vienna
Austria
tino.lindner-silwester@hoerbiger.com

5th Conference of the EFRC
March 21-23, 2007
Prague, Czech Republic

Abstract:

It is well-known that the achievable lifetime of a dry-running piston rod packing seal is significantly dependent on the temperature level the sealing elements are exposed to during operation. Thus, a deeper understanding of the various thermophysical processes governing the non-lube operation of a packing is crucial a) for assessing the major influencing factors that give rise to the current application limits of dry-running packings and b) for developing improved packings capable of coping with demanding applications.

The presented approach towards gaining that fundamental understanding consists in the creation of a novel theoretical model that accounts for all the complex mass and energy transport phenomena, the development of a test compressor (“**multi-purpose test compressor**”, MPTC) on which measurements previously regarded as impracticable to take can be performed during operation, and fundamental investigations into transfer film phenomena. In this paper the simulation model is presented and its predictions are compared to measurements taken at the MPTC.

1 Introduction

It has become common for many reciprocating compressors to operate in non-lubricated mode for a variety of reasons such as costs and environmental aspects. Such dry-running operation of a reciprocating compressor poses a great challenge especially to the piston rod sealing system (pressure packing). In absence of any lubricating oil much more frictional heat is released in the pressure packing during operation of the compressor. Depending on how much frictional heat is released and how efficiently it is removed, the rod might heat up to considerable temperature levels. High rod temperature levels in turn significantly increase the wear rates of the sealing elements (packing rings) of the pressure packing.

In this paper a mathematical model is presented that allows to predict the temperature level the rod heats up to when sealed by a dry-running pressure packing. Once the rod temperature distribution is known, the counter surface temperature of the individual packing rings, i.e. the temperature the rings are exposed to where they contact the rod, can easily be calculated. This counter surface temperature together with the pressure loading gives each ring's thermomechanical load collective. Given the significant effect of the counter surface temperature on the operational behaviour of a dry-running packing, the presented model, together with a fundamental understanding of the mechanisms governing the wear¹, allows to identify and quantify all the factors and parameters that determine the limits of stable operation of a pressure packing. Gaining a thorough understanding of how these limits come about constitutes, on the other hand, a sound basis for developing improved packings.

2 The thermophysical model

An investigation is taken into the operational behaviour of a dry-running reciprocating compressor whose rod of length L_{rod} and diameter d is sealed by n packing ring sets of width b against ambient pressure. $L_{PR,i}$ denotes the distance between the lower face of the piston and the midplane of the i -th ring set at bottom dead centre $z=0$, and $L_p=L_{PR,n}-L_{PR,1}$ is the sealing length of the packing (cf. Fig. 1).

2.1 Energy balance of rod

Starting point of the investigations is the heat diffusion equation of the rod. Any variations of the rod temperature T across the rod's cross section are neglected so that T is a function of distance x along the rod and time t . The x -axes is fixed with the rod and shall point towards the crankcase with $x=0$ and $x=L_{rod}$ corresponding to the locations of the lower face of the piston and the crosshead, respectively.

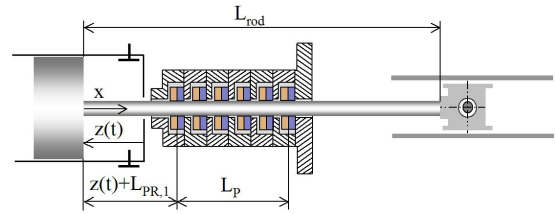


Figure 1: Geometry of problem

The unsteady temperature distribution $T(x,t)$ is governed by

$$\rho c \frac{\partial T}{\partial t} = \lambda \frac{\partial^2 T}{\partial x^2} - \frac{4}{d} \dot{q}^{(conv)} + \frac{4}{d} \dot{q}^{(fric)} - \frac{4}{d} \dot{q}^{(ring)} \quad (1)$$

where ρ , c , and λ denote, respectively, the density, the specific heat capacity, and the heat conductivity (assumed not to vary significantly in the considered temperature range) of the rod. The convective heat flux to the gas surrounding the rod is denoted by the superscript (conv) whereas the superscripts (fric) and (ring) mark the flux of heat corresponding to the generation of frictional heat and the heat flux removed from the rod by the packing rings, respectively.

At the two end surfaces of the rod the boundary conditions

$$T(x=0,t) = T_1, \quad T(x=L_{rod},t) = T_2 \quad (2)$$

are prescribed where T_1 is the piston bulk temperature and T_2 the bulk temperature of the crosshead. For determining the value of the former the empirical relationship $T_1 = T_s + 2/3(T_d - T_s)$ is used where T_s is the suction and T_d the discharge temperature. For T_2 a value in the order of $(60 \dots 70)^\circ\text{C}$ is in most cases a reasonable choice. However, it should be noted that especially the value of T_2 has no noticeable effect on the peak temperatures of the rod.

Since the focus of the presented investigations is on the steady thermal state where the relation

$$T(x,t) = T(x,t + \tau)$$

holds with τ denoting the time duration of one revolution of the crankshaft, no initial conditions have to be prescribed. In order to be able to directly solve for the rod temperature distribution in the final steady state without having to account for the transient starting phase, it is advantageous to decompose the rod temperature according

$$T(x,t) = T_m(x) + T_f(x,t), \quad T_m(x) := \frac{1}{\tau} \int_0^\tau T(x,t) dt \quad (3)$$

into a time-averaged mean value T_m and a fluctuating component T_f . An order-of-magnitude estimation shows that the fluctuating component T_f is negligibly small. This important finding

- allows to determine the distribution of the time-averaged rod temperature $T_m(x)$ without having to solve for the fluctuating component $T_f(x,t)$ and
- reduces the heat diffusion equation (1) from a partial differential equation to an ordinary one.

Since all subsequent considerations refer to the time-averaged rod temperature T_m , the subscript m will be dropped from now on to keep the notation compact.

The convective heat flux to the gas surrounding the rod is assumed to be expressible in terms of a heat transfer coefficient α according

$$\dot{q}^{(conv)}(x,t) = \alpha(x,t) [T(x) - T^{(gas)}(x,t)] \quad (4)$$

where the heat transfer coefficient as well as the temperature of the gas $T^{(gas)}$ will in general vary both in time and space. Buoyancy effects are of no significance in the present problem so that the value of α is not affected by the temperature difference $T - T^{(gas)}$ driving the heat transfer to the gas. However, the dependence of α on several properties of the gas that themselves vary with temperature may introduce a slight variation of α with the rod temperature. Since this variation is smaller than the unavoidable uncertainty as to the exact value of α (unsteady turbulent gas flow,...), α will be regarded as independent of the rod temperature.

2.2 Time-averaging of rod energy balance

Applying the time-averaging process (3) to the heat diffusion equation (1) and the boundary conditions (2) gives

$$\frac{d^2 T(x)}{dx^2} - \frac{4\alpha_m(x)}{\lambda d} T(x) = \frac{4}{\lambda d} \dot{q}_m(x) \quad (5)$$

and

$$T(x=0) = T_1, \quad T(x=L_{rod}) = T_2 \quad (6)$$

where the abbreviation

$$\dot{q}_m(x) := (-\dot{q}_m^{(fric)}(x) + \dot{q}_m^{(ring)}(x) - [\alpha T^{(gas)}]_m(x)) \quad (7)$$

is used. Herein,

$$[\alpha T^{(gas)}]_m(x) := \frac{1}{\tau} \int_0^\tau \alpha(x,t) T^{(gas)}(x,t) dt \quad (8)$$

is the distribution of the time-averaged product of heat transfer coefficient and temperature of the gas surrounding the rod. Time-averaging of the released frictional heat and the heat removed from the rod by the packing rings gives the remaining two terms appearing on the right-hand side of (7).

The function $\alpha_m(x)$ that represents the variation of the time-averaged heat transfer coefficient along the rod plays an important role in the analysis. Basically there are three regions along the rod to be distinguished from each other in this respect:

- region A...the compression chamber where the effect of the gas flow through the valves on the convective heat transfer can be of importance.
- region B...here heat is transferred convectively to the gas in the packing cups. This process can be significantly affected by the magnitude of the packing leakage.
- Region C...the remainder of the rod (distance piece,...) where the gas is usually at ambient pressure. Here any gas flow is solely induced by the rod's motion.

Further complications arise from the fact that, especially in region A, the gas may undergo considerable pressure and temperature changes. Simple relationships for the convective heat transfer that can be found in the literature usually hold for much more idealized configurations so that they cannot be applied to the current problem.

Hence, numerous CFD calculations have been performed to derive universally valid dimensionless expressions relating α to all significant parameters of the problem (geometry, operating conditions, gas properties,...).

To keep the analysis as simple as possible without losing track of the important effects, a simplified distribution $\alpha_m(x)$ will be used for which α_m is assumed to vary in a stepwise constant manner along the rod. The rod is partitioned into three regions of constant α_m by looking at the rod at half-stroke position (cf. Fig. 1). Region A extends from $x=0$, i.e. the lower face of the piston, to $x=s/2+L_{PR,1}$, where s stands for the piston stroke. In region B that extends from $x=s/2+L_{PR,1}$ to $x=s/2+L_{PR,1}+L_P$, the value of α_m is determined by averaging over the individual cups and multiplying the obtained value by a geometrical correction factor that accounts for the fact that parts of the rod surface are not in contact with the surrounding gas but with the counter surfaces of the packing rings. Region C covers the remainder of the rod.

If the right-hand side of (5) were known, the linearity of the problem would allow to express the rod temperature distribution in terms of the Green's function $G(x,\xi)$ of the problem according to

$$T(x) = T_1 + x \frac{T_2 - T_1}{L_{rod}} + \frac{4}{\lambda d} \int_0^{L_{rod}} \left[\dot{q}_m(\xi) + \alpha_m(\xi) \left(T_1 + \xi \frac{T_2 - T_1}{L_{rod}} \right) \right] G(x,\xi) d\xi. \quad (9)$$

Herein, $G(x,\xi)$ gives the value of the temperature the rod would reach at the location x if a properly normalized heat sink of unit strength acted at the location ξ with both ends of the rod kept at zero temperature. For solving the subsequently derived equations it will be of great importance to have an analytical expression for $G(x,\xi)$. This fact is the root cause for approximating $\alpha_m(x)$ by a step function as $G(x,\xi)$ can be derived analytically for such a variation of α_m .

However, the solution (9) is just a formal one as the right-hand side of (5) is not independent of the resultant rod temperature distribution but will turn out to even depend on integrals over the rod temperature distribution. Thus equation (5) in fact constitutes an integro-differential equation that can be reduced to an integral equation by using the concept of a Green's function.

2.3 Frictional heat generation

The amount of frictional heat generated as well as the positions along the rod where frictional heat gets released are crucial pieces of information that have to be incorporated into the analysis. Fig. 2 shows in a schematic manner how the way the gas pressure is broken down in the counter surface from p_i (acting in the i -th packing cup) to a lower level p_{i+1} (acting in cup $i+1$) gives rise to an unbalanced force $F^{(unbal)}$ in radial direction with which the ring set is pressed against the rod. In presence of a relative motion between the ring and the rod, this contact force is accompanied by a tangential force of sliding friction opposing the relative motion. Work has thus to be done on the rod to keep it moving. Neglecting any changes in the internal energies of the rod and the rings associated with ring wear and the formation of a transfer film, this work can be regarded as a release of frictional heat in the areas where the rings contact the rod.

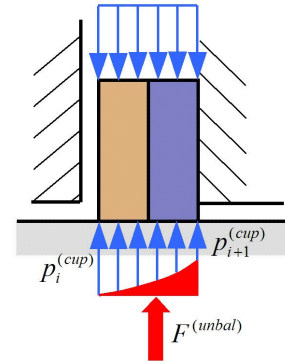


Figure 2: Relationship between gas pressure distribution in counter surface and radial unbalanced force

The determination of how much frictional heat gets released on the average at a certain location x along the rod can thus be split into the following subproblems:

- Derivation of a relationship between the radial unbalanced force and the pressure differential across a ring set. This relationship depends on the gas pressure distribution in the counter surface and is thus a “fingerprint” of the ring design.
- Determination of the cup pressure distribution $p_i^{(cup)}(t)$, i.e. how the instantaneous cylinder pressure is broken down to ambient pressure by the individual packing rings.

- Translation of the sequence of instantaneously released frictional heat quantities into distribution of time-averaged release of frictional heat along the rod.

2.3.1 Gas pressure distribution in counter surface gap

Even though the surfaces of the rod and the packing rings are nominally flat, the actual (microscopic) area of contact between them is considerably smaller than the macroscopic one. Contact spots are interspersed with gaps through which gas can leak under the action of a pressure gradient. A mean gap height h can be defined in a purely geometric manner or by equating the leakage rate of the actual configuration with a hypothetical one where the gas is forced to flow through plane-parallel walls separated from each other by a distance h . Attempts to calculate the leakage rate through areas of contact in general rest upon the assumption that both ways to determine h give the same result. The value of h is usually determined by means of the geometrical concept of the so-called ‘‘Abbott bearing curve’’². The obtained leakage rate will in any case be a sensitive function of h .

For the current analysis that is focused on the gap pressure distribution rather than on the rate at which gas leaks through, it will turn out to be sufficient to assume that h does not vary (on a macroscopic length scale) in the contact area. The gap pressure distribution is not affected by the value of h in the subsequently considered limiting case of sufficiently small values of h .

Assuming ideal gas behaviour and the flow to be adiabatic, an order-of-magnitude analysis (assuming h to be in the order of microns) of the Navier-Stokes equations gives the following:

- The flow is an isothermal one so that density variations are linearly related to pressure variations.
- The inertia terms (unsteady and convective) may be omitted, i.e. the flow is a quasi-steady one governed by the equilibrium between pressure forces and viscous forces.
- The gas pressure does not vary across the film so that the pressure field is two-dimensional.
- The shearing of the fluid brought about by the relative motion between rod and ring has a negligible effect on the pressure field.

Taking into account that the dynamic viscosity of gases changes but little with pressure, the 2d pressure distribution is governed in this thin-film approximation by $\Delta p^2=0$ where Δ denotes the Laplacian. The square of the absolute gas pressure obeys thus Laplace’s equation. For a ring pair consisting of a radial ring and a stop-tangent ring, a typical pressure distribution (widths of wear compensation gaps neglected in right-hand side of Fig. 3, x-axes and y-axes point in circumferential and axial ring direction, respectively) is depicted in Fig. 3.

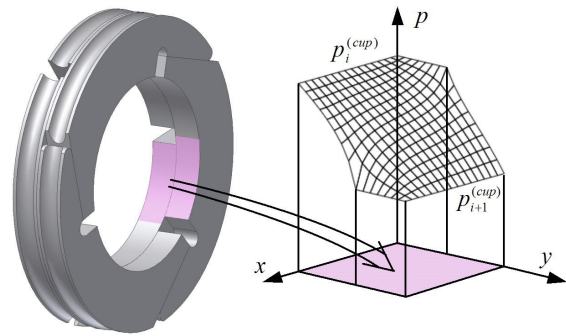


Figure 3: Gas pressure distribution in counter surface

Once the pressure distribution in the contact area is known, mechanical equilibrium of the ring gives the unbalanced force. The frictional heat generated is

$$\dot{Q}_i^{(fric)}(t) = \mu_{fric} F^{(unbal)}(p_i^{(cup)}(t), p_{i+1}^{(cup)}(t)) v_{rod}(t)$$

where μ_{fric} and v_{rod} denote the coefficient of sliding friction and the piston speed, respectively. For any ring design this relationship is expressible in the form

$$\dot{Q}_i^{(fric)} = \mu_{fric} \Delta p_i^{(cup)} f\left(\frac{p_{i+1}^{(cup)}}{p_i^{(cup)}}\right) b d \pi v_{rod} \quad (10)$$

where all effects (ring design, gas compressibility) are accounted for by the function f that in general has to be determined numerically. The garter spring loading, albeit usually of negligible effect compared with the pressure loading, may be added to (10).

2.3.2 Cup pressure distribution

The way the cylinder pressure is broken down to ambient pressure by the individual rings is the result of each ring's relationship between applied differential pressure and leakage across the ring. Contrary to labyrinth seals where there are well-defined leakage paths, pressure packings are gas-tight seals where any leakage is the sole result of geometric imperfections associated with unavoidable manufacturing tolerances.

In each packing cup the gas occupies a certain volume V_i . These volumes are assumed as being connected in series via prescribed orifices. The flow through these orifices is modelled as an adiabatic, inviscid nozzle flow. Especially for single-acting rings the backward and forward "shuttling" of the rings under the action of dynamic forces has a significant effect on these orifice areas that has to be taken into account.

Both the pressure and the temperature of the gas are assumed to be spatially uniform in each cup. Assuming furthermore ideal thermal and caloric behaviour of the gas, the mass and the energy balance of each cup give the following set of $2(n-1)$ first-order ordinary differential equations

$$\begin{aligned} \frac{dp_i^{(cup)}}{dt} &= \frac{R}{V_i} \left[\dot{m}_{in,i} \kappa T_{in,i}^{(cup)} - \dot{m}_{out,i} \kappa T_i^{(cup)} + \frac{\kappa-1}{R} \dot{Q}_i \right] \\ \frac{dT_i^{(cup)}}{dt} &= \frac{R T_i^{(cup)}}{p_i^{(cup)} V_i} \left[\dot{m}_{in,i} (\kappa T_{in,i}^{(cup)} - T_i^{(cup)}) - \right. \\ &\quad \left. - \dot{m}_{out,i} T_i^{(cup)} (\kappa-1) + \frac{\kappa-1}{\kappa} \dot{Q}_i \right] \end{aligned} \quad (11a), (11b)$$

where the subscripts (in) and (out) mark the mass rates and the temperature levels at which gas flows into respectively out of each cup. In the first cup the gas is assumed to undergo the same changes of state as the gas in the cylinder. R and κ denote the special gas constant and the ratio of the specific heat capacities, respectively.

The supply of heat to the gas in each cup is due to convective heat exchange with the packing housing and the rod. This exchange of heat is proportional to the respective driving temperature difference with the coefficient of proportionality given by the product of heat transfer coefficient and corresponding surface area. The packing housing is assumed to act as a heat sink whose temperature T_h is not affected by the amount of heat getting absorbed by it. The exchange of heat with the rod is driven by the difference between $T_i^{(gas)}$ and the average temperature $T_i^{(rod/gas)}(t)$ of that region of the rod surface that is in contact with the gas in the i -th cup at time t .

The heat transfer to the gas in the cups, while significantly affecting the gas temperature, has virtually no effect on the cup pressure distribution. Thus, the amount of frictional heat generated by each ring can be calculated to a very good approximation by assuming the gas in the cups to undergo adiabatic changes of state. Contrarily, the temperature of the gas in each cup is closely related to the rod temperature via exchange of convective heat. The rod temperature is in turn affected by the rate at which heat leaves the rod. This coupling effect will be considered in detail in section 2.5.

2.3.3 Distribution of time-averaged release of frictional heat along rod

The crankcase kinematics $z(t)$ allows to relate the amount of frictional heat generated (given by the values $p_i^{(cup)}(t)$, $i=1\dots n$, and equation (10)) to the position x along the rod where it gets released. This release of frictional heat is assumed to be concentrated in the mid-plane of each ring set instead of being distributed over the whole area of contact which leads to the expression

$$\dot{q}_i^{(fric)}(x,t) = \mu_{fric} |v_{rod}(t)| \Delta p_i^{(cup)}(t) f\left(\frac{p_{i+1}^{(cup)}}{p_i^{(cup)}}\right) \cdot b \delta(x - [z(t) + L_{PR,i}]) \quad (12)$$

where Dirac's delta function δ ensures that the heat flux diverges at $x=z(t)+L_{PR,i}$ in such a manner that the overall amount of frictional heat released is given by (10). Time-averaging (12) finally gives the result

$$\dot{q}_{m,i}^{(fric)}(x) = \frac{\mu_{fric} b}{\tau} \left(\Delta p_{i,I}^{(cup)}(x) f\left(\frac{p_{i,I}^{(cup)}}{p_{i+1,I}^{(cup)}}\right) + \Delta p_{i,II}^{(cup)}(x) f\left(\frac{p_{i,II}^{(cup)}}{p_{i+1,II}^{(cup)}}\right) \right) \quad (13)$$

Herein, $\Delta p_{i,I}^{(cup)}(x)$ ($\Delta p_{i,II}^{(cup)}(x)$) denotes the differential pressure acting on the i -th ring set at the instant of time when the mid-plane of the i -th ring set passes the location x during the suction (compression) stroke.

Hence, the function $z(t)$ that relates the position of the piston with time (i.e. crank angle) has to be inverted so that a certain position z of the piston can be related to the corresponding crank angle. Since the required inverse z^{-1} cannot be obtained analytically for non-vanishing values of the rod ratio, the smallness of the latter is made use of by applying perturbation methods to derive an approximate expression for z^{-1} .

It is remarkable that the piston speed, while being the quantity to give rise to the generation of frictional heat, no longer appears in expression (13).

This is due to the fact that the mean amount of frictional heat generated at a certain location x is given by both the amount of frictional heat getting generated at the instant of time when the ring is passing x and the time $t^{(\text{pass by})}$ it takes the ring to pass this location. Since the amount of heat is proportional to the rod speed, whereas the time $t^{(\text{pass by})}$ is inversely proportional to it, the rod speed cancels out in (13). However, the fact that the frictional heat generation rises in proportion to the speed is reflected in the appearance of τ in (13).

2.4 Heat transferred through packing rings

Packing rings made of PTFE based materials are in general poor conductors of heat with thermal conductivities λ_{PR} typically in the order of 0.5W/(m K). An order-of-magnitude analysis of the rod energy balance thus leads to the result that only a very small percentage of the frictional heat gets transferred away by the packing rings³. Following this line of argument one might arrive at the conclusion that attempts to increase λ_{PR} (within realistic limits, i.e. up to a factor in the order of five to ten) are barely worth the efforts. However, this reasoning will turn out to be incorrect.

The convective heat exchange between the gas and the packing rings is in any case no major influencing factor (which has been confirmed by CFD calculations) and thus neglected in what follows. The ring set with all its cuts and joints is regarded as an uncut single ring made of an isotropic and homogeneous material whose physical properties do not vary with temperature. The axisymmetric distribution of the ring temperature $T^{(\text{ring})}$ and hence the heat transfer through the ring is governed by the unsteady heat diffusion equation. Along the area of contact with the packing housing, T_h is prescribed as boundary condition. Along the contact area of the i -th ring with the rod, the reciprocating rod motion gives a temperature varying in time in accordance with (cf. Fig. 4)

$$T(x = z(t) + L_{PR,i}) = a_{0,i}/2 + a_{1,i} \cos(\omega t) + a_{2,i} \cos(2\omega t) + \dots \quad (14)$$

that is prescribed as boundary condition. The periodicity allows an expansion into a Fourier series. The coefficients $a_{k,i}$ of this Fourier series are given by

$$a_{k,i} = \frac{2}{\tau} \int_0^{\tau} T(z(t) + L_{PR,i}) \cos(k \omega t) dt .$$

For practical purposes the Fourier series is truncated at $k=2$.

The linearity of the unsteady heat diffusion equation allows to split this problem into a) the determination of the steady temperature distribution the ring adopts when it is kept at $T_i^{(\text{ring})} = a_{0,i}/2$ and $T_i^{(\text{ring})} = T_h$ at the areas of contact with the rod and the packing housing, respectively, and b) the determination of the unsteady temperature distribution that occurs when the ring is exposed to a temperature that varies according to $a_{1,i} \cos(\omega t) + a_{2,i} \cos(2\omega t)$ at the area of contact with the rod while $T_i^{(\text{ring})} = 0$ along the area where the ring contacts the packing housing. The mean heat flux through the i -th ring is given by the solution of a) and reads

$$\dot{Q}_{m,i}^{(\text{ring})} = \lambda_{PR} S \frac{a_{i,0}/2 - T_h}{\Delta r} d \pi b \quad (15)$$

where Δr is the radial ring height and S is a geometry-dependent shape factor that essentially accounts for the deviation of the heat flow from the radial direction. S has to be determined numerically.

Fluctuations of the counter surface temperature around the mean value $a_{0,i}/2$ as expressed by the Fourier coefficients $a_{1,i}$ and $a_{2,i}$ give rise to corresponding temperature fluctuations in the interior of the ring around values given by the steady-state ring temperature distribution a). These fluctuations follow from the solution of problem b). Problem b) involves two different time-scales, $t_1 = \tau$ and a diffusive time scale given by $t_2 = L^2/a$ whereby L is a typical length scale of the problem and a denotes the thermal diffusivity of the ring material. The value of t_2 is a measure for the time it takes a sudden temperature disturbance imposed at $x=0$ to become noticeable at $x=L$. For typical materials and geometries $t_2 \gg t_1$, so that in packing rings unsteady temperature fluctuations just take place in a very small region surrounding the counter surface (cf. Fig. 4).

Hence, for these unsteady phenomena neither the curvature of the ring nor the deviation of the heat flow path from the radial direction are of significance so that problem b) can be treated to an excellent approximation as if it only involved the unsteady heat transfer through a plane wall. The unsteady temperature field of the latter configuration is depicted in the bottom picture of Fig. 4. Here it can be seen how temperature waves getting induced by a sinusoidal fluctuation of the counter surface temperature propagate into the material. The penetration depths of these waves are much less than 1mm.

For the present problem in which the counter surface temperature varies according to (14) we get

$$\dot{Q}_{f,i}^{(ring)}(t) = \lambda_{PR} \left(a_{1,i} \sqrt{\frac{\omega}{2a}} [\cos(\omega t) - \sin(\omega t)] + a_{2,i} \sqrt{\frac{2\omega}{2a}} [\cos(2\omega t) - \sin(2\omega t)] \right) .$$

It should be noted that the unsteady transfer of heat through the rings, although vanishing in the temporal mean, has an important effect on the rod temperature distribution. The rings, on the one hand, take away the heat (15) from the rod which is the quantity appearing in an order-of-magnitude analysis of the global energy balance of the rod. On the other hand, the rings take away an additional amount of heat where the temperature of the rod is high and deliver it back to the rod where its temperature is low. Both this “temperature-equalizing” effect and the fact that the packing rings remove heat away from where it is generated make rings more efficient in cooling the rod than one would expect on basis of a global energy balance.

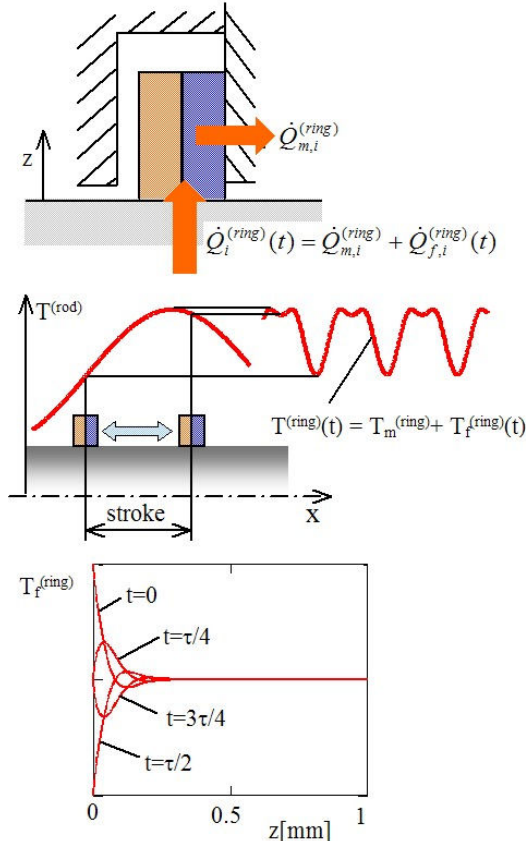


Figure 4: Unsteady transfer of heat through packing ring set (top) arising from periodic fluctuations of ring's counter surface temperature (middle) with temperature waves propagating less than half a millimetre into ring (bottom)

To finally derive the time-averaged amount of heat removed from each location x along the rod by the rings, the same time-averaging procedure as performed in the transition from (12) to (13) has to be applied. In contrast to the release of frictional heat, however, the speed of the rod that enters the problem via the substitution $dt=dx/v_{rod}$ in the time-averaging integral this time does not cancel out. As a result, the integrand appearing in the time-averaging integral diverges at the limits of integration where the rod speed becomes zero whereas the integral itself of course remains finite. A coordinate expansion of the integrand around its limits of integration avoids convergence problems in the numerical evaluation of these integrals.

2.5 Convective heat transfer to gas

For the convective transfer of heat to the surrounding gas, the temperature of the latter is one of the major influencing factors. The term (8) is approximated according to

$$[\alpha T^{(gas)}]_m(x) \approx \alpha_m(x) T_m^{(gas)}(x)$$

where $T_m^{(gas)}(x)$ is the mean gas temperature the location x of the rod surface is exposed to. The temperature of the gas in the compression chamber and in the distance piece shall not be affected by any exchange of heat with the rod with the temperature of the gas inside the compression chamber varying in accordance with the ideal pV diagram and the gas in the distance piece being at a constant level ($\approx 60^\circ\text{C}-70^\circ\text{C}$).

The temperature of the gas in the individual cups, on the other hand, will in any case be significantly affected by how much heat is exchanged with the rod and the packing housing as well as by the amount of gas leaking through the packing. These effects are expressed in (11b). The numerically proven fact that the fluctuations $T_{f,i}^{(gas)}$ of the temperature of the gas in each cup are in any case small compared to the absolute values of the mean gas temperatures $T_{m,i}^{(gas)}$ is taken advantage of by time-averaging (11b) and neglecting $T_{f,i}^{(gas)}$ against $T_{m,i}^{(gas)}$ (but taking the cup pressure fluctuations into consideration). This results in a linear system of $n-1$ equations

$$A \bar{x} = \bar{b} \tag{16}$$

where the coefficients of the matrix A are time-integrals over the cup pressure and over the exchanges of mass between neighbouring cups, both taken from the adiabatic calculation of the cup pressure distribution.

The column vectors x and b contain the variables $T_{m,i}^{(gas)}$ and integrals over the rod temperature distribution, respectively. These integrals represent mean values $T_{m,i}^{(rod/gas)}$ of the rod temperature that together with the mean gas temperatures $T_{m,i}^{(gas)}$ give the temperature differences driving the convective exchange of heat between the rod and the gas in the individual cups.

Hence, these integrals constitute averages over both time and space. It is reasonable to assume these mean rod temperatures $T_{m,i}^{(rod/gas)}$ to be given by the arithmetic mean (=spatial average) $1/2(a_{0,i}/2+a_{0,i+1}/2)$ of the temperatures the counter surfaces of the i -th and $i+1$ -th ring are exposed to in the (temporal) mean. The advantage of this choice is that these quantities also appear in the expression for the heat transferred through the packing rings so that no new quantities involving integrals over the rod temperature distribution are introduced.

Solving equation (16) for x allows to express each temperature $T_{m,i}^{(cup)}$ as a linear combination of the mean rod temperature levels $T_{m,j}^{(rod/gas)}$, $j=1,\dots,n-1$, according to

$$T_{m,i}^{(cup)} = g_i \left(T_{m,1}^{(rod/gas)}, T_{m,2}^{(rod/gas)}, \dots, T_{m,n-1}^{(rod/gas)} \right) \quad (17)$$

where the functions g_i give the way in which $T_{m,i}^{(gas)}$ is linked with $T_{m,j}^{(rod/gas)}$ as well as, via gas leaking through the packing, with the mean temperatures $T_{m,j}^{(rod/gas)}$, $j=1\dots n-1$, $j \neq i$, of the rod regions in contact with the gas in all the other cups.

By means of the inverse z^{-1} the time duration each location x of the rod spends for instance in the compression chamber or in contact with the gas in the i -th cup can be determined. This knowledge and the temperature level the gas adopts at the instant of time when it is in contact with the location x are required for determining $T_m^{(gas)}(x)$. However, the temperature of the gas in the packing cups is not known in advance. Since a) the unknown values $T_{m,i}^{(cup)}$ enter the expression for $T_m^{(gas)}(x)$ in a linear manner and since b) (17) relates the values $T_{m,i}^{(cup)}$ in a linear manner to the Fourier coefficients $a_{0,i}$, there is also a linear relationship between $T_m^{(gas)}(x)$ and the spatial integrals $a_{0,i}$ over the rod temperature distribution. This is of importance for the structure of the resultant equation governing the rod temperature distribution.

2.6 Solution of resultant equation

Inserting all the expressions into (9) gives, after some rearrangement, a Fredholm integral equation of the second kind

$$T(x) = F(x) + \sum_{i=1}^n \int_{L_{PR,i}}^{L_{PR,i}+\delta} T(\xi) K_i(x,\xi) d\xi \quad (18)$$

with separable Kernel

$$K_i(x,\xi) = \sum_{j=1}^3 \alpha_{i,j}(x) \beta_{i,j}(\xi) .$$

For $n=1$, a solution to the integral equation can be obtained by inserting the ansatz⁴

$$T(x) = F(x) + \sum_{j=1}^3 B_j \alpha_j(x)$$

into (18) which gives a system of linear equations governing the coefficients B_j . This solution strategy can be generalized to an arbitrary number n of packing rings.

3 Experimental setup

A compressor was developed by HOERBIGER to provide a means for testing rings and packings under challenging real world conditions. This compressor, referred to as multi purpose test compressor (“MPTC”) for the sake of emphasizing the versatility of the genuine HOERBIGER design, is capable of compressing different gases at different speeds (up to 1500rpm) in two stages to pressure levels up to 400bar. The stroke of the machine is 88.9mm. In the development of the design special attention was paid to rendering a close up view into what is happening during operation of the compressor possible (cylinder pressure, packing leakage, pressure and temperature of gas in individual cups, packing housing temperature, heat removed by packing cooling system). Apart from these rather common measurements it has become possible to measure – to the author’s knowledge for the very first time ever – the distribution of the rod temperature during operation of the compressor. This major achievement is realized by means of a pyrometer specially suited for measuring metallic surfaces at comparatively low temperatures. The contactless rod temperature measurements are taken through two holes in the packing case (cf. Fig. 5) that are sealed by quartz glasses. The transmissivity of the latter is matched to the spectral range of the pyrometer. The very fast response time (down to 1.5ms for temperatures higher than 130°C) of the pyrometer allows to get a signal varying in time in the manner sketched in Fig. 4 that can be converted into a rod temperature distribution by means of the crankcase kinematics.

The shaded rectangular areas depicted in Fig. 5 extend over the regions of the rod that are accessible to temperature measurements.

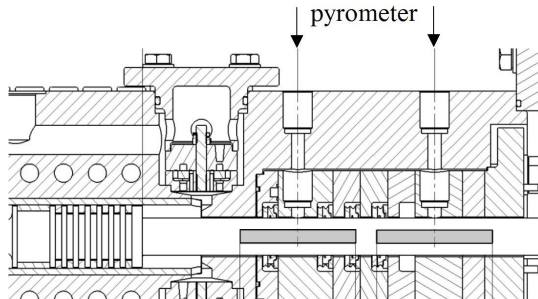


Figure 5: Configuration of pressure packing of 1st stage of MPTC

4 Comparison of theory with experimental data

The sealing characteristics of a common radial-tangential ring pair (made of a PTFE-PPS compound and equipped with an additional backup ring) was tested. This test was conducted at a speed of 700rpm (mean rod speed 2.1m/s) with air getting compressed from 50bar to 80bar. The rod, measuring 28mm in diameter, was sealed by four ring sets against ambient pressure.

In the contactless measurement of the rod's temperature, the emissivity of the rod surface plays a crucial role. Any transfer film covering the rod significantly affects the value of this emissivity. Hence it is advantageous to use data recorded shortly after starting the test for comparison purposes as no considerable transfer film formation can be expected to have taken place during the very first test phase. Besides, deviations of the rod roughness from its initially established value of $R_a=0.2\text{mm}$ are also not to be expected in these early test phases. Both facts ensure that the coefficient of sliding friction does not vary noticeably along the rod. It should be noted, however, that the present formulation of the problem allows for a straightforward incorporation of such an effect.

From measurements of both the cup pressure distribution and the leakage of the packing, the equivalent orifice areas of the individual packing ring sets can be inferred. These areas have to be provided as input data for the model. The coefficient of sliding friction remains then the only unknown parameter.

Fig. 6 shows that good agreement between the measured and calculated rod temperature distribution can be achieved for $\mu_{\text{fric}}=0.34$. This value, quite high due to no transfer film having established on the rod yet, also matches reasonably well with what is found on HOERBIGER's tribological test rigs.

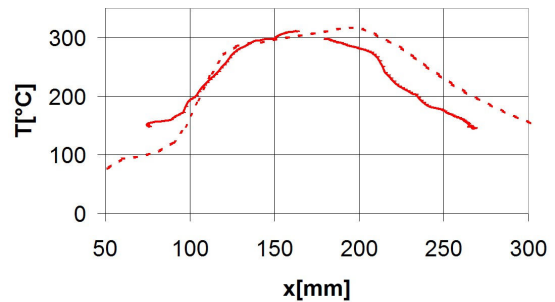


Figure 6: Comparison between measured (solid lines) and calculated (dotted line) rod temperature distribution (working medium air, $p_s=50\text{bar}$, $p_d=80\text{bar}$, $n=700\text{rpm}$, radial / tangential ring pair, $\mu_{\text{fric}}=0.34$)

A more stringent test of the model's accuracy can be realized by taking measurements of a different ring design made of the same material so that there remains no unknown adjustment parameter. To this end, tests of a new HOERBIGER ring design were also conducted. As can be seen in Fig. 7, the agreement between theory and experiment is this time even more impressive.

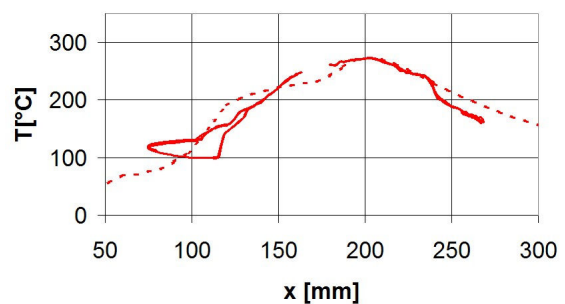


Figure 7: Comparison between measured (solid lines) and calculated (dotted line) rod temperature distribution (working medium air, $p_s=50\text{bar}$, $p_d=70\text{bar}$, $n=700\text{rpm}$, pressure balanced ring, $\mu_{\text{fric}}=0.34$)

It should be noted that the tests also validate the statement concerning the smallness of the rod temperature fluctuations. The solid lines depicted in Fig. 6 and Fig. 7 are conversions of time-dependent temperature signals recorded over several cycles into rod temperature distributions. Hence, if there were noticeable temperature fluctuations, i.e. if the rod temperature at a certain location were not the same during the suction and compression stroke, the conversion would not give a single line but a closed loop. The loop visible on the left side of Fig. 7 is not associated with such temperature fluctuations but with the automatic switch in the response time of the pyrometer when the temperature falls below or exceeds certain threshold values.

One might wonder why the peak rod temperature only goes down by about 30°C when switching from a radial-tangent ring set to a pressure-balanced design. This only moderate decrease is due to the difference in thickness b (with which the frictional heat generation rises in linear proportion, cf. (10)) between the pressure balanced ring design ($b=10.5\text{mm}$) and the radial-tangential ring set ($b=8\text{mm}$).

5 Conclusions

In this paper a mathematical model is presented that predicts the temperature the piston rod and the packing rings heat up to during non-lube operation. The model incorporates, amongst others,

- the effect of gas compressibility on the frictional heat generation,
- the unsteadiness of the heat transfer through the packing rings,
- a coupling between the rod temperature and the temperature of the gas in the individual packing cups so that the impact of the packing leakage on the rod temperature is accounted for,
- the variance of the convective heat transfer coefficient with several parameters (gas properties, geometry, speed, pressure,...),
- and the variations of the locations along the rod where frictional heat gets released.

Especially the last point is crucial for understanding the thermal problems occurring in short stroke applications.

When going to higher speeds and shorter strokes in such a manner that the mean rod speed remains constant, the overall amount of frictional heat generated also remains constant. The presented model agrees with observations in so far that it predicts a rise in the peak temperatures. Models⁵ that ignore the change in the locations along the rod where frictional heat gets released are not capable of distinguishing between applications having the same mean rod speed.

Remarkable agreement is found between theoretical predictions of the rod temperature distribution and measurements taken at HOERBIGER's MPTC. The model thus proves to be a powerful tool for understanding application limits and for improving the performance and reliability of present pressure packings.

6 Acknowledgements

Special thanks go to Andreas Dittmann, Alexander Edelbacher, and Martin Lagler for assisting in taking the measurements on the MPTC and to Peter Steinrueck for initiating and funding this fundamental research.

7 References

- ¹ Dittmann, A.; Spiegl B.; Steinrück, P.: "Fundamental Research on Tribology of PTFE Wear Parts Opens Windows of Opportunity for Improved Materials". 4th EFRC conference (2005), 75-82.
- ² Kragelski, I.V.; Dobycin, M.N.; Kombatov, V.S.: "Grundlagen der Berechnung von Reibung und Verschleiß". VEB Verlag Technik Berlin (1982).
- ³ Radcliffe, C.D.: "A New Design of Non-Cooled Pressure Packing for Improved Life and Reliability". 2nd EFRC conference (2001), 1-9.
- ⁴ Grosche, G.; Ziegler, V.; Ziegler, D.; Zeidler, E.: Teubner-Taschenbuch der Mathematik. Teil II, B.G. Teubner Stuttgart Leipzig (1995).
- ⁵ Heinrichs, K.; Strümke, M.: "Berechnung der Gleitflächentemperatur in trockenlaufenden Kolbenstangendichtungen". Wiss. Z. Techn. Hochsch. Magdeburg 28 (1984), Heft 4, 86-89.

Dry-running sealing systems in practice – new challenges by new materials

by:

**Dr. Norbert Feistel
Research and Development
Burckhardt Compression AG
CH-8404 Winterthur
Switzerland**

norbert.feistel@burckhardtcompression.com

**5th Conference of the EFRC
March 21-23, 2007
Prague, Czech Republic**

Abstract:

Advances in the tribology of dry-running friction pairs as well as the design of sealing elements and systems have greatly improved performance compared with earlier types of dry-running sealing systems made of plastic. Amid the euphoria over this positive development, however, it is often overlooked that many old recommendations on the handling of dry-running systems remain valid and that some of the new materials have peculiarities which need to be accounted for. A certain level of expertise in design and maintenance of modern dry-running sealing systems is needed to fully exploit their potential and maximize their life cycles. Even high-grade materials can soon fail in an absence of the conditions necessary for stable operation, as the examples provided further below clearly demonstrate.

1 Introduction

Around the year 1910, mention was first made of a use of graphite as a sealing material in steam turbines¹. This was followed by continual improvements in the after-treatment and impregnation of graphite as a solid lubricant. Discovered in 1938, however, the material PTFE went on to dominate dry-running applications in reciprocating compressors. By the end of the 1970s, a multitude of filled PTFE materials were in existence, but without having achieved any significant increases in service life or load parameters. Such improvements were not realized until the mid-1980s, when polymer blends and modified high-temperature polymers were introduced.

Compared with earlier types of dry-running sealing systems made of plastic, advances in the tribology of dry-running friction pairs as well as the design of sealing elements and systems have greatly improved performance. Unfortunately, this positive development has been attended by a misinterpretation of dry-running technology as an easily operable and maintainable alternative to oil lubrication. There is a tendency to disregard that many old recommendations on the handling of dry-running systems remain valid and that some of the new materials have features requiring special attention.

Since friction and wear are system properties, tribological optimization must address general system design instead of focusing exclusively on the basic or counter body. The numerous interactions between dry-running friction partners and the broad spectrum of gases being compressed pose special challenges here. A certain level of expertise in design and maintenance is needed to fully exploit the potential of modern dry-running systems and maximize their life cycles. Even high-grade materials can quickly malfunction in an absence of the conditions necessary for stable operation. In such cases, the wrong conclusions are often drawn and the dry-running material simply replaced. It must be noted here that modern dry-running materials like polymer blends and high-temperature polymers are three to five times more expensive than common, filled PTFE.

2 Different approaches to dry-running materials

The dry-running capabilities of sealing and rider rings are attributable to solid lubricants present as

matrix material or filler in one of the friction partners. Solid lubricants here include compounds with layer lattices (e.g. graphite, molybdenum disulphide), soft metal compounds without layer lattices (oxides, fluorides etc.) and organic compounds (e.g. polytetrafluorethylene). Nearly all dry-running reciprocating compressors today employ plastic sealing elements with differing contents of polytetrafluorethylene (PTFE), a plastic material from the group of fluoropolymers.

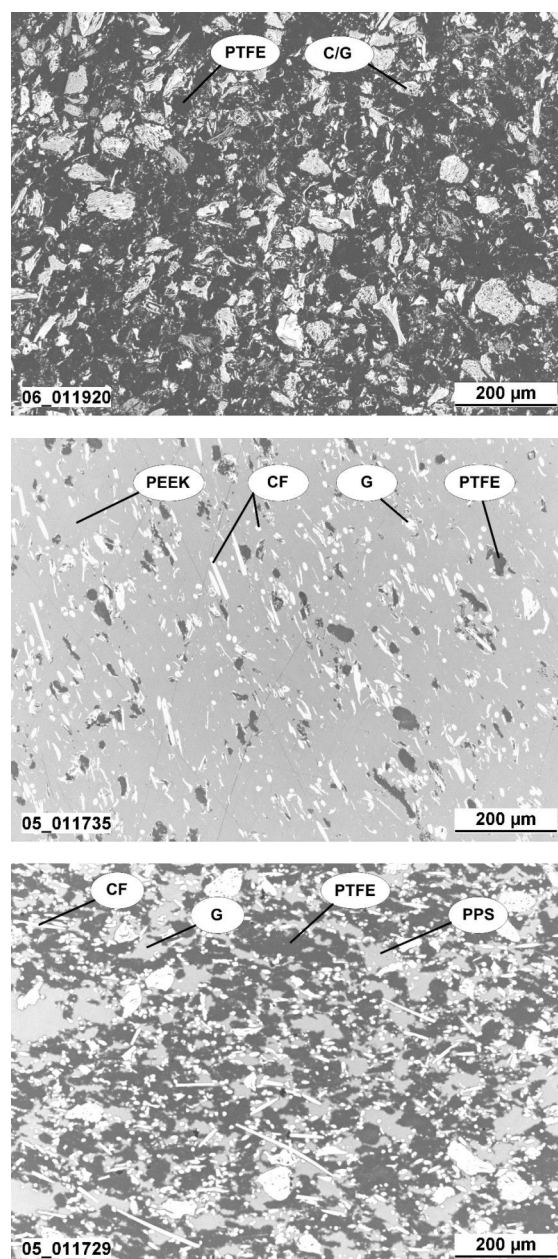


Figure 1: Micrographs of various dry-running materials: PTFE filled with carbon/graphite (top), modified PEEK (centre), PTFE-PPS polymer blend (bottom) on a scale of 100:1

Though pure PTFE is an excellent solid lubricant, its low mechanical strength and its high susceptibility to creep makes it quite unsuitable for use as a sealing or guiding system in reciprocating compressors. A typical method of offsetting these disadvantages for practical applications is to mix the PTFE with inorganic fillers like carbon, graphite, glass fibre, copper, bronze, ceramics or molybdenum disulphide making up a total proportion of 25 - 35 % by weight. PTFE serves as the matrix in this original group of dry-running materials, termed filled PTFE materials in the following. A typical member of this group, PTFE filled with carbon/graphite, is shown in Figure 1 [top].

Modified high-temperature polymers are a completely different type of dry-running material. Not defined precisely as yet, this material group includes thermoplastics and duroplastics with high temperature strength. The sealing and rider rings in a reciprocating compressor are made of materials such as polyetheretherketone (PEEK), polyphenylsulfide (PPS), polyimide (PI), polyamidimide (PAI) and epoxy resin (EP). In their pure form, these plastics are not suitable as dry-running materials and hence need to be "modified" through an addition of solid lubricant, preferably PTFE, but also carbon/graphite, molybdenum disulphide etc. The proportion of PTFE here is usually 10 - 15 % by weight. Figure 1 [centre] shows a modified PEEK filled with carbon fibre, PTFE and graphite.

Over recent years, polymer blends have also been used increasingly in the manufacture of dry-running sealing and guiding elements. Polymer blends can generally be considered as alloys of different polymers whose characteristics exceed those of their original constituents. Dry-running sealing and rider rings for reciprocating compressors usually comprise a PTFE matrix containing inorganic fillers and an additional plastic to a proportion of 15 - 35 % by weight. Plastics commonly employed here are PEEK, PI, PPS and, of late, PPSO2 (polyphenylsulfone). Figure 1 [bottom] shows a PTFE-PPS blend filled with carbon fibre and graphite.

Manufacturers are cautious about disclosing details concerning their polymer blends' compositions, mixture ratios and, in particular, production parameters. In an absence of clear distinctions or definitions with respect to the category of filled PTFE materials (the values mentioned above serve purely as standard measures), many manufacturers simply include blends into the said category.

However, the blends are distinctive in terms of certain special properties and their much higher price. Polymer blends' enormous potential becomes most evident in combination with dry gases, as demonstrated plainly by bench tests on hydrogen (dew point of about -65 °C) with dry-running packings each comprising six sealing elements (suction pressure = 1.4 MPa, final pressure = 4 MPa, $C_m = 3.4$ m/s). Figure 2 shows the average wear rates of sealing systems comprising PTFE-PPS blends compared with PTFE filled with carbon/graphite after 500 hours of operation. Although the wearing properties of polymer blends differ widely by manufacturer, even the "poorest" quality exhibits just half the wear rate of the PTFE filled with carbon/graphite.

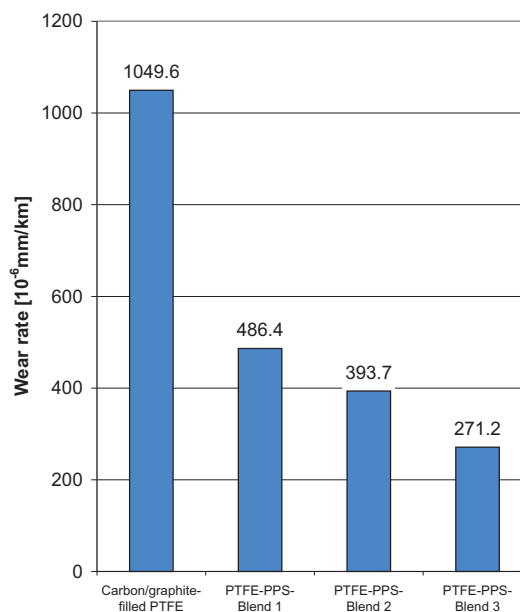


Figure 2: Wear rates exhibited in dry hydrogen by various PTFE-PPS polymer blends in comparison with PTFE filled with carbon/graphite

3 Mechanical properties

The low mechanical strength and high creep sensitivity of filled PTFE materials are caused by the PTFE matrix despite the effect of the fillers. In the course of the years, these material-specific features have been accounted for by a use of relatively large cross-sections and – wherever necessary – tension and anti-extrusion rings. Due to their extreme toughness, however, filled PTFE rings are not vulnerable to breakage during installation and thus easy to handle.

Today, modified high-temperature polymers are normally used for applications involving high pressure differences and/or temperatures. Some high-temperature polymers have a remarkable load capacity. For instance, modified PEEK (10 % PTFE, 10 % graphite and 10 % carbon fibre by weight) at a temperature of 250 °C has a tensile strength of 18 MPa, higher still compared with filled PTFE (35 % carbon and graphite powder by weight) whose tensile strength at room temperature is 10 MPa².

However, the high modulus of elasticity and low toughness of many high-temperature polymers prove disadvantageous during assembly of sealing elements, loading under dynamic pressure differences and wear compensation. In a bending test conducted according to DIN 53 452 at room temperature, the PEEK material described above exhibited an elasticity modulus of 3856 MPa and a breaking elongation of just 3.4 %. By comparison, PTFE filled with carbon/graphite exhibited an elasticity modulus of 1285 MPa and a breaking elongation of 16.4 %². Due to the considerable differences in material characteristics, one-piece piston rings made of modified PEEK should therefore not be dimensioned wholesale with the cross-sections commonly used with filled PTFE. This must be noted especially when post-converting sealing elements made of high-temperature polymers.

A conflict of aims arises from the small piston diameters typically involved in compression stages loaded with high pressure differences. Simple assembly and uniform contact with the cylinder wall entail small cross-sections which, however, reduce the permissible load capacity and radial wear (i.e. short life cycle). Consequently, very small piston diameters can necessitate a transition to a built-up piston (very elaborate) or the use of two-piece piston rings (lower sealing efficiency). Especially the dry-running compression of light gases such as hydrogen to high pressures thus requires expert knowledge of the relationships between sealing element design and material properties³.

Polymer blends' properties are influenced particularly by the proportion of the additional plastic and the production parameters. The strength of such blends usually lies closer to that of filled PTFE materials than high-temperature polymers. However, the additional plastic lowers PTFE's toughness, so that polymer blends with a high proportion of this plastic can become quite brittle. Some PTFE-PPS types at room temperature have a breakage elongation of 2 % - 3 % which is lower

yet than the above-mentioned value for modified PEEK. If PTFE piston rings are to be replaced by ones made of polymer blend in order to lengthen service life, their low breakage elongation must therefore be considered. For the piston ring displayed in Figure 3 with an outer diameter of 160 mm, a radial thickness of 12.5 mm and an axial height of 8 mm, an FEM analysis⁵ yielded a maximum elastic elongation of 2.5 % during fitting on the piston. Although filled PTFE rings pose no problems here, polymer blends are susceptible to failure by fracture at room temperature.

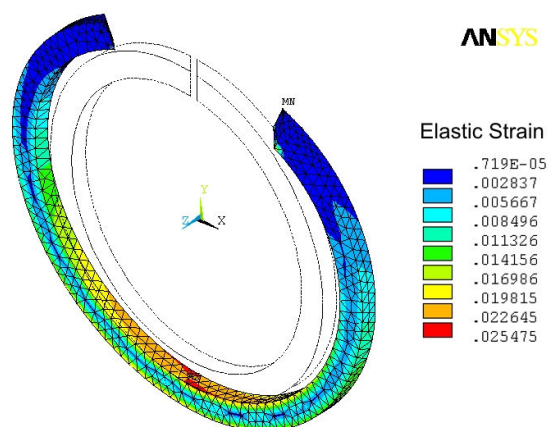


Figure 3: Elastic elongation of a piston ring during fitting on the piston - FEM calculation

4 Resistance to chemicals

Among the plastic materials, especially fluoropolymers are extremely resistant to chemicals. PTFE sealing elements withstand nearly all chemicals ranging from common solvents to strong acids and bases. PTFE sealing elements with a BAM certificate can even be installed in oxygen compressors. PTFE is also approved for direct contact with foodstuffs. It is only from a temperature of 330 °C that fluorine-based gases are released (inhalation causes nausea and fever).

Much greater attention needs to be paid to the chemical resistance of high-temperature polymers and polymer blends. Polymer blends' chemical resistance is influenced decisively by the additional plastic. PTFE-PPS types undergo a non-critical reaction with hydrogen, occasionally emitting a distinct odour of hydrogen sulphide after extended operation during bench tests. Even PEEK which is notably more resistant to chemicals than many other plastics imposes several restrictions in direct comparison with PTFE.

For instance, PEEK is not suitable for use in oxygen compressors, nor is it resistant to certain acids and inorganic reagents.

Although PEEK has been tested against a long list of chemicals under a variety of conditions, this list by no means covers all possible substances inside a process-gas compressor. Sealing elements made of modified PEEK have been known to occasionally pose problems, especially in polyolefine applications. Figure 4 shows fibre-filled PEEK after a few hours of operation in a propylene compressor.

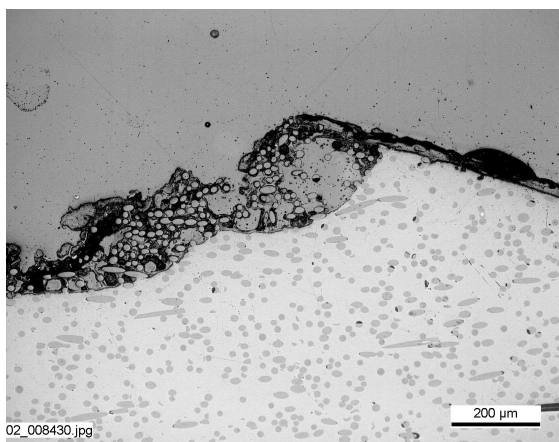


Figure 4: Chemical changes in the surface of fibre-filled PEEK

Laboratory investigations⁴ revealed matrix damage and depletion at the surface. Furthermore, an elementary analysis of the damaged ring zones uncovered a large number of inorganic components absent in the original material. In view of an especially high concentration of aluminium, the cause of the damage was assumed to be triethylaluminium (TEA) used as a catalyst in polymerization processes. Such problems can usually be solved through use of a different dry-running material. However, it becomes clear that materials other than standard, filled PTFE intended for use in process-gas compressors require critical examination in terms of chemical resistance.

5 Significance of the transfer film to dry-running

It is frequently assumed that the initial, plastic-to-metal frictional contact between a dry-running sealing or rider ring and its counter body is converted through formation of a transfer film into plastic-to-plastic contact which ultimately ensures a low and stable wear rate for dry-running applications.

However, the friction and wear characteristics of dry-running applications are influenced decisively by intensive interactions taking place between the friction partners. Investigations by Vetter and Tomschi^{6,7} showed that tribo-chemical reactions of the basic and/or counter body with components of the intermediate material or ambient medium result in material conversion during wear, thus frequently determining its extent and nature. In the case of suitable dry-running pairs, original plastic-to-metal contact is hence replaced after a sufficiently long running-in period by a combination of a boundary layer on either side.

Care is taken during the design phase to achieve favourable conditions for transfer film formation by providing a suitable roughness on the counter-body surface. Since the introduction of filled PTFE in dry-running applications, maintaining a minimum roughness of the hard counter body proved to be advantageous over an extremely smooth surface. Various friction theories explain the suitability of rough texture by pointing out the growing influence of the adhesive component of friction as roughness decreases, which, on some materials, overcompensates the loss in deformative and abrasive resistance. Though pure PTFE paired with a smooth steel surface only exhibits a low degree of adhesion, it is still more significant as the polymer cohesion which makes possible a transfer of material. The multitude of filled PTFE materials used in dry-running applications must also be considered in terms of their filling and reinforcement substances which, compared with pure PTFE, can notably alter running-in characteristics, particularly with regard to the tribo-chemical processes mentioned earlier. If the equally large number of counter-body materials is taken into account too, the impracticality of a universal, optimal roughness range soon becomes obvious. Recommendations by various manufacturers of sealing elements cover a range of approximately 0.1 µm - 0.6 µm Ra.

In a crosshead compressor, particularly the dry-running piston-rod sealing system can be sensitive to inadequate roughness. Heat dissipation in this zone is limited compared with the cylinder region. The increase in friction power resulting from a negative change in friction characteristics here can lead to a sharp rise in temperature and, consequently, wear rate.

This encourages a high rate of material transfer to the piston rod, correspondingly impairing heat dissipation from the friction surfaces and potentially resulting in damage to individual sealing elements or even complete thermal failure of the dry-running sealing system (Figure 5).



Figure 5: Plastic deformation and damage to a packing ring caused by high temperatures resulting from inadequate piston-rod roughness

In the case of polymer blends and high-temperature polymers, the effect of the additional or other plastic on running-in characteristics must be noted besides the influence of inorganic fillers. These materials, too, can be susceptible to inadequate roughness. Figure 6 shows piston-rod temperatures measured during the running-in period by an infrared sensor for two different roughness values. At a roughness of $0.11 \mu\text{m Ra}$, the PTFE-PPS blend selected here reproducibly exhibits a higher temperature curve than at a roughness of $0.20 \mu\text{m Ra}$. That this behaviour is not simply attributable to a presence of PPS was demonstrated by tests on a different manufacturer's PTFE-PPS blend which - despite a similar composition - permitted thermally stable operation at low temperatures with a roughness of $0.11 \mu\text{m Ra}$. Accordingly, influential parameters here include not only the number, type and mixture ratio of the fillers, but also PPS type, particle size and production parameters. This clearly reveals that transfer film formation essential for proper functionality of dry-running pairs is even more complex in the case of polymer blends and high-temperature polymers, and that the desired wear characteristics might not be achievable given incorrect implementation.

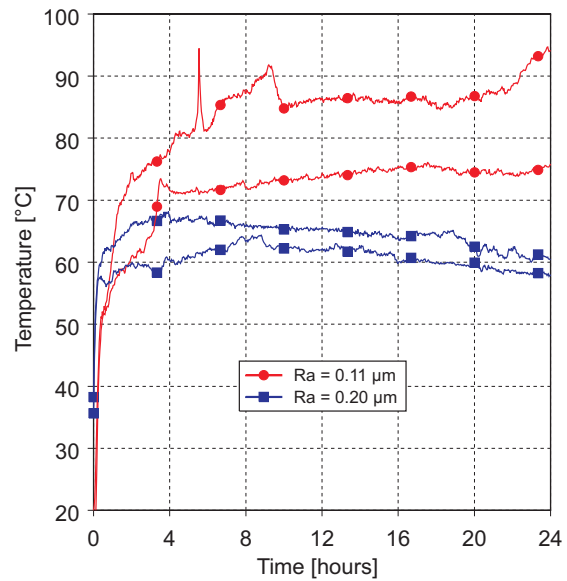


Figure 6: Piston-rod temperatures measured at different roughness values by an infrared sensor during the running-in period of dry-running packings

Though an increase in surface roughness improves the thermal conditions with many dry-running materials, it also increases the abrasion of the soft friction partner, so that a compromise is needed to avoid unnecessarily high wear during the running-in period. A properly designed surface roughness keeps the degree of wear during the running-in period within moderate limits; the roughness peaks abraded and wear particles deposited in this process give rise to a friction surface which is very smooth but not covered entirely with transfer film (Figure 12, phases 0-2).

6 Phenomena during commissioning

The friction values of dry-running friction pairs remain notably higher than those of oil-lubricated systems, even if polymer blends and high-temperature polymers are employed. Their favourable wear characteristics do not necessarily imply a low coefficient of friction, so that high temperatures can occur especially during a commissioning of new dry-running friction pairs. However, it must be noted that friction pairs often exhibit a lot of scattering during the running-in period, so that even slight changes in initial condition can have a major impact later⁸.

6.1 Mechanical test run

During the mechanical test run of a new dry-running compressor, the sealing systems are operated under apparently favourable conditions without being subjected to loads by pressure differences. Dry-running sealing and guiding systems can nevertheless pose thermal problems in this situation. In particular, an absence of gas leakages in the case of piston-rod sealing systems notably impairs convective heat transfer from the piston rod to the packing cups. This can sharply raise temperatures to a point where the sealing elements begin to suffer thermal damage. In severe cases, piston-rod temperatures of more than 200 °C were measured after a four-hour test run.

The friction power arising during operation without compression is attributable to the garter springs or tension rings of the packing rings. These components are meant to ensure that the sealing elements maintain contact with the piston rod despite progressive wear. As tests with differently pre-stressed packing rings have shown, however, spring designs generating unnecessarily high forces in the sealing elements' new state should be avoided wherever necessary. If a critical force is exceeded at a given, average piston velocity, the piston rod's temperature rises sharply, making it necessary to stop the test. The two maximum values shown in Figure 7, therefore, indicate the temperatures on termination of the tests conducted. Below the relevant critical force, the piston rod's temperature under the given test conditions stabilizes to a maximum value of 140 °C after about two hours. The specified piston-rod temperatures are average values obtained with a hand-held measuring device during two measurements conducted near the packing flange at the piston's outer and inner dead centres immediately on completion of each test.

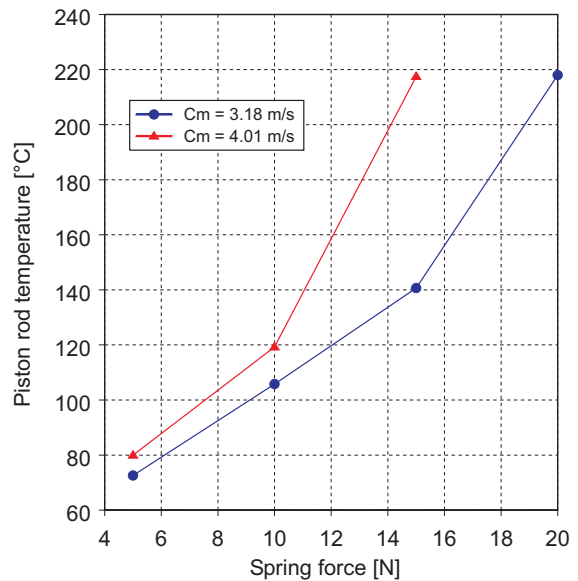


Figure 7: Piston-rod temperatures during the mechanical test run with various garter spring forces and average piston velocities C_m

Besides the packings, the rider rings of horizontal compressors can pose thermal problems during the mechanical test run. In the absence of hot compressed gas, the rider rings are heated solely by the friction power at the contact surface. In combination with the plastic materials' poor heat conductivity, this potentially results in an uneven load-bearing profile with a segment angle of less than 120 degrees used as a design basis, thus increasing surface pressure and correspondingly raising temperatures. In extreme cases, the high temperatures may even cause a blue discoloration of the cylinder wall. During regular operations involving compression, however, the rider rings achieve a much more favourable load-bearing characteristic.

6.2 Commissioning of new friction pairs

High temperatures can occur temporarily also during the commissioning of new sealing systems with compression. Figure 8 shows piston-rod temperatures measured by means of an infrared sensor during commissioning of new packings consisting of PTFE-PPS polymer blend. These are average temperature values along the piston stroke. Comprising six sealing elements each, the two packings differ in terms of the sealing and cover rings' axial width of 4 mm and 7 mm respectively. Evidently, the temperatures in the initial phase of operation are notably higher but subside by up to 40 °C after 1 - 2 days.

This temperature rise can also be observed on the sealing elements with a narrow axial width of 4 mm, although their temperature in the stationary state is notably lower than that of the 7-mm variant. In addition to formation of the transfer film, frequently a transition to a more favourable pressure distribution within the sealing system takes place during the running-in period, which also positively influences the temperature.

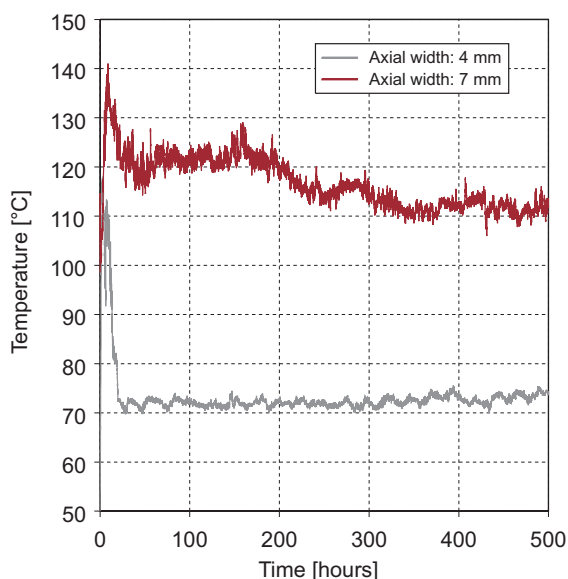


Figure 8: Piston-rod temperatures measured during the running-in period of new polymer blend packings with an axial segment width of 4 and 7 mm ($P_s = 1.4 \text{ MPa}$, $P_d = 4 \text{ MPa}$, $C_m = 3.4 \text{ m/s}$)

7 Inspection and maintenance of friction surfaces

The running-in period is completed once a dynamic equilibrium dependent on the load parameters has been attained between the friction pair's boundary layers. This state of equilibrium is characterized by constant friction, constant average friction heat and constant wear rate. Dry-running sealing and rider rings operated under such conditions at a stable and low wear rate often exhibit a smooth, shiny surface on visual inspection (Figure 9 [centre]).

A rise in the load parameters of a given tribological system increases the wear rate in the state of equilibrium and consequently shortens service life. Load parameters exceeding a tribological system's limit usually result in changes to the main wear mechanisms.

Such systems do not attain a steady state, and rapid failure of the sealing elements ensues. Unfavourable tribological conditions during operation are often manifested in the form of matt, furrowed surfaces of sealing and rider rings on their removal (Figure 9 [bottom]). However, laboratory analyses are needed to define the wear characteristics more precisely.

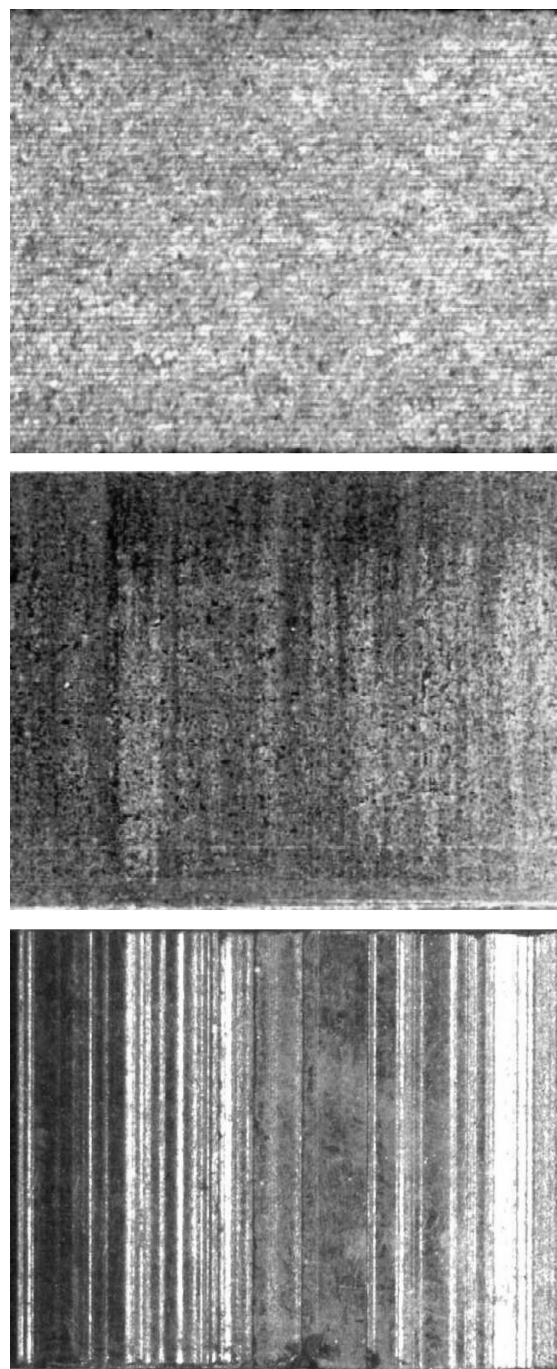


Figure 9: Various friction surfaces of dry-running piston rings: New state (top); operation at low wear (centre) and under unfavourable tribological conditions (bottom)

Of great significance to an evaluation of dry-running conditions is the friction surface of the counter body coated with transfer film. From the macroscopic point of view, favourable wear conditions are often characterized by a not completely closed transfer film (Figure 10 [bottom]). This transfer film's appearance can vary from one friction pair to another. In a hydrogen compressor equipped with a nitrided-steel piston rod, for instance, favourable wear conditions lead to a dark-grey transfer film for PTFE filled with carbon/graphite. PTFE-PPS polymer blends can exhibit light-grey, brown and rust-coloured transfer films, while a light-grey transfer film is often observed in the case of modified PEEK.

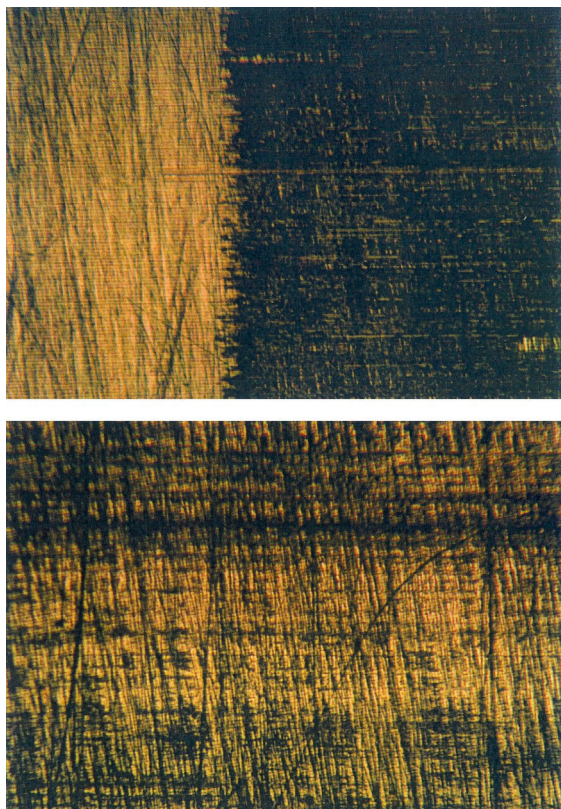


Figure 10: Normal (bottom) and undesirable (top) transfer film for PTFE filled with carbon/graphite on a nitrided-steel piston rod (125:1)



Figure 11: Damage to rider rings resulting from high temperatures during dry-running under unfavourable tribological conditions

A closed, deep-black transfer film (Figure 10 [top]) or a complete absence of transfer film on the friction surfaces indicates unfavourable tribological conditions. Wear characteristics can be impaired by unsuitable friction pairs, excessively high load parameters (pressure, velocity, temperature), inadequate cooling and undesirable intermediate substances such as infiltrating lubricating oil. An increase in friction power caused by deteriorating tribological conditions can also lead to a notable temperature rise in the cylinder. This can have particularly negative consequences for rider rings made of polymer blend, these often being characterized by a combination of low ductility and a large dimension as well as a high coefficient of thermal expansion in the axial direction. Additional temperature stress can damage such rider rings despite careful design based on the compression temperatures (Figure 11).

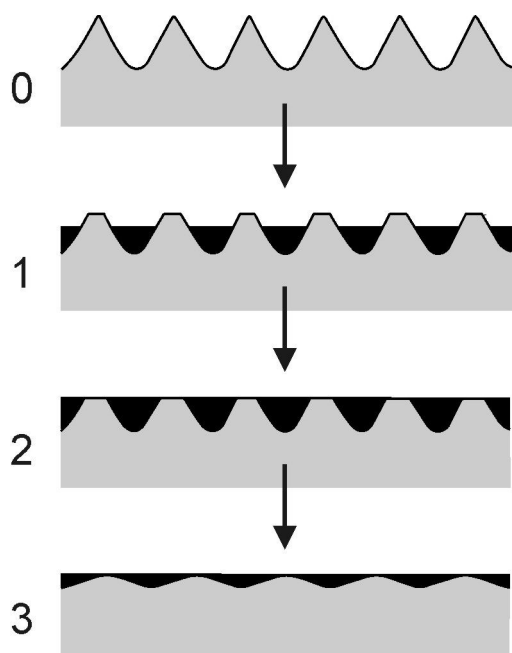


Figure 12: Schematic representation of the various phases of transfer film formation

Even if initial indications of life cycle are favourable, tribological conditions for dry-running can deteriorate in the course of operations – this sometimes taking several years – and ultimately shorten the life cycle to a point where dry-running is no longer possible (Figure 12, phase 3). The real cause of the problem is often not immediately identifiable. Because operation at high compression temperatures and cooling problems lead to similar signs of damage, the wrong conclusions are occasionally drawn here. Such unfavourable tribological conditions can arise, for instance, through a combination of soft counter-body materials and abrasive fillers. Of a gradual nature, these processes eventually hinder the formation and maintenance of a stable transfer film. Especially abrasive materials include glass fibre and ceramics among filled PTFE materials, and carbon fibre among modern polymer blends and high-temperature polymers⁹. Depending on the type involved, the abrasiveness in the latter group is notably lower than that of glass fibre but nevertheless significant especially in combination with PEEK. It must also be noted that the abrasive effect of fillers in applications involving a reciprocating compressor lasts for several years, not just a few hours or days as in the case of most laboratory tests¹⁰. The life cycle of dry-running friction pairs is threatened, in particular, by a counter body of a low hardness such as austenitic cast iron (Ni-Resist) in combination with abrasive, filled plastic. A minimum hardness of 220 HB is needed here.

Especially with high load parameters, however, counter-body materials should have notably higher hardness values between 900 and 1400 HV in order to ensure stable dry-running for as long as possible.

Unfavourable tribological conditions are also created by gas contaminations which can severely impair the functionality of dry-running systems. Although some dry-running materials are offered for operation with gas contaminations, negative consequences can still be expected. Depending on particle size and hardness, impurities in the gas have a range of effects on the sealing and rider rings as well as the counter bodies. Given a constant ingress of hard particles – e.g. aluminium oxide – with a size exceeding 10 µm, even nitrided steel with a hardness of over 900 HV can quickly wear down. Hard particles of a smaller size have a seemingly harmless polishing effect on the counter body, often manifested in the form of a mirror-finish surface without any recognizable transfer film. Under such conditions, life cycles of just 4000 to 6000 hours are achieved in practice despite a use of high-grade polymer-blend sealing and rider rings, while similar applications without gas contaminations easily provide 16,000 hours of operation. Though counter-body surfaces can be protected by appropriate, rather expensive coatings, there is no effective measure for protecting sealing or rider rings. Instead of implementing elaborate protective measures inside the compressor, it is advisable to minimize the ingress of gas contaminations here.

The decisive role played by transfer film in ensuring favourable friction and wear characteristics makes it clear that, despite all the progress made in the area of dry-running materials, the friction surfaces of dry-running sealing and rider rings still require care and attention in order to consistently achieve target life cycles. Due to a present lack of quantitative measurement for evaluating transfer film, however, reliance on experience is necessary. By no means practical is a general overhaul of all friction surfaces as part of every service. In principle, however, transfer films should be removed on a change of dry-running material, and an appropriate roughness should be set for the new material. Bench tests have shown that negligence here can lead to major thermal problems particularly during replacement of filled PTFE or polymer blend with modified PEEK and vice versa.

8 Summary

Modern dry-running materials such as high-temperature polymers and polymer blends provide a basis for notably improving the performance of oil-free reciprocating compressors. However, the differences between the mechanical properties of these materials and conventional, filled PTFE must be considered when designing and handling sealing and rider rings in order to preclude failure by fracture and malfunctions during installation and subsequent operation. In terms of chemical resistance, too, the new materials have posed problems previously not known during operations with filled PTFE.

The transfer-film formation phase of importance to dry-running has also been made more complex by high-temperature polymers and polymer blends. The usually expensive, high-performance materials respond to deviations from ideal conditions with higher temperatures and shorter life cycles. High temperatures may occur especially during commissioning of new sealing systems. This must be considered already during the mechanical test run which, due to operation without compression, gives rise to unfavourable heat transfer conditions especially for the packings.

Even if high-performance materials are employed, conditions necessary for stable dry-running can gradually deteriorate in the course of operations and ultimately shorten the life cycle to a point where dry-running is no longer possible. This can be caused especially by a combination of soft counterbody materials and abrasive fillers or gas contaminations. Despite a use of high-grade polymer blend here, a shortening of target life cycles by roughly one-third has been observed in practice.

Of great significance to an evaluation of dry-running conditions is the friction surface of the counter body coated with transfer film. Due to a present lack of quantitative measurement for evaluating transfer film, however, reliance on experience is necessary. For this reason, the design and maintenance of high-performance dry-running systems should be left to experts.

Notation

PTFE	Polytetrafluorethylene
PEEK	Polyetheretherketone
PPS	Polyphenylsulfide
CF	Carbon fibre
C	Carbon powder
G	Graphite powder
Ps	Suction pressure
Pd	Discharge pressure
Cm	Average piston velocity

References

- ¹ Hüttner, W.:
Tribologische Eigenschaften und Anwendungsgebiete von Carbonwerkstoffen (TriboCeram) Frankfurt, 1989, Schriftenreihe »Praxisforum« 12/89, S. 227 - 262
- ² Ritter, U.:
Physikalisch-mechanische Werkstoffuntersuchungen an Kolbenringmaterial Unveröffentlichter Bericht von Sulzer Innotec, Winterthur, 1994
- ³ Feistel, N.:
Influence of piston-ring design on the capacity of a dry-running hydrogen compressor 3rd EFRC-Conference, Vienna, Austria, 2003, S. 141 – 149
- ⁴ Dörner, G.:
Worn glassfibre reinforced PEEK sealing ring of a polypropylen compressor Unveröffentlichter Bericht von Sulzer Innotec, Winterthur, 2002
- ⁵ Retz, N.:
Untersuchungen zur Montage von Kunststoff-Kolbenringen mittels FEM Unveröffentlichter Bericht von Burckhardt Compression AG, Winterthur, 2006
- ⁶ Vetter, G.; Tomschi, U.:
Zur Tribologie der Trockenlaufdichtungen von Hubkolbenverdichtern Pumpen + Kompressoren 1, 1995, S. 66 – 78
- ⁷ Tomschi, U.:
Verschleißverhalten von Trockenlaufwerkstoffen für Abdichtelemente in Kolbenkompressoren Dissertation Universität Erlangen-Nürnberg, 1995

- ⁸ Uetz, H.; Wiedemeyer, J.:
Tribologie der Polymere
München/Wien: Carl Hanser Verlag 1985
- ⁹ Flöck, J.; Friedrich, K.; Yuan, Q.:
On the friction and wear behaviour of PAN- and
pitch-carbon fiber reinforced PEEK composites
Wear, 225-229, 1999, 304 - 311
- ¹⁰ Klein, P.; Zhang, Z., Friedrich, K; Theiler, G.;
Hübner, W.:
Zur Bildung von Transferfilmen bei ausgewählten
PTFE-Compunds
Tribologie+Schmierungstechnik, 4/2003 S. 32-36



Evaluation of the Coefficients used for simulation for Cylinder Valves for Reciprocating Compressors

by:

M.Schiavone, F.Manfrone, E.Giacomelli

Dott.Ing.Mario COZZANI S.r.l.

Arcola (SP)

Italy

info@cozzani.com

**5th Conference of the EFRC
March 21-23, 2007
Prague, Czech Republic**

Abstract:

As valves represent the most critical component of the reciprocating compressor, they need particular care in designing. For these reasons during the initial design stage valve simulation and related reciprocating compressors simulation are necessary and carried out today with advanced mathematical models. In order to have a simulation closer to the real operation, the mathematical models, simple stage or multistage, have to incorporate some coefficients.

The work presented in this paper concerns the determination of the flow coefficient. The work shows the influence of some intrinsic and extrinsic valve features on said coefficient. This paper studies also the flow coefficient in very high pressure valves. These analyses have been carried out by CFD calculation methods and experimental tests.

1 Introduction

The automatic valve has always been considered one of the most critical component of the reciprocating compressor. The valve features strongly influence the reliability and efficiency of the whole machine. As well as the valve influences the compressor, in the same way the compressor influences the valve. Such correlation requires a very deep cooperation between compressor and valve manufacturers starting from the very beginning of designing.

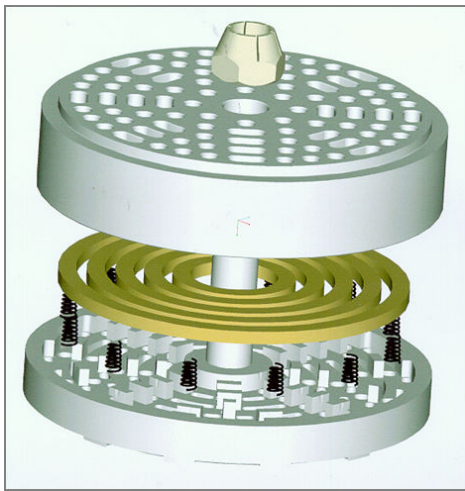


Figure 1: automatic valve with concentric rings

Like every critical compressor component, the valve is object of continuous evolutions and researches. In this context of optimisation, consequence of hardware and software systems evolution, the developments and improvements of calculation methods play a very important role. Simulating in very short time the real valve and compressor behaviour is essential to optimise the product by limiting at the minimum the experimental activities.

2 Simulation program

A mathematical model simulating the cylinder valve behaviour is based on two differential equations: the first describes the gas flow through the valve, the second describes the plate movement law.

Software and program languages, like Matlab Simulink, are able to solve such systems of equations in a simultaneous way.

Figures 2 and 3 show the scheme of a dynamic simulator realized and developed by Cozzani.

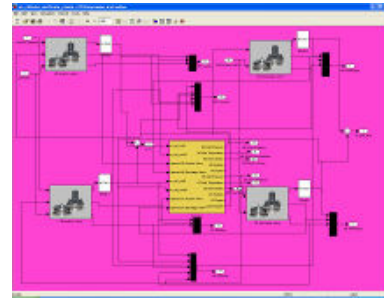


Figure 2: Cozzani's dynamic mono-stage simulator

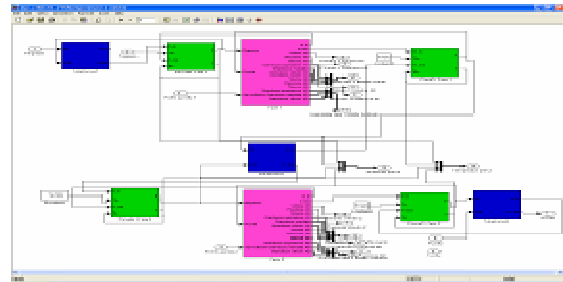


Figure 3: Cozzani's dynamic multistage simulator

As input data we can mention the geometrical features of the compressor (stroke, cylinder diameters, clearance, speed, number of valves, etc), the working conditions (gas, pressures, temperatures, etc), the valves features (lift, sections, spring load and preload, flow coeff., etc).

As output data we can find the shutter movement, the impact speed of the shutter, the power consumption, the eigenfrequency of the valve, the capacity, the PV cycle, etc.

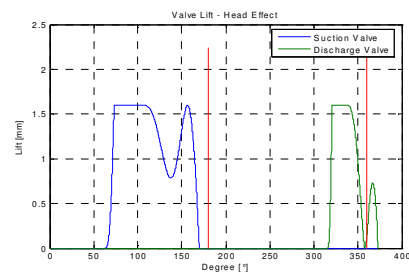


Figure 4: Suction and discharge shutter movements

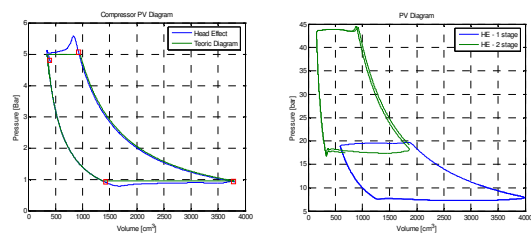


Figure 5: PV cycle for mono-stage and two-stage compressors

The software validation has to be carried out by comparison with experimental tests, according to our ISO 9001 certification, see figure 6.

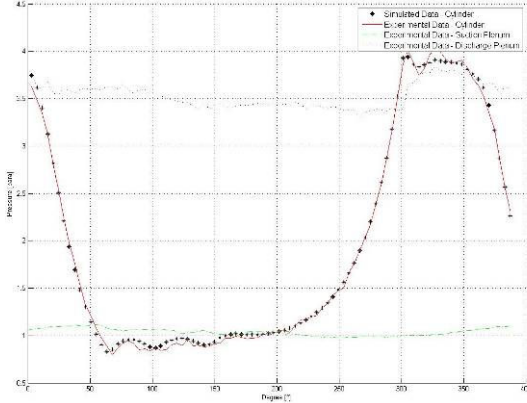


Figure 6: Comparison between Cozzani simulation and experimental data

3 Valve coefficients

The input data have to include different coefficients, the main ones are: drag, flow, sticking and restitution.

The work presented in this paper concerns the determination of the flow coefficient, but we report here below the definition of them all.

3.1 Drag coefficient C_d

The drag coefficient is a dimensionless quantity that describes a characteristic amount of aerodynamic drag of the shutter caused by fluid. This coefficient depends on the shutter shape.

3.2 Sticking coefficient C_s

This coefficient depends on the sticking effect of the shutter on the guard. The sticking, due to the presence of oil in the cylinder, causes a delay in the valve closing.

The delay time is defined as the time that the shutter, subject to a given force, takes to unstick from the guard.

$$\tau_{delay} = C_{ST1} \cdot e^{-C_{ST2} \cdot F}$$

This coefficient mainly depends on the oil viscosity.

It is obvious that through simulations it is possible to eliminate this delay selecting the right springs.

3.3 Restitution coefficient C_R

The restitution coefficient is defined as the ratio between the velocity after and before the shutter impact. The value goes from zero (anelastic impact) to one (elastic impact). This coefficient mainly depends on the shape and material of the shutter.

3.4 Flow coefficient K_s

The Flow coefficient is defined as the ratio between the effective passage area and the geometric one. It depends on the intrinsic valve features (channels geometry, shutter shape, etc.) and on the external valve ones (gas, velocity, etc). The formula used for gas is:

$$K_s = \frac{\dot{M}_{in}}{A_r P_1 \sqrt{\left[\left(\frac{P_2}{P_1} \right)^{2/k} - \left(\frac{P_2}{P_1} \right)^{(k+1)/k} \right] \frac{2k}{R \cdot (k-1) \cdot T_1}}}$$

\dot{M}_{in} is the mass capacity at inlet, A_r the minimum passage area inside the valve, T_1 the inlet temperature and P_1 e P_2 are the inlet and outlet pressures.

4 Determination of K_s

In order to evaluate the effective influence that the intrinsic and extrinsic parameters have on K_s , a series of CFD analysis have been done on different types of valves. In this presentation we can just show you our analysis on flat shutter valves and on special valves for very high pressure. We define a valve type all the valves characterized by the same channel dimension, same number of channel (depending on the size), and same shutter shape. These analysis have been done using advanced software: PRO-ENGINEER to do the models, GAMBIT as preprocessor and FLUENT 6.2.16 as solver. The theoretical results have been done compared with values obtained by experimental tests carried out in University Laboratories.

4.1 Ks in flat shutter valves

The parameters chosen for the study are listed in table 1 and shown in figure 7

D [mm]	Size
C [mm]	Channel dimension
α [mm]	Channel inclination
L [mm]	Lift
$\Gamma (=2\beta/\pi)$	Seat and guard ribs
N° di Reynolds Re	Inlet speed
MW [kg/kmol]	Molecular weight

Table 1: Parameters

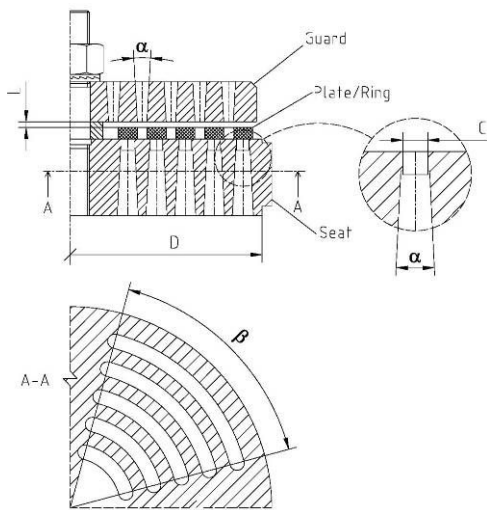


Figure 7: Geometrical valve parameters

2D axial symmetric simulations have been done to quickly evaluate the influence of some parameters (size, channel dimension, channel inclination, lift, inlet speed, molecular weight) on Ks.

Obviously a valve is a 3D component, having ribs that interfere with the flow and consequently influence the pressure drop. In order to evaluate the importance of ribs and to do a comparison between theoretical and experimental data 3D simulations has been done.

4.1.1 Theoretical analyses

In order to simplify the present lecture, it has been considered only valve having flat shutters. Figure 8 shows the 2-D model, where D is the pipe diameter that defines the valve size, the lengths H_1 and H_2 are the pipe length, upstream and downstream the valve, dimensioned to allow a full development of the flow streams.

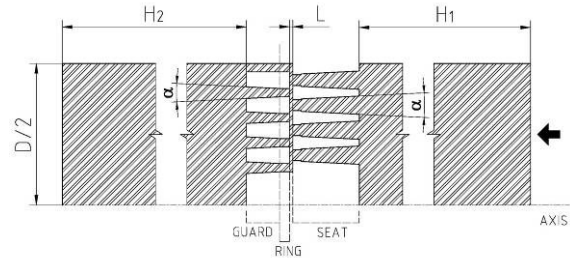


Figure 8: 2D model of a ring valve

Figure 9 shows the mesh used. It is formed by quadrangular cells suitably intensified around the critical area.

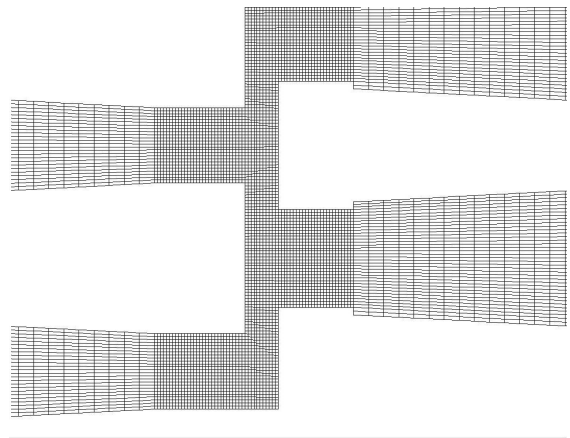


Figure 9: Mesh 2D

Once the boundary conditions have been defined, as the internal valve flow is turbulent, we chose a first order k- ϵ RNG solver. Figure 10 shows the velocity distribution inside the valve, while fig. 11 the pressure distribution. These figures help to understand the most critical valve points.

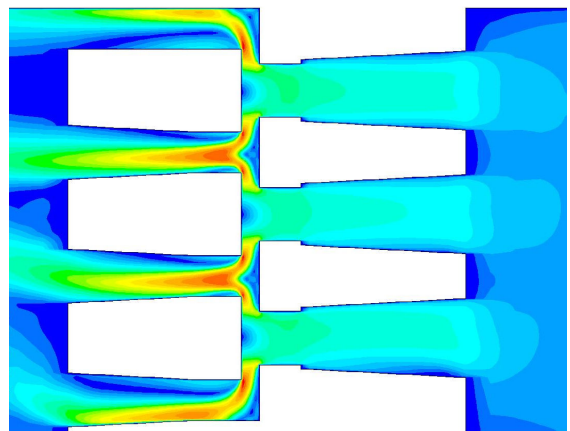


Figure 10: CFD 2D velocity distribution

VALVES

Evaluation of the Coefficients used for Simulation for Cylinder Valves for Reciprocating Compressors

Fabione Manfrone, Massimo Schiavone, Enzo Giacomilli; COZZANI

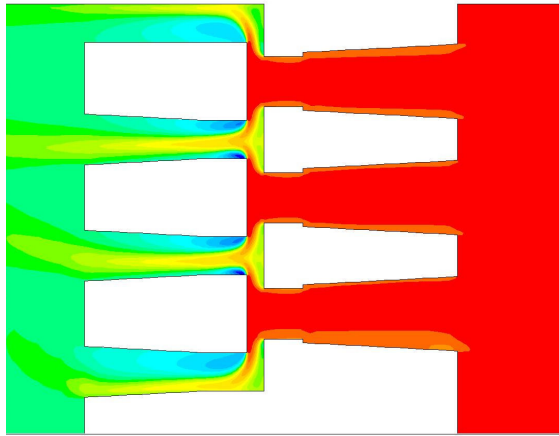


Figure 11: CFD 2D total pressure distribution

The figures below show CFD simulation results.

Figure 12 shows the relationship between K_s and molecular weight at three different lifts ($L1 < L2 < L3$). Three different gases (H_2 , air, CO_2) have been analysed. The results are:

- at fixed lift, K_s does not change with the molecular weight
- K_s decreases when the lift increases.

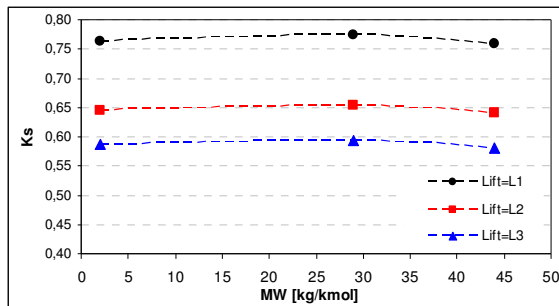


Figure 12: K_s vs. molecular weight

Figure 13 shows the relationship between K_s and the Reynolds number at three different lifts ($L1 < L2 < L3$). In the range analysed, the result is:

- at fixed lift, K_s does not change with the Re .

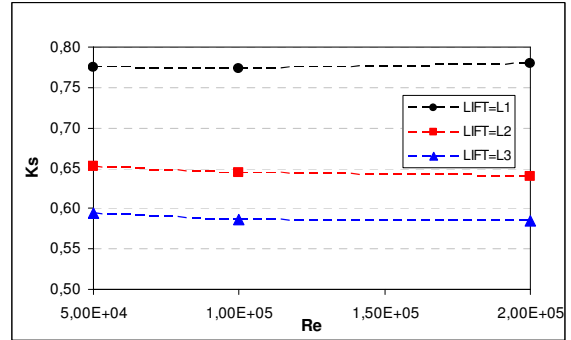


Figure 13: K_s vs. Re

Figure 14 shows the relationship between K_s and the channel inclinations at three different lifts ($L1 < L2 < L3$). The result is:

- at fixed lift, K_s does not change with the channel inclinations.

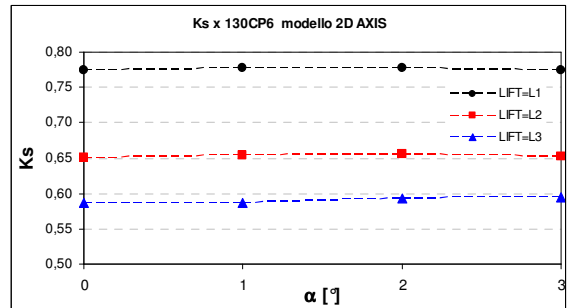


Figure 14: K_s vs. channel inclinations

Figure 15 shows the relationship between K_s and valve size at three different lifts ($L1 < L2 < L3$). The result is:

- at fixed lift, K_s is almost constant with the valve size.

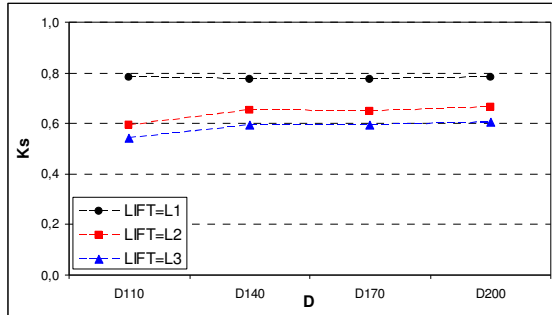


Figure 15: K_s vs. valve size

Figure 16 shows the relationship between K_s and channel dimension at three different lifts. The result is:

- at fixed lift, K_s increases when the channel dimension increases ($C1 < C2 < C3$)

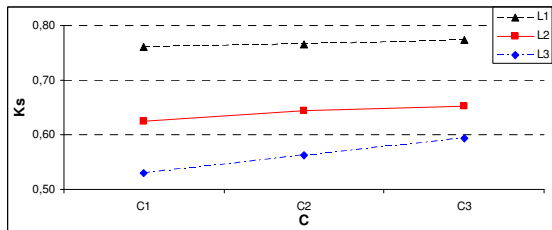


Figure 16: K_s vs. channel dimension

As it has been told before, the 2-D model cannot evaluate the seat and guard ribs influence on the K_s . For this reason 3D models have been used for the CFD simulations.

Figure 17 shows the mesh of the 3D model. The number of cells used for a 3D model is over two million versus the one hundred thousand cells used in a 2D model.

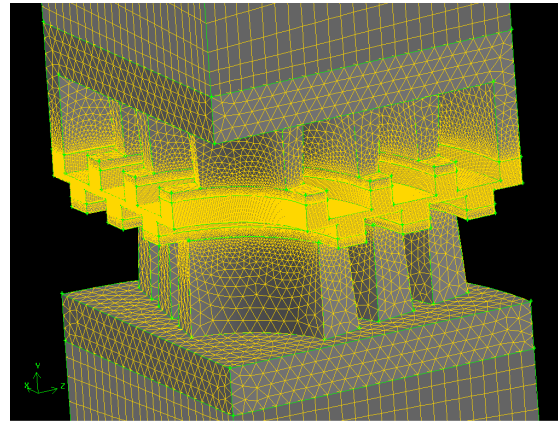


Figure 16: Mesh 3D

Figure 17 shows the velocity distribution inside the valve, while fig. 18 the total pressure distribution.

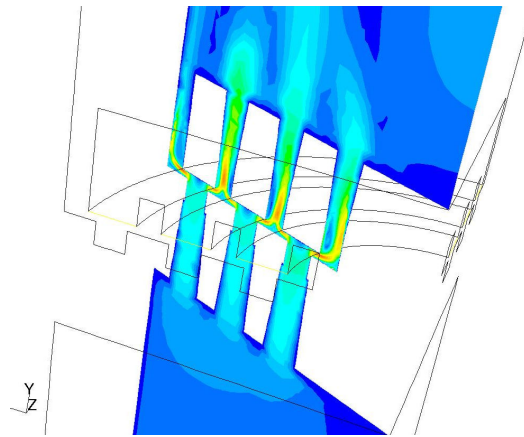


Figure 17: CFD 3D velocity distribution

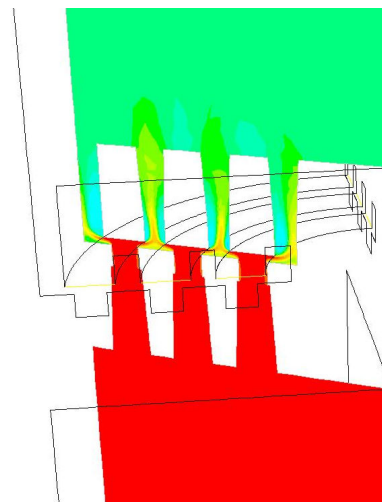


Figure 18: CFD 3D total pressure distribution

Figure 19 shows the relationship between K_s and the rib angle at three different lifts. The result is:

- at fixed lift, K_s decreases when the rib angle increases.

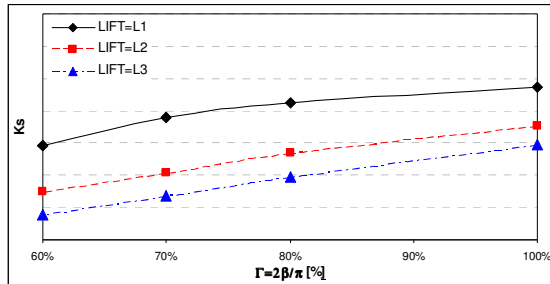


Figure 19: K_s vs. rib angle

The study proceeded on another valve type characterized by different channels number, channels dimensions, and shutter shape.

TYPE 2 has channels higher in number and smaller in dimension than TYPE 1. Moreover the shutter of TYPE 2 is a plate instead of rings.

Figure 20 shows the comparison between the two different studied types, 1 and 2. The result is

- K_s changes with the type. Type characterized by smaller channels has a lower K_s , even if the effective area increases.

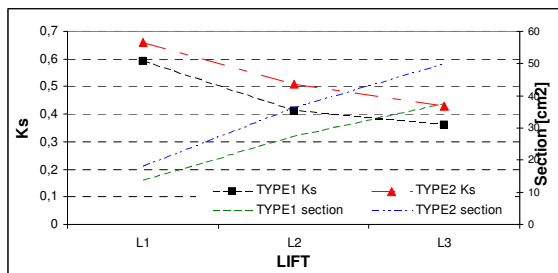


Figure 20: K_s vs. valve type

4.1.2 Experimental test and comparison with simulation.

Figure 21 and 22 show the air test plant used to take capacity measurements.

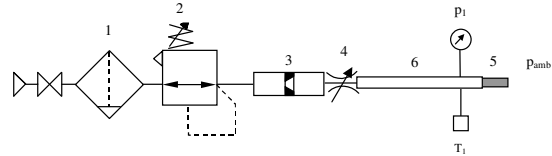


Figure 21: Test plant Scheme



Figure 22: Air test plant

The test plant, equipped with proper instrumentation for data acquisition, is arranged with flanges to house the valves. The tests have been done by feeding the valve with constant downstream pressure, equal to the environment pressure, and by applying different fixed upstream pressures, using a control valve.

Different valve types, varying size and lift, have been tested. Consequently, it has been possible to draw the curves of pressure loss versus flow.

The data have been processed to allow the comparison with the theoretical analysis.

Figure 23 shows the experimental results of the K_s with the Reynolds number, confirming the trend of figure 12.

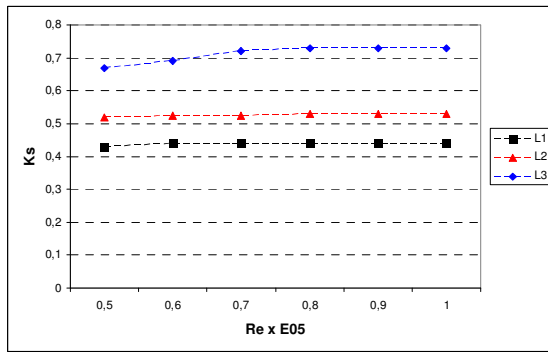


Figure 23: experimental curve Ks-Re

Figures 24 and 25 show the results on the previously studied types: the TYPE 1 with large channels and the TYPE 2 with small and narrow channels.

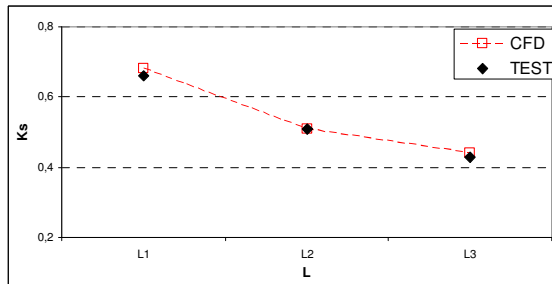


Figure 24: Ks comparison between theoretical and experimental data on TYPE 1

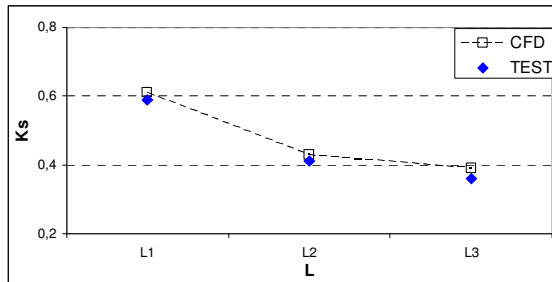


Figure 25: Ks comparison between theoretical and experimental data on TYPE 2

These analyses confirm that Ks changes with the lift and every valve type is characterized by its own Ks curves.

It is confirmed that some valve parameters, such as inlet velocity, molecular weight, channels inclination, and valve size, have a negligible influence on Ks. On the contrary, other parameters, such as lift, channels dimension and ribs, have a heavier influence on flow coefficient.

The statement that Ks depends only on the lift is too restrictive, a more realistic result is reached considering the relationship between Ks and the seat and guard ribs.

4.2 Ks in very high pressure valve

The second part of this study has been done on a monopopet valve. The goal is to evaluate the influence of valve geometrical parameters on the Ks in a condition of very high pressure, (till 300Mpa), and heavy molecular weight.

Considering the gas condition, as the density is very high, the experimental and theoretical analysis have been done using water as fluid.

For the incompressible fluid Ks has to be calculated by the following formula:

$$K_s = \frac{\dot{M}_{in}}{A_r \sqrt{2g\Delta P}}$$

The following valve geometry has been designed only for theoretical study on Ks, and it has no other purpose.

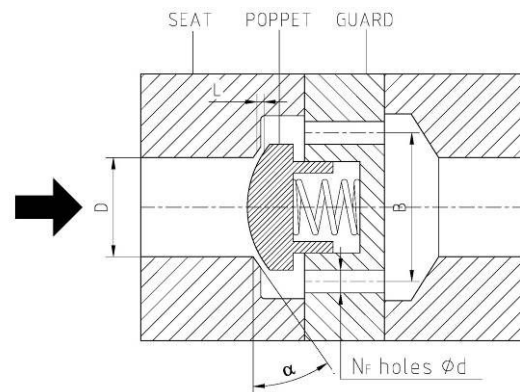


Figure 26: Test valve drawing

Figure 26 shows the parameters used for the analysis (D, α, L, N_F e d).

4.2.1 CFD Analysis

The theoretical analysis have been done using the same technique previously used on the flat shutter valves: CFD-2D axial symmetric to evaluate rapidly the influence of some parameters on Ks, and CFD-3D to evaluate other parameters and to compare theoretical and experimental results.

In order to use an axial symmetrical 2D model, the guard holes have been modelled as a circular crown (wideness equal to “s”) having the same passage area of the said holes (see figure 27).

VALVES

Evaluation of the Coefficients used for Simulation for Cylinder Valves for Reciprocating Compressors

Fabione Manfrone, Massimo Schiavone, Enzo Giacomilli; COZZANI

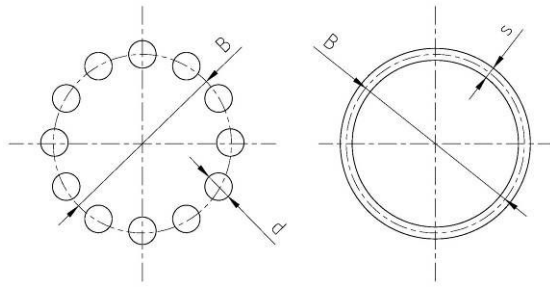


Figure 27: Guard simplification from holes (left) to circular crown (right)

Figure 28 shows a 2D axial symmetrical model, meshed through triangular cells, appropriately intensified around the critical area.

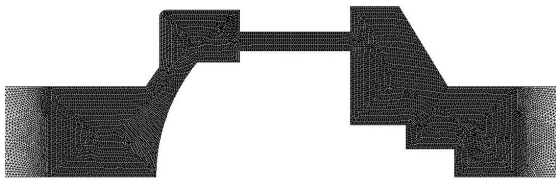


Figure 28: 2D asymmetrical Meshed

It has been chosen a first order segregated k-ε RNG solver. Figure 29 shows the velocity distribution and figure 30 the total pressure distribution.

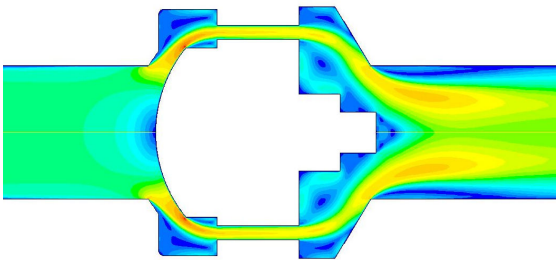


Figure 29: Velocity distribution

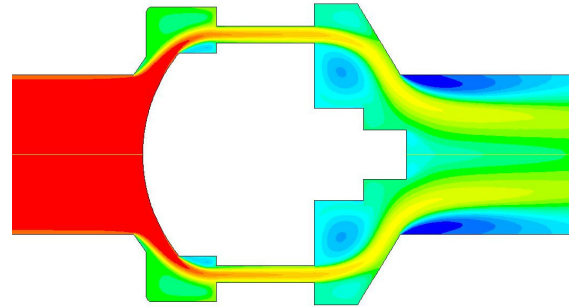


Figure 30: Total pressure distribution

Figure 31 shows the relationship between K_s and lift ($L_4 < L_5 < L_6$) at three different values of the inlet diameter (D).

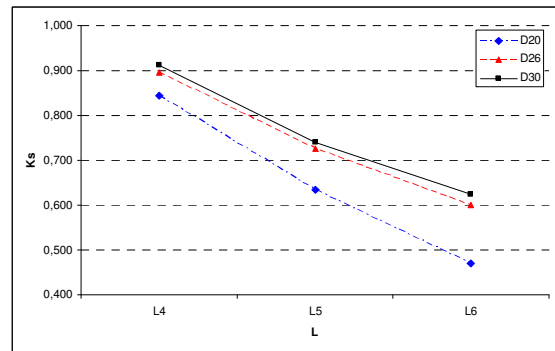


Figure 31: K_s vs. lift and inlet diameter

Figure 32 shows the relationship between K_s and lift ($L_4 < L_5 < L_6$) at three different values of the crown wideness ($S_1 < S_2 < S_3$).

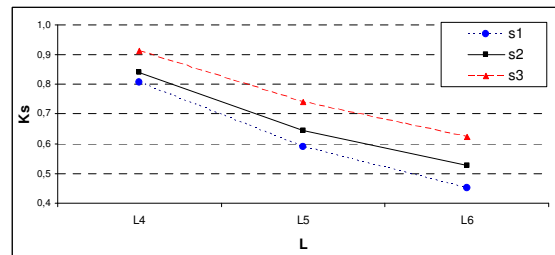


Figure 32: K_s relationship between lift and crown wideness

3D simulation have been done to verify the 2D simplification and to compare theoretical and experimental results.

Figure 33 shows a 3D model meshed through tetrahedral cells (1127641 cells).

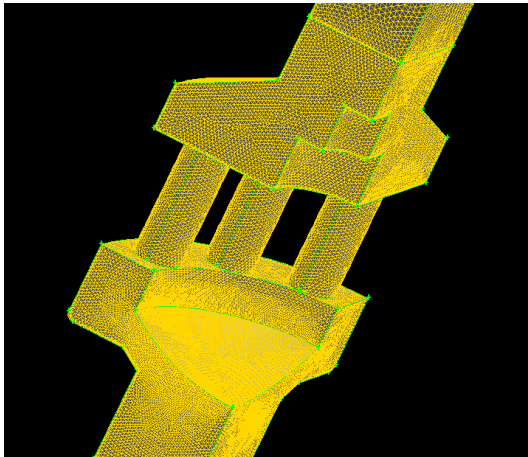


Figure 33: 3D Mesh

Figure 34 shows velocity path lines inside the valve.

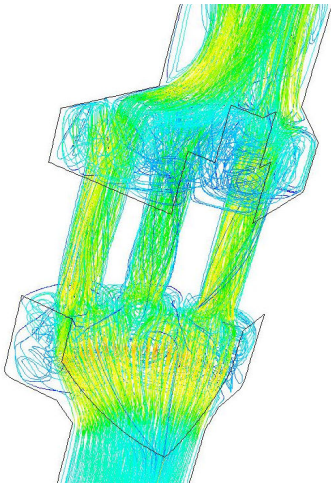


Figure 34: Velocity path lines

Figure 35 shows the discordance between 2D and 3D analysis, due to the simplification done. The result is that we can use 2D models to determine the influence of some parameters, but we can not use them to find the real value of the K_s .

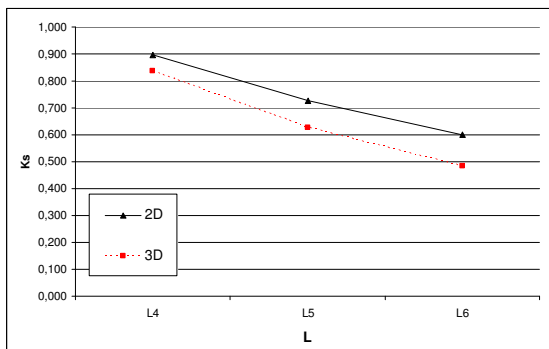


Figure 35: Comparison between 2D and 3D

4.2.2 Experimental test and comparison with the simulation.

Figure 36 shows the water test plant used to take capacity measurements.

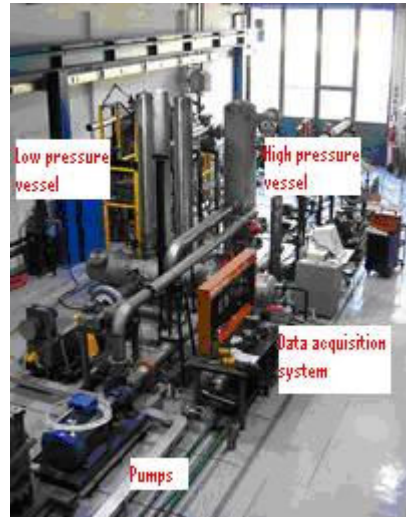


Figure 36: Water test plant

The plant is composed by two pumps (the first one acted by an asynchronous motor and the second one by a direct current motor), two tanks, temperature and pressure sensors, flow meter, and data acquisition system with dedicated software.

The tests have been done by feeding the valve with different values of flow rate and by applying a constant downstream pressure. Of course the flow rate values used are the same of the ones used in theoretical analysis.



Figure 37: Valve under test

Different valves, characterized by different lifts, have been tested. For every test the curves of flow and pressure have been drawn, see figure 38.

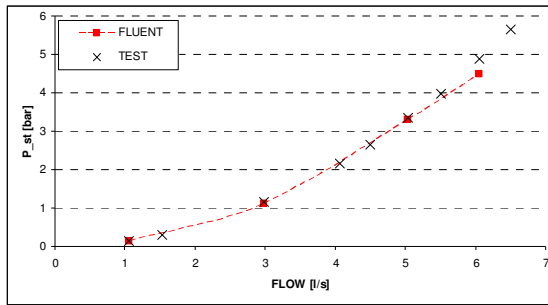


Figure 38: Pressure vs. flow

The data have been processed to obtain the relationship between K_s with the flow. Figure 39 shows the comparison between theoretical and experimental results.

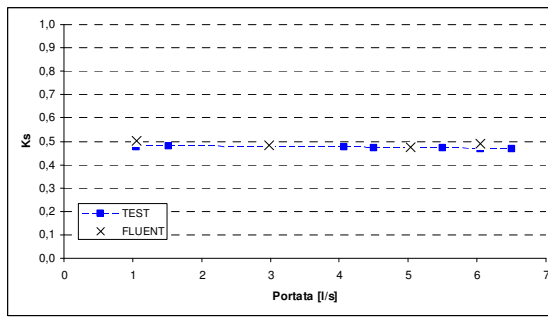


Figure 39: K_s vs. flow: comparison between theoretical and experimental results

Also for this second part of the study, as the first one, we can confirm the high utility of advanced software to calculate the K_s .

It was found that some valve parameters, such as lift, inlet channel dimension, and guard ribs, have a heavy influence on flow coefficient.

The experimental test made using water as fluid gave a very good correspondence with the theoretical simulations.

5 Conclusions

Valve optimisation is obtained thanks to the calculation techniques improvement, possibility offered by continuous hardware e software systems evolution.

Cozzani valves are designed by using a self developed valve simulation program that allows to optimise the compressor and valves performance. The correspondence of the theoretical results to the reality is based on the knowledge of the coefficients defined in chapter 3.

The work presented in this paper shows the utility of CFD simulations to determinate the flow coefficient. Using the 2D and 3D simulations in a matched way it is possible to find the influence of valve parameters on said coefficient.

2D axial symmetrical models are very useful for a sensibility study, while the 3D one to evaluate the influence of the ribs and to do a comparison between theoretical and experimental data.

It was found that some valve parameters, such as inlet velocity, molecular weight, channels inclination, and valve size, have a negligible influence on K_s . On the contrary, other parameters, such as lift, channels dimension and ribs, have a heavier influence on flow coefficient.

The results are valid for very high pressure valve too.

The results had been validated through a series of experimental test carried out in University Laboratories.

References

- ¹ API Standard 618 "Reciprocating Compressors for Petroleum, Chemical and Gas Industry Services", 4th Edition, June 1995
- ² Shapiro," The Dynamic and Thermodynamics of Compressible Fluid Flow", Wiley 1953
- ³ Fluent User's Guide 6.1
- ⁴ O. Acton, C. Caputo, "Macchine a fluido", Collana UTET.
- ⁵ A. Bianchi, M. Schiavone, "New profile for Thermoplastic Shutter of Compressor valve", 2EFRC-Conference 20001 Den Haag.
- ⁶ Warsi, Z.U.A. "Fluid Dynamics and Computational Approaches" CRC Press, 1993.



Semi-Active Compressor Valve Development and Testing

by:

Brun, Klaus
Mechanical and Fluids Engineering
Southwest Research Institute®
San Antonio, Texas
United States
klaus.brun@swri.org

Platt, John P.
BP Company
Houston, Texas
United States
plattjp2@bp.com

Gernentz, Ryan S.
Mechanical and Fluids Engineering
Southwest Research Institute®
San Antonio, Texas
United States
ryan.gernentz@swri.org

Smolik, Mitchel A.
Mechanical and Fluids Engineering
Southwest Research Institute®
San Antonio, Texas
United States
mitchel.smolik@swri.org

5th Conference of the EFRC
March 21-23, 2007
Prague, Czech Republic

Abstract:

A novel semi-active reciprocating compressor valve was designed, fabricated, and tested to address performance limits of current technology compressor valves. This valve's concept is based on a conventional plate valve design but replaces the valve springs with an electromagnetic coil that senses position and provides an opposing force prior to the plate's impact (i.e., although actively controlling the motion of the plate, this valve does not require pressure sensors or shaft encoders for control). By reducing the valve plate's opening and closing impact velocities, one can effectively design an infinite fatigue life plate valve. Two semi-active valve models were developed, built, and tested: a benchscale model and a prototype model. Both valves were mounted in a 250 HP reciprocating compressor and tested over a wide range of operating conditions. The benchscale semi-active valve tests demonstrated the feasibility of the concept, while the subsequent prototype tests provided endurance and performance optimization.

1 Introduction

The operation of a reciprocating compressor is closely linked to the performance of its valves, in terms of both life and efficiency. These compressors have traditionally used passive valves to control the suction and discharge flow process of the compressor cylinder. However, valve failures are generally cited as the most common cause of scheduled and unscheduled compressor outages, and the single largest maintenance cost items on reciprocating compressors are valve replacements and repairs. With the emergence of larger machines operating over wider speed and pressure ratio ranges over the last 15-20 years, this trend has worsened. Consequently, the industry has to consider improvements in valve technologies to be able to compete with alternative compression technologies.

To address these needs, the Gas Machinery Research Council, BP Exploration & Production Company, and the Department of Energy funded a multi-faceted program to develop advanced reciprocating compressor valve technologies¹. One promising technology that was identified early on in the program was a semi-active compressor valve (SAV). This technology, which is described in detail in this paper, has the potential to improve both valve life and efficiency, while minimizing the failure risk that has traditionally been associated with the usage of fully active compressor valves. The conceptual development, design, fabrication, and testing of the prototype semi-active valve are described in this paper.

1.1 Background

The life of a conventional reciprocating compressor valve is typically one to six months for many pipeline applications and shorter for many upstream and process applications. Valve failures can be divided into two major categories: Environmental and Mechanical. Environmental causes are principally due to corrosive contaminants, foreign material, debris, liquid slugs, or improper lubrication. These environmental failures can usually be prevented by the proper choice of valve material and conditioning of the gas stream (filtration, separation, etc.).

On the other hand, mechanical causes are the result of high cycle fatigue and abnormal mechanical motion of the valve, caused by high valve lift, valve operation at off-design conditions, valve flutter, pulsations, and/or spring failure. Some of these can be controlled by careful analysis and design of valve components (i.e., guard, seat, sealing element(s), springs, and damper plates) for fixed compressor operating points. However, mechanical valve failures are generally more difficult to control as they are principally related to valve internal mechanical behavior and material limitations—especially for the compressor operator, who has limited access to design and materials data of the valves. Also, valves are designed for a single optimal operation point; hence, valve operation is impaired and life is often reduced when the operating conditions deviate significantly from the design point.

In the traditional compressor valve design, an increase in valve life (reliability) directly relates to a decrease in valve efficiency. This relationship is due to an increase in valve lift (and flow-through area) being limited by the corresponding increase in the valve impact force. As impact velocities increase due to higher valve lift or valve operation at off-design conditions, the velocities cause excessive impact stresses and an accelerated material damage/fatigue rate to the valve. Also, above a certain impact velocity, valve plate failure is attributable to plastic deformation of the valve springs. These springs consequently fail to provide adequate damping for the plate. Clearly, reducing impact velocity can greatly increase the life of a valve plate and springs. Thus, a lack of durability and low efficiency of the current technology passive valve designs demonstrates the need to control valve motion.

1.2 Semi-Active Valve Concept

To address this need, SwRI[®] engineers have developed a new valve concept that provides electromagnetic damping and creates a soft landing at both the valve seat on closing and at the valve guard on opening. The concept is to utilize a conventional plate valve design but to replace or augment the valve springs with an electromagnetic coil that senses position and provides an opposing force prior to the plate's impact.

This concept is referred to as a “semi-active electromagnetic plate valve” because it is still passively activated by gas forces and only actively controlled prior to impact (i.e., although actively controlling the motion of the plate, this valve does not require pressure sensors or shaft encoders for control). Furthermore, should any of the control mechanisms fail, this valve assembly will continue to act as a passive valve.

Figure 1 shows the first conceptual schematic and iteration at this type of design: The valve consists of a plate valve with a single or multiple moving shafts (connected to the plate) that are effectively the motion element within an electromagnet. The basic functional principle behind the valve is that control is only needed at certain times in the valve’s plate motion cycle: just prior to the opening and closing impacts of the plate. The pressure forces (just like in a conventional valve) start the opening movement; however, once in motion, the electromagnets sense a current and then actively control the valve motion to limit the impact velocity.

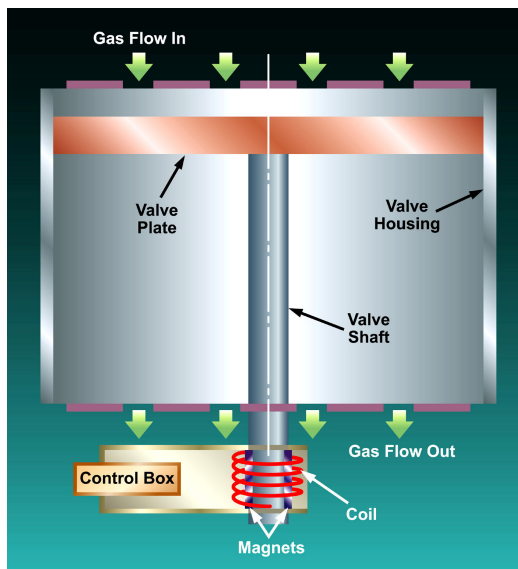


Figure 1. Electromagnetic Linear Valve

Figure 2 shows a typical opening motion profile of a plate valve and how the plate impact can be damped (rounded) using an electromagnetic actuator. By only controlling the plate’s motion prior to the impacts, the electromagnetic control power requirements are minimized, and the valve’s plate transient time performance should not be significantly affected as shown in the figure.

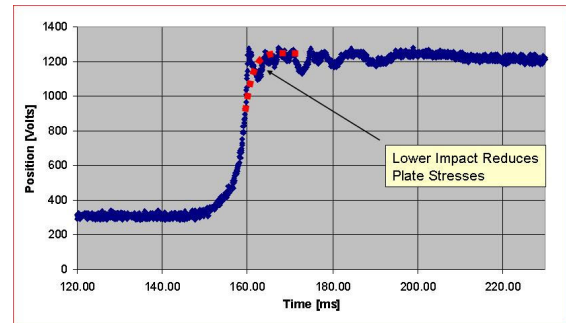


Figure 2. Valve Plate Opening Motion Profile

1.3 Concept Advantages

Previous research work within this program demonstrated that the life of a compressor valve could be significantly enhanced by reducing plate impact velocities². For example, Figure 3 shows Stress-fatigue (S-N) curves of a common valve plate PEEK material. The S-N curve relates cyclical stress level applied to the material to the number of cycles required for failure of the material. The figure demonstrates that if impact stresses are sufficiently reduced, fatigue life is effectively infinite for this material. Thus, the SAV could potentially achieve significantly enhanced valve life by actively limiting the impact forces of the plate.

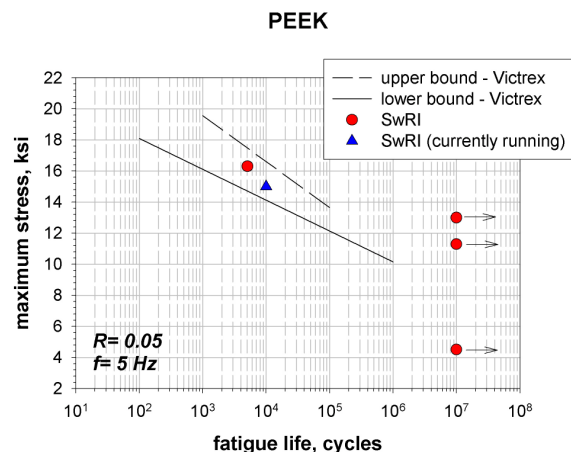


Figure 3. Fatigue Curves for PEEK Plate Material

Furthermore, since the impact velocity can be controlled on-line and actively, the lift may be increased, thus, increasing the efficiency.

This feature not only provides the operator with improved efficiency but also has the potential to allow the operator to selectively optimize the compressor operation for improved life versus improved efficiency to match his unique production/operation requirements. The valve self-regulates to the operating point of the compressor as the sensing is based on the movement of the valve plate itself (i.e., if the speed of the compressor changes, the valve will follow the speed in real time without operator input required). Finally, as previously described, the valve is intrinsically fail-safe as it reverts back to passive operation if the semi-active valve's electronic controls or mechanical parts should fail.

2 Semi-Active Valve Design and Implementation

In designing a reciprocating compressor valve, desirable functional attributes include good sealing, rapid opening and closing, sustained high flow area (when open), minimum bouncing upon impact, tolerance of impact forces and maximum temperatures, and low flow resistance. Two semi-active valve models were developed over the last 18 months: a benchscale model to prove the concept and a prototype model to test semi-active valve performance and endurance. Both models utilized a conventional plate valve as the basis of their design, but the benchscale model primarily utilized off-the-shelf components for the electromagnetic damper/sensor to minimize cost and time while the prototype model was a clean-sheet-of-paper design that is capable of prolonged normal operation under a realistic compression conditions. Both designs are described in some detail below.

2.1 Semi-Active Valve Control Requirements

During most of the operational cycle, the function of the semi-active valve is identical to that of a conventional passive valve: when a differential pressure exists across the plate that exceeds the spring force against the plate, the plate will be accelerated. Only when the velocity of the plate (as sensed from the electromagnetic coil) exceeds a preset limit will a current be induced into the coil to produce an opposing force on the plate. This slows the plate motion and provides for a soft landing of the plate on the valve's seat or guard.

Figure 4 shows two distinct regions in which plate control is advantageous. The valve plate experiences the highest velocities in Region 1. During this opening event, the control system stays passive until partway through the stroke. The control system then provides a force opposite the direction of the gas forces. In Region 2, the valve is fully open and gas is flowing. Too much opposing force at this point would cause the valve to close prematurely and initiate flutter. Thus, in this region, the control system is inactive. In Region 3, the valve shuts and seals against the seat. Although this event is not as severe as the opening, the control system gently limits the velocity to avoid plate bouncing after the closing event. Some spring force is required after Region 3 to maintain the closed position of the valve while the cylinder builds pressure. The intensity of the controlling forces is varied based on the velocity of the valve and the control requirements, giving it the ability to adjust to changing operating conditions and improved cycle performance.

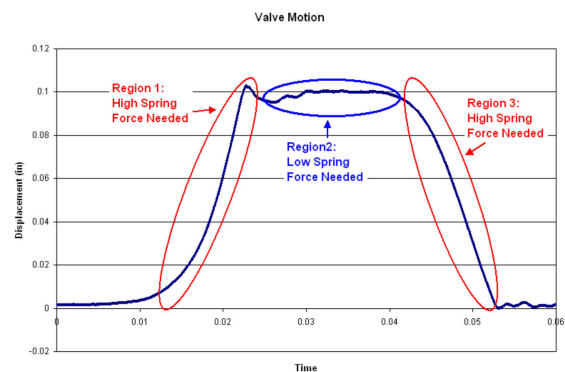


Figure 4. Regions of Control for Valve Motion

Control is achieved using the valve plate velocity as an input. (The coil's output voltage is linearly proportional to velocity.) The coil signal is converted to a digital signal and fed to a controller, which determines the plate's velocity and determines the proper level and synchronized timing of the controller's response output to provide velocity reduction prior to plate impact. The digital output is converted to an analog voltage signal, is strengthened by an amplifier, and fed directly back into the control coil of the electromagnet. The control requirement for the semi-active valves was implemented using a PC with AD and DA cards as well as a conventional audio amplifier as shown in Figure 5.

VALVES

Semi-Active Compressor Valve Development and Testing, Klaus Brun, John P. Platt, Ryan Gernentz, Mitchel Smolik;
SOUTHWEST RESEARCH INSTITUTE, BP EXPLORATION & PRODUCTION TECHNOLOGY

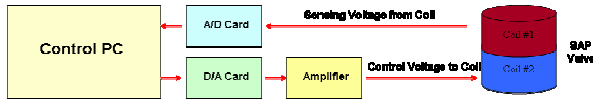


Figure 5. Semi-Active Valve Control Logic

Controls software was written in Visual Basic and LabVIEW to provide a user-friendly interface for the operator that allows for real-time adjustment of the valve performance. This feature allows the operator of the compressor to optimize the valve for either enhanced efficiency or plate life, depending on his operational requirements. Figure 6 shows a screen shot of the control's user interface.

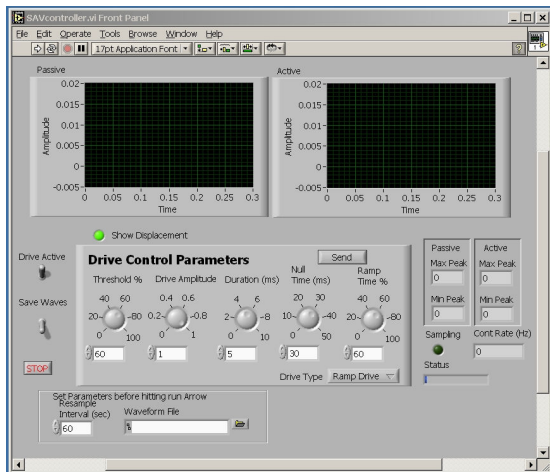


Figure 6. Control Interface of the Semi-Active Valve

2.2 Semi-Active Valve Benchscale Model

To demonstrate and test the concept of a semi-active compressor valve, it was decided to initially build a low-cost benchscale model utilizing primarily off-the-shelf items. The actuator for this first iteration was a dual voice coil from a loudspeaker mounted outside of the compressor assembly. Three long actuator shafts were utilized that were guided through the valve cage and connected the loudspeaker coil to the plate valve. To pressure isolate the valve from the ambient, a large cone had to be mounted over the loudspeaker coil. Figure 7 shows a schematic of this design. Clearly, this semi-active valve assembly was very heavy, bulky, and not practical for actual field installation.

However, the benchscale model proved valuable to demonstrate the function and feasibility of the concept.

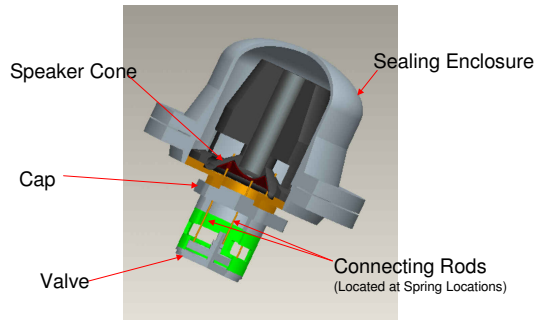


Figure 7. Benchscale Semi-Active Plate Valve Design

The benchscale model semi-active valve was fabricated and mounted onto a 250 HP Ariel compressor at the SwRI Metering Research Facility closed loop. This closed piping loop allows compressor operation using natural gas or other gas mixtures over a wide range of pressure and flow conditions (i.e., it provides an ideal facility to test compressor valves under realistic operating conditions). Pressure ratios up to 2.0 from suction pressures between 50 to 150 PSIA can be tested for compressor speeds between 300 to 900 RPM. Figure 8 shows the benchscale semi-active valve model mounted in the 250 HP compressor. An optical position probe was also mounted to verify the effect of the electromagnetic control on the motion of the plate.

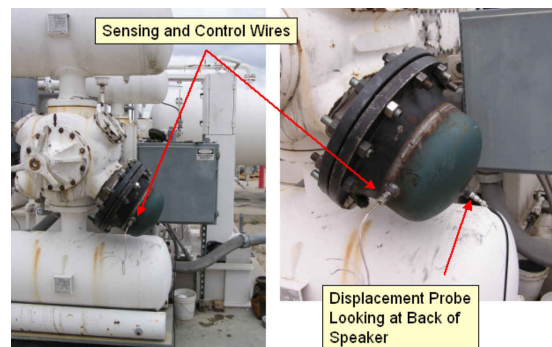


Figure 8. Benchscale Semi-Active Valve Mounted in Compressor for Testing

For the tests, the compressor was run at a low 1.1 pressure ratio, 50 PSIA suction pressure, and 700 RPM using nitrogen as the test gas (for safety reasons). Measurement results for the optical position probe traces are seen in Figure 9.

This figure shows the motion trace of the plate valve for uncontrolled versus semi-actively controlled operation. Clearly, the opening impact of the plate is significantly damped when operating in semi-active mode. For this case, the actual opening impact velocity of the plate was reduced from 0.55 m/s to 0.02 m/s. Based on an S-N curve for PEEK material, this impact velocity reduction results in a plate life improvement factor of approximately 100. The benchscale tests, thus, demonstrated that it is feasible to utilize a semi-actively controlled valve to control and significantly soften impact velocities and increase life of a compressor valve.

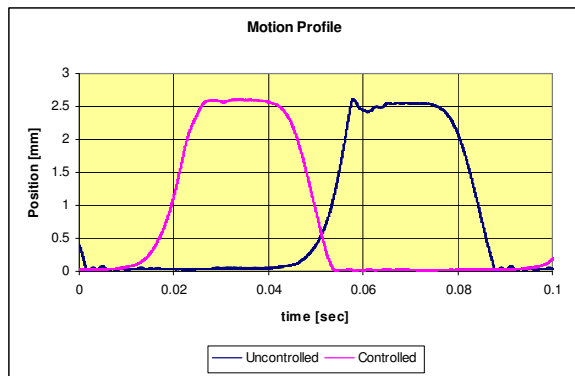


Figure 9. Controlled versus Uncontrolled Motion Using the Benchscale Semi-Active Valve

2.3 Semi-Active Valve Prototype Model

Once the feasibility of the semi-active valve function was demonstrated, a full prototype of the concept was designed and fabricated. The prototype model was built to perform extended performance and endurance testing at the previously described closed loop facility and subsequently field trials at an actual compressor station. To meet the wide range of operating requirements of the valve, a clean-sheet-of-paper design was developed that had to meet the following criteria:

- ❑ Extended operation for at least 1,000 operating hours under realistic compression conditions.
- ❑ Reduction of the plate impact velocities by at least 60% under all operating conditions.
- ❑ Self-regulating operation for all speeds up to 900 RPM.
- ❑ Safe operation on natural gas or any other flammable hydrocarbon gas.

- ❑ Retrofittable to existing compressor installations.

Figure 10 shows a design drawing of the semi-active valve prototype model. The valve utilizes four electromagnetic actuators, and the entire assembly fully fits within a standard valve cage (i.e., there are no extensions outside the conventional cylinder geometry other than the control cables). Actuators and sensors are isolated from the gas flow and pressure balanced using filter screens. The cage was custom made from a solid piece of material, with pockets for the actuators, tapped holes for filter screens, and provisions for mounting the necessary sensors. All plate valve components are taken from a conventional commercial valve with only small machining modifications applied. An LVDT position transducer was also mounted to verify the semi-active valve performance—this LVDT would not be part of an actual commercial design but was useful for testing purposes.

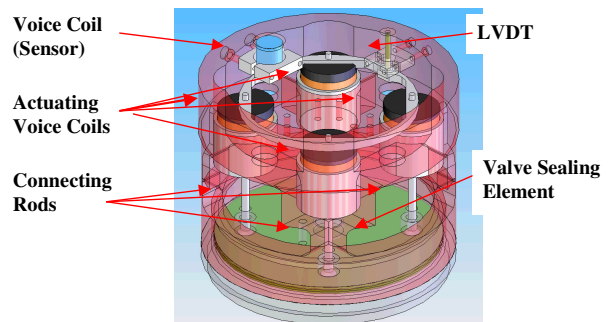


Figure 10. Semi-Active Valve Prototype Design Drawing

Figure 11 shows the final fully fabricated semi-active valve prototype. This valve was mounted in the 250 HP Ariel compressor and closed-loop that was previously described. Testing with natural gas in the loop is ongoing, and so far, about 100 total operating hours have been accumulated over various test runs. Speeds have been varied between 500 and 900 RPM, and pressure ratios up to 1.5 were tested. A number of different control schemes have been tested to identify an optimal control output signal shape, force, and timing for valve plate control algorithms. Figure 12 shows a typical time trace of the sensing coil and the output signal to the control coil; in this case, the output signal was a simple Dirac-Delta function. Other output functions include a square wave, a saw-tooth wave, and a simple proportional control.

Results from the semi-active valve tests at the closed-loop facility have verified that the semi-active valve is capable of significantly reducing the impact velocities (and even completely stopping) of the valve plate for any of the operating conditions tested so far (i.e., the desired electro-magnetic damping was achieved). The valve self-regulates to any speed and plate velocity changes, and the operator can manually override the controller to adjust the control force level. Testing also showed that the valve reverts to passive operation and continues to function when the control mechanism is disabled (or fails). These tests will be continued until September 2006 at which time the semi-active valve assembly will be removed from the current facility and installed at an actual compression station for start of field trials.



Figure 11. Assembled Semi-Active Valve

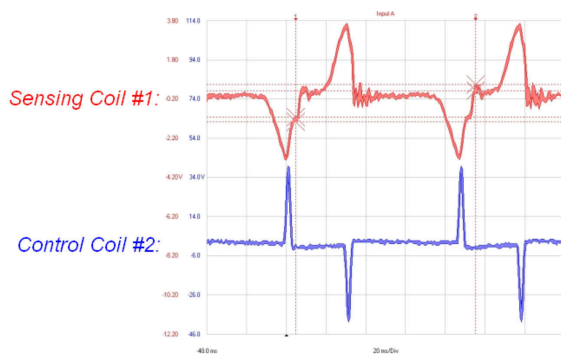


Figure 12. Sensing and Output Coil Time Trace During Semi-Active Valve Operations

3 Summary and Conclusions

A novel semi-active reciprocating compressor valve was designed, fabricated, and tested to address and performance limits of current technology compressor valves. This valve's concept is based on a conventional plate valve design but replaces or augments the valve springs with an electromagnetic coil that senses position and provides an opposing force prior to the plate's impact. This concept is referred to as a "semi-active electromagnetic plate valve" because it is still passively activated by gas forces and only actively controlled prior to impact (i.e., although actively controlling the motion of the plate, this valve does not require pressure sensors or shaft encoders for control). By reducing the valve plate's opening and closing impact velocities, one can effectively design an infinite fatigue life plate valve.

Two semi-active valve models were developed, built and tested: a benchscale model to prove the concept and a prototype model to test semi-active valve performance and endurance. Both models utilized a commercial plate valve as the basis of their design, but the benchscale model primarily utilized off-the-shelf components for the electromagnetic damper/sensor to minimize cost and time, while the prototype model was a clean-sheet-of-paper design that is capable of prolonged normal operation under a realistic compression conditions. Also, a semi-active valve controller was implemented utilizing a PC with AD and DA cards, as well as a standard audio amplifier. Both valves were mounted in a 250 HP reciprocating compressor and tested over a wide range of operating conditions.

The benchscale semi-active valve tests demonstrated the feasibility and practicality of the concept. Subsequent testing of the prototype semi-active valve model provided the following test results and demonstrated the valve's principal features:

- ❑ Reduction of the plate impact velocities up to 100% was achieved for all tested operating conditions (i.e., the actuators were capable to completely stop the plate).
- ❑ The valve automatically self-regulates to any compressor speed and operating conditions without operator input.

- ❑ The valve can safely operate with natural gas.
- ❑ The current prototype design is retrofittable to existing compressor installations.
- ❑ The valve reverts to passive operation and continues to function when the control mechanism fails or is disabled.

Additional endurance testing is ongoing to quantify the service life of the prototype valve and to optimize the valve control performance. Once this endurance testing is completed, the valve will be installed in an actual compression station for field trials.

3.1 Acknowledgements

The authors would like to acknowledge the Gas Machinery Research Council, the United States Department of Energy, and BP Exploration & Production Company for their financial and technical support of this valve research program.

References

-
- ¹ Deffenbaugh, D. M., Brun, K., Harris, R. E., Harrell, J. P., McKee, R. J., Moore, J. J., Svedeman, S. J., Smalley, A. J., Broerman, E. L., Hart, R. A., Nored, M. G., Gernentz, R. S., and Siebenaler, S. P. "Advanced Reciprocating Compression Technology (ARCT)," Southwest Research Institute Final Report prepared for U.S. Department of Energy – National Energy Technology Laboratory, December 2005.
 - ² Brun, K., Nored, M. G., Smalley, A. J., and Platt, J. P., "Reciprocating Compressor Valve Plate Life and Performance Analysis," Proceedings of 4th Conference of the EFRC, Antwerp, Belgium, June 9-10, 2005.



Elastomeric Materials Applied to Reciprocating Gas Compressor Valves

by:

Kevin Durham
Director of Engineering
Cook Manley
Stafford, Texas
United States of America
kevind@cookmanley.com

5th Conference of the EFRC
March 21-23, 2007
Prague, Czech Republic

ABSTRACT:

The history of valves in reciprocating gas compressors is dominated with the use of rigid materials from metal to thermoplastic polymers. Research started in 1998 investigating the application of elastomeric materials has resulted in elastomeric valve designs that not only improve the sealing capabilities of the valve elements but increase the durability and robustness of compressor valve performance. Specifically, compressor valves fail when the valve element loses its ability to form a gas tight seal. The leaking gas causes operating temperatures to rise as the leak path grows and failure progresses. Valve elements made from rigid materials can fail from damage caused by solid particles in the gas impinging upon the surface of the element or by the damage accumulated from the repeated impacts between the valve seat and the moving valve element.

The flexible nature of elastomeric materials has been used to overcome the disadvantages of rigid valve elements. Elastomers can readily conform to or around irregular surface and still create a gas tight seal and the inherent energy damping properties of elastomers significantly reduces the damaging effects of cyclic impacts with the valve seat. The discussion of this technology will center on some failure modes of reinforced composites currently being used and the methods in which elastomeric materials can overcome the limitations of rigid components and dramatically improve compressor valve performance.

Introduction:

It seems simple enough. Design a mechanical device that opens and closes with each stroke of a compressor, create a leak tight seal to prevent reverse flow and repeat this process up to 1200 times a minute for several years. The devil, of course, is in the details and in spite of their seemingly simple features, gas compressor valves are complex and dynamic devices whose service life is strongly influenced by the operating environment and, more importantly, the materials of construction. Adjusting the spring forces and changing the valve lift can result in improved valve life but changing these variables can never completely neutralize the damage caused by liquids or solids entrained in the gas stream or the stresses caused by variable operating conditions. The factors opposing reliable valve operation are numerous and as our understanding of compressor valve operation and failure grows, more creative methods are being applied to overcome the obstacles to long term performance.

In general, the effectiveness of any device is often attributed to the performance of the materials from which the device is made and compressor valves are no exception. Unfortunately the long history of compressor valves is populated with a relatively few novel changes in the materials of construction. Plates with a rectangular cross section were used first because metals were inexpensive, the ordinary shapes were easy to produce and pressure drops through the valve and the subsequent horsepower consumption weren't driving forces for change. Plates could be stamped, lapped and placed into service and if corrosion was a problem, stainless steels could be used which seems odd since the early valves probably didn't operate long enough for corrosion to take place.

In the early 70's, polymer technology had evolved to the point where engineered, reinforced thermoplastics achieved thermomechanical properties significant enough for them to be considered for use in reciprocating compressor valves. The cost of injection molding machines was such that more and more companies began to look at ways to use plastic composites in place of metal components. Space vehicles benefit most from weight reductions but injection molding parts out of thermoplastic materials allows for more complicated shapes to be made at a lower cost in addition to the benefits of less weight. Injection molding technology and the availability of robust thermoplastics opened the door for engineers to try

these materials in reciprocating compressor valves and in 1972, this is exactly what happened. Today thermoplastic valve elements are very common while metal plates are being used less frequently and are typically called for in services where high temperatures prohibit the use of thermoplastics. Modern metal valve plates perform very well but, in general, valves with plastic elements perform better.

In the present day operating environment, compressor operators are placing severe demands on reciprocating compressors. These machines must be reliable, durable and efficient. The pressure drop through the valve (power consumption) is now a critical selection factor given the present cost of energy and of course, long term operation is what everyone wants. Ten years ago 18 months of continuous operation was a significant achievement but now, in many applications, it's commonplace. The problem facing the valve industry now is that compressors are getting faster, smaller and, regardless of size, service life expectations are getting longer. A three year continuous run is a common goal. Engineered thermoplastics offer impressive performance (on paper) but these materials are sophisticated systems with a number of parameters that make them unpredictable and difficult, if not impossible, to engineer with great precision. What are the valve manufacturers going to do to meet these challenging requirements?

The purpose of this paper is to introduce and report on the use of elastomeric materials in reciprocating compressor valves. While elastomeric materials have problems of their own, they also have a number of key properties that could allow for dramatic improvements in the service life of conventional valves with rigid elements. A valve element should be of an aerodynamic shape to reduce the pressure drop through the valve and reduce power consumption, flexible enough to seal over a variety of surface imperfections and robust enough to handle the cyclic loading and constant impacts that are characteristic of the compressor valve operating environment.

VALVE ELEMENTS:

Valve elements are the critical component of the compressor valve. If the elements are unable to create a gas tight seal, a leak occurs and the valve begins to overheat. If the element is unable to efficiently absorb the kinetic energy during the impacts with the seat and guard, yielding and or

fractures can develop leading to an unscheduled shutdown of the compressor. The amount of effort needed to push gas through a compressor valve is greatly influenced by the shape of valve element and the magnitude of the valve travel (lift) with higher lifts and contoured shapes requiring less power to move gas through the compressor valve.

Power Consumption: It is generally held that increasing the lift of the valve to lower the pressure drop and horsepower consumption will result in a reduction of the valve service life. How much service life is lost is extremely difficult to quantify and highly dependent on the service environment but historically, a trend has evolved and most compressor valve manufacturers agree that valve lift and valve service life are inversely related. The effect of increasing lift on valve service life is usually determined by trial and error; change the lift and see what happens. While this approach is crude, it does yield results if one can afford the time, expense and aggravation.

Valve elements made from metal are very difficult to form into aerodynamic shapes. Sophisticated, multi-axis machine tools are needed and invariably, these shapes require the element to make contact with and seal on two surfaces simultaneously thus requiring very high machining tolerances and surface finishes in order to be functional. Thermoplastic materials make aerodynamic shapes possible but it is still anything but routine and the cross section of metal valve elements is almost exclusively rectangular. Very little progress here over the years as there are very few contoured valve elements in the market.

The Gas Tight Seal: Leaking valves run hot and the temperature of the valve will continue to increase as the severity of the leak increases. Compressor cylinders and compressor valves depend on the process gas to remove heat from the cylinder. A leaking valve prevents all of the hot gas from being expelled and the resulting reduction in heat transfer causes temperatures to increase. Given that there are solids entrained in just about every gas stream, damage to the sealing surfaces is assured. How long the surfaces remain in a condition good enough to make a seal is a function of the size and density of the solids in the gas stream. Metal surfaces, once damaged, are unlikely to recover but thermoplastics have shown the ability to tolerate surface damage and actually recover their profile and continue to operate with an effective seal. This is one reason why thermoplastic parts out perform their metal counterparts. With a lower mass, the thermoplastic valve elements generate less kinetic energy ($KE=(1/2)mass*velocity^2$). A valve element

that could adapt to changes in the profile of the sealing surfaces and better tolerate solids in the gas stream could substantially improve the service life of the valve.

Damage from Impulse Loads: Valve elements open and move to a position against the valve guard under the influence of differential gas pressure and valves close under the influence of springs but even when well controlled, the elements still strike the seat with some velocity. As the valve springs fatigue over time and operating conditions change, the plate velocity at closing increases. Impulse loads are defined as the time for a mass to change velocity. The mathematical equation is:

$$F = \frac{mass * \Delta velocity}{\Delta Time}$$

The time to stop the plate will always be very small because in most cases the valve elements and the surfaces to which they mate are rigid. It's not possible to appreciably increase the duration of the stopping event in these cases. Lowering the magnitude of the impulse loads during the opening and closing events will lower the energy that initiates yielding in the parts and provides the driving force for the nucleation of fractures. In elastomers, energy is dissipated by the ability of the polymer chains to slide relative to one another (hysteresis damping) thus limiting the magnitude of the energy transmitted to the sealing surface of the valve seat. The compression of an elastomer is a time dependent event and if we assume that the elastomer remains unchanged as the compressor speed increases, the elastomer will behave more like a rigid solid because there will be insufficient time for the polymer chain motion to occur. In general, increasing the compressibility or flexibility of a material making contact with another object will increase the time duration of the stopping event. Elastomers in many cases have a lower density than thermoplastics so the mass of the element can be reduced and the element velocities can be controlled to some degree by reducing lift and designing effective spring systems.

Now that we have some of the history of compressor valve elements and listed some of the more important properties a successful valve element would embody, what is wrong with the thermoplastic materials currently being used and if what we have is limited in some way, what is being considered to address the problems? There are claims being made that the life of a reinforced polymer composite valve element can be predicted and even if mathematical equations could be derived to consider all of the factors working against the valve element, these equations most likely could not be solved in any useful time

period. It's easier to predict the weather. Useful solutions to valve reliability are going to come not from mathematics but from the creative application of materials not normally considered for use in compressor valves. This paper will consider the use of elastomers (rubber).

ELASTOMERS:

Elastomers are long chain molecules (polymers) similar to rigid thermoplastics however the elastomers operate well above their glass transition temperature (T_g) and they feature a lightly cross linked structure that affords them the ability to undergo large deformations with relatively small applied stresses. This ability to deform and recover is what permits elastomers to be used extensively in places where a gas or fluid tight seal is required. Furthermore, elastomers have the ability to dampen vibration, dissipate shock energy better than rigid materials and elastomers do not fracture in the strict definition of the term. Effective use of elastomers has the potential to significantly increase the mean time between failures and indeed, there are compressors operating at this moment where extraordinary valve life has been realized.

Elastomers are materials in which there is crosslinking between the polymer chains the crosslink density (the number of crosslinks per polymer chain) strongly influences the mechanical properties of the elastomer and the particular atoms in the molecules on the chains their bonding

structure dictate the chemical resistance properties of the compound. Without cross linking, the polymer chains would slide passed one another, the material would behave in a viscoplastic manner and the strains caused by applied stresses would not be recoverable. Think of this behavior as being analogous to a thick liquid. Cross linking (see fig #1) is a chemical bond (usually covalent) that

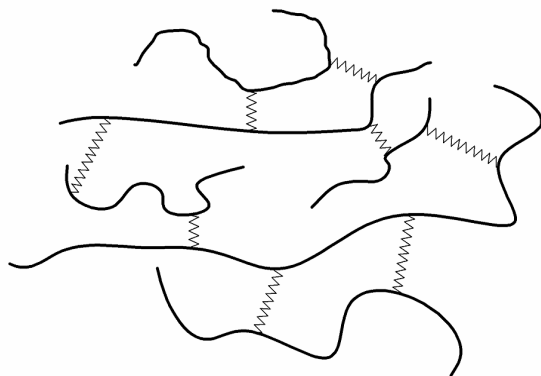


Figure 1

firmly attaches one polymer chain to another and provides a mechanism for enabling elastic behavior. Typically crosslink densities for elastomers are on the order of one crosslink for every one hundred molecules on the polymer chain. Crosslink density can be controlled to a very high degree and manipulating the number of cross links permits the stiffness of the material to be changed over a wide range. For example, when the crosslink density approaches 1 in 30 the material becomes rigid. Controlling the stiffness of the elastomer is one variable used to successfully apply elastomers to reciprocating gas compressor valves.

Much like cooked spaghetti, polymer chains in their natural conformation are entangled with one another and they become straightened only after a stress is applied. Polymer chains consist of thousands of molecules (mers) bonded to one another and each of these bonds has some degree of freedom to rotate thereby allowing a single polymer chain to take on a tremendous number of conformations. Double and triple bonds between molecules are very stiff, restrict rotation and provide a pathway for chemical attack. Consequently, some of the more useful elastomers are comprised of polymer chains dominated by single bonds. If it were possible to hold each end of the polymer chain and apply a tensile force, the molecular bonds would rotate (see figure #2) and permit the polymer to uncoil and straighten in response to the applied stress. If the ends of the chains continue to be pulled apart, a point would be reached where all of the bond rotations would have taken place, the polymer chains would be fully uncoiled (as much as their bonds would allow) and

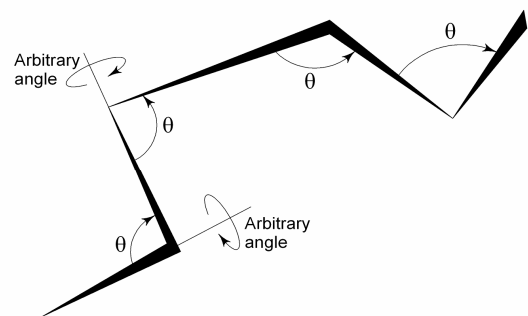


Figure 2

further tension on the chains would begin to stretch the atomic bonds between molecules. The material will rupture/tear when the applied loads exceed the strength of the intermolecular bonds along the polymer backbone. All of this behavior is fundamentally different from metal and thermoplastics.

Thermodynamic Basis for Elasticity:

Elasticity comes from the resistance of the chains to uncoil and this can be explained thermodynamically using the first and second laws and the concept of entropy.

The change in internal energy for any process (first law) is:

a) $dU = dQ + dW$

Where: dU = change in internal energy
 dW = work done on the system from external sources
 dQ = heat absorbed by the system from the surroundings

The change in entropy in a reversible system (second law) is:

b) $dS = dQ * \frac{1}{T}$

Where: dS = the change in entropy of the system
 T = temperature

Combining (a) and (b), the change in internal energy for reversible processes is:

c) $dU = TdS + dW$

Work is defined as a force acting through a distance (l):

$$W = f * l$$

and the change in work is therefore:

d) $dW = f*dl$ when the force applied is constant.

Combining (c) and (d) and solving for the force (f) results in:

e) $f = \frac{dU}{dl} - T \frac{dS}{dl}$

Where: T = constant temperature

Simply stated, equation (e) says that the internal energy and the entropy can be changed when a force is applied to a system. In elastomeric

systems, the entropy term dominates and the first term can be ignored because the chains uncoil and molecular bonds rotate leading to a more ordered microstructure as the polymer chains are pulled into alignment by the applied load. This decrease in entropy (more order) is brought about by the uncoiling of chains and bond rotations rather than stretching the atomic bonds directly as in metal or composite systems. The atomic bonds in polymer chains do not see any effects until the polymer chains are as straight as their structures will allow. Equation (e) is a mathematical statement of the loss of entropy that occurs under applied loads. Pulling the polymer chains into alignment takes them from a probable arrangement to a less probable arrangement and an entropic driving force results in the polymer chains desiring to return their coiled, disordered state and we see this macroscopically as an elastic response to an applied stress. When the stress is removed, the part returns to its original configuration. The details of elastic behavior have been omitted because they are beyond the scope of this paper and are not necessary to convey the macro behavior of elastomers being introduced in this paper.

Design:

With a Poisson ratio very near 0.5, elastomers are considered to be constant volume materials. In practice this presents the very real problem of containment when the elastomer parts are stressed. A pressure or load in one area results in a response in another. The volume displaced due to the applied stress appears elsewhere and the need to know where and in what form this volume appears adds

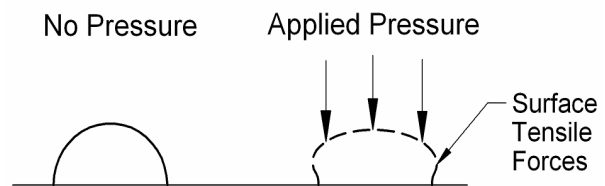


Figure 3

complexity to the application of elastomers. Figure #3 shows schematically how an arbitrary elastomeric shape might deform under an applied pressure force. The regions of concern are the bulges that tend to form perpendicular to the applied force. The surfaces of these bulges are home to locally high tensile forces and as the radius of the bulge gets smaller with increasing loads, the tensile forces increase dramatically. These areas of high tensile forces must be managed and evaluated because this is where tears in the elastomer will

VALVES

The Application of Elastomeric Materials to Reciprocating Compressor Valves, *Kevin Durham; COOK MANLEY*

evolve and thereby initiate destruction of the part. If the surface tensile loads exceed the material properties, a rupture will occur and under cyclic loads the fracture will grow until the part is damaged and its ability to form a seal is lost.

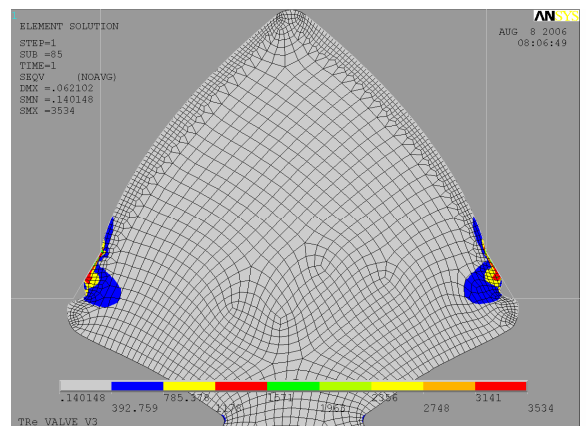
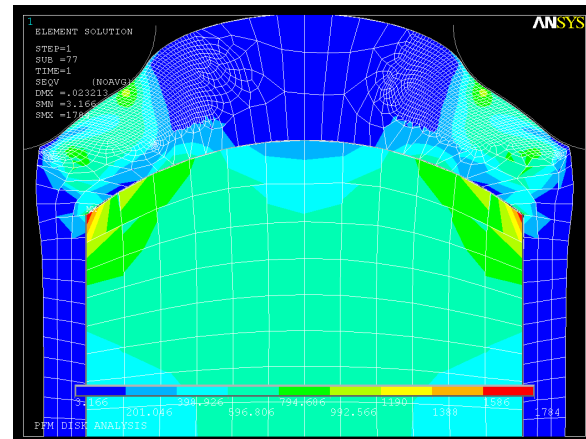
The solution to the constant volume behavior is anything but trivial because elastomeric deformation is inherently non-linear and FEA software is required to model the deformation and calculate the stresses. The construction of a physical test to validate the computer model is highly recommended. Only when the behavior is accurately modeled can the material and geometry be manipulated to arrive at designs that permit high differential pressures to be applied that do not exceed the material limits. Design of an acceptable geometry is a time consuming iterative process and stress-strain curves for uniaxial and biaxial tension are needed by the FEA software to model the material behavior under load.

The application window for elastomers is highly dependent on the geometry of the part but in general, the low strength of elastomers is a real problem since there are only a few process services that operate at these low pressures. FEA analysis showed that rigid thermoplastics with an elastomeric overlay could tolerate a differential pressure of 600 psid. This differential pressure would allow for a rather wide application of elastomeric valve elements but field tests demonstrated that the mechanical interaction between the elastomer and the substrate is problematic and limits the application pressure to 200 psi. Further study and FEA analysis reveals that valve elements made from solid elastomer materials can eliminate the need for a rigid substrate and allow for highly aerodynamic shapes. Eliminating the substrate should permit higher differential pressures to be tolerated. At the time of this writing, field tests on prototype geometries were being conducted with positive results.

The point of applying elastomers is to allow deformation to occur so as to greatly increase the surface contact area and make it more difficult for one or even a series of surface defects to link up to form a leak. The probability of a leak occurring is inversely proportional the contact area between the elastomer part and the opposed sealing surface. A robust and durable seal results in a compressor valve and damage tolerance is significantly increased when the valve element has the ability to conform to damaged surfaces. The initial designs and field results indicate that the elastomer concept is viable and that elastomer parts can outperform their thermoplastic and metallic counterparts by a

wide margin in terms of service life, seal integrity and substantial reductions in valve pressure drops.

Examples of Elastomeric Valve Elements:



If element fractures are not considered, it is safe to say that compressor valves develop leaks because of damage to the valve element, the valve seat or both. Whether the damage occurs from impingement by solids entrained in the gas stream or by plastic deformation caused by high cycle fatigue and differential pressure, leaks evolve when the sealing element and the valve seat are no longer in continuous contact. A leak path permits gas to wash back and forth with each compressor stroke and locally high temperatures combined with an accumulation of damage from subsequent strikes from solids results in a progressive failure of the valve seal. The region of interest is then the line or surface that is created when the element and the sealing surfaces of the seat come together. This is where the gas tight seal is formed.

There is some debate about which mode of contact is more effective – line contact or surface contact. Both are capable of creating a gas tight seal and both have experienced reasonable success in actual compressor service. A general inspection of why

VALVES

The Application of Elastomeric Materials to Reciprocating Compressor Valves, *Kevin Durham; COOK MANLEY*

and how leak paths form in compressor valves with rigid elements allows one to see that seals formed by line or surface contact fail by the same process. The following figures schematically depict the process of leak path formation in line and surface contact designs.

Figure #4 depicts surface contact. The dashed lines indicate the width of the contact surface and the irregular shapes are intended to show physical damage that can occur from entrained solids. The

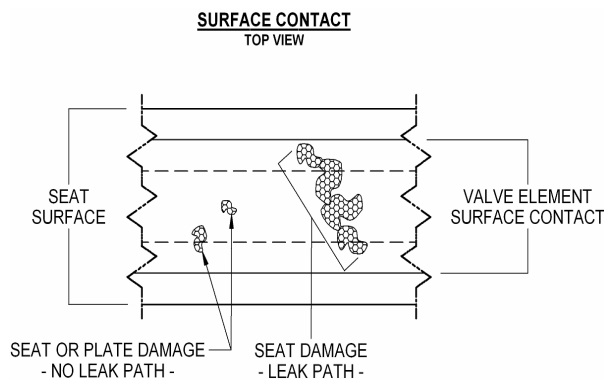


Figure 4

left side of figure #4 shows two impact regions that are not in close proximity to one another and consequently there is a smaller but still continuous region of contact that takes place between the valve seat and the valve element. There is no leak path and the seal is intact.

The right hand side of figure #4 depicts how a series of impacts can be arranged to allow for a

leak path to be created. Once gas begins to flow, local temperatures rise and as more solids impinge upon the surfaces, more leaks are created and valve performance deteriorates until the compressor is shutdown and the parts are replaced. Figure #6 (“side view”) shows how the rigid valve element spans the damaged area but does not fill the depression thereby allowing gas to pass under the

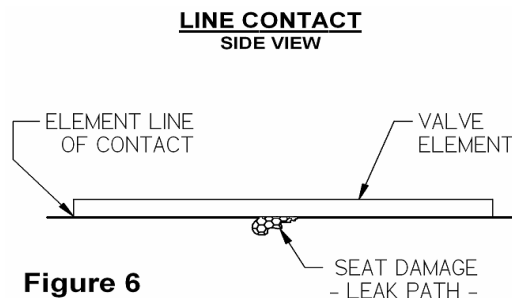


Figure 6

valve element. The damage is shown to occur on the valve seat but it could occur on the valve element or both. The key point is that valve

elements made from rigid thermoplastics or metals cannot deform enough to fill these damage craters and restore the continuous surface required to maintain the gas tight seal.

In line contact, the gas tight seal is dependent on a very narrow region of contact between the valve element and the valve seat. It may take one or only a few strikes from solid particles in the gas to breach the contact line and create a leak path. It is reasonable then to assume that it is more likely that a single strike by a solid particle of the appropriate size could result in the loss of the seal and the probability of this occurring is even more likely as the region of contact between the element and seat becomes more narrow. A schematic showing how damage from one strike could result in a leak path is shown in figure #5. While the diagrams depicting how leak paths are formed are simplified, the

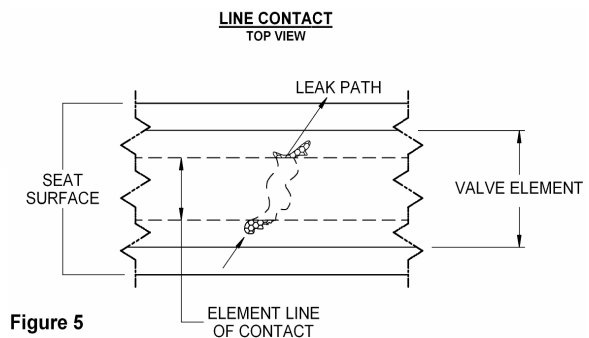


Figure 5

mechanisms do in fact exist. The “side view” sketch at the left is most descriptive of what happens when rigid thermoplastics or metal valve elements are used. The element materials are too stiff to allow for the elements to deform and fill the voids left by impact damage. It is true and it has been observed that thermoplastics will absorb solid particles and allow the gas tight seal to remain intact. The catch is that the particle must be of such a size that will allow it to be pressed completely into the thermoplastic element so as to restore the original surface profile of the part. Anything protruding above the surface will effectively hold the valve element open thereby creating a leak path and a source of heat in the valve. Metal valve elements are even less responsive and do not show any ability to “heal” themselves. It would seem then that materials with the ability to tolerate entrained solids would be highly desirable but however attractive these properties are, flexible materials do not exhibit great strength. Making use of these flexible (elastomeric) materials requires a new set of problems to be addressed.

Why Developing this Technology is Important:

In recent years, compressor valve technology has become stagnant. There have been incremental changes to materials and some of the shapes of the valve elements have changed but they are still made from metal or rigid thermoplastics and published documentation does not reveal any new methods for accurately selecting or designing rigid polymers for use in reciprocating compressor valves. As noted previously, the factors that dictate the performance of engineered thermoplastics are numerous and many are inherently uncontrollable. How do you control or predict the size, orientation and distribution of the reinforcing fibers between the time the raw pellets are melted and the finished part falls out of the injection molding machine? It can't be done. Fibers are broken while in transit through the injection molding machine and their positions and distributions are randomized when the molten plastic is shot into the mold yet the fibers play a crucial role in the mechanical performance of the finished part. If one cannot control the length of the fibers, their location or their orientation then how can a claim be made that mechanical properties be predicted and controlled to a level of precision that would allow for service life to be predicted? There are other factors such as crystal size and distribution that can increase or decrease the performance of the polymer. Thermoplastics are noble materials and their use is increasing but we do not understand them well enough nor can we control their properties with enough precision to make the claim that there is nothing else out there that cannot surpass their performance.

Elastomers come with a new set of problems but many of the variables that dictate their behavior are not random and most of them are mechanical in nature and can be modeled with non-linear FEA software. Elastomeric materials offer the potential to overcome several of the barriers to advancement:

- 1) Aerodynamics – Complex shapes are more easily and less costly to make if they can be molded rather than machined to finish shape.
- 2) Flexible Valve Elements – The ability to conform to irregular surfaces implies that less than perfect aerodynamic shapes can be produced and a gas tight seal can be achieved because of the flexibility of the elastomer materials. Tight production tolerances are eliminated without loss of performance. To achieve the same

function with rigid materials (thermoplastics or metals) would be far more costly. Plastics shrink when cooled from the mold and machining/lapping operations would be needed to make the parts for a gas tight seal.

- 3) Reduced Valve Horsepower – Aerodynamic parts improve gas flow and reduce valve pressure drops. Pressure drops can be reduced with no increase in lift and in some cases a more efficient geometry can reduce valve loss horsepower with a reduction in lift. In addition, stagnant regions in the valve can be reduced so as to prevent solid debris from collecting in the valve.
- 4) Valve Dynamics – Elastomeric materials dampen energy which means that during the valve motion, less energy is transmitted to the seats and guards. The elastomeric elements won't cause seat recession as can sometimes occur when rigid parts strike one another over long periods of time.
- 5) Unlike injection molded thermoplastics, elastomers can be treated as homogeneous materials and this allows them to be readily analyzed by non-linear FEA techniques. The randomness in the fiber reinforced composites can lead to serious errors in FEA results when these materials are assumed to be homogenous. Non-linear analysis requires a new set of skills but elastomers can be modeled with substantial accuracy.

The inherent low strength of elastomers is the most formidable obstacle facing their use in compressor valves. Differential pressure forces can easily deform the elements and a great deal of creativity is required to manage the deformation without increasing the stiffness of the material to a level that approaches the plastics that are being superseded. The good news is that it can be done and it has been done. There are compressors operating today that have experienced increases in the mean time between valve failures that can be measured in *years* over previously used composite materials. Expanding the pressure envelope by testing a variety of elastomers and geometries is the focus of current research.

Observations/Conclusions:

A number of compressors are operating with elastomeric valve elements and in each case, elastomers were applied after the composite

materials failed to perform. Damage tolerance has been increased as expected and a compressor field analyzer confirmed a reduction in impact energy of 60% compared to a non-elastomeric valve element of the same geometry.

In spite of their low strength and the difficulties in non-linear analysis, elastomers have shown themselves to be viable materials for compressor valve elements. Desktop computing and advanced FEA codes have made it possible to analyze the non-linear behavior of elastomeric materials and make effective designs that minimize the weakness of the materials and maximize the strengths. Good, reliable sealing in reciprocating gas compressor valves will always be in demand and elastomer technologies are poised to take compressor valve reliability to heights well beyond the reach of rigid thermoplastics.

REFERENCES

- (1) Mechanical Properties of Polymers and Composites 2nd Ed, by L. Nielsen and R. Landel, Marcel Dekker 1994
- (2) Fundamentals of Polymer Science, by P.Painter and M. Coleman, Technomic Publishing 1994
- (3) Mechanics of Composite Materials 2nd Ed, By R. Jones, Taylor and Francis 1994.
- (4) The Physics of Rubber Elasticity 3rd Ed, by L.R.G Treloar, Clarendon Press 1975.
- (5) "Polymer Toughness and Impact Resistance", William Perkins, Polymer Engineering and Science, December 1999, Vol 39 No 12, pages 2445-2460.
- (6) "Changes in Mechanical Behavior During Fatigue of Semicrystalline Thermoplastics", Alan Lesser, Journal of Applied Polymer Science, 1995, Vol 58, pages 869-879.
- (7) "Mechanisms of Fatigue in Short Glass Fiber Reinforced Polyamide 6", J.J Horst and J. L. Spormaker, Polymer Engineering and Science, November 1996, Vol 36 No 22, pages 2718-2726.
- (8) "Fibre Orientation Effects on the Fracture of Short Fibre Polymer Composites: on the Existence of a Critical Fibre Orientation on Varying Internal Material Variables", S.Fara and A. Pavan, Journal of Materials Science, 2004, Vol 39 pages 3619-3628.
- (9) "Microfailure Behavior of Randomly Dispersed Short Fibre Reinforced Thermoplastic Composites Obtained by Direct SEM Observation", N.Sato, T.Kurauchi, S.Sato and O. Kamigaito, Journal of Materials Science, 1991, Vol 26 pages 3891-3898.
- (10) "Mechanisms of Fatigue Fracture in Short Glass Fibre-Reinforced Polymers", R.W. Lang, J.A. Manson and R.W. Hertzberg, Journal of Materials Science, 1987, Vol 22 pages 4015-4030.
- (11) "The Effect of Loading Rate on the Fracture toughness of Fiber Reinforced Polymer Composites", George C. Jacob, J. Michael Starbuck, John F. Fellers, Srdan Simunovic and Raymond G. Boeman, Journal of Applied Polymer Science, 2005, Vol 96, pages 899-904.
- (12) "Fatigue Behavior Characterization of the Fiber-Matrix Interface", R.A Latour Jr., J. Black, Journal of Materials Science, 1989, Vol 24 pages 3616-3620.



Burckhardt Compression

Further Improvement of Pulsation and Vibration Studies for Reciprocating Compressors

by:

**Georg Samland, Nicole Retz
Research & Development
Burckhardt Compression AG
Winterthur, Switzerland**

**5th Conference of the EFRC
March 21-23, 2007
Prague, Czech Republic**

Abstract:

Pulsation and mechanical response analyses have proven to be effective tools to predict pulsations and vibrations for reciprocating compressors.

The precise modeling of the complete pipe system is necessary for the pulsation study. Subsequently the pulsations and pulsation-induced shaking forces are calculated and compared with maximum allowable values.

For the mechanical response study a mechanical model is built up which includes all important components influencing the mechanical natural frequencies and cyclic stresses. The mechanical model is excited by the pulsation induced forces and corresponding phases. Subsequently, the vibrations and cyclic stresses in the pipe system are calculated. A full Design Approach 3 analysis of the API Standard 618 also includes the detailed modeling of the compressor manifold. Therefore, the so-called compressor manifold vibration or better compressor manifold stiffness is considered in the analysis too.

Highly loaded compressors such as secondary compressors are showing remarkable cylinder displacements during operation. A further improvement for the vibration study could be realized by taking these forced cylinder displacements and corresponding phases into account. The results help to minimize the need for subsequent costly and time-consuming corrective measures.

The paper describes such an enhanced pulsation/vibration study for a secondary compressor and shows the comparison between calculated and measured results.

1 Introduction

Reciprocating compressors are used in major industries in a wide range of applications and processes. Key factors for a reliable and safe reciprocating compressor operation are amongst others pulsation and vibration issues. Pulsation and vibration may disturb safe and reliable operation and control of pulsation and vibration in accordance with the API 618 is mandatory to avoid vibration problems and to optimize the dynamic behavior.

It is common practice to carry out the pulsation and mechanical analysis during the design stage of an installation. These analyses include the investigation of compressor manifold vibrations, which are the vibrations of compressor cylinders, distance pieces, crosshead guides, pulsation dampers and piping.

In the 4th edition of the API Standard 618¹ the compressor manifold analysis is mandatory if a Design Approach 3 analysis has been specified. To keep the costs to a minimum, economic models have to be used to analyze the compressor manifold vibrations accurately. /3/ describes these kind of analyses for standard horizontal and vertical reciprocating compressors and shows the agreement between calculated and measured values.

However, these analysis are not limited to standard compressors, it also makes sense to apply this kind of analysis to so-called hyper or secondary compressors.

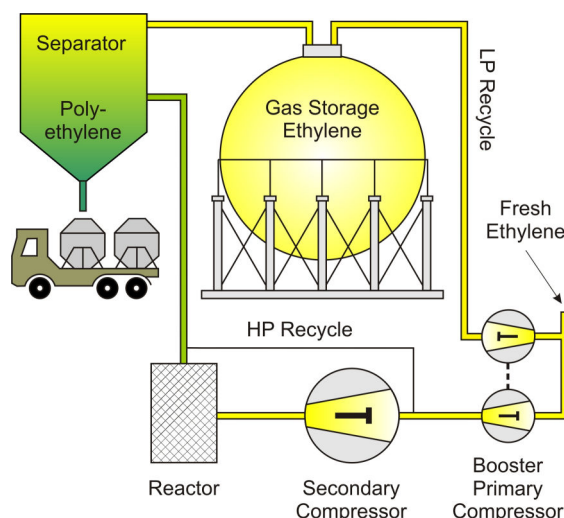


Figure 1.1: Schema of ldPE production

Secondary compressors are used in low-density polyethylene (ldPE) plants, where ethylene or ethylene vinyl acetate mixtures are compressed from 1 bar suction pressure up to over 3000 bar discharge pressure. Figure 1.1 shows the schema of ldPE Production. Compression is done within seven or eight stages in two compressors. The compressor for the lower pressure range is divided into two parts. The booster part compresses the recycled gas to fresh ethylene pressure, which typically is between 15 and 30 bar. The primary part compresses the gas up to the feed pressure of the secondary compressor (approx. 270 bar). Finally, the two stage hyper compressor delivers discharge pressure required at the reactor inlet.

2 Compressor manifold analysis according to the API Standard 618 and comparison with measurement

The procedure of a compressor manifold analysis according the API Standard 618 is as follows³:

The first step in the analysis is to generate the mechanical model of the pipe system. The second step is to generate mechanical models of the compressor parts. These parts will be assembled and the lower mechanical natural frequencies and mode shapes will be calculated. For those cases where acoustical and mechanical natural frequencies coincide (worst-case situations), a forced response analysis must be carried out to calculate:

- Vibration levels of compressor and piping
- Cyclic stress levels in piping and pulsation dampers

Vibration and cyclic stress levels must be compared with allowable levels and in case of exceeding, modifications have to be investigated to finally achieve acceptable levels.

Such an analysis has been carried out for a secondary compressor installation (8 cylinders) and the appropriate supports and orifices were determined in order to fulfill the above mentioned API guideline.

After start-up of the compressor, the customer reports high vibration primarily at the 2nd stage discharge piping of the secondary compressor.

An intense measurement campaign was started in order to find out the root cause for the vibration and to provide a solution for the problem.

PULSATIONS & VIBRATIONS

Further Improvement of Pulsation and Vibration Studies for Reciprocating Compressors, *Georg Samland, Nicole Retz;*

BURCKHARDT COMPRESSION

Figure 2.1 shows a sketch of the secondary compressor and exemplarily the location of two measuring points (cylinder and discharge piping). The vertical, axial and horizontal directions are also defined. All figures, tables and diagrams refer to these directions.

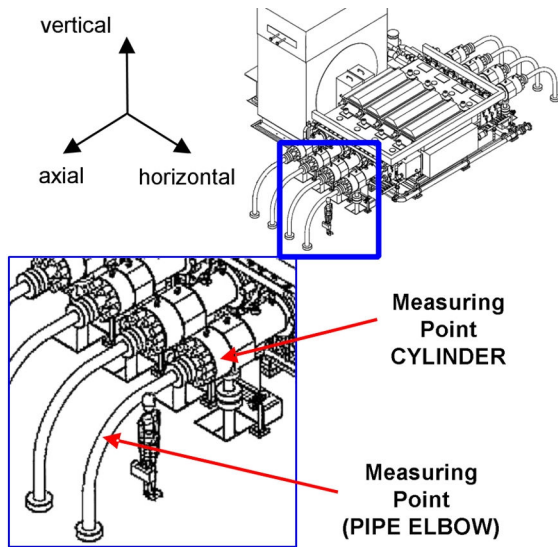


Figure 2.1: Measuring points (horizontal direction) at the secondary compressor discharge piping

The vibration velocity time signal is shown in figure 2.2 for the horizontal direction. The corresponding RMS-, peak-to-peak values and amplitudes for vibration displacement, velocity and acceleration are listed in Table 2.1.

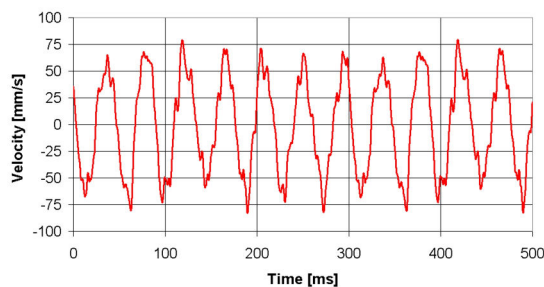


Figure 2.2: Vibration velocity time signal at the pipe elbow (horizontal direction)

DISCHARGE PIPE ELBOW				
PERPENDICULAR				
		RMS	0-P	P-P
Displacement	s (mm)	98.1	185.18	370.36
Velocity	v (mm/s)	12.59	33.07	66.14
Acceleration	a (m/s ²)	14.924	288.64	577.28
HORIZONTAL				
		RMS	0-P	P-P
Displacement	s (mm)	340.62	614.88	1229.76
Velocity	v (mm/s)	45.66	83.7	167.4
Acceleration	a (m/s ²)	19.349	193.485	386.97

Table 2.1: RMS-value and amplitude for vibration displacement, velocity and acceleration at the pipe elbow

The gap between these measured vibration displacement values and the theoretically determined values are shown in figure 2.3.

Remarkable differences can be noticed for the 1st and 7th harmonic. The measured high horizontal vibrations are showing an existing out-of-plane force and a research into an out-of-plane excitation source suggests itself.

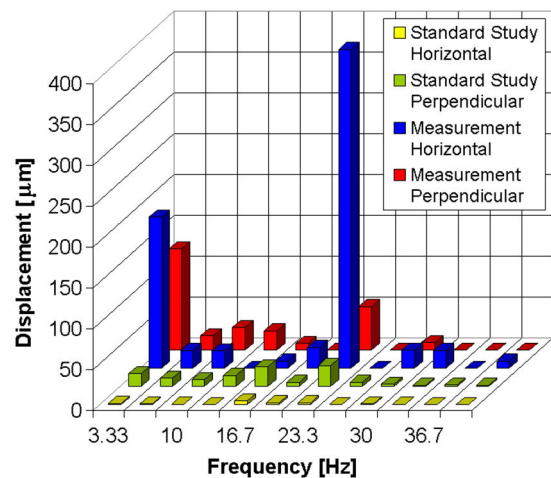


Figure 2.3: Comparison of measured and calculated vibration displacements amplitudes at the pipe elbow

3 Approach to improve the vibration analysis

It is a known fact that the pulsation and vibration study only includes in-plane shaking forces for a pipe bend. This is due to the fact that a fluid flow through a pipe bend could only generate forces acting in the plane of the pipe bend. Therefore, it is obvious that out-of-plane (horizontal direction of the measurement) results are missing in a standard pulsation and vibration study.

Especially for larger compressors, compressor manifold vibrations are important as the mass of compressor parts and pulsation dampers increases, which leads to low-resonance frequencies, which may be excited by pulsation forces, by gas loads in the compressor cylinder, and by unbalanced forces, and moments of the compressor.

One excitation source could be the deformation behavior of the compressor structure. It is well known that highly loaded compressors such as secondary compressors are showing remarkable cylinder movements in all directions during operation. Therefore, the idea came up to take these forced cylinder displacements and corresponding phases into account and to implement them into the compressor manifold study.

A further improvement for the vibration study should be realized by this approach and the results should help to minimize the need for subsequent costly and time-consuming corrective measures.

The paper describes such an enhanced vibration study for the secondary compressor and shows the comparison between calculated and measured results.

4 Preliminary static analysis

4.1 FE-model and boundary conditions

In order to calculate the deformation behaviour of the secondary compressor under load a 3D-CAD model of the hyper compressor including frame, crankshaft, distance pieces, cylinders and cylinder supports have been setup. Frame and distance pieces have been modelled in detail whereas crankshaft and cylinders were modelled with simplified cylindrical volumes. This partial simplification of the solid model is necessary in order to reduce the amount of elements and calculating time.

The 3D-CAD model was imported into the finite element (FE) program and prepared for the analysis. The final model consists of 155'000 elements and 271'000 nodes. Contact elements were included at the bearings between crankshaft and compressor frame. Figure 4.1 shows the FE model of the hyper compressor.

The load boundary conditions on the FE-model are the gas forces acting on each cylinder and the forces acting on the crank shaft. The crank case and the cylinder supports have been fixed at the bottom.

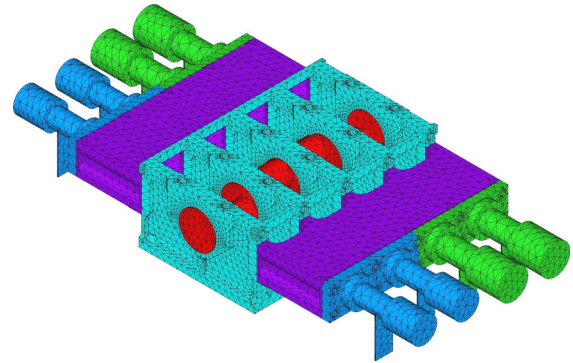


Figure 4.1: FE model of the hyper compressor

The gas forces on the individual cylinders are calculated for each crank angle with an appropriate compressor sizing program. Taking into account the inertia and the operating speed, the resulting forces on the crankshaft pins were also calculated. Figure 4.2 shows the force progression over one revolution on a 2nd stage cylinder (gas force) and the crankshaft pin (resulting force).

Due to the fact that hyper compressors are operated in the low speed range (180-200 rpm) and therefore the dynamic effects are not dominant, it is sufficient to carry out a static structural analysis for several load steps. Preliminary studies turned out that a calculation is accurate enough using load steps with a crank angle difference of 10 degrees. Therefore 36 load steps are finally used for one revolution. The FE model of the crankshaft is rotated for each load step according to the crank angle.

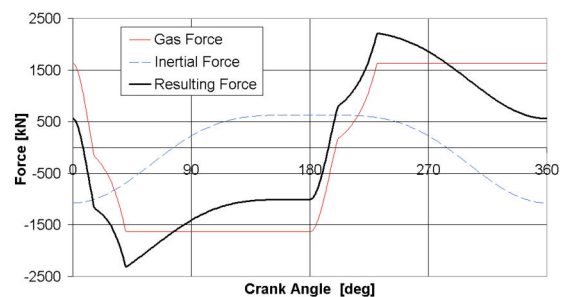


Figure 4.2: Gas- and resulting force during one revolution

4.2 Results of the static analysis

The deformation of the compressor over one revolution of the crankshaft is calculated in several nonlinear static analyses. The cylinder movement at the connecting flange to the piping is determined for all directions. Exemplarily the displacement results of a cylinder over one revolution are shown in Figure 4.3.

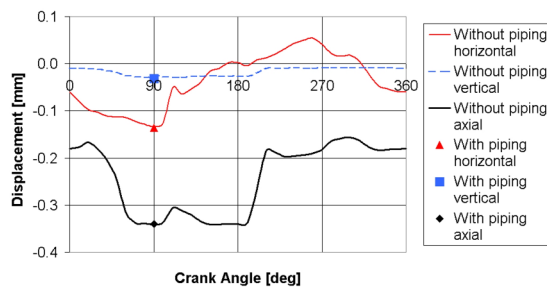


Figure 4.3: Displacements of a cylinder with and without attached piping in all three directions

Additionally, preliminary studies were carried out to answer the question whether attached discharge and suction piping have an influence on the overall cylinder movement. Figure 4.4 shows the total displacement of the compressor with discharge piping attached to 2nd stage cylinders at an angle of 90 degrees.

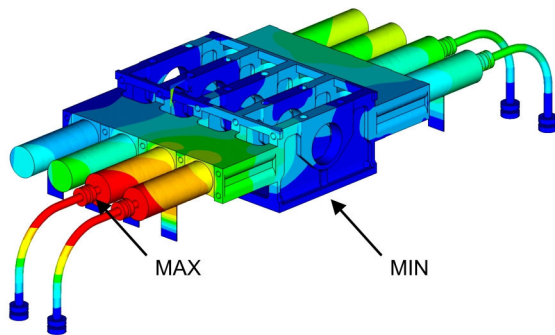


Figure 4.4: Total displacement of the hyper compressor due to gas forces with attached 2nd stage discharge piping at a crank angle of 90°

The cylinder displacement with attached discharge piping at a crank angle of 90 degrees is also shown in Figure 4.3. The comparison of all calculations for different “with and without” piping configurations showed that the piping has only a small influence on the global movement of cylinders. Therefore the piping can be excluded from the static analysis and thus leading to a further reduction of analyzing time.

The cyclic cylinder displacements are of interest for the harmonic response analysis. If these cyclic cylinder displacements are of similar shapes and if they are only depending on the load it might be possible to use a general load curve with an offset for each cylinder for the vibration analysis.

To compare the cyclic cylinder movements the results have been superimposed, so that the curves are independent of offset and phase. E.g. the axial displacement in figure 4.3 has a large negative offset while the cylinder on the opposite side (not shown) has a large positive offset with a phase shift of 180 degrees. To eliminate the offset a Fourier analysis has been carried out. The first Fourier coefficient is the offset and was set to zero.

Figure 4.5 shows calculated, superimposed cyclic movements of all cylinders in horizontal, axial and vertical direction (directions as defined in Figure 2.1).

The results for axial movements are quite similar for all cylinders (1st and 2nd stage). The results for vertical movements are showing small differences between 1st and 2nd stage cylinders. Due to the fixed cylinder support, the amplitude of the vertical direction is about a magnitude lower. The horizontal movement of a cylinder depends on the cylinder location at the frame. For example, a cylinder in the middle has an influence on adjacent cylinders, so they are partially out of phase to the corresponding gas load.

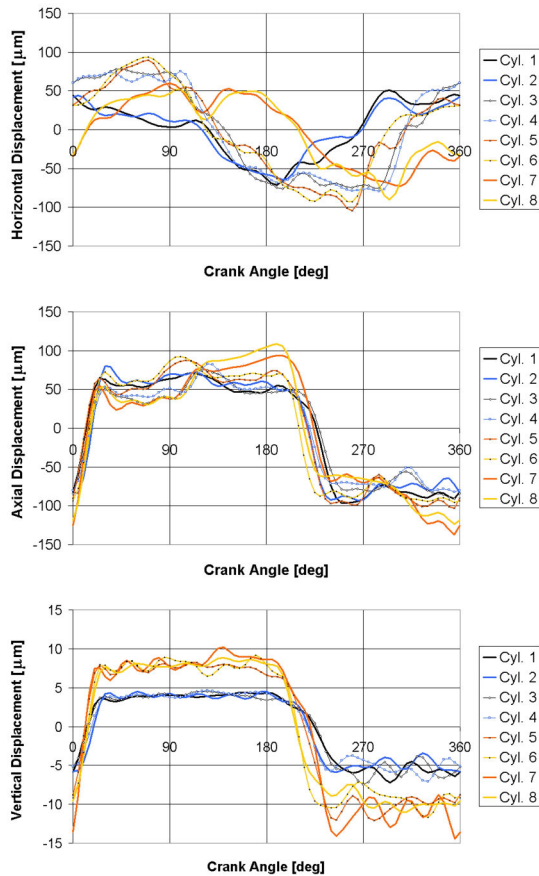


Figure 4.5: Fast Fourier Transform for horizontal, axial and vertical movement of the cylinders due to gas forces

The result especially for the horizontal component shows that a general cyclic displacement behavior does not exist. Therefore, an individual analysis for specific compressor configurations has to be carried out in order to get the input for a following harmonic response analysis.

4.3 Comparison of the static results with measurements

For the harmonic response calculation of the vibration analysis the Fourier coefficients of the cyclic cylinder movement are needed. Figure 4.6 shows calculated horizontal displacement components for first 12 orders. The cyclic movement of the cylinders was measured and the comparison of calculated and measured displacements of a cylinder in horizontal direction is also shown in Figure 4.6. At the cylinder an amplitude for the first order of 187 µm was measured and the analysis result matches quite good with a value of 154 µm.

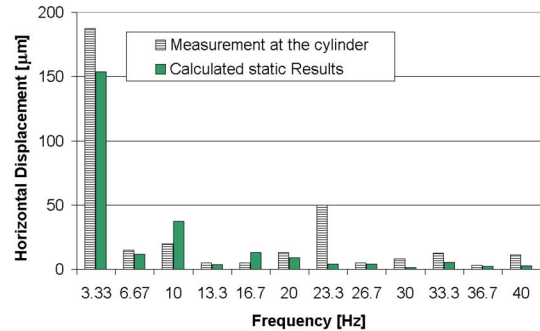


Figure 4.6: Measured and calculated horizontal displacement at the cylinder

5 Extended vibration study

A simple FE-model for the vibration study typically is built up with pipe- and beam elements. However it is important that the simplified compressor model is accurate enough, e.g. modeling of the cylinder support to simulate a realistic vibration behavior.

5.1 Modal analysis

Due to the measured values (shown in Figure 2.3) a natural frequency of the system seems to occur at a frequency of 23.3 Hz (7th order). Therefore in an additional step a modal analysis of the simplified pipe- and beam model was carried out. Figure 5.1 shows the result for the first natural frequency (23 Hz) of the discharge elbow pipe of the 2nd stage. This natural mode shows a displacement in the horizontal direction.

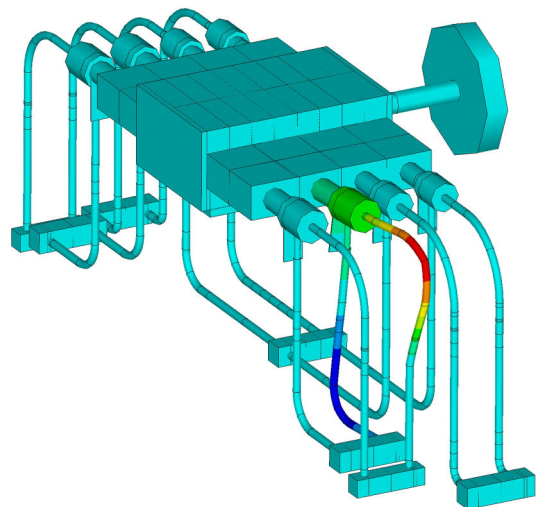


Figure 5.1: Natural frequency at the elbow pipe of the 2nd stage (23 Hz)

5.2 Results of the extended vibration analysis and comparison with measured values

The model for the vibration analysis is now extended with the cyclic cylinder deformations. Due to some limitations of the FE program⁴ the displacements have to be transferred into corresponding forces acting at the cylinders. This was done within an additional static analysis. Figure 5.2 shows the result for such an improved vibration study for the horizontal displacement component at a discharge elbow pipe.

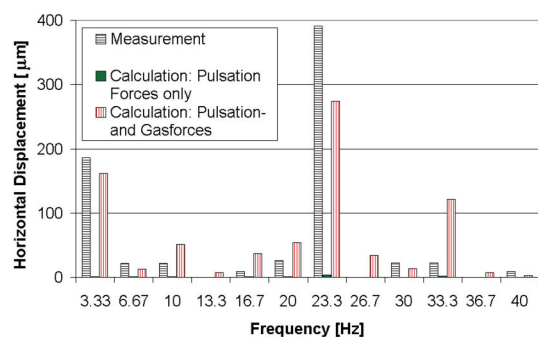


Figure 5.2: Measured and calculated (dynamic) results at the elbow pipe

The calculated results are now matching quite well with the measured results.

The standard vibration study without forced cylinder displacements shows only a slight displacement in horizontal direction (Figure 2.3), even if a natural mode exists for the examined piping configuration at 23 Hz (see chapter 5.1). The reason for this discrepancy is the missing horizontal excitation. Within the extended vibration study the horizontal displacement of the elbow pipe is excited due to forced cylinder movements.

This example shows the necessity and the benefits of an improved pulsation and vibration study. The results of such a study are helping to minimize the need for costly and time-consuming corrective measures as shown in the following chapter.

5.3 First corrective measures

During the measurement campaign, the effects of connecting neighboring elbow pipes with stiffening bars have been examined. Especially the horizontal vibrations at 23 Hz (7th order) could be reduced to an acceptable value. The reduction of the vibration level is shown in Figure 5.3.

Taking the modified boundary conditions (coupled discharge elbow pipes) into consideration the analysis also shows a corresponding reduction (Figure 5.3). Therefore using such an improved pulsation and vibration analysis might have helped to optimize the discharge piping configuration in an early stage of the project.

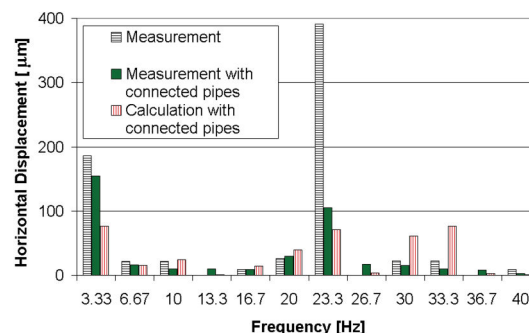


Figure 5.3: Influence of connected elbow pipes on the horizontal displacement behavior

6 Summary and conclusions

Reciprocating compressors, including pulsation dampers and connected pipe system, are often the heart of an installation and should therefore operate reliably. Compressor manifold vibrations can contribute to fatigue failure of the system that can lead to unsafe situations, loss of capacity, increase in maintenance and repair costs.

To avoid these situations a compressor manifold analysis has to be carried out in an early stage of the design. In the API Standard 618 such an analysis is mandatory in a Design Approach 3 analysis.

For such an analysis, the dynamic properties (stiffness and mass) of compressor parts have to be modeled in a proper way to accurately predict the natural frequencies and consequently the dynamic response (vibrations and cyclic stress levels) of a compressor manifold. Pulsation and mechanical response analyses have proven to be effective tools to predict pulsations and vibrations for reciprocating compressors.

The precise modeling of the complete pipe system is necessary for the pulsation study. Subsequently the pulsations and pulsation-induced shaking forces are calculated and compared with maximum values allowed.

For the mechanical response study a mechanical model is built up which includes all important components influencing the mechanical natural frequencies and cyclic stresses. The mechanical model is excited by the pulsation induced forces and corresponding phases. Subsequently, the vibrations and cyclic stresses in the pipe system are calculated. A full Design Approach 3 analysis of the API Standard 618 also includes the detailed modeling of the compressor manifold. Therefore the so-called compressor manifold vibration or better compressor manifold stiffness is considered in the analysis too.

Measurements have shown that for specific compressor configuration horizontal vibration displacement, velocity and acceleration components are dominant for pipe bends. The excitation source could be found in the global deformation behavior of the compressor structure. Highly loaded compressors such as secondary compressors are showing remarkable cylinder displacements during operation. A further improvement for the vibration study could be realized by taking these forced cylinder displacements and corresponding phases into account. Such an enhanced pulsation/vibration study for a secondary compressor has been performed. The calculated and measured results agree very well for the enhanced study.

The results are helping to minimize the need for subsequent costly and time-consuming corrective measures. For example, investigations on how to combine some of the discharge pipes are possible in an early stage of the project.

This procedure supports the effort of continuously improving the reliability and efficiency of reciprocating compressors.

7 References

- ¹ API Standard 618, 4th edition, June 1995, "Reciprocating Compressors for Petroleum, Chemical and Gas Industry Services".
- ² Pyle, A., Eijk, A., Elferink. H., "Coming 5th edition of the API Standard 618, Major changes compared to the API 618, 4th edition", 3rd EFRC Conference, 27-28 March 2003, Vienna
- ³ Eijk, A., Samland. G., Retz N., Sauter D., "Economic Benefits of CAD Models for Compressor Manifold Vibration Analyses according to API 618", 3rd EFRC Conference, 27-28 March 2003, Vienna
- ⁴ ANSYS Users' Manuals, Release 10.0, SAS IP, 2005



Dynamic analysis of large intercoolers and tubular reactors installed in LDPE plants with an Hypercompressor

by:

Marco Passeri

Matteo Romiti

Stefano Generosi

Engineering

GE Infrastructure, Oil & Gas

Florence, Italy

**5th Conference of the EFRC
March 21-23, 2007
Prague, Czech Republic**

Abstract:

The development of the market of large-scale LDPE plants requires larger and larger compressor and plants. Such extreme applications, involving ultra-high pressure piping and potentially high-pressure pulsations need a very detailed dynamic analysis of the complete plant. Special attention must be paid to the vibration aspects of intercoolers and tubular reactor, which may represent the most critical part of the system because generally mounted on tall steel structures. Due to the long delivery of such components, a proper selection should be done at an early stage, when just a preliminary layout and equipment drawings are available. This implies the assessment of plant pulsation-induced forces and the subsequent definition of layout adjustments and of piping supports locations, type and supporting structures. The study must take into consideration the actual jacketed tube configuration (i.e. concentric process and cooling medium pipes), to avoid internal vibrations, which are difficult to be monitored and may produce unexpected failures. The final review of the plant arrangement should bring just minor adjustments.

1 Introduction

Low Density Polyethylene plants have critical equipment like intercooler and tubular reactors operating up to very high pressures, up to 350 MPa or -50,000 psi.

Pulsation and vibration control on high-pressure piping is necessary to prevent failures caused by cyclic stresses, due to both internal pressure fluctuations and vibrations [7]. These stresses are also a consequence of the thermal expansion of the piping. Pressure and flow pulsations generate acoustic energy that interacts with the plant's mechanical system to cause mechanical vibrations. The magnitude of the vibrations depends on the amplitude and frequency of the acoustic pulsations and on the elasticity, mass and damping effect of the mechanical system. Considering that the damping effect is very low when large vibrations are encountered, it is essential to predict the behaviour in advance, so that unexpected vibrations do not occur during plant start-up, as these can cause significant production losses.

For these applications, API states, "the corresponding cyclic stress should be carefully evaluated". The usual approach starts maintaining the total pressure pulsation within reasonable values, then the analysis continues to verify, piping supports locations, and relevant supporting structures. Furthermore special attention must be dedicated to the intercoolers and tubular reactor that are generally mounted on tall steel structures and may be the most critical part of the system. The jacketed piping (an internal process pipe surrounded by an external cooling pipe) must be included in the model to prevent internal vibration problems, difficult to detect and able to produce unexpected failures. In fact, it is very difficult to modify on site the internal pipe pins or their location.

The goals of safety and reliability can only be achieved by a thorough analysis of all components and aspect of the pulsation and vibration effects. Innovative methods of simulation and modelling improve the ability to evaluate piping and equipment behaviour, obtain greater efficiency and achieve smooth, safe plant operation.



Figure 1: Hypercompressor LDPE

The unsteady gas flow of reciprocating compressors generates pressure pulsations that are increased by acoustical resonance, in relation to plant configuration and fluid characteristics. High vibration and noise levels, and reduced performance are possible consequences [3, 4, 5, 6]. Therefore an effective plant design requires:

- an acoustical analysis, to avoid acoustical resonance and to control pressure pulsation and shaking forces level;
- A mechanical analysis of the piping system, intercoolers and tubular reactor structures to avoid mechanical resonance and maintain vibrations and stresses within the limits.

Some guidelines should be followed in the design of the structure, piping supports and piping jackets so that to minimize the modification during the study stage.

2 Nomenclature

Dkn	oscillation amplitude of the kth degree of freedom in the nth natural mode
FE	Finite Elements
F _n	generalized force of nth mode $\sum_j F_j D_{jn}$
m _n	generalized mass of the nth mode $\sum_j m_j D_{jn}$
N	Number of the degrees of freedom, equal to the number of the calculated natural frequencies
t	time
x	coordinate distance along the axis of the tube from an arbitrary origin
x _k	displacement of the kth degree of freedom
θ _n	angle of phase
ω	Exciting frequency
ω _n	frequency of the nth mode shape

3 Acoustical analysis

The plant configuration can be analyzed under all operating conditions through a digital study, including speed variation, capacity control and multiple compressors running in parallel. Piping, cylinders, valves, orifices, intercooler and reactor must all be considered in the study [6, 7].

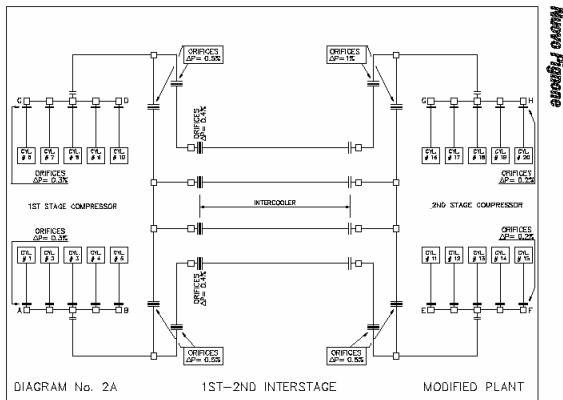


Figure 2: Example of typical interstage

For all significant points the pressure pulsation level, shaking forces acting on the equipment and piping (bends, change of size, etc.) are calculated and compared with the limits requested by the customer or with the internal experience. At very high pressure, the speed of sound in ethylene considerably varies (as a function of pressure and temperature (1000 – 2000 m/sec.) Since these compressors operate in a wide range of pressures and temperatures, it is easy to fall in resonance with some natural acoustic frequencies. Wavelengths are very long (300 – 600 m); therefore required adjustments changes in pipe length and in the position of piping connections may be in the order of several meters and therefore difficult to achieve [7].

The most frequent remedy is the use of orifices, located in positions where the maximum velocity of the standing wave field occurs. In fact damping efficiency increases with the drop in pressure, which in turns depends on the square of the instantaneous gas velocity through the orifice itself. The standing wave field is the addition of several harmonic components, each with a certain frequency, module and phase. The orifice positions are selected so that the predominant harmonics are damped out.

However residual pulsation, even if limited can have high harmonic components and, due to the high mean pressure, may still generate high shaking forces. The pressure pulsations and their phase are recorded so that they can be applied at each discontinuity points of the mechanical model during the mechanical analysis.

4 Piping Vibration and Cyclic Stress

The mechanical study investigates the natural frequencies and the forced response of the plant, to keep vibration amplitudes and stresses within allowable limits. This is achieved firstly by defining the number and position of piping supports so that the mechanical natural frequencies are separated from the most significant exciting frequencies [5]. Guidelines, based on experience and preliminary acoustic analysis, lead the initial mechanical design. In general use of such guidelines prevent significant modifications due to the final mechanical analysis. Typically the guidelines set the allowable values of:

- Minimum piping mechanical frequency
- Maximum force applicable at each support
- Maximum span between two consecutive supports
- Size (function of pipe elevation) of beams of racks

In general, high mechanical natural frequencies allow for better mechanical behaviour; therefore care should be given to maximizing overall stiffness and minimizing improperly supported masses. Some practical advice in this regard includes the following:

- Piping should be placed as close as possible to the ground for easier application of stiff supports;
- Concentrated masses such as elbows, tee joints, valves etc should be adequately supported;
- Supports and supporting structures should be much stiffer than supported components;
- An axial constraint should be provided for any straight pipe sections to contrast axial shaking forces.

The mechanical analysis starts with the FEA calculation of piping mode shapes and associated natural frequencies [4].

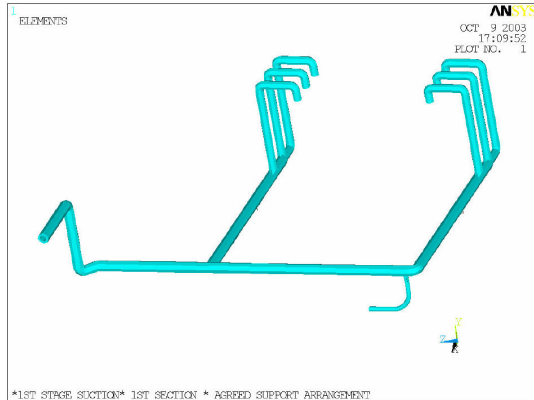


Figure 3: Finite elements model of suction pipe

The piping shaking forces determined with the pressure pulsation analysis are automatically introduced as input data during the final mechanical tuning of the plant. In this phase, the dynamic behavior of the complete piping system is investigated. When required, a combination of additional orifices and supports can be chosen so that the overall impact on the plant's cost and performance is minimized [4].

First step is to verify piping support locations and types. Once the locations and types of supports determined, it is possible to calculate supporting reaction forces so that the suitability of standard supports can be verified and, in case, adjusted to withstand to these loads. Then, the overall forced response of the piping system is calculated, using the technique of "modal super-imposition", as the sum of the response of each mode to the exciting harmonics, each with its module and phase. For a system having N degrees of freedom the response to harmonic excitation is given by:

$$x_k = \sum_{n=1}^N \frac{D_{kn} F_n}{\omega_n^2 m_n} \frac{1}{\sqrt{(1 - \omega^2 / \omega_n^2)^2 + (2\zeta \omega / \omega_n)^2}} \sin(\omega t - \theta_n)$$

Once the total response of the piping system in terms of vibration amplitude has been calculated, the relevant stresses are also obtained.

Then, the procedure explained in ASME VIII-2 appendix 5 is applied to calculate the maximum alternate stress. The stress is compared with the allowable cyclic stress limit, to verify its suitability. The actual cyclic stress limit for carbon steel is defined either according to customer specification or starting from the API cyclic stress limit of 179 MPa (26000 psi), reduced to take into account stress concentration and safety factors [2].

The allowable vibration amplitude is generally based on either API limits or Customer experience. The program may be used for design purposes (by imposing the displacement, velocity or acceleration limit) or as a verification tool, in case of field problems. [4].

5 Intercoolers and tubular reactors vibration and cyclic stress

Of course a complete procedure cannot be limited to the piping analysis therefore the study should continue to verify that intercooler and reactor structures are adequate to maintain vibrations and cyclic stress within allowable limits. Considering the high cost of this equipment, the experience of the manufacturer and designer, may be not sufficient to avoid dynamic problems. A dynamic study is really recommended in new applications in term of plant size or operating parameter.

Finally, the jacketed pipe (an internal process pipe surrounded by an external cooling pipe) should be verified to ensure that internal pins are properly designed to avoid vibration problems that are more difficult to monitor and that, in most cases, can produce failure prior to giving evidence of the phenomena except for the noise.

Considering the great difficulty that can be encountered implementing the pins design in the field, unless the application is very similar in terms of compressor arrangement and piping size to one already running smoothly, it is advisable to confirm the design of the pins with an accurate vibration check. Guidelines, based on experience and preliminary analysis, must lead initial mechanical design of the structure piping supports and piping jackets so that to minimize the modification during the study stage.

- Span between two piping supports must assure a minimum mechanical frequency higher than the main harmonic component of the exciting forces (e.g. 5th one in case history described later). This span represents an initial guideline for the main structures spacing.
- Maximum friction force applicable at each support (considering the minimum friction factor) shall allow movements only for thermal loads (i.e. fixed point for relatively low dynamic forces)

PULSATIONS & VIBRATIONS

Dynamic Analysis of Large Intercoolers and Tubular Reactors Installed in LDPE Plants with a Hyper Compressor

Marco Passeri, Matteo Romiti, Stefano Generosi; GE OIL & GAS

- Size (function of pipe elevation) of beams of racks sufficiently rigid to avoid coincidence of mechanical natural frequency and main harmonic component of the exciting forces. In case high elevated structure are necessary due to physical constrains the introduction of a central concrete tower is suggested.
- Main racks beam must be wind braced so that to maximize the structure stiffness using the minimum size of beam.
- Internal pins on jacketed pipe must be spaced so that to assure a minimum mechanical frequency higher than the main harmonic component of the exciting forces (e.g. 5th one in the case history described later)
- Internal pins on jackets must be located at the minimum distance (e.g. 300 mm from external supports)
- Generally the pins allow the axial sliding, therefore each straight jacket pipe shall have a tube assembly so that to allow an axial constrain at the inner pipe.

In the following chapter a case history has been reported to describe GE Oil & Gas approach to the integrated study of intercoolers and tubular reactors and the complete procedure attended in the vibration analysis.

6 Case history

6.2 Model description

The case considered represents the dynamic model of a large intercooler installed in a plant for the production of low-density polyethylene and connected to a GE O&G compressor, type 20PK/2.

The compressor train considered insists in two different streams each one connected to 5 cylinders (72° phased) therefore the main harmonic component present on the common line is the 5th one and its multiples. In the case considered the 5th harmonic order of the nominal compressor speed (i.e. 214 RPM) corresponds to 17.8 Hz.

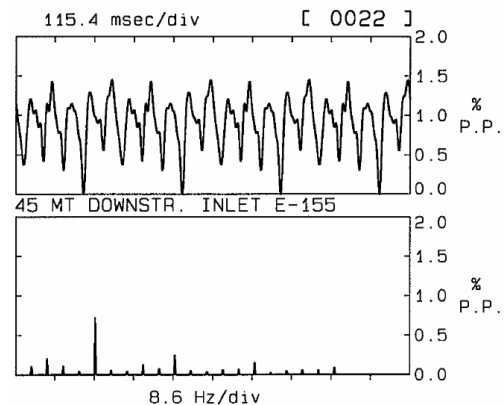


Figure 4: Pressure Pulsation spectral analysis



Vertical column pipes composed the intercooler steel structure, horizontal bracing pipes and wall beam pipes. All sliding pipe supports have been considered dynamically fixed with the High Pressure-pipes, due to the high friction forces. The HP piping and jacket have been simulated on the model so that to verify the internal pins spacing suitability. In the FEM model all these items were modeled with PIPE elements with the relative diameter and thickness.

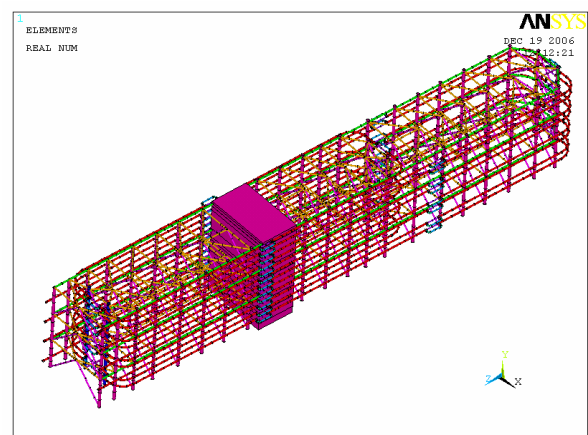


Figure 5: Intercooler structure FEM model

The concrete tower that supported the steel frame structure has been modeled with a single beam with appropriate inertia and material properties (see Fig. 6). Ground flexibility of the anchor tower is taken into account introducing three spring elements with the appropriate rotational and axial stiffness. The equivalent beam simulating anchor tower is connected to the structure by rigid links (see Fig.7). Two different damping materials relative to steel structure ($\xi = 0.02$) and concrete tower ($\xi = 0.05$) have been considered in the model. Figure 3 and 4 shown some views of Ansys model.

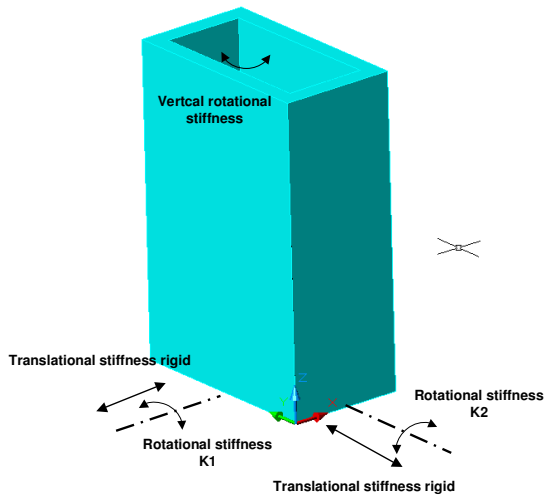


Figure 6: Anchor tower

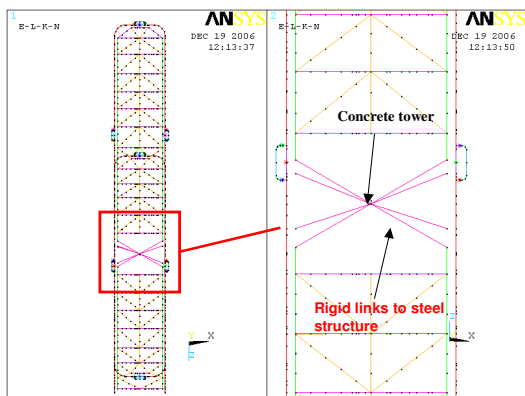


Figure 7: Anchor tower FEM model

6.3 Original structure mechanical natural frequencies

The mechanical natural frequencies and the mode shapes of the original structure were calculated using Ansys code and GE O&G proprietary code. From the modal analysis it resulted that the 1st natural frequency (i.e. 15.102 Hz) was near the 5th harmonic component (i.e. within the frequency tolerance of $\pm 20\%$ approx around the 5th harmonic order of nominal compressor speed) and that the relative mode shape is such as to be excited by the shaking forces acting on the axial direction (long side) of the intercooler piping system (Fig. 8).

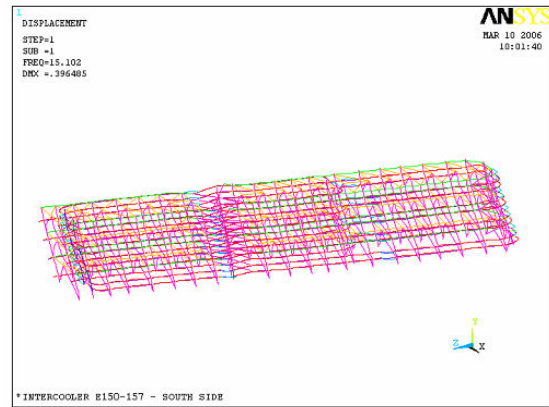


Figure 8: 1st Mode – resonance condition with 5th harmonic

6.4 Harmonic analysis

The amplitudes of the input pulsation shaking forces were obtained from the results of acoustical simulation. A forced response analysis was performed using proprietary software.

This program has been developed to automatically couple, in resonance condition, each calculated mode shape with each harmonic component of the shaking forces that falls within the defined margin. Furthermore the study performs the analysis for of all the examined operating conditions, to define the “worst case condition”. In the specific case this was detected with the 5th harmonic component under a specific operating condition.

PULSATIONS & VIBRATIONS

Dynamic Analysis of Large Intercoolers and Tubular Reactors Installed in LDPE Plants with a Hyper Compressor

Marco Passeri, Matteo Romiti, Stefano Generosi; GE OIL & GAS

As explained above once the worst-case condition was determined by GE O&G code the same case was performed by means of Ansys code. The analysis was carried out considering a tolerance of $\pm 20\%$ approx around the 5th harmonic order of nominal compressor speed). The pressure pulsation loads relevant to 5th harmonic applied to intercooler structure FEM are shown in fig 9.

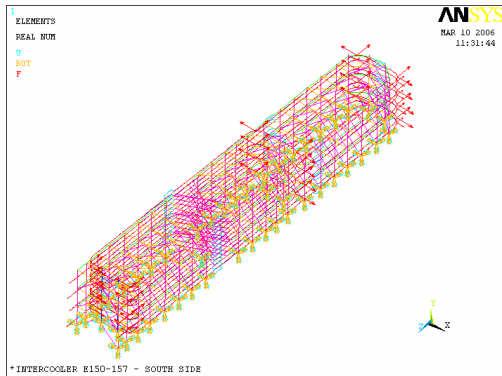


Figure 9: Pressure pulsation loads applied

The results of the original layout indicated that in the range of frequency considered (i.e. 14.3 Hz-21.4 Hz) there is a peak of resonance coupling the 5th harmonic component and mode shape corresponding to 1st natural frequency with maximum vibration amplitude of 1160 μm peak to peak (allowable 393).

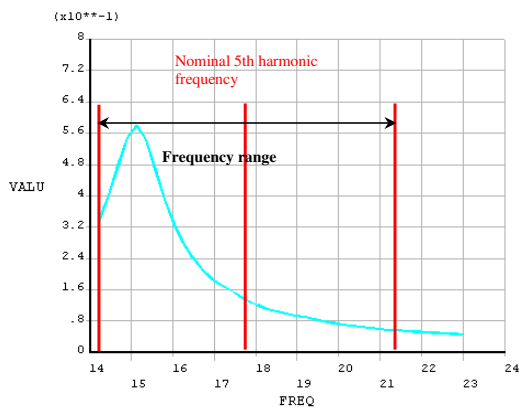


Figure 10: Forced response frequency range

The deformed shape relative to the forced response analysis shows that the high vibration levels were not due to local movements but to the whole structure, moving in the direction of the long side of the intercooler.

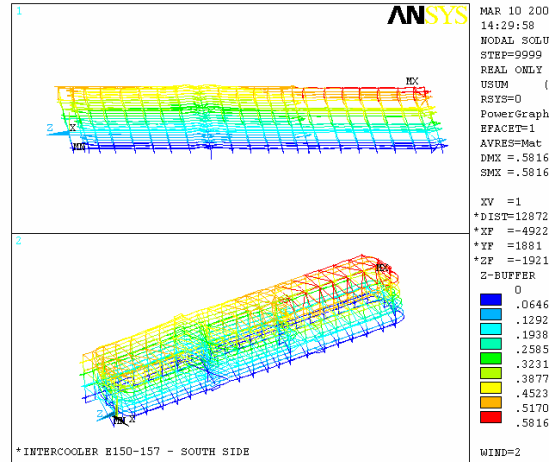


Figure 11: Vibration amplitude at resonance frequency (max 0.58 mm zero to peak = 1160 micron p.p.)

Vibration limit curve based on “Standard piping vibration criteria and verified by GE O&G field measurements (black line) with indicated maximum calculated vibration amplitudes at resonance frequency (blue circle) are show in Fig 12.

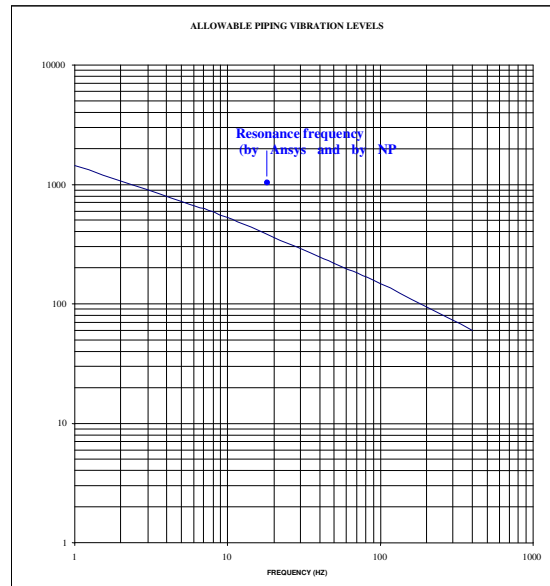


Figure 12: Vibration limit curve of original structure

On the basis of forced response analysis performed the following conclusions have been drawn:

- 1st mode shape of the structure excited by 5th harmonic component, if coupled in full resonance, cause resonance vibration amplitudes that strongly exceed the limit indicated in Fig.12.
- The deformed shape of the structure with high vibration levels strongly depends on the characteristic and base constrains of concrete tower, unable to be a fixed point for the dynamic behaviour of the intercooler.

Considering above evaluation it was decided to introduce some modifications that imply the increasing of original structure stiffness and reduction of the applied shaking forces so that to minimize the max vibration amplitude in the whole range (i.e. at least +/- 20%) considered in the analysis as per standard procedure.

6.5 Proposed modified structure

In order to reduce vibration amplitudes the following modifications were been evaluated:

Introduction of lateral bracings $\phi 139.7 \times 8$ mm in the steel structure to increase stiffness. This should be made in both lateral frame beams (blue color on FEM model).

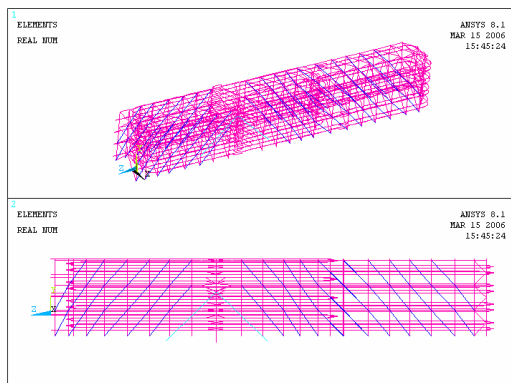


Figure 13: Lateral bracings added plus raked props on both side

As evidenced from forced response analysis, in order to avoid deformations of the whole structure that cause high values of vibrations, the concrete anchor tower must act as a fixed point for the dynamic behavior of the intercooler, breaking off the continuity of the deformations.

Two solutions have been studied, with a different impact in the re-design of the concrete tower and the structures connected:

- Introduction of three raked props on both sides of the column (see fig. 14)
- Enlargement of the anchor tower, as shown in Fig. 15, with a significant increase of inertia properties and ground stiffness.

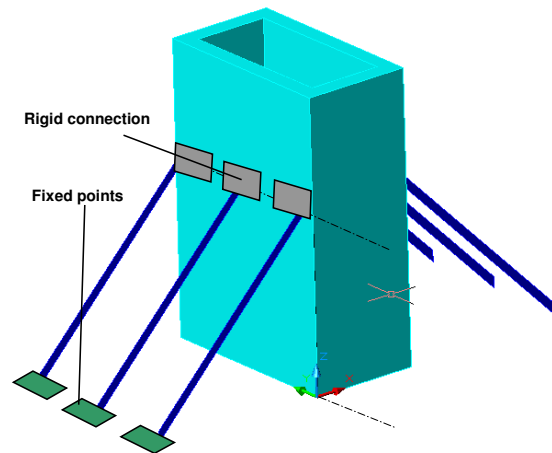


Figure 14: 1st proposed solution

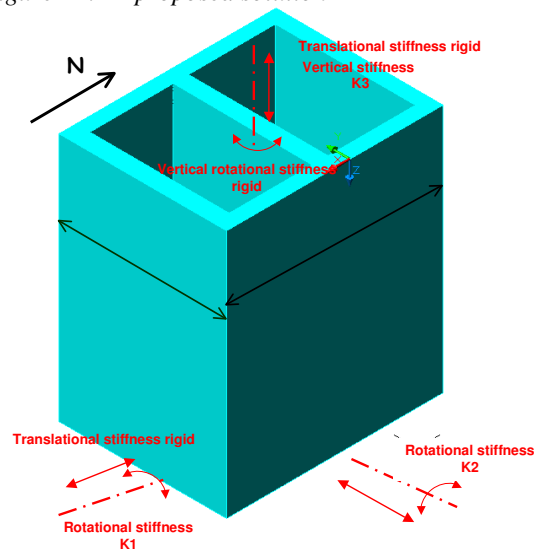


Figure 15: 2nd proposed solution

The second solution was then selected, because the stage of the project did allow such modification, more effective both from structural and design point of view. The FEM model was updated with the 2nd solution (i.e. structure with a larger concrete tower Fig.16). In the picture a not hollow anchor tower is shown, however in the study an equivalent section with proper inertia properties was considered.

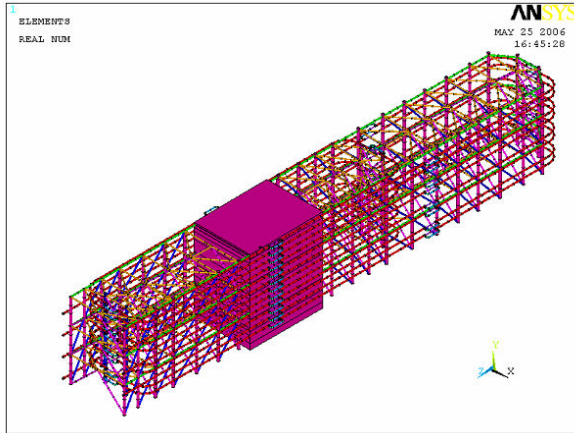


Figure 16: FE model modified structure

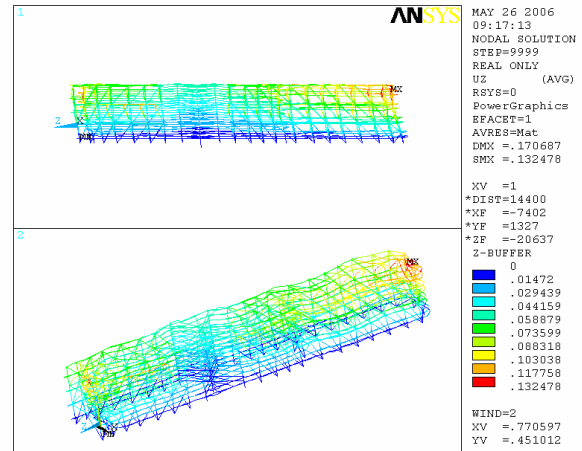


Figure 18: Max Vibration amplitude by Ansys - modified model at upper extreme of range

6.6 Harmonic analysis

Forced response analysis was been repeated by GE O&G and Ansys codes using the modified model. Results of the analysis evidenced that the axial mode shape became the 6th mode (i.e.25.1Hz) and came out of 5th harmonic component range tolerance. The concrete anchor tower turned out to be sufficiently stiff to de-couple the two steel sides of the structure. This time the “worst case condition” was detected, with a lateral mode shape, still close to resonance with the 5th harmonic component.

The resonance curve calculated by Ansys for the axial mode shape is shown in Fig. 17. The study shows that, in the considered frequency range, the enlarged concrete anchor tower, together with additional orifices, produces a drastic reduction of the axial mode shape peak-to-peak vibration amplitude, from 1160 micron to 264 micron peak to peak, at the upper limit of frequency range (see Figs. 17 and 18).

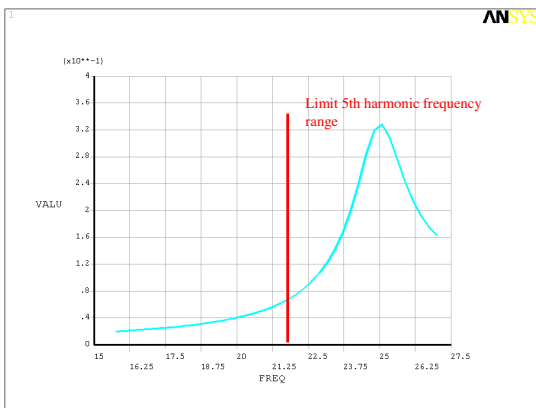


Figure 17: Resonance bell curve axial displacements

In the modified configuration the resonant mode shape involving axial displacement is out of the frequency range and the vibration amplitude in axial direction at the extreme of the range is within allowable limits.

The max. vibration amplitude detected by Ansys code with the modified layout is caused by a lateral mode shape, as indicated in fig 20, with max peak-to-peak amplitude equal to 284 micron.

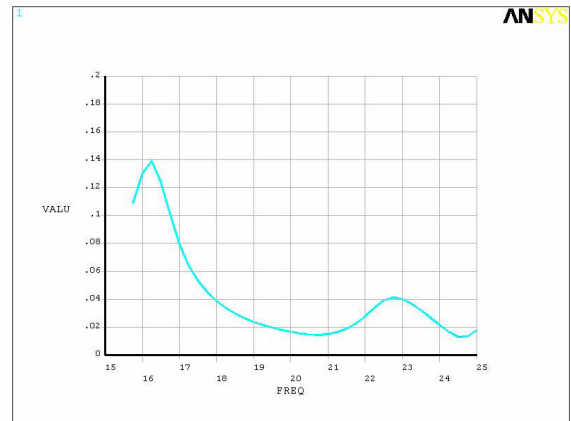


Figure 19: Resonance bell curve lateral displacements

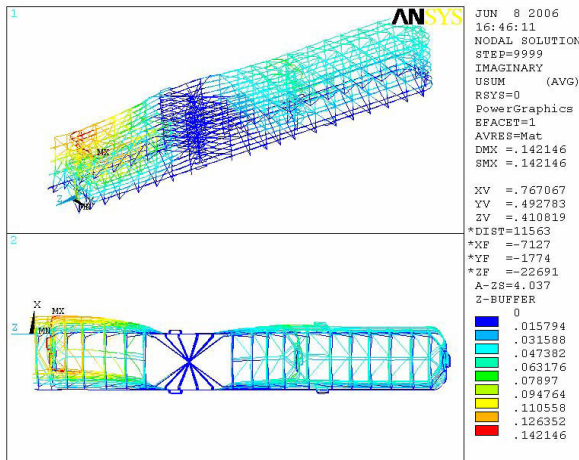


Figure 20: Max Vibration amplitude detected with a lateral mode shape

With the 2nd solution the maximum cyclic stress detected with GE O&G code is 13.4 N/mm² (allowable 20.6 N/mm²). In conclusion, the max vibration amplitude was dramatically improved from 1160 micron (peak to peak) to 264 micron for axial mode and 284 for lateral mode, by stiffening the structure and adding the required orifices. It should be noted that the worst case occurring in the range of +/-20 of the frequency has been considered for judging the suitability of the structure.

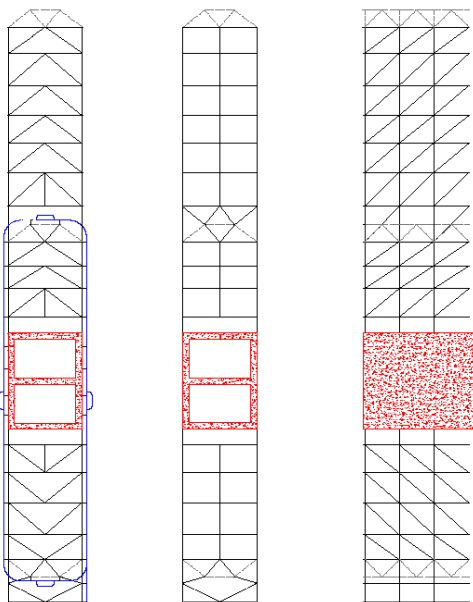


Figure 21: Final structure layout

6.7 Forced response of intercooler piping jackets

As described above, the jacketed piping (i.e. internal process pipe and external pipe) was included in the model and verified to ensure that internal pins were properly designed to avoid internal vibration. The standard support tightening has been considered sufficient to stop the dynamic forces, therefore the piping supports were considered as they were rigidly connected to the structure.

The amplitude of dynamic reaction forces acting on the support and equipment due to pressure pulsations were calculated. These values were calculated by a technique of “modal superposition” (static forces are not included). The forces resulting from dynamic analysis were multiplied by a factor 1.5 to take into account any contingencies. In fig 22 a part of the jacket pipe is shown, internal pin and relevant FEM model.

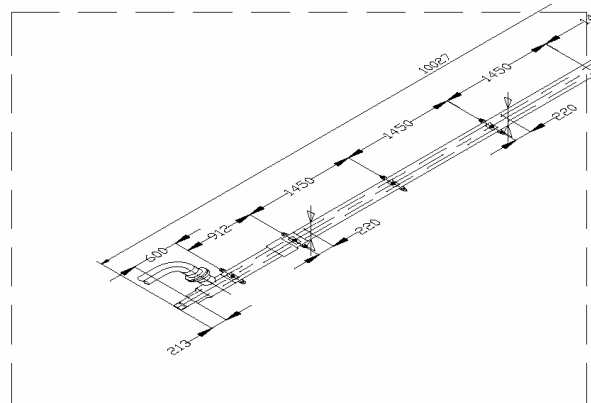


Figure 22: Jacketed pipe

7 Conclusions

Design is important for safe, reliable operation of hyper-compressors and their connected piping system.

The recommended procedure is to perform a preliminary acoustical and mechanical study of the complete plant prior to proceed with procurement of the material. When a complete preliminary study procedure is followed, the final acoustical and mechanical study is expected to only require minor modifications, such as orifices and/or change in some support types or additional wind braces.

The pulsations have to be analyzed with advanced modeling methods. Since they have an appreciable impact on both the compression cycle and valve operation, a proper evaluation of these phenomena is required. The vibration level is strongly influenced by the piping arrangement and supporting structure. Therefore only a depth static and dynamic analysis can assure proper performance, reliability and availability of the whole plant. Such an approach requires a strong cooperation between compressor manufacturer, equipment manufacturer, end user, engineering contractor and vibration specialists since any decision must be taken in a short time and necessary modifications must be shared among all involved specialist.

These calculations should be repeated in case of machine up rating involving modification of compressor components, piping arrangement or operating conditions.

8 Acknowledgments

The authors wish to thank GE Infrastructure, Oil & Gas and Nuovo Pignone S.p.A. for granting permission to publish the information reported in this paper.

9 References

- [1] API 618 STD fourth ed., June 1995, "Reciprocating Compressor for Petroleum, Chemical and gas Industry services" American Petroleum institute. pp. 37-42 and 147-148)
- [2] ASME - Boiler and Pressure Vessel code, sect. VIII Div. 2 2001, The American Society of Mechanical Engineers
- [3] Giacomelli E., Passeri M., Giusti S., Zagli F., Generosi S., 2004, "Modeling of Pressure Pulsations for Reciprocating Compressors and Interaction with Mechanical System", Proceedings of ESDA, Engineering System Design and Analysis, 19-22 July, Manchester, UK, The American Society of Mechanical Engineers.

[4] Giacomelli E., Passeri M., Zagli F., Generosi S., 2004, "Control of Pressure Pulsations and Vibrations in Hyper-compressors for Ldpe Plants" ASME/JSME Pressure Vessels and piping conference, PVP – Vol. 473 High Pressure Technology 2004, Innovations and advances in High Pressure Technologies, July 25-29 2004 S.Diego California U.S.A. PVP2004-2281, The American Society of Mechanical Engineers.

[5] Giacomelli E., Passeri M., Zagli F., Ranfagni L., 2004, "Acoustic and Mechanical Analysis of Reciprocating Compressors-Optimizing Plant Reliability and project Schedule", ICEM 12-12th Int. Conference on Experimental Mechanics, 29 August –2 September, Politecnico di Bari, Italy, McGraw-Hill...

[6] Generosi S., Passeri M., 1995, "The Control of Vibrations Induced by Reciprocating Compressors on Plant Piping: New Developments in Calculation Methods", *Quaderni Pignone* N. 56

[7] Giacomelli E., Passeri M., Giusti S., Zagli F., Generosi S., 2004, "Modeling of Pressure Pulsations for Reciprocating Compressors and Interaction with Mechanical System", Proceedings of ESDA, Engineering System Design and Analysis, 19-22 July, Manchester, UK, The American Society of Mechanical Engineers.



Mitigation of high-frequency pulsations, using Multi Bore Restriction Orifices

Leonard van Lier and Harry Korst
Department of Flow and Structural Dynamics
TNO Science and Industry
Delft
The Netherlands
Leonard.vanlier@tno.nl

5th Conference of the EFRC
March 21-23, 2007
Prague, Czech Republic

Abstract:

In reciprocating fluid displacement systems, a trend toward high-speed machinery and application of stepless reverse-flow capacity control system is observed. Badly designed compression systems may cause excessive high-frequency noise and vibration levels, which are a risk from a structural integrity point-of-view. Furthermore, noise levels, conflicting with both environmental and HSE legislation may result in reduced system capacity or even process shutdown. Therefore, a robust system design should focus on the mitigation of high-frequency pulsations in an early design stage. This paper highlights the multi-bore orifice plates (MBRO's) as powerful damping devices of in-line, high-frequency pressure pulsations. MBRO's provide efficient pulsation damping behavior at high frequencies (up to 1 kHz) where conventional (single bore) orifices plates fail. Within the TNO research program, in collaboration with Hoerbiger, prediction models have been developed that describe the static and dynamic performance of MBRO's. Experimental validation confirms the validity of these models. The models have been integrated in the TNO prediction tools (PULSIM) for pulsation analysis of reciprocating fluid machinery.

1 Introduction

Developments in compressor technology, such as reverse-flow capacity control systems and high speed machinery, have led to unwanted effects, such as high frequency pulsations, vibrations, cyclic stress levels and noise radiation [1].

A commonly used mitigation tool to reduce pulsation levels in a pipe system attached to reciprocating machinery are restrictions orifice plates. For these simple (single bore) configurations, analytical models are available to predict the acoustic behaviour in the low-frequency limit. These so-called quasi-steady models are valid for low values of the Strouhal number fd/U . The damping effect of orifice plates is a complex physical mechanism, associated with interaction between the acoustic field and unsteady vorticity shedding. Part of the acoustic energy of the pulsations is converted into turbulence and hence dissipated into heat. An important parameter that determines the amplitude of the effective damping effect is the static pressure drop over the orifice plate. For reliable design tools, it is therefore necessary to have accurate prediction models for the static pressure drop.

Peters [2] illustrates that single bore restriction orifices are effective only up to a certain frequency limit. By applying multi bore restriction orifices, the upper frequency limit will be shifted to higher frequencies. This upper limit is determined by the orifice geometry (orifice hole diameter) and the flow speed, displaying a strouhal number behaviour.



Figure 1: Single bore and multi bore orifice plates

A first step is to develop more advanced models for the static orifice behaviour (static pressure drop). For single bore restriction orifices, empirical models are available. Based on relatively simple physical modelling, a more general model is derived, that predicts more accurately the pressure drop of a single bore orifice and that allows for prediction of multi bore restriction orifices as well.

Important model input parameters are:

- Number of holes (N)
- Individual hole diameter (D_o)
- Orifice thickness (L)
- Position of orifice in the pipe system
- Beveling of the orifice edges
- Wall friction

The prediction model has been validated using an extensive experimental survey, and a significant increase in accuracy is observed, relative to the existing models.

Analytical models for the dynamic behaviour (acoustic damping) exist for quasi-steady conditions only. Experiments were used to determine scaling rules that give empirical relations for the upper frequency limit as function of the orifice and flow parameters. A general and robust relation was found from the experiments.

This relation and the advanced models for the static behaviour are integrated in the TNO prediction software PULSIM, and in a stand-alone prediction tool. This extension of the PULSIM capabilities is thought to be a useful and practical extension, which allows low-noise design of high-speed compression systems with flow capacity control, in an early design stage.

2 Static behaviour MBRO's

A general and common way to express the static pressure drop over a constriction element in a flow is the non-dimensional pressure loss coefficient K_w . It is normalized with the dynamic pressure:

$$K_w = \frac{\Delta p}{\frac{1}{2}\rho U^2} \quad (1)$$

The flow velocity U is defined as the velocity in the pipe. A useful empirical relation that is commonly used for single bore restriction orifices is Kramer's formula [3]:

$$K_w \approx 2.7 \frac{(1-\alpha)(1-\alpha^2)}{\alpha^2} \quad (2)$$

This relation gives an order-of-magnitude estimate of the pressure loss coefficient as a function of the open area ratio α .

Preliminary experiments indicated however, that this relation is not appropriate for prediction of Multi Bore Restriction Orifices and cannot account for effects of the orifice location in the pipe system [2]. Therefore it was decided to investigate possibilities for more advanced modelling, starting from simple physical models.

The mechanism can be illustrated best by considering figure 1.

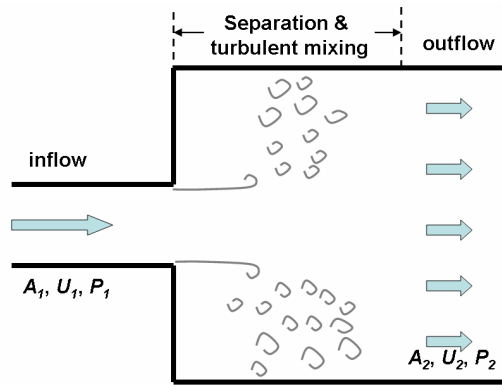


Figure 2: General expansion with separation, turbulent mixing area and reattached outflow

When the flow meets a sudden expansion of the duct, the flow will separate due to the adverse pressure gradients. The separated flow will re-attach after a turbulent mixing region. The initial pressure is not fully recovered, but is partly lost into heat, via turbulent decay. The pressure loss due to an expansion from area A_1 to A_2 is given by Miller [4] (pressure loss is based on U_1 , the flow speed in the upstream part).

$$K_w = \left[1 - \frac{A_1}{A_2} \right]^2 \quad (3)$$

Flow contractions are always associated with pressure gradients alligned with the flow direction: these are reversible processes and therefore no significant turbulence is generated. For prediction of pressure loss, only the flow expansion phenomena need to be considered

2.1 Vena contracta effect

When considering the pressure loss due to an orifice, an additional phenomenon occurs that is crucial for correct prediction of the pressure loss: the vena contracta effect.

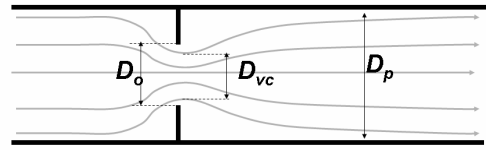


Figure 3: Vena contracta effect in a constriction

The flow contracts to an effective diameter, that is smaller than the geometrical diameter of the constriction. Instead of using the pressure loss associated with the expansion from the orifice hole diameter (D_o) to the pipe diameter (D_p), the expansion from the vena contracta (D_{vc}) to the pipe diameter (D_p) should be considered. The contraction coefficient ϕ is the ratio of the cross section of the contraction to the cross section of the orifice hole ($\phi = A_{vc}/A_o \sim (D_{vc}/D_o)^2$) and has a typical value of 0.6-0.8. Its exact value depends on the open area ratio and an empirical relation is given by Miller [4].

2.2 Orifice thickness

When considering orifices, 2 cases should be distinguished: a thin orifice, where the orifice thickness L is small compared to the orifice diameter D , and a thick orifice, where the orifice thickness is large compared to the orifice diameter.



Figure 4: Thin and thick orifice configurations

In the thin orifice ($L/D \ll 1$), the flow expands in a single step from the vena contracta diameter to the pipe diameter. In a thick orifice ($L/D > 1$), the flow expands in two steps: first from the vena contracta to the orifice hole diameter, (re-attachment in the orifice hole). Second, the flow expands from the orifice hole diameter to the pipe wall diameter. The 2-stage expansion process, causes a smaller pressure loss than the single stage expansion in a thin orifice. The ratio L/D is a critical parameter, especially in the case of Multi Bore Restriction Orifices. For intermediate cases ($L/D \sim 1$), an empirical transition function is applied.

2.3 Wall friction effect

In a thick orifice ($L/D > 1$), wall friction effects need to be considered in the prediction model for the pressure loss. This is especially true for MBRO's. The additional pressure drop associated with wall friction, for an orifice with N holes, with an individual diameter D is described by [4]:

$$K_{w, friction} = f_D \frac{L}{D} \sqrt{N}, \quad (4a)$$

with the Darcy friction factor f_D given by:

$$f_D = 0.25 \left[\log \left(\frac{k}{3.7D} + \frac{5.74}{Re^{0.9}} \right) \right]^{-2}, \quad (4b)$$

with k the wall roughness and Re the Reynolds number in the orifice hole.

2.4 Orifice position

When an orifice is not placed in a uniform pipe, but immediately upstream of a large vessel (for example a pulsation damper), the pressure loss changes. This is due to the fact that the flow does not expand to the pipe wall diameter, but to the effective diameter of the large vessel. This effect can be accounted for by considering the effective diameter of the large volume. Also when the orifice is placed immediately downstream of a large volume, the pressure loss is affected. This, however, is a result of the modified vena contracta behaviour, due to the modified inflow conditions. Both effects are included, using models described by Miller [4] and Idelchik [5]. For the intermediate cases (orifice located close to volume, at a distance dx) an empirical transition function is applied.

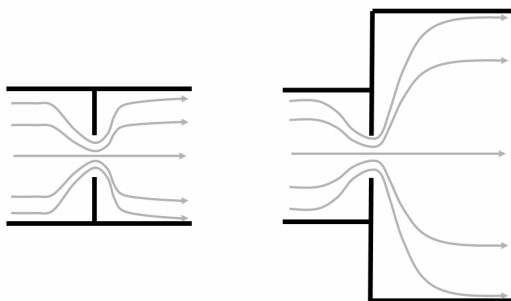


Figure 5: Orifice location: in pipe and upstream of a vessel

In general, the pressure drop of an orifice increases when it is placed close to a large volume, and deviations up to 90% may occur, when the simple formula (2) is applied.

2.5 Beveling of orifice edges

When the upstream edge of an orifice is beveled, the vena contracta will be affected: a smaller contraction (larger contraction coefficient) will be observed, and hence a lower pressure loss. This effect is included in the model, using the results of Idelchik [5]. Beveling the downstream edge, does not affect the vena contract behaviour, but reduces the effective orifice length.



Figure 6: Orifice with beveled upstream and downstream edges

3 Experimental validation

To validate the performance of the prediction model and the improvement relative to the simple empirical relation (2), an extensive set of experiments was performed.

3.1 Experimental setup

The experiments were carried out at TNO's flow test rig facility.

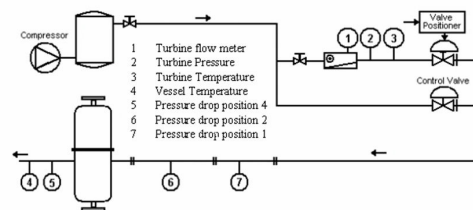


Figure 7: Experimental setup for static pressure loss measurements

The compressor delivers air at a pressure of approximately 7 bar. A control valve reduces the pressure to nearly atmospheric conditions, allowing to control the flow between 0 and 100%. With a static pressure sensor, the absolute pressure drop over different orifices was determined, accounting also for the intrinsic pressure drop, due to friction effect in the pipe system. The static pressure drops were determined in an indirect way, which is a significant improvement, relative to the method applied in [2]. That method was limited to orifices placed relatively far from the large vessel. Furthermore, the measurement accuracy in [2] was limited, because pressure losses were determined too close downstream of the orifice, in the pressure recovery region.

The pressure loss coefficients were determined by measuring the flow speed with a turbine flow meter, and determining the density from a static pressure and temperature measurement. The following experimental parameters were investigated:

- Orifice design: open area ratio α : 0.3 - 0.6
- Orifice design: number of holes N : 1 - 81
- Orifice design: orifice thickness L : 6 - 20 mm
- Orifice design: straight and beveled edges
- Orifice position: 7 positions up and downstream of a large vessel
- Flow speed U : 5 - 20 m/s.

3.2 Results

As an illustration, the effect of changing the number of holes, while keeping the open area ratio constant, is illustrated in figure 7. We compare the improved model prediction with the old Kramers model (equation 2). Since we keep the open area ratio constant ($\alpha=0.4$), the Kramer model (equation (2)) predicts a single value, independent of the number of holes. This is clearly not appropriate: increasing the number of holes, while keeping the open area ratio constant decreases the pressure loss. Furthermore, the Kramers formula seems to predict significantly too high values for the pressure loss, which may lead to insufficient accuracy margin when designing orifice solutions.

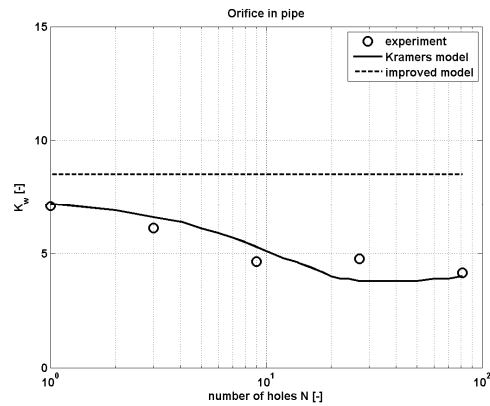


Figure 8: Comparison of Kramers model, improved model and experiments: orifice in pipe

Furthermore, the Kramers formula cannot deal with the effect of the orifice position. This is illustrated in figure 8. The effect of the position is evident: placing an orifice closer to a large vessel will increase the pressure loss.

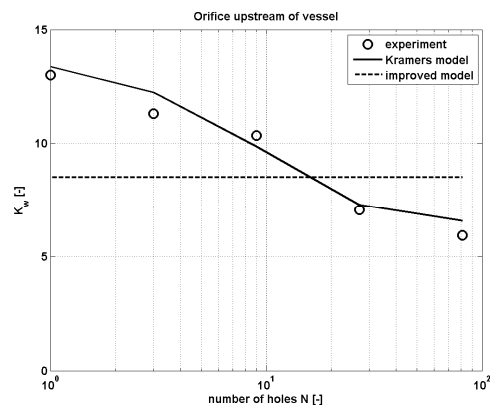


Figure 9: Comparison of Kramers model, improved model and experiments: orifice upstream of vessel

The overall conclusion regarding the prediction model for pressure loss, is that a significant improvement is obtained with the new model, compared to equation (2). Many important engineering parameters were incorporated into the new model, like number of holes, orifice location, orifice thickness and beveling properties. The prediction results are all within 20% of the experimental data.

4 Dynamic behaviour of MBRO's

Single Bore Restriction Orifices are commonly used to reduce low-frequency pulsations ($f < 100$ Hz) and reliable (quasi-steady) models are available to predict the performance [2],[6],[7]. However, at higher frequencies SBRO's are generally less effective, as they only generate additional pressure losses, without adding significant damping.

In this frequency range, quantitative modelling of the damping effect is not straightforward, and out of the scope of this paper. Aim of this study is to determine experimentally how large the damping effect of MBRO's is, compared with quasi-steady theory, and to determine empirical guidelines that indicate the maximum frequency for which a given MBRO design displays significant damping behaviour.

4.1 Quasi-steady modelling

Peters and others [7] present a quasi-steady theory for the damping efficiency of a single bore restriction orifice, located in a uniform pipe, or at the exit of a uniform pipe. The quasi-steady theory is valid, when the Strouhal number, associated with the flow and the acoustic field, is small compared to unity:

$$Sr = \frac{fD_p}{U} \ll 1 \quad (5)$$

For MBRO's, this requirement can be formulated in terms of the individual hole diameter, and to the velocity in the vena contracta, which leads to smaller values of the Strouhal number, and presumably to a larger range of frequencies where quasi-steady behaviour is observed. Experimental confirmation of this was one of the goals of this study.

For a single bore restriction orifice at a pipe exit, the quasi-steady theory predicts a value for the reflection coefficient at the orifice location, that is related to the flow Mach number M and the pressure loss coefficient K_W :

$$R \approx \frac{MK_W - 1}{MK_W + 1} \quad (6)$$

Similar expressions can be derived for an orifice located at a distance x from the pipe exit. Equation (6) illustrates that for a given $M - K_W$ combination, a reflection-free termination is observed. Hence, no pressure build-up due to resonances will occur and the system has minimal pulsation levels.

Relation (6), valid for SBRO's allows for a generalization for MBRO's, by simply assuming that the K_W values obtained via the models described in the previous section, can be applied.

Changing the number of holes has two effects: it shifts the location of the minimum in R , and it affects the amplitude of the reflection coefficient. The lower the amplitude of R , the more efficient pulsations will be suppressed.

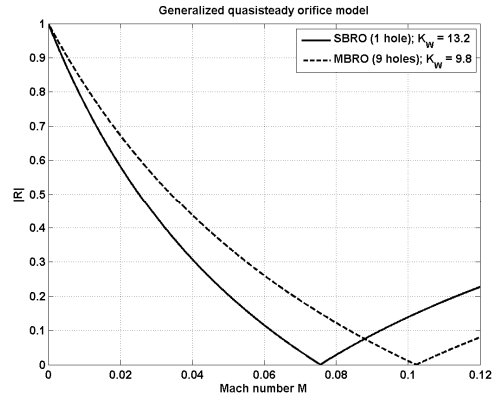


Figure 10: Generalized quasi-steady model for SBRO and MBRO with equal open area ratio α .

The assumption that this generalized models, and the predicted damping efficiency is valid for MBRO's was one of the goals of the experiments. Finally, the experiments should indicate the range of applicability, or the cut-off frequency f_c for efficient damping behaviour.

We choose the Standing Wave Ratio as a measure to quantify the damping efficiency of the orifice:

$$SWR = \frac{1 + |R|}{1 - |R|} \quad (7)$$

A low value of the Standing Wave Ratio (minimum 1) indicates a low value of R and hence a strong pulsation suppression. In this case the nodes and anti-nodes of the system are comparable, and no strong build-up of energy (resonances) can occur. A high value of the SWR indicates a reflection coefficient close to unity, and strong pressure build-up in the pipe system.

4.2 Experimental setup

In order to determine the standing wave ratio, or the reflection coefficient at the orifice location, the acoustic field needs to be decomposed in the downstream travelling wave (p^+) and the upstream travelling wave (p^-). The measurement technique commonly applied to determine reflection coefficients is the 2-microphone method, allowing to separate these 2 travelling wave components.

See [7] for a more detailed description of the 2-microphone method.

A comparable experimental setup was applied, as described in section 3. In this case however, a siren was applied, to generate strong and controlled pulsations. A frequency range of 20-900 Hz was applied, but the existence of higher-order harmonics allows also for evaluation at individual, higher frequencies. A set of 8 dynamic pressure transducers (PCB116 series) was applied to reconstruct the standing wave pattern in the upstream part of the pipe. Various sensor spacings were applied, in order to be able to cover the complete frequency range from 12 Hz to 2.2 kHz. A 8 channel DIFA analyzer was used for the data-acquisition and FFT-processing. For selection of appropriate transducer pairs, a minimum coherence of 0.9 was required. However, most data points had a coherence superior to 0.999.

The orifices plates are mounted at various upstream locations of the vessel ($dx = 0, 0.125, 0.25$ and 0.49 meter). Various orifice plates have been evaluated, with different number of holes, and thicknesses. Finally the tests have been repeated at various flow speeds.

For a fair assessment of the effect of the number of holes, orifices with different number of holes, but with the same K_W value must be compared. This is be done by fixing the orifice pressure loss, by means of taping-off some individual holes. Changing the position is clearly not a fair comparison, because the orifice position is an important parameter for the damping efficiency. To determine the number of holes that need to be shut-off, to reach a given pressure loss, we used the prediction model described in section 3. Validating this by measuring the actual pressure loss, confirmed again that the prediction tool works well, within 10% accuracy.

4.3 Results

An example of the reconstruction of the standing wave pattern is shown in figure 11.

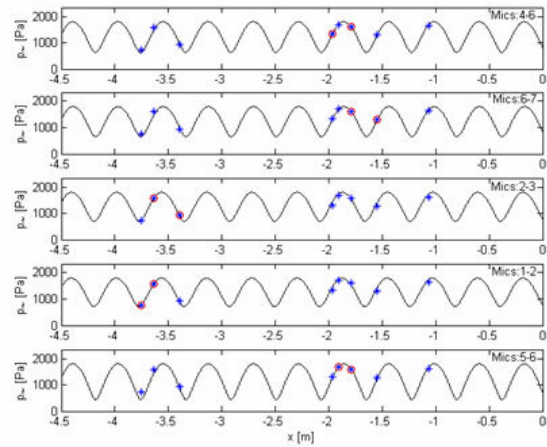


Figure 11: Two-microphone method: illustration of reconstructed standing wave pattern in upstream pipe section

An example of a measurement result is shown in figure 12.

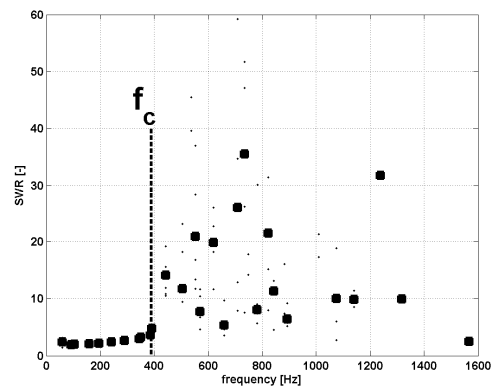


Figure 12: Example of standing wave ratio as a function of frequency, illustrating the cut-off frequency at 400 Hz

The trend is very obvious: a low-frequency region is observed, where low SWR occur, indicating that the pulsations are strongly suppressed by the orifice. Above a certain cut-off frequency (in this case at 400 Hz), the standing wave ratios increase significantly and the scatter becomes considerable. The large scattering is due to resonances that are excited in the large vessel downstream of the pipe.

A first check is if the measured standing wave ratio in the low-frequency range, corresponds to the predicted standing wave ratio, using the generalized quasi-steady model. This is confirmed by the figure below:

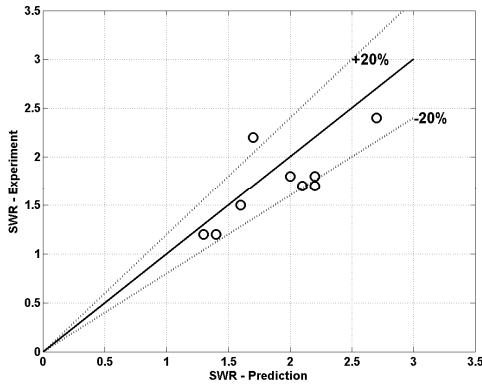


Figure 13: Standing wave ratios: generalized quasi-steady model prediction, and experimental result

The predicted value for the SWR, using the generalized quasi-steady model and the measured value in the low frequency range are consistent.

The second result is the value of the cut-off frequency f_c , above which the effective pulsation suppression is lost. This value depends on the number of holes and increases with increasing number of holes. It depends also on the flow velocity and increases with increasing flow velocity. The location in the pipe system is a crucial parameter. Two effects happen here:

- The pressure loss depends on the location relative to a large vessel (aerodynamic effect, see section 2.4)
- The standing wave pattern affects the damping efficiency (acoustic effect). Quasi-steady theory indicates that no damping occurs when the orifice is located at a velocity node.

When the orifice is located at $1/4\lambda$ from the pipe exit, the pulsation suppression reduces to zero. At frequencies where this $1/4\lambda$ distance occurs, the experimental SWR increase to very high values. This confirms that orifices are only effective when applied close to the pipe exit.

A general relation between the cut-off frequency f_c for an orifice located at the ideal location (pipe exit) can now be established, based on the complete dataset.

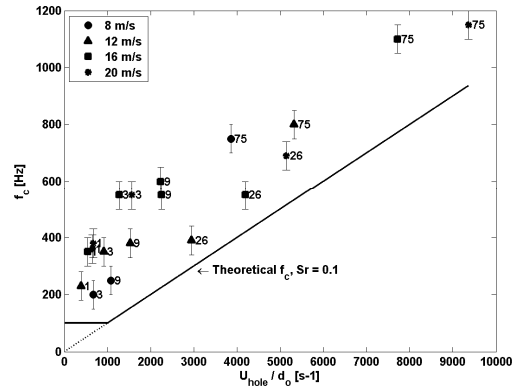


Figure 14: Relation between cut-off frequency and U/d for various orifices

A conservative estimate is made, in order to avoid over-optimistic estimates of the cut-off frequency:

$$f_c = 0.1 * \frac{U_{hole}}{D_o} \tag{8}$$

U_{hole} is the flow speed in the individual holes, and D_o is the individual hole diameter.

5 Prediction tools

The findings described in the previous sections have been implemented into engineering tools. Both as a stand-alone tool and fully integrated into the TNO PULSIM software, the knowledge can be applied in projects and allows for an efficient application of restriction orifices in piping systems.

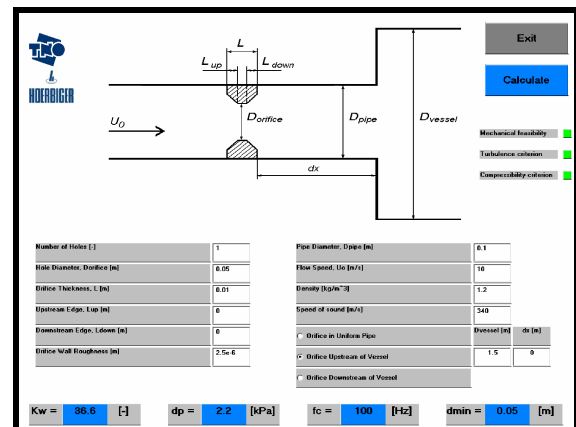


Figure 15: Standalone prediction tool for the static and dynamic behaviour of orifices

These tools give a fast and accurate prediction of the pressure loss coefficient for a given MBRO design, taking into account all the parameters discussed above: number of holes, hole diameter, location relative to large vessels, beveling properties, flow speed and wall roughness. Moreover, several automatic checks are performed that evaluate the validity of the mechanical construction, the compressibility criterion and Reynolds number criterion. This allows for a fast and reliable design and application of the orifice. Finally the software indicates the cut-off frequency f_c up to which the given orifice will perform efficiently.

6 Conclusions

The static pressure loss over an orifice is an important parameter that describes the pulsation suppression capabilities. Therefore, a more accurate model is required, than is currently available. A model with extended functionality has been developed. Extensive measurements confirm that the accuracy of this model is a significant improvement, compared with existing models.

A generalized quasi-steady model is validated, that extends existing models for application on MBRO's. This generalized quasi-steady model has been validated with measurements.

The cut-off frequency, up to which effective pulsation suppression occurs, has been determined empirically, and a robust relation in terms of orifices and flow properties has been postulated.

The findings of this research have been implemented in a commercially available stand-alone tool, and are integrated in TNO's PULSIM software. This ensures that the advanced functionality becomes available in pulsation studies, allowing for an efficient application of orifices in reciprocating compression installations.

TNO recommends to apply MBRO's only in case they are really needed, that is when high-frequency problems exist, that cannot be resolved with conventional orifices. This recommendation is strongly related to the fact that MBRO's may suffer from fouling and corrosion, to a larger degree than conventional SBRO's. With the results from this research and the tools that were developed, the design choice whether to apply MBRO's or SBRO's, can be made conveniently.

7 Acknowledgements

The results presented in this paper were obtained with the kind support of Hoerbiger.

8 References

- [1] H.Korst & W.Brocatus, "Noise reduction at a NAM compressor station", 4th EFRC conference Antwerp 2005.
- [2] M.C.A.M. Peters, "damping of low frequency noise in piping systems by means of perforated plates", ImechE conference 2003.
- [3] H.Kramers, Physical transport phenomena, 1961
- [4] D.S.Miller, Internal flow systems, 2nd edition, 1989.
- [5] I.E.Idelchik, Handbook of hydraulic resistance, 3rd edition, 1996
- [6] D.W.Bechert, "Sound absorption caused by vorticity shedding demonstrated with a jet", Journal of Sound and Vibration, 70(3), 1980.
- [7] M.C.A.M.Peters et al, "Quasisteady aero-acoustic response of orifices", Journal of the Acoustical Society of America, 110 (4), 2001.



Practice Report – Design and Commissioning of New Compressor Units

by:

Claus Pollok

Gas Storage Construction & Operation

E.ON Hanse AG

Hamburg

Germany

claus.pollok@eon-hanse.com

**5th Conference of the EFRC
March 21-23, 2007
Prague, Czech Republic**

Abstract:

E.ON Hanse AG installed in 2002 one 4 cylinder compressor unit and in 2006 two 4 cylinder compressor units at the Natural Gas Underground Storage Reitbrook near Hamburg. This script describes the practical application of the current standards related to these projects and gives numerous information's for planning and operation of reciprocating compressors. The section about the pulsation investigation before and after the installation of Pulsation-Damper-Plates gives detailed information's about the reason and effect of pulsation related to reciprocating compressors.

1 Introduction

1.1 General

Most natural gas consumed in Germany is used for heating. Due to differences in energy consumption over the seasons of the year and weekday / weekend cycles, consumption can vary considerably every day. Delivery rates per hour can be up to 25 times higher in winter than in summer.

For both technical and economic reasons, natural gas producers strive to keep gas production rates constant throughout the year. In contrast to this gas consumption rates vary considerably all the year round. As a result the need arises for storage of natural gas, i.e. accumulation of excess summer production quantities in order to cover peak winter demand.

E.ON Hanse purchases natural gas on the basis of long-term contracts covering the entire year. E.ON Hanse procures its natural gas on a "take or pay" basis, i.e. the entire quantity ordered is paid for whether delivered in full or not. This type of contract minimizes supply costs and ensures competitive prices for our customers. E.ON Hanse operates two giant storage facilities of completely different design located in Hamburg -Reitbrook and in Kraak (near Schwerin, Mecklenburg-Vorpommern) which accumulate excess summer production for use in the winter months. In addition E.ON Hanse has a cooperation agreement with Kiel City Works (Stadtwerke Kiel) for sharing of their storage facility in Kiel-Rönne.

Approx. 800,000 gas consumers are listed in the supply area of E.ON Hanse which extends from the Danish border to the Polish border. The customers are provided (sales by 31-12-2002) with 44.5 bn kWh of natural gas. Since 1973 the natural gas storage plant at Reitbrook / Hamburg is operated in cooperation with GdF (formerly PREUSSAG/Mobil Oil) by using the gas oil reservoir.

The Reitbrook gas storage facility has a "working" gas capacity of around 350 million m³, with a maximum output rate of 350,000 std.m³/h.

This development has been necessary by the increase of a maximum gas supply per hour from 140,000 std.m³/h coal derived gas in 1960 up to more than 600,000 m³/h natural gas in 1985 and up to approx. 900,000 std.m³/h at present time.

1.2 Compressors for Gas Storage

When the natural gas storage plant at Reitbrook was set into operation in 1973 it has been equipped with three W CUB - 2 H compressors with a capacity each of 9,600 std.m³/h by 21.6 bar on suction side, driven by one 8 cylinder gas- engine with the power of 625 kW.

The primary gas pressure delivered by the suppliers was in the range of 35 -40 bar for a long time. The current pressure operating conditions caused a positive effect for compressor operation at 40 bar. The output of each compressor rises up to approx. 20,000 std.m³/h.

In the subsequent years the compressor capacity had to be improved. In consequence to this two units of the same type have been installed in the years 1982 and 1986 each with a capacity of 20,000 std.m³/h. In total 5 compressors were in operation at the storage plant at the end of 1986.

Due to the storage expansion and technical upgrade in 1995 a DR CUB 4-OF6XH 1 compressor with 40,000 std.m³/h output at 40 bar suction pressure has been installed. This compressor was also equipped with a gas driven engine. The 12 cylinder Waukesha V engine delivers a power output of 1,664 hp/1,224 kW.

Now approx. 120,000 std.m³/h was the maximum capacity of the 6 installed compressors for storing.

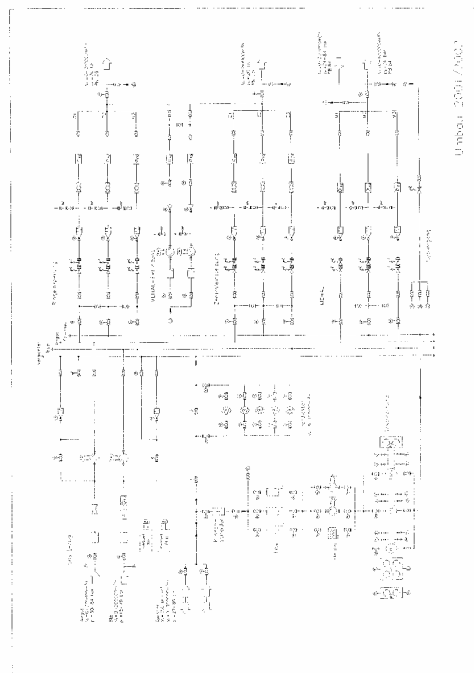


Figure 1: General layout of the natural gas storage plant Reitbrook in 2001/02

In the year 2000 our natural gas storage plant in Kraak (located near Schwerin) was set into operation.

In addition to the Kraak activities the condition of the almost 30 years old compressors in Reitbrook were reconsidered. In comparison to the 2 new compressors installed in Kraak with automated and remotely controlled operation, the equipment in Reitbrook could be described as the "old" compressors.

The decision was made to replace at first the oldest machines by a new unit with a nominal capacity of 60,000 std.m³/h. This has been decided under the aspect of potential failure, low automation level and technical availability. Next step should be done, to prepare the specification and commit the parameters for the basic design of the new compressor.

2 Basic Design

The price, the performance, the quality, the delivery date and the references belong to the essential aspects of a budget planning. For preparing the specifications, construction and inquiry specification we cooperated with an external engineering partner.

Basic values were:

A nominal design capacity of 60,000 std.m³/h at 40 bar suction pressure and 80 bar pressure at the outlet. Remote control operation and an electrical motor with frequency converter (FC) for a broad working range.

The preference of an FC operated electrical engine based on the fact, that in 2002 our "Hein Gas GmbH" company has been a subsidiary company of the Hamburg electrical power supplier HEW (currently Vattenfall). There was no problem to sign an acceptable contract for delivery of electrical energy at that time.

By the way, the electrical engine allowed the use of the existing foundation founded on caisson piles of one of the dismantled compressors.

2.1 Legal Requirements

Natural Gas Storage Plants are erected and operated in accordance to the German Mining Law (BBergG / Bundesberggesetz). The approval by the responsible state's mining authority requires all interventions and changes at the existing plant and the construction of new plants. I would like to skip the permission procedure without any explanation. It is a special theme.

2.2 Technical Requirements & Standards

DIN V 19250 Basic safety analyses for Measurement and Control Safeguard (MCS), May 1994 –cancelled 2004 see chap 2.2.5

DIN V 19251 Electrical instrumentation safeguards, February 1995–cancelled 2004 see chap 2.2.5

DIN EN 12583 Gas compressor plants, functional requirements, Nov. 2000

DVGW G 497 compressor units, March 2001,

2.2.1 DIN V 19250 Safety Analysis

Step 1 Risk Estimation

In this preliminary standard the basic safety analyses are treated for instrumentation safeguards. It becomes a qualitative method to the risk estimation described which then leads in the specification of the required classes in this preliminary standard that to this preliminary standard there are no corresponding international standards notwithstanding this one. To tighten the discourse by this preliminary standard the result is anticipated that analysis of the reciprocating compressor unit in the required class 3 (AK 3) has been on safety.

2.2.2 DIN V 19251 Measurement and Control Safeguards

Step 2 Requirements

For the application field of this preliminary standard there are no corresponding international standards at that time in 2002. The standard shall fulfil the choice of electrical instrumentation equipment with protections in order to avoid injuries of persons which can be caused by operation of the technical facilities and plants as agreed on.

Table: Specification of the requirements

Fault		
Without influence on the protection	With influence on the protection	
	Active fault	passive fault
Harmless, protection not touched	Harmless, triggering of protection in safe condition	Dangerously, protection blocked

2.2.3 DIN EN 12583 "Gas Supply Systems - Compressor Stations"

This standard describes the essential requirements for compressor units. It is applied to compressor units with an operation pressure of more than 16 bar and a total working output of more than 1 MW.

Topics of EN 12583 e.g.:

- Safety
- Quality assurance
- Environmental protection
- Planning, erection, examination
- Location and layout
 - layout
- Fence around areas --
 - limited access areas
 - explosive areas
 - streets and accesses
 - distances between facilities
 - electrical facilities
 - sign and signals
- Gas piping
- Compressor unit
 - engine / motor
 - compressor
 - unit control system (UCS)
- Modes
- Safeguards
- Supervision, rule and control equipment
- Alarm units
- Emergency shut down
- Safety pressure limiter (switch /valve)
- Safety temperature limiter
- Pumping prevention
- Revolution speed limit (safety revolution speed limit switch)
- Protection against inadmissible vibrations
- Flame monitoring system of the gas turbine
- Condition monitoring system (CM-System)
 - utilities of the compressor unit
- Gas warning installations
- Fire protection system
 - control and regulation of the station
- SCS system controlled of
- Emergency shut down of the station
- Gas warning installations
- Fire protection unit
- Control and supervision of the fittings of a station
- Business
- Maintenance
- Removal from service and disposal

Protection against inadmissible vibrations/condition monitoring system (CM):

In coordination with the experts it is definitely possible, to use the CM as a protection against inadmissible vibrations. This CM equipment would be safety relevant, as an element of the safety chain. The CM Condition Monitoring would be part of the experts' check scale in this constellation.

We decided to install a separate vibration switch. The advantage is now, that this item is not part of the monitoring CM and not to be inspected by the expert as an element of the safety chain. Changes of the limiting values up to the stop command remain in the exclusive responsibility of the operator. A change in the checked and approved safety chain is not necessary.

2.2.4 DVGW G497 Worksheet Compressor Units

The requirements listed in the mentioned worksheet are related to EN 12583 "Gas Supply Systems - Compressor Stations" as supplementary, obligatory requirements to the mentioned standard (DIN).

2.2.5 Amendment Conversion of IEC 61511, DIN V 19250 and VDI/VDE 2180

IEC 61511	DIN V 19250 (cancelled 2004)	VDI/VDE 2180
	AK (class)	range
	AK 1	risk range I
SIL 1	AK 2	
	AK 3	
SIL 2	AK 4	risk range II
SIL 3	AK 5	
	AK 6	risky to handle only by process control instrumentation & utilities
SIL 4	AK 7	
	AK 8	

3 The Decision for Compressor

The decision included all specified requirements and led to a 4 piston, double acting compressor (JGK 4). The supplier changed after signing the contract. The involved disciplines are listed below: Compressor delivery and engineering by a subsidiary company.

Electrical Engineering:
 Piping Engineering:
 PLC-Programming:
 Electrical Installation:
 Piping:
 Monitoring System:
 Time Schedule, Control and Supervision:
 Hein Gas / E.ON Hanse
 Examination: TÜV-Nord



Figure 2: Compressor unit 7 with new installed suction side piping and operation panel.

The contracting company closed the compression department a few weeks after contract signing. The skilled staff found a new job in Hamburg by the a 100% subsidiary company of Hein Gas currently E.ON. It should be mentioned, that also for experienced engineers such developments are consistently full of quite a number of problems which can get relevant regarding milestones at least, too.

This special situation required new milestones to be agreed on with the involved companies. The new compressor was ready for test operation as scheduled on July, 1st-2002 and could be tested during storage period over 3 months.

4 Upgrade of the Auxiliary Facilities

Due to the installation of the compressor 7 the compressor house has been equipped with a new gas detecting system and a new fire control unit. For the compressor engine separate 10 kV feed has been installed. We changed numerous ball-valves and installed maintenance-free ball-valves with electrical actuator in order to provide a remote controlled operation of the compressor unit.

5 Test Operation Experience

During test operation we tested the designed volume regulation control. We had no volume regulation of this type installed at any of our other compressors before. Our interest was appropriately high on that utility. We found out, that we did not need such volume regulation unit for storage operation and we decided to implement speed control additionally. The speed regulation range reaches from 600 to 1,000 min⁻¹ and covers the required operation range.

In fact we had a lot of problems with the interface between the frequency converter (FC) and the compressor PLC Programmable Logic Controller, Simatic S7, caused by the interface data log. These failures were eliminated during test operation.

6 Vibration Topic

Prior to the installation of the compressor unit 7 we have done no arithmetical vibration investigation. From our point of view the reason for this decision is given by only changing one unit and not erecting a new station.

At the end of the storage period and test operation we had the pulsation and piping vibration behaviour due to the installed new compressor at the maximum storage pressure of 80 bar investigated by a specialized company.

The piping system jointed to the compressor should be examined and if necessary the excitation mechanism of the inspected vibration situation should be indicated. It should be mentioned that during the test operation stronger vibrations of the piping where indicated particularly at a higher maximum storage pressure.

Figure 3 shows the layout of the compressor unit with some of the measuring points for examination. Figure 4 shows the measured increased vibrations in the comparison with the reference value of permitted piping vibrations.

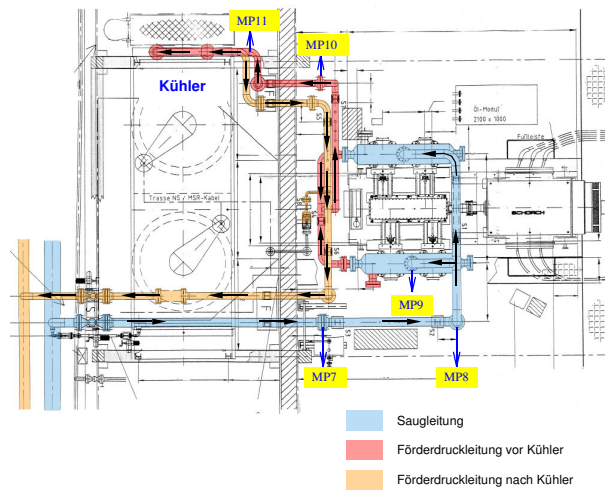


Figure 3: Layout of compressor unit with part of the vibration measuring installation (MP).

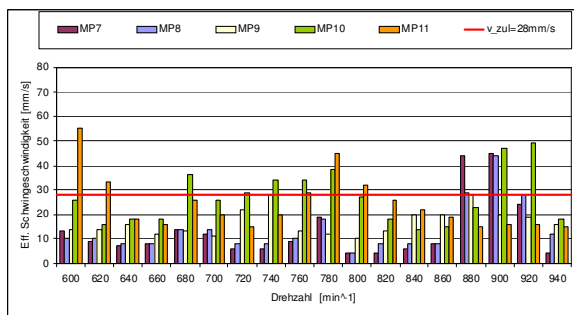


Figure 4: Measured vibration velocity at measuring installation as shown in figure 3 diagrammed here above rotational speed.

By analysis of the reasons for the established increased vibrations three different mechanisms were detected:

- acoustic resonance between cylinder rooms and outlets of the pulsation dampeners at the pressure sides
- internal frequencies of the mechanical piping in the cooling section
- increased pressure pulsations into the pressurised pipe end

The results of the investigation for reduction of the vibration values we installed pulsation damper plates at the outlet flanges of the compressor. At this stage an additional fastening and stiffening of the horizontal piping installation should be decided later on, depending on the results of additional investigations.

The positive effect of the pulsation damper plates was confirmed by testing in 2003. Figure 5 above shows in an abridged version the measured pressure of the 1st cylinder. It is easy to recognize the increased pressure pulsations as a single frequency when outputting the gas. Due to these effects the increased piping vibrations cause an additional dynamic load of approx. 2 t (load) to the crankcase.

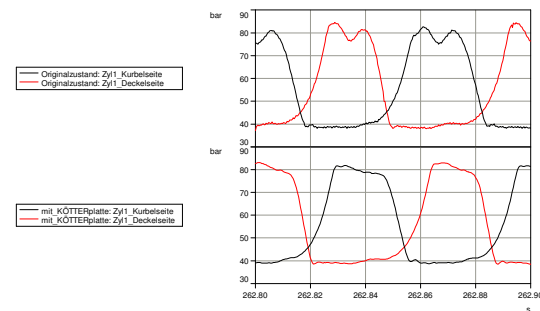


Figure 5: Measured indication pressure in the original condition (above: 90 Hz pressure pulsation, outputting the gas) and after installation of pulsation damper plates (below.)

Recorded cylinder pressure with installed pulsation damper plates at the same operation conditions is shown in figure 5 below. The pressure pulsations when outputting the gas with fault cannot be measured any more. By the reduction of the pulsations the vibration behaviour of the compressor and the pipes could be improved (figure 6). The results of the latest investigation after installing the pulsation damper plates shows only a low vibration modulation at the pipes of the gas cooling unit. The vibrations shall be reduced by installing additional pulsation damper plates according to the plates principle.

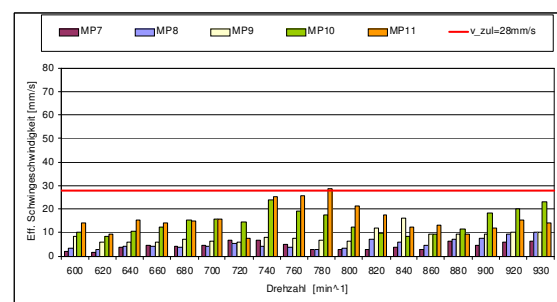


Figure 6: Measured vibration velocity after using the pulsation damper plates according to the plates principle at different test points illustrated here above rotational speed (cf. illustration 4.)

We enlarged the pulsation investigation by the investigation of the torsion vibration behaviour at the compressor 7. During design the torsion vibration calculations led to an elastic clutch as well as to an additional flywheel that have been provided at the compressor side drive shaft of the motor.

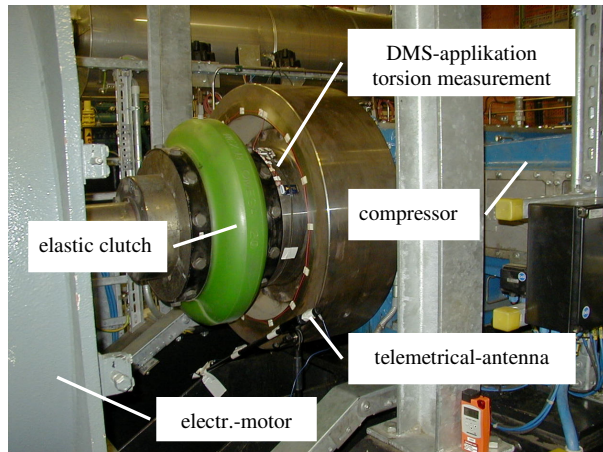


Figure 7: Torsion vibration metering installation close to the elastic clutch.

The intended result (due to these modifications in order to move the first torsion natural frequency below the operating speed) could be confirmed by technical investigation. During all operation periods of the compressor no significant overlaid torsional wave stated the static rated torque over the complete speed range.

Thanks to these examinations it could be confirmed in conclusion that the compressor with vibration engineering aspects could be operated continuously without any restrictions.

7 Conclusion

The test operation that has been performed immediately after putting into operation allowed us a very conscious discussion of the new compressor. All involved employees exchanged their own observations and by this they have contributed to a meanwhile successful operation of the compressor unit with a considerable reduction of breakdowns. The interface problems mentioned in section 5 between the frequency changer and the compressor PLC controlled were solved in a durable manner. In the meantime, we have operated six storage periods with the compressor without problems. The convenient and simple operation of the compressor out of the control room fulfils our ideas.

We carried out further investigations of pressure pulsations and piping vibrations after the assembly of additional pulsation damper plates at the compressor 7 in February 2004. The vibration reduction has been provably very successful.

8 Amendment Gas- Engines

By operating reciprocating compressors with gas engine we experienced that there are currently no gas engines available that can be installed in explosive zone (1) without extensive modifications. That's why it is recommended for design engineers to involve motor damage experts for motor specification and preselection in time.

9 References

- Development of the natural gas storage plant Reitbrook respecting gas economic requirements. Dr. Ing. Ralf Luy E.ON Hanse AG Report no. 16414-1,001 Investigation of the pressure pulsations and piping vibrations at the compressor 7 UGS Reitbrook. Dr. Ing. Johann Lenz and Ing. Grad. Joachim Holstein, Kötter Consulting Engineers, 2003
- Report no. 16414-1,002 Investigation of torsion vibration analysis at the compressor 7 UGS Reitbrook. Dr. Ing. Johann Lenz, Kötter Consulting Engineers, 2003

Reciprocating Compressor Foundations They do not last forever

By:

Robert van Lienen

**Regional After Market Sales and Product Manager for GHH Hyper
Compressors**

Robert.vanLienen@NEAC.de

And

Harry Lankenau

Head of Technical Service and Engineering

Harry.Lankenau@NEAC.de

NEAC Compressor Service GmbH & Co. KG

Uebach-Palenberg

Germany

5th Conference of the EFRC

March 21-23, 2007

Prague, Czech Republic

Abstract:

After 30 and more years of operation the foundation of a reciprocating compressor as well as the frame itself may no longer be in proper condition and further operation considered being unsafe.

Unbalanced dynamic foundation loads commonly accompanied by severe oil contamination typically initiate the deterioration of the concrete strength. Rocking and twisting movement of the machine on the foundation may also damage the frame that is resting on the grouting, sole plates or steel blocks.

That is the time to consider a sound reconditioning of the foundation and check of the integrity of all compressor parts with refurbishment or replacement of parts where necessary.

When the compressor has been opened and removed from the foundation the amount of work becomes clear – including the 'surprises', which are not visible from the outside.

Since unit downtime is of the essence the repair activities may require significant manpower in the field as well as capable tools and large milling machines in the workshop. Only specialists with the know-how, experience and capacity are able to perform all necessary steps in parallel and in close coordination.

This paper will outline the procedure of a typical compressor revamp in conjunction with successfully performed foundation repair and reconditioning.

1 Introduction

Piston compressor foundations and also their frames typically suffer long term deterioration from:

- Unbalanced mass loads
- Oil penetration into the concrete
- Unfavourable ambient conditions
- Loose or cracked foundation bolts

Depending on the magnitude of the unbalanced mass forces and/or moments the foundation may be subject to severe loads over the period of its lifetime. In conjunction with oil penetrating into the concrete – e. g. due to missing oil resistant paint – foundations may lose their capabilities and yield to the constant dynamic loads (picture 1.1 and 1.2)



(Picture 1.1: Oil Penetration into Foundation)

Ice formation during winter time and possibly also aggressive product dripping down from the machine over the years may further contribute to its deterioration.

Foundation bolts, being submerged in concrete or grout, possibly come loose with time due to the phenomena outlined above.

Once the foundation is no longer man enough to hold the compressor down on its surface the frame will start to move. Relative movement between surface and frame then propagates the commencing self destroying effects in terms of impact forces initiated by the rocking machine and/or already loose or broken foundation bolts. That is usually the end of the foundation.

Quick and easy repair is hardly a sound and lasting solution (picture 1.2) and may incorporate the risk of damage of the entire compressor unit.



(Picture 1.2: Example of poor Foundation Repair)

Since also large machines are built with tolerances in the range of 10th and 100th of an mm any kind of frame twisting or rocking may have a critical effect e. g. on the bearing way alignment with subsequent bearing damage. Misalignment of cylinders and cross head guides may lead to increased friction and consequently to unfavourable running conditions. Forces and moments of the frame and internals may increase with material stress becoming closer to the yield limits. In worst case those are even exceeded.



(Picture 1.3: Example of catastrophic Damage)

Catastrophic scenarios could be the last consequence of negligence as shown above (picture 1.3); that, however, is neither the machine nor the customer being discussed in this paper.

2 BASELL Hyper Compressors

BASELL Polyolefins in Wesseling (near Cologne) in Germany is operating a number of GHH Hyper Compressors in their various Ethylene plants (picture 2.1).

OPERATING & MAINTENANCE

Reciprocating Compressor Foundations – They do not last forever, *Robert van Lienen, Harry Lankenau; NEAC COMPRESSOR SERVICE*



(Picture 2.1: BASELL Polyolefins in Wesseling)

“BASELL is the world's largest producer of polypropylene and advanced polyolefins products, a leading supplier of polyethylene and catalysts, and a global leader in the development and licensing of polypropylene and polyethylene processes. BASELL, together with its joint ventures, has manufacturing facilities around the world and sells products in more than 120 countries.” (Source: Website <http://www.basell.de/>)

To create polyethylene so called hyper compressors are used which pressure ethylene up to max. 3000 bar which is then sent to a reactor where the ethylene polymerisation takes place. Picture 2.2 shows typical products made from polyethylene.



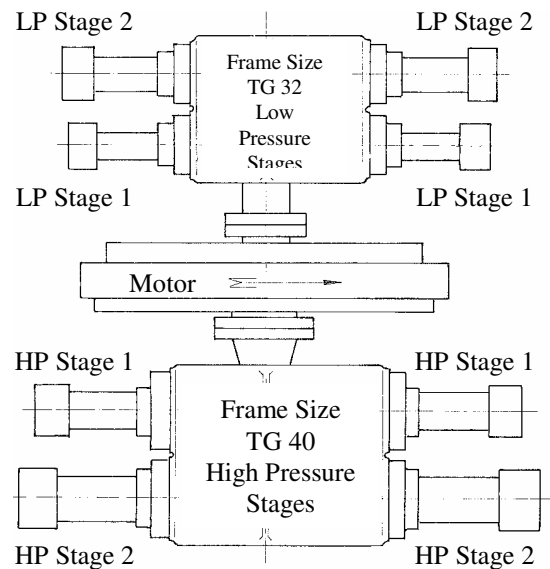
(Picture 2.2: Final Polyethylene Products)

The typical technical datasheet for such a GHH Hyper Compressor reads as follows:

Manufacturer:	GHH
Type:	B4g 40-32 / 105-87 / 82-68
Year built:	1973
Commissioned:	1974
No. of stages:	2 x 2
Gas:	Ethylene
Max. Pressure:	3000 bar
Flow:	15700 / 7700 Nm ³ /h
Rated Power:	4780 kW
Speed:	132 rpm
Piston Speed:	1.77 / 1.42 m/s

The lay-out of a tandem unit is depicted in picture 2.3.

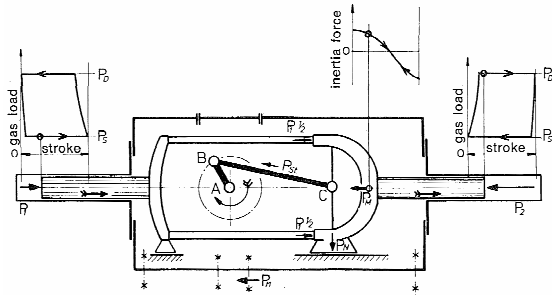
Two compressors of different size are combined with the electric motor located between both units. The TG 32 frame size is the low pressure and the TG 40 frame size the high pressure side.



(Picture 2.3: Tandem Hyper Compressor)

The operating principle is somewhat different from a common piston compressor. Two opposite plungers are linked through one common kind of special crosshead which is driven by one connecting rod (picture 2.4).

Hence, both opposite plungers are operating in phase, in contrast to a typical boxer type compressor where opposite pistons (plungers) are acting in opposite phase.



(Picture 2.4: Hyper Operating Principle)

Consequently the mass forces of the two opposite plungers – with the common crosshead - are not balanced.

Since masses being moved back and forth are large, the inertia forces are a major dynamic load factor – despite the comparably low speed of such machines.

After many years of operation the foundation of one of the GHH Hyper Compressors (picture 2.5) was no longer in proper condition and further operation was considered to become unsafe.



(Picture 2.5: Hyper Compressor)

The compressor frame had started to rock on the concrete. The knocking sound was already noticeable.

Already in 2002 it became obvious that lifetime of the concrete was slowly coming to an end and the link to the compressor frame had lost its initial strength. Major revamp would be required in the foreseeable future.

In September 2005 BASELL took the decision to do comprehensive repair work at the foundation and overhaul of the compressor crank cases.

BASELL decided to partner with NEAC Compressors Service being the OEM with the former GHH Hyper Compressor legacy.

2.1 Problem Area No. 1: Crank Case Damage and Wear

The hyper compressor frame is typically resting on special levelling and supporting blocks (picture 2.1.1).



(Picture 2.1.1: Hyper Frame on Support Blocks)

Since the deteriorated foundation allowed the frame to move up and down, the bottom of the frame was hammering on the support blocks (picture 2.1.2) with increasing impact as wear propagated.



(Picture 2.1.2: Hyper Frame Levelling Support)

Consequently the bottom of the frame was severely deformed as shown in picture 2.1.3.



(Picture 2.1.3: Frame Bottom Hammering Marks)

It was quite obvious that it had become impossible to create a good link between crank case and foundation with mating surfaces being in such poor condition.

2.2 Problem Area No. 2: Foundation Wear and Deterioration

Already before lifting the crank case from the supporting blocks it was clearly visible that oil had severely penetrated into the foundation over the past years and softened major parts of the concrete block (picture 2.2.1).

Cracks in the foundation that had been created at some time intensified the oil penetration and concentration all across and also deep inside the concrete.



(Picture 2.2.1: Oil Penetration into Foundation)

Last but not least a large oil puddle showed up when the crank case had completely been removed from its supporting structure (picture 2.2.3).



(Picture 2.2.3: Oil Puddle on Top of Foundation)

2.3 Problem Area No. 3: Overloaded Crank Case Supports

The levelling support blocks did not remain unharmed. The constant regular hammering over years left its signs of impact overload on almost each of the blocks (picture 2.3.1).

Some of them had also lost their close contact to the machine.



(Picture 2.3.1: Support Blocks in bad Condition)

2.4 Consequential Damage

The disassembly of the compressor internal parts revealed quite a critical condition of the main bearings (picture 2.4.1).

OPERATING & MAINTENANCE

Reciprocating Compressor Foundations – They do not last forever, *Robert van Lienen, Harry Lankenau; NEAC COMPRESSOR SERVICE*



(Picture 2.4.1: Severely worn Bearing)

Wear and cobblestone formation had become excessive and a number of particles had cracked off near the main bearing shell split line (picture 2.4.2 and 2.4.3).

Cobblestone formation is a clear indication of long term fatigue bearing overload which here must assumed to be mainly based on frame movement and twisting phenomena.

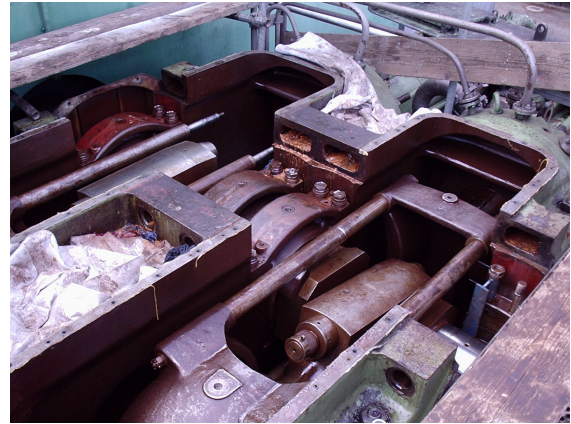


(Picture 2.4.2: Cobblestone Formation)



(Picture 2.4.3: Cobblestone Formation)

Relevant bolts in the crank case (picture 2.4.4) holding the bearing shells in place had also cracked at some unknown time in the past.



(Picture 2.4.4: Hyper Crank Case)

Pictures 2.4.5 to 2.4.7 are showing the fractured surfaces of the bearing cover bolts.

It goes without saying that these cracks must be assessed as being critical for the integrity of the entire compressor.



(Picture 2.4.5: Fractured Bolt Surfaces)



(Picture 2.4.6: Fractured Bolt Surface)



(Picture 2.4.7: Fractured Bolt Surface)

3 Repair Procedure and Solutions for each Problem Area

After BASELL had taken the decision to place the order for this complete revamp of the foundation and the compressor with NEAC the actual work at site started in November 2005.

Since unit downtime was of the essence the repair activities required significant manpower in the field as well as capable tools and large milling machines in the workshop where specialists with the know-how, experience and capacity were able to perform all necessary steps in parallel and in close coordination with each other.

At first the complete compressor unit had to be dismantled piece by piece (picture 3.1).



(Picture 3.1: Hyper Unit Disassembly)

The crank case was then lifted from its foundation for sound inspection (picture 3.2).



(Picture 3.2: Frame being lifted from Foundation)

3.1 Solution for Crank Case Damage and Wear

After opening and removal of the compressor from the foundation it had become clear that comprehensive investigations referring to the integrity of all compressor parts were necessary with relevant machining according to findings.

Therefore various parts were shipped to the NEUMAN & ESSER Workshop for

- Condition and dimension checks
- Repair and/or machining
- Replacement of parts where necessary

After a thoroughly conducted assessment of each compressor part the scope of rework and parts replacement was defined.

OPERATING & MAINTENANCE

Reciprocating Compressor Foundations – They do not last forever, *Robert van Lienen, Harry Lankenau; NEAC COMPRESSOR SERVICE*

The frame was set up on a large milling machine where all major surfaces were machined as required (picture 3.1.1).



(Picture 3.1.1: Hyper Frame on Milling Machine)

Only with adequately selected and available tools which can handle the dimensions and at the same time keep the required tight tolerances it is possible to provide for the high level of rework quality being of utmost importance here (picture 3.1.2).



(Picture 3.1.2: Large Milling Head at Work)

Picture 3.1.3 shows the bottom of the crank case during the machining process.



(Picture 3.1.3: Frame on Milling Machine)

When the milling tool had done its work, all mating surfaces had been refurbished and the frame was ready for reassembly (picture 3.1.4).



(Picture 3.1.4: Crank Case after Machining)

3.2 Solution for Foundation Wear and Deterioration

Due to the high level of deterioration the decision had to be taken to chisel off the oil contaminated soft and cracked portions of the concrete down to a solid and healthy core (picture 3.2.1).

OPERATING & MAINTENANCE

Reciprocating Compressor Foundations – They do not last forever, *Robert van Lienen, Harry Lankenau; NEAC COMPRESSOR SERVICE*



(Picture 3.2.1: Jackhammers in Action)

The reinforcement was improved through extra steel bars being added to the existing grids (picture 3.2.2)



(Picture 3.2.2: Improved Steel Reinforcement)

After the new concrete had been filled into the form work and completely dried a high quality non-shrinking epoxy grout was then poured on top to creep underneath and around the sole plates creating a robust surface (picture 3.2.3)



(Picture 3.2.3: Epoxy Grout being poured)

Prior to the epoxy grouting new sole plates had been put in place and aligned which would later carry the refurbished hyper frame.

The target of the epoxy grout is not only to enable the concrete block to bear the frame loads of the hyper compressor but also to avoid any oil penetration.

3.3 Solution for overloaded Crank Case Supports

The final layout of the reconditioned foundation is shown in picture 3.3.1 right before the frame is being put back in place.



(Picture 3.3.1: Reconditioned Foundation)

Special steel blocks were fitted and aligned ready to withstand the static and dynamic forces and moments which will later be transferred from the compressor through the crank case into the ground.

The position of the new blocks is as close as possible to the anchor sleeves to keep deformation - due to limited material stiffness - as low as possible (picture 3.3.2).



(Picture 3.3.2: New Steel Block)



(Picture 3.4.2: Anchor Bolts entering Sleeves)

3.4 Reassembly Procedure

One day it was the time for the refurbished crank case to fly in and get settled again (picture 3.4.1)



(Picture 3.4.1: Frame flying in)

Service technicians were assisting to guide the anchor bolts into their foundation sleeves and to make sure that the crank case would be positioned at its proper place (picture 3.4.2).

Picture 3.4.2 shows the frame being lowered and close to touch base on its new bed.



(Picture 3.4.2: Frame close to touch Base)

Afterwards the reassembly of the machines and the motor was performed with high accuracy to ensure best alignment of all components being inserted back into the frame.

4 Conclusion

After months of continuous shift work – sometimes under extreme weather conditions at site – and with dead lines to be met, the complete job was performed in close cooperation between BASELL and NEAC.

OPERATING & MAINTENANCE

Reciprocating Compressor Foundations – They do not last forever, *Robert van Lienen, Harry Lankenau; NEAC COMPRESSOR SERVICE*

It was in the nature of the job that also surprises had to be expected and handled – when opening and removing the crank case, during machining and manufacturing of parts, when the foundation was reconditioned and during reassembly.

After recommissioning the hyper compressor was reported to behave like a “snoring cat”. Vibrations being measured had come down to a very low level (compared with those before the revamp).

This paper shows that in heavy machinery “soft footing” can lead to unpredictable behaviour and cause severe damage inside the compressor.

Only through looking at the “total picture” and overhauling all elements which are involved in the “soft footing” – including the compressor frame – one can achieve reliable and trouble free operation.



Extensive Optimisation Analyses of the Piping of two large Underground Gas Storage Ariel compressors

A. Eijk and H.J.C. Korst
TNO Science & Industry
Delft, The Netherlands

G. Ploumen
Plant Manager
Essent Epe, Germany

D. Heyer
HGC
Hamburg, Germany

**5th Conference of the EFRC
March 21-23, 2007
Prague, Czech Republic**

Abstract:

Two large identical 6-cylinder Ariel JGB/6 compressors of each 7.5 Mw, are used for the underground gas storage (UGS) plant of Essent in Epe, Germany.

The compressors can be operated at a wide range of operating conditions, e.g. variable suction and discharge pressures, 2-stage mode during gas storage, 1-stage mode during gas withdrawal, capacity control by speed variation and valve lifters.

The system should operate safe, reliable and efficient for the complete range of operating conditions, which could be met with an extensive optimisation analyses during the design stage of the project.

For that purpose TNO has carried out a damper check, a pulsation and mechanical response analysis of the piping, a compressor manifold analysis and a thermal stress analysis.

This paper will indicate the different steps in the optimisation process and will focus on the interaction between the different analyses.

Finally, the results of vibration measurements after start-up of the system will be presented.

1 Introduction

ESSENT ENERGIE is a major gas distributor of low caloric LC-gas to private, small consumers as well as to the midstream power and gas sector in the Netherlands. The gas portfolio is about 11 billion m³ per year including supply of gas to gas-fuelled electricity power stations.

ESSENT ENERGIE is trading with gas on the Dutch gas market and follows a strategy to meet current and future demands of the market that undergoes changes in line with its liberalisation.

The new build gas storage will permit supply of additional gas quantities into the distribution grid in seasonal periods of peaking demand and serve as balancing and trading tool.

The cumulative storage capacity established in the cavern field “Epe” by the gas distributing companies Ruhrgas, RWE and Nuon forms one of the greatest underground gas storage in Central Europe.

Generally the gas storage facilities of ESSENT ENERGIE are located on the already existing storage field “Epe” close to the city of Gronau, and will exist of 4 caverns with a working volume of 200 million cubic meter and the installations for compressing, gas treatment, reducers, and the auxiliary equipment.

The salt deposit is a flat Zechstein salt formation of about 400 m thickness in an average depth of 1000 to 1400 m below surface. A massive bank of sandstone that is about 600 m thick overlies it.

Foreseen are operations with the plant on base of seasonal- as well as day-to-day base following the gas demands or trading opportunities. Therefore, an excellent flexibility, availability and reliability of the plant are obliged. The plant has a high grade of automation in such a way that operation and monitoring from distance is possible.

The main technical data for the compressor selection are as follow:

- Suction pressure range: 40-70 barg (design 40 barg)
- Discharge pressure range: 80-220 barg (design 220 barg)
- Flow rate Injection: 50.000-100.000 Nm³/h (design 100.000 Nm³/h)
- Flow rate Withdrawal: 100.000-200.000 Nm³/h (design 200.000 Nm³/h)
- Flow rate First gas fill in: 30.000-50.000 Nm³/h

To realise the different operation modes and wide range of pressure and flow requirements of the storage, it has been selected 2 reciprocating compressors units, which have been engineered and delivered by HGC Hamburg Gas Consult GmbH.

The selected compressor is a 6-throw compressor (Brand “Ariel”, type JGV 6) equipped with 3 cylinders for stage 1 and 3 cylinders for stage 2 as shown in figure 1.

The compressor is driven by a frequency controlled electrical driver with a max. power output of 7.400 kW. The speed range can vary between 400-750 rpm, for first gas fill in operation the speed can be reduced up to 300 rpm. The driver is water cooled and air purged in order to fulfil the requirements of explosion zone 1.

For capacity control reasons each cylinder of stage 1 is equipped with pneumatically operated suction valve unloaders (located head end side). The flow rate will be automatically controlled and adjusted, based on the given parameters by the plant operator.

Based on the requested operation mode (injection / withdrawal) the cylinders can operate in serial mode (two stage compression) or in parallel mode (single stage compression).

The compressor train with compressor, driver and coupling is mounted on a common steel skid, the steel skid incl. the before mentioned main equipment was delivered in 1 piece at side (total weight of appr. 80.000 Kg).

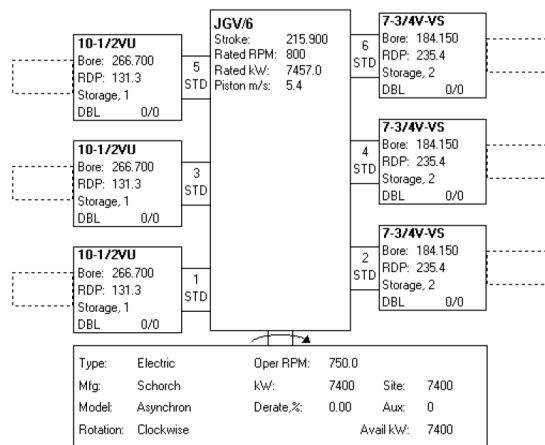


Figure 1: Compressor configuration

The following analyses were carried out for this system:

- acoustical damper optimisation;
- acoustical pulsation analysis of the piping ;
- thermal stress analysis
- compressor manifold vibration analysis;
- mechanical response analysis of the piping;

This paper will discuss the different analyses to achieve an optimum design from the static (thermal) and dynamic (vibrations) point of view.

Finally also the results of the measurements during start-up of the system will be summarised.

2 Acoustical damper optimisation

2.1 Introduction

The first step in the dynamic analysis is the damper check^{2,4}. During this check the dampers are investigated without any interaction of the future pipes systems. This check is therefore also called the endless line check. The main objective of this check is to determine if the volumes of the dampers are large enough to attenuate the compressors' flow pulses to acceptable levels. During the damper check TNO recommends a residual pulsation level at the line connection of 70-80% of the allowable levels according API-Standard 618¹.

The four criteria against which the dampers are judged are:

1. Pulsation at the line flange should be smaller than 70% - 80% of API-618 levels;
2. Pulsation levels at the cylinder flanges should be minimised (preferable to within the API-618 levels);
3. Pulsation induced vibration forces on damper shells, nozzles and internals should be minimised (no absolute criterion);
4. The pressure loss across the damper ('pulsation suppression device') should be within acceptable limits (API-Standard 618, paragraph 3.9.2.2.4).

The calculation have been carried out with the digital program PULSIM^{2,3} for the conditions as summarised in table 1.

Table 1: Investigated conditions

Ps bar	Pd bar	Occurring Part loads [%]				Remark
		1	2	3	4	
41	201	100	83	67	50	2-st. operation
41	101	100	83	67	50	2-st. operation
71	201	-	-	67	50	2-st. operation
71	101	-	-	67	50	2-st. blow through
51	71	100	83	67	50	1-st operation

2.2 Results

The damper check has led to a complete redesign of the original design of the suction and discharge 1st and 2nd stage dampers. Especially for the 1st stage dampers a significant increase in volume was necessary to achieve acceptable pulsation levels at the line connections.

All recommended modifications resulting from the damper check have been incorporated into the final design of the dampers of which a sketch of the final dampers is shown in figure 2 and 3 and photos are shown in figure 4 and 5.

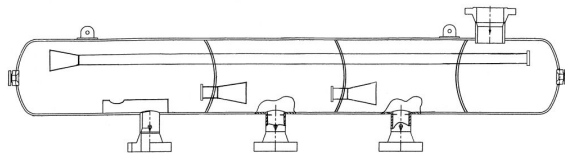


Figure 2: Sketch of the final 1st stage suction damper

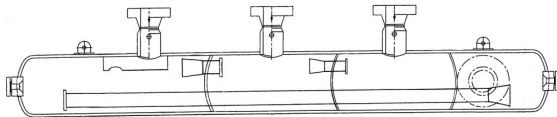


Figure 3: Sketch of the final 1st stage discharge damper



Figure 4: Photo of the suction damper



Figure 5: Photo of the discharge damper

3 Pulsation analysis of the pipe system

3.1 Introduction

In the pulsation analysis the complete pipe system, including the optimised pulsation dampers as discussed in the acoustic damper check has been investigated for the worst-case situations.

The investigated pipe system includes the entire gas storage plant starting from the main transport (feed)line up to the four transport lines to the four caverns. In this way the interaction between the two machines during parallel operation and the effect of pulsations on for instance the accuracy of the flow metering equipment, could be assessed during the early design stages.

The calculated pulsation levels are compared with allowable levels according API 618. In case of exceedings of allowable levels, modifications (e.g. orifice plates) have been investigated.

The calculation have been carried out for the conditions as summarised in table 1.

3.2 Results

For all parts of the system, the pulsation levels exceed the allowable levels for all investigated duties and loads. The most important resonances were standing waves between dampers, separators and closed side branches.

The highest calculated pulsation levels were respectively 3.7, 7.7 and 3.2 times the API 618 level for the suction 1st stage, interstage and discharge 2nd stage piping.

From the calculations it appeared that allowable pulsation levels could be achieved with 6 orifice plates installed in the system. The optimum location of the orifice plates was at the inlet and outlet of pulsation dampers and separators.

The effect (vibrations) of the residual pulsation levels has been investigated further in the compressor manifold analysis, see chapter 5, and in the mechanical response analysis of the piping, see chapter 6.

4 Thermal stress analysis

4.1 Introduction

The first step in the mechanical analysis of the system is a static (thermal) stress analysis in order to verify that the stresses in the piping do not exceed the piping code limits of ASME B31.3⁵. Also nozzle loads on equipment (vessels, dampers, and coolers) have been calculated and checked against the allowable levels of API 661⁷ for the air-fin cooler and against allowable levels as specified by the manufacturer of the dampers and separators.

The original locations of the supports were given by HGC and the type of supports had to be designed and optimised in this stress analysis.

The support layout must also be designed in such a way that the vibration and cyclic stress levels do not exceed allowable levels as explained in chapter 5 and 5.

The static (thermal) and dynamic support layout compete with each other in many cases. From the static (thermal) point of view a more flexible system is required than from the dynamic point of view.

Introducing additional supports, which are required to keep the vibrations within allowable levels, can introduce too high thermal pipe stresses and nozzle loads of attached equipment

This means that there is a strong interaction between the static (thermal) and dynamic design.

To achieve an optimum support layout both for the static and dynamic design, the following steps have been carried out:

Step 1: Design of the support layout from the static (thermal) point of view in such a way that pipe code stresses and nozzle loads do not exceed allowable levels;

Step 2: Adjust the support layout from step 1 in the vibration analysis. Assume that each support is able to restrain the dynamic motions (dynamically fixed);

Step 3: In case additional modifications are necessary in the vibration analysis, adjust the additional supports in the static stress analysis and repeat step 1. If all static stresses and nozzle loads are within allowable levels, determine if all supports are able to restrain the dynamic motions: repeat step 2. If the friction force is too low on a support (dynamically loose) to restrain the dynamic loads, the required normal force, which is necessary to restrain the dynamic loads, has been adjusted in the static analysis;

Step 4: Check with the model of step 3 if all thermal stresses and nozzle loads are within allowable levels.

The calculations have been carried out for the following cases:

- Case 1: Compressor A in operation and compressor B not in operation;
- Case 2: Compressor B in operation and compressor A not in operation;
- Case 3: Compressor A& B in operation.

The expansion of the compressor at the location of the cylinder nozzles has been taken into account.

4.2 Type of supports

The following type of supports has been applied in the system:

- Weight only support: restrains only the downwards vertical motion, see figure 6;
- Guide: restrains the lateral movement in both directions, see figure 7;
- Directional anchor: restrains the axial movement in both directions;
- Valve/flange support: restrains only the downwards vertical motion, see figure 8;
- Any combination of the above mentioned supports excluding or including spring constructions, see figure 8 and 9.

Normally rigid clamp type supports are advised in systems which are subjected to vibrations. However, for those supports where the friction force (as calculated in the thermal stress analysis) is smaller than the pulsation-induced reaction force (as calculated in the mechanical response analysis) the supports are dynamically loose. This means that the support is not able to restrain the vibrations at that location. To restrain the vibrations and to keep the static pipe stresses within allowable levels, spring hold down type supports can be applied, see figure 8. The disadvantage of a spring hold down is that it is possible that they can become loose after a while which is caused by the dynamic loads which act on the support. It is strongly recommended to include the check on the correct function of these supports frequently during the periodically maintenance program.



Figure.6: Example of a weight only support



Figure 7: Example of a guide support



Figure 8: Example of a combination of valve with spring type support



Figure 9: Example of a weight only with a spring hold down support

4.3 Pipe stress code requirements

Piping:

In order to comply with the requirements of the ASME B31.3 it is necessary to construct load cases to satisfy the sustained, occasional and expansion stress conditions

Sustained stress (primary stresses)

The hoop (membrane) stress due to internal pressure shall not exceed S , the piping material allowable stress at maximum metal temperature
 Longitudinal stresses S_L due to pressure, weight shall not exceed S_h , the piping material allowable stress a maximum metal temperature.

Operating stress:

Operating stresses are calculated in a similar manner to sustained stresses. These are not required to be “Code Checked”, however, the code requirements for the sustained, and expansion cases must be met.

Expansion stress (secondary stress)

This is in fact the total displacement range S_E due to all displacement strains on the piping system. These can be from thermal expansion of piping and/or connecting equipment (e.g. compressor), deflection of piping restraints and from movements resulting from vessel motion. The allowable stress range is:

$$S_A = f [1.25 (S_c + S_h) - S_L]$$

Where:

f = stress range reduction factor

S_c = allowable stress at minimum metal temperature

S_h = allowable stress at maximum metal temperature

S_L = calculated sustained stress due to weight, pressure etc.

4.4 Results

Pipe system

After several iterations of the different steps as indicated in chapter 4.1, the final support layout is such that the maximum pipe stresses are as follows:

Table 2: Table with a summary of the maximum calculated pipe code stress

	Stresses in % of the allowable stress	
	Sustained load	Expansion load
Case A	47	4
Case B	47	22
Case C	50	27

Nozzle loads

With the optimised support layout it appeared that the loads on nozzles of some pulsation dampers, separators and air-fin coolers exceed allowable levels. To decrease the nozzle loads on dampers and separators, stiffening rings are applied.

The loads on the air-fin coolers could not be decreased without a rigorous change of pipe routing. However, this appeared not to be feasible.

A more flexible pipe routing would also lead to higher vibration levels. From experience it is known that the allowable levels according API 661 are normally rather low. In many cases the actual nozzles can be much higher than the allowable loads. Detailed FE calculations have been carried out therefore by the manufacturer to check the integrity of the nozzles with the calculated loads. From the calculations it appeared that the nozzles can sustain the calculated loads.

5 Compressor manifold analysis

5.1 Introduction

Compressor manifold vibrations^{8,9} are a specialized and complicated form of vibration of a part of the piping, pulsation dampers and compressor parts such as cylinders, distance pieces, crankcase and crosshead guides.

If not properly controlled, these vibrations can cause fatigue failure of the system because compressor manifold mechanical natural frequencies can be excited by gas loads in the cylinder, by pulsation-induced forces in the cylinder and/or pulsation dampers, or by mechanical loads of the compressor. Figure 10 shows an example of a compressor manifold.

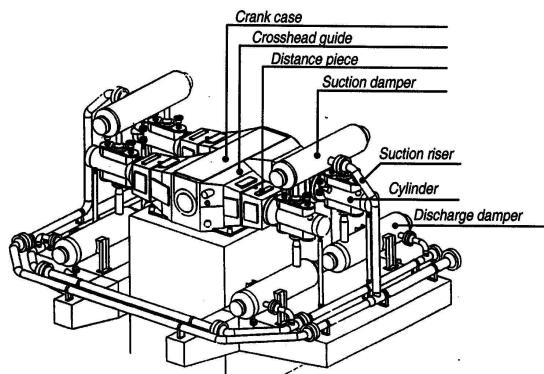


Figure 10: Example of a compressor manifold

The first step in the analysis is to generate a Finite Element model of the pipe system. The second step is to generate a Finite Element model of the compressor parts. These parts will be assembled and the calculations of the lower mechanical natural frequencies has been carried out. For those cases where acoustical and mechanical natural frequencies coincide (worst-case situations), a forced response analysis has been carried out to calculate:

- Vibration levels of compressor, dampers and a part of the piping;
- Cyclic stress levels in piping and pulsation dampers.

Vibration and cyclic stress levels must be compared with allowable levels and in case of exceeding, modifications have to be investigated to finally achieve acceptable levels.

5.2.1 Development of Finite Element Model of the compressor

Solid models⁹ of the compressor parts were created using Solid Works 2004 using 2D and 3D technical drawings obtained from Ariel. The solid models were simplified by removing small details such as fillets, rounds, and small holes. These details were not included in the solid model to help reduce the size of the finite element model.

These details will not have a significant effect on the accuracy of the finite element model.

The compressor frame, crosshead guide, crosshead guide support and end covers were given material properties of grey cast iron ASTM 278 Class 30.

The frame covers and crosshead guide covers were given material properties of aluminium. The covers were rigidly connected to the compressor frame and crosshead guide. Several models were created with different element sizes. A modal analysis was conducted on each model to determine the change in the calculated modal response. The finite element model using an element size of 100 mm was found to be an acceptable compromise between model size and convergence in the calculated modal response. A plot of the complete finite element model is shown in figure 11.

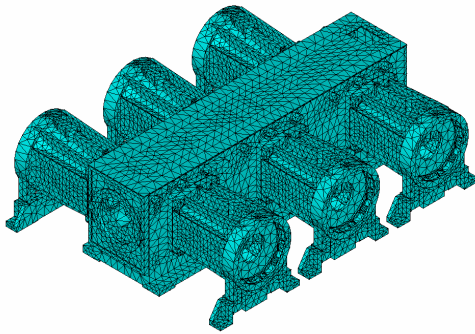


Figure 11: FE model of the compressor

A summary of the model statistics for the 100 mm element size model is shown in table 3.

Table 3: Model Summary

Element type summary		
ANSYS Type	Amount	Comment
Solid187	108083	Solid elements
Mass21	3644	Mass elements
Conta174	9647	Bonded contact elements
Target170	9647	Bonded target elements

Finally a substructure has been generated to decrease the computer calculation time. From calculations it appeared that with 3500 so-called Master Degrees of Freedom (MDOF's) the maximum difference between the natural frequencies of the substructure differs less than 2% from the complete FE model which is an acceptable accuracy. In table 4 a summary of the 10 lower mechanical natural frequencies have been given.

Table 4: Summary of mechanical natural frequencies

Mode shape number	Frequency [Hz]	
	Substructure 3500 MDOF	Complete FE Solid Element Model
1	142.76	141.30
2	158.45	156.69
3	162.68	162.56
4	167.84	167.71
5	176.45	176.30
6	180.46	178.23
7	190.66	190.47
8	199.25	196.44
9	204.54	201.76
10	208.18	205.91

5.2.2 Compressor manifold model

To complete the compressor manifold model the substructure of the compressor model has been extended with the compressor cylinders, the pulsation dampers and a part of the suction 1st stage, interstage and discharge 2nd stage piping. The piping around the compressor has been modelled up to the first two supports upstream and downstream the pulsation dampers. The compressor cylinders, the pulsation dampers and the piping have been modelled with beam type elements (ANSYS: PIPE16 and BEAM4).

The complete compressor manifold model is shown in figure 12.

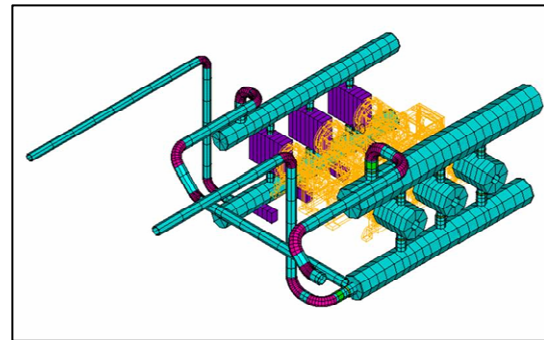


Figure 12: Compressor manifold model

5.2 Results

The calculations have been carried out with the finally accepted modifications of the pulsation analysis and for the following selected worst-case situations out of the complete range:

- $P_{\text{suction}} = 41 \text{ bar}$, $P_{\text{discharge}} = 207 \text{ bara}$, 100% load condition
- $P_{\text{suction}} = 70 \text{ bar}$, $P_{\text{discharge}} = 207 \text{ bara}$, 50% load condition

The vibration and cyclic stress levels have been calculated which are caused by the pulsation-induced forces and by the gas stretching forces on the cylinders.

For the original layout the maximum calculated vibration level and cyclic stress levels exceed the allowable levels on the dampers and piping at many compressor speeds. This can lead to fatigue failure of piping the piping at some locations. The highest calculated values occur at 50% load at a compressor speed of 741 rpm and at a frequency of 94.7 Hz of which a mode shape is shown in figure 13.

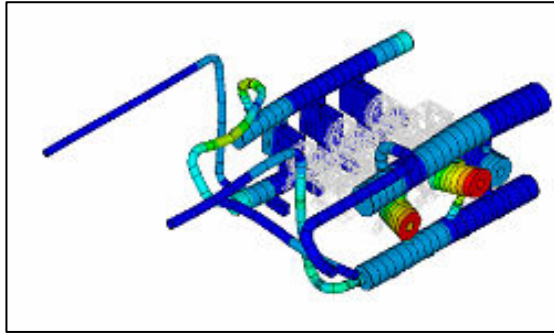


Figure 13: Mode shape at 94.7 Hz

To decrease the vibration and cyclic stress levels finally the following modifications are advised, see figure 14 and 15:

1. Install HEB 200 braces between the main HEB 200 beams of the 1st and 2nd stage discharge damper support
2. Install an outboard cylinder supports at each cylinder.
3. Install a HEB 200 structure on which the outboard cylinder supports must be mounted.
4. Install additional supports close to the discharge pulsation dampers.
5. Due to the fact that supports at high elevated piping could not be installed the suction and discharge piping of the 1st are connected to each other.

With the advised modifications the vibration levels exceed the allowable levels at the suction 2nd stage damper at a speed of 690 rpm at 50% load condition.. However, due to the high elevation of the damper it was not possible to mount a support at this location. Therefore, it is advised to exclude this condition out of the operation envelope.

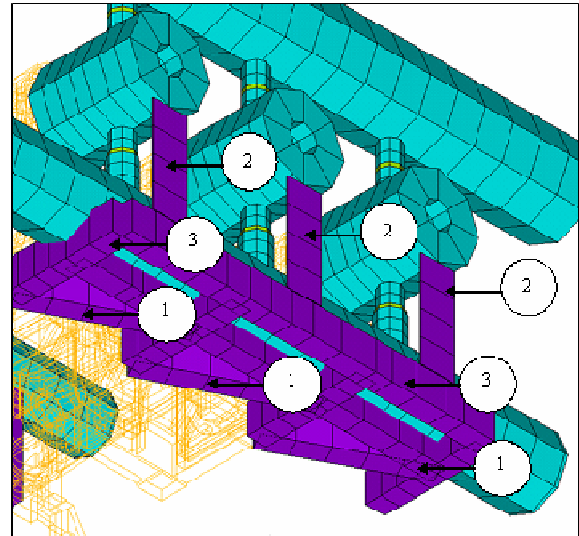


Figure 14: Advised modifications (bottom view of compressor manifold)

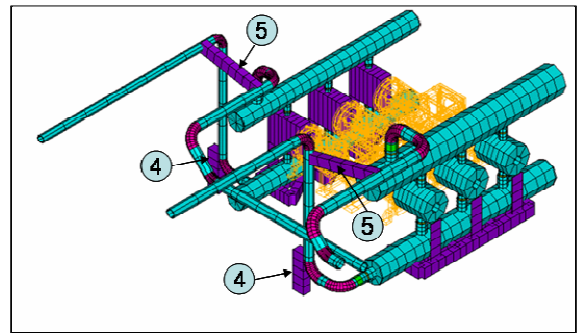


Figure 15: Advised modifications (isometric view)

6 Mechanical response analysis piping

6.1 Introduction

A mechanical response analysis of the pipe system has been carried out with the support layout of step 1 of the thermal stress analysis as discussed in chapter 4.1,. For this purpose a detailed (ANSYS beam type) FE model has been generated including all flexible beams, pipe racks and air-fin coolers, see figure 16.

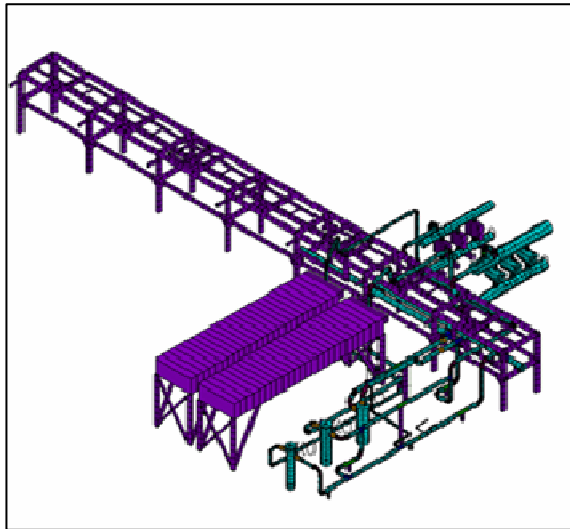


Figure 16: FE model of the complete pipe system

The calculations of the vibration and cyclic stress levels have been carried out with the finally advised modifications of the pulsation analysis for the following worst-case situations:

- $P_{\text{suction}} = 41 \text{ bar}$, $P_{\text{discharge}} = 207 \text{ bara}$, 100% load condition
- $P_{\text{suction}} = 70 \text{ bar}$, $P_{\text{discharge}} = 207 \text{ bara}$, 67% load condition

6.2 Results

With the results of the support layout of step 1 of the thermal stress analysis, the vibration levels exceed the allowable levels at several locations and at several compressor speeds. The maximum calculated vibration level was 4.2 times the allowable level. The maximum calculated vibration level occurs at a compressor speed of 628 rpm at 100% load.

The maximum calculated cyclic stress was within the allowable level according API 618. This means that fatigue failure of the piping, caused by pulsation forces, will not occur.

To decrease the vibration levels, several additional pipe supports, several additional braces, and/or several changes of the pipe rack were necessary.

Finally, 11 additional pipe supports, 5 modifications of the support steel structures and 5 modifications of the pipe rack were necessary to achieve acceptable vibration levels.

To achieve these results, several iteration steps, as discussed in chapter 4 were necessary between the static and dynamic analysis.

7 Measurements

7.1 Introduction

During start-up of the system vibration measurements have been carried out. The objective of the measurements is to check if the actual field vibrations are acceptable and to compare them with the calculated values.

The measurements have been carried out at three test runs at respectively 61, 35 and 38 locations. The suction 1st stage pressure was varied between 40 -70 bar and the discharge pressure was fixed at 170 bara. The measurements have been carried out at several unloading conditions and over the full speed range for parallel operation of two compressors (worst-case situation).

7.2 Results

Compressor cylinders

From the results it appeared that the vibrations are within allowable levels.

Pulsation dampers

From the results it appeared that the vibration levels are within allowable levels. The trend of the vibrations, especially for the high elevated suction dampers (higher at higher speeds), show a rather good agreement between measurements and calculations.

Large header piping

From the results it appeared that the vibrations are within allowable levels.

Small bore piping

From the results it appeared that the vibration levels are unacceptable high which could lead to fatigue failure. This was mainly caused by the fact that several supports do not make any contact by incorrect mounting, see figure 17. To decrease the vibration levels it was advised to install additional spring hold down supports and to brace the lines according API 618, chapter 3.7.1.7 and 3.9.3.12.

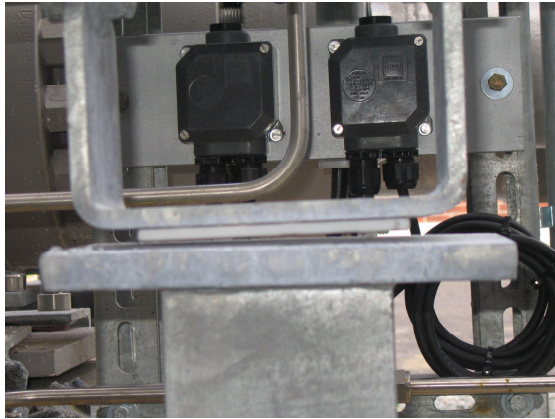


Figure 17: Support without any contact

Small bore instrument lines

High vibrations have been observed in small-bore instrument lines. It was advised to support these lines towards the nearest points of sufficient stiffness.

Air-fin cooler

Unallowable vibrations have been measured in the middle of the coolers close to the e-motor location, see figure 18. Despite the fact that the cooler was included in the model, the high vibrations were not predicted. This is probably caused by the fact that the model did not include all important details of the structure of the e-motor, which has an influence on the natural frequencies. It was advised to add a robust set of full-cross bracings to the 15m long air-fin cooler. After the installation of these measures the vibration levels were acceptable.



Figure 18: Air-fin cooler

8 Conclusions

From this project it appeared that extensive static (thermal) and dynamic iteration analyses according ASME B31.3 and API 618 are necessary to optimise the layout of the rather complex compressor system which can operate at a wide variety of operation conditions.

During the analyses the layout of the pulsation dampers, piping and support layout has been optimised in such a way that the system can operate safe, reliable and efficient for the long term.

The interaction between the static and dynamic analyses is essential to achieve the optimum solution and several iterations between these analyses were necessary.

An advantage of extensive simulations in comparison with trying to optimise the system with only field measurements is that the system can be optimised for all possible operating conditions. Especially measuring at different discharge pressures and unloading conditions for gas storage systems can be very difficult and time consuming.

Finally, vibrations measurements have been carried out during start-up of the system. From the results it appeared that the vibration levels on some small bore piping and air-fin coolers were unacceptable. A number of smaller adjustments to the supporting arrangement provided satisfactory results.

9 Acknowledgements

The authors would like to thank Essent for publishing the results of this project.

References

- ¹ API Standard 618, 4th edition, June 1995, "Reciprocating Compressors for Petroleum, Chemical and Gas Industry Services.
- ² Egas, G., Building Acoustical Models and Simulation of Pulsations in Pipe Systems with PULSIM3, "Workshop Kolbenverdichter", 27-28 October 1999, Rheine, pp 82-108.
- ³ Bokhorst, E., and Korst, H., Smeulers J.P.M. and Bruggeman, J., "PULSIM3, A Program for the Design and Optimization of Pulsation Dampers and Pipe System," *Proceedings of the Euro_Noise*, 1995, pp. 751-756.
- ⁴ Pyle, A., Eijk, A., Elferink, H., "5th edition of the API Standard 618", 3rd EFRC Conference, 27-28 March 2003, Vienna
- ⁵ ASME B31.3, "Process Piping"
- ⁶ Eijk, A., Egas, G., Effective Combination of On-Site Measurements and Simulations for a Reciprocating Compressor System, 2nd EFRC Conference, 17-18 May 2001, The Hague
- ⁷ API 661, "Air-cooled heat exchangers for general refinery services"
- ⁸ Eijk, A., Smeulers, J.P.M., Egas, G., "Cost-effective and detailed Modelling of Compressor Manifold Vibrations", Pressure Vessel and Piping Conference, Montreal, Canada, July 1996. PVP-Volume 328, pp 415-424
- ⁹ Eijk, A, Samland, G, Retz, N, Sauter, "Economic Benefits of CAD-Models for Compressor Manifold Vibration Analyses according to API 618", 3rd EFRC Conference, 27-28 March 2003, Vienna



Minimization of Gas Loss During Condensate Drain

by:

Dr. Ernst Huttar

Dipl. Ing. Rainer Scheifinger

Dipl. Ing. Thomas Heumesser

Mechanical Design and Control Engineering

LMF AG

Leobersdorf

Austria

thomas.heumesser@LMF.at

**5th Conference of the EFRC
March 21-23, 2007
Prague, Czech Republic**

Abstract:

In the last years LMF has realized a lot of innovations with the goal to save the environment in very different ways. In the field of tailor-made compressors, solutions to reduce the CO₂ pollution by recompressing flair gas are successfully installed in plants as well as on offshore platforms. Other LMF solutions to reduce the power consumption of compressors while operating under different load conditions have the approval of a wide population of compressor users.

In this lecture an alternative method will be presented, where the blow out time for condensate from separators is optimized in a way that the time when the flow of condensate ends followed by a gas stream. This right moment is detected and the condensate valves are closed. This easy solution can be used in all cases, for all pressures and even in applications where usually automatically, very sophisticate condensate drainers with level transmitters are applicable.

1 Introduction

One of the main targets during the last decade was to protect environment as far as it is possible for a machinery company producing compressors. To achieve this goal, a lot of very different solutions may be implemented.

One aim is to limit or stop any loss of CO₂ or any other relevant gas amount which has to be calculated as CO₂ value. To achieve this goal, normally a new process gas compressor is necessary, mainly to recompress flare gas, which is normally led to a flare to be burnt. The flare gas compressor recompresses the gas and adds it to another gas stream, which is a technical and commercial advantage. The second aim is to limit gas losses through any condensate drain, separated in a scrubber at each compressor stage. The third aim is the reduction of operating expenses, mainly electrical, natural gas or diesel fuel equivalent as compressor drive power source.

Any solution depends on customer specifications. The later described control sequence may technically be used on any compressor, but highly sophisticated specifications often promote other condensate drain separation possibilities.

The following chapters will first present a more complex solution, which also needs much higher investment cost and technical engineering. Secondly a very simple way to solve the condensate outlet of

condensate separation vessels will be discussed, also if this solution has disadvantages. The only benefit is the investment effort of this solution. The third possible way shown in the lecture has technical advantages, especially the reduction of gas loss and connected power consumption, all realized with low investment cost.

2 Tailor made condensate drains

2.1 Technical solution

As already said, this solution is normally specified by customers or design companies for process gas compressors. Each specification may include different requests for scrubbers and all instruments and valves necessary or connected to the condensate drain pipes and control logic. The mechanical type of the scrubber vessel is normally not the reason for differently or additionally mounted instruments.

According to the compressed gas flow, the condensate amount for each stage and separation may be calculated. Level measurement instruments have to be mechanically mounted on the scrubber. Different measurement principles may be necessary. For example, radar level instruments, differential pressure transmitters, magnetic level instruments etc. may be used. Additionally the number of instruments depends on the specification, for example one instrument for control, one for



Figure 1: Flare gas compressor package for a FPSO in the North Sea

shutdown purposes or also two out of three same or even different instruments with one or more physical measurement principles might be necessary. All these instruments will only give the information for the condensate level. According this level one or two on/off valves, sometimes in this case even control valves will be used for opening and closing the condensate drain to let out only the fluid and no process gas.

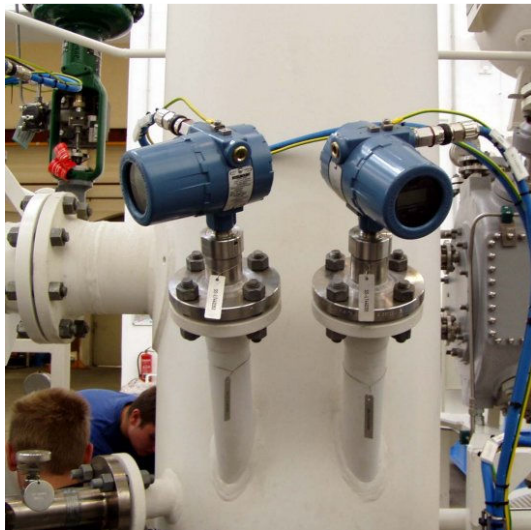


Figure 2: Double radar level instruments on a condensate scrubber

2.2 Principle of operation

Depending on the instruments, the condensate level is measured and four switch and/or alarm levels are used. The high and low switches for opening and closing the drain valve, the low alarm/shutdown switch point for closing the ESD valve and the high alarm/shutdown for stopping the compressor because of the risk of condensate fluid to be transferred to the next stage compressor cylinder.

Some solutions include on/off valves, others may additionally include control valves for condensate drain outlet. In the case of control valves, normally the condensate level will be controlled electronically, to achieve a stable level during compressor operation.

2.3 Commercial impact

The described principle is technically the best solution for any condensate drain. The main reason for any other strategy to solve condensate drains are the investment costs. Basically all manufacturers face the same situation on the sales side, prices are

too high, solutions are too sophisticated, everybody has to reduce the financial effort for solving technical issues.



Figure 3: Condensate drain system of a process gas compressor unit

3 Simple condensate drains

3.1 Technical solution

A very different solution is used on small compressors, built without special specifications. Each condensate drain is equipped with a scrubber, the condensate flow is only controlled by a simple solenoid valve, no level measurement or other instruments are used. Normally this way is used on air cooled high pressure compressors, utilised for industrial air, industrial gases, CNG and a lot of other purposes.

3.2 Principle of operation

The control sequence for opening and closing the solenoid valve depends on a fixed time stamp, which means that the valve is switched after a timer controlled lead time. Also the opening time is fixed and does not depend on the amount of condensate in the scrubber. This solution is simple enough, so that any compressor control basis may be used.

The simplest electric sequence may be controlled by easy, manually adjustable time relays and contactors.

More complex solutions may be programmed in any programmable logic controller. If a simple human machine interface is used, timers for switch interval and opening time may be adjusted by the operator according to the compressed gas humidity and the predicted amount of condensate. Additionally a programmable controller is able to manage the sequence of more condensate valves of the different stages of the same compressor. The loss of gas and pressure is the main reason to control also the sequence. If not only one solenoid valve opens at the same time, the pressure drop and consequently the loss of flow and power is much bigger than necessary.

The main disadvantage of the described solution is the fixed time sequence, which basically does not depend on humidity, temperature or any other parameter. This leads to longer opening times and therefore bigger losses of gas and drive energy. Manual adjustment may help a little, but does not really solve the problem.



Figure 4: Human machine interface for the manual condensate drain adjustment

Especially on mobile units, for example ship bound air compressors, the condensate amount may vary a lot. In northern areas the temperature is cold and the air is dry, in tropic atmosphere high temperatures are possible combined with relatively high air humidity.

Any fixed condensate drain time sequence can only be arranged for the worst case, not to get any condensate passover to the next stage cylinder. Therefore opening times of the solenoid valve are normally much too long, the pressure loss during drain period is high, energy and compressed gas is lost.

3.3 Commercial impact

The simple condensate drain solution is a very cheap way. Investment costs are low, but the operational risk may be very high. If the gas quality is stable, the humidity does not change and the climatic effects do not have to be considered, no operational consequences have to be kept in mind. In such a case, any more sophisticated solution is neither necessary, nor recommended.

4 Simple, energy saving condensate drains

4.1 Technical solution

The simple and energy saving solution is mechanically not so much different to the previously one described. After each compressor stage the compressed gas is cooled down and the condensate is separated in a scrubber. Normally an easy cyclone separator is sufficient. The drain pipe is equipped with a simple solenoid valve, which switches the drain line. No other instruments are used, especially no level transmitter is necessary. The only additional signal necessary is the line pressure in the compressor stage somewhere near the separator connection. This pressure transmitter is no additional device, because the transmitter is used to monitor and display the stage pressure.

4.2 Principle of operation

The operational sequence for the condensate drain is slightly changed compared to the simple mode, but the simple mode is included as basic operation mode.

The whole sequence has to be programmed in a programmable logic controller. Any contactor and relay circuit with solid state time relays is no possible way to control this solution logically.

The basic time depending sequence programmed in the programmable logic controller is equivalent to the simple logic, described before. If the solenoid valve is opened by the control system, the pressure transmitter of the same stage is monitored. The valve will be closed the moment the stage pressure drops. This incidence happens, if the condensate fluid has left the separator and only the gas or air is led to the drain piping. This sequence opens the solenoid valve only as long as some fluid is inside the separator and does not loose any gas during the condensate drain.

As the compressor control system is equipped with a human machine interface with graphic display, some more adjustments may be done. The necessary pressure drop may be changed as a percentage value from the relevant stage pressure. The basic time sequence may be changed manually to adapt the time intervals according to the gas quality. An alarm is displayed, if the relevant stage pressure does not drop, in this case the valve closes after a fixed programmed time delay.

As long as the sequence works properly, no gas is let out to the drain piping, only fluid is flowing through the drain valves. An additional automatic adaptation may also be actuated. The mechanical parameters like piping diameters, pressure in the stage, temperature after the cooler, etc. stay the same during normal operation. Therefore the time the solenoid valves is kept open is equivalent to the amount of condensate in the separator. If this time gets longer and longer, the amount of condensate fluid is higher. As the control system may detect this instance, because of the time the valve keeps open, the time based sequence may be adapted to shorter time intervals between the valve opening steps.

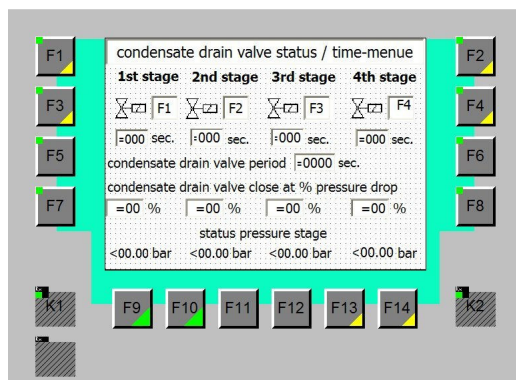


Figure 5: Human machine interface for the energy saving drain system

The advantage of this program logic is the reduction of gas losses through the condensate drain system. As the pressure drop in the compressor stages is limited during condensate blowoff, no additional power is necessary to compensate the gas loss. Climatic changes may also be compensated automatically.

The described solution and control strategy may be used on any type of compressor as long as condensate separators are used and does not depend on the compressed gases. Experience in the field is confirmed by customers and the performance is satisfactory. Further development may be included and added if necessary.

4.3 Commercial impact

This simple energy and gas saving solution is a very cost saving possibility for condensate drains. No investment for additional parts is one of the main advantages. The effort lies only in software and programming and may also be added to already operating compressor units.

5 Conclusion

The target to limit the gas loss at any condensate drain of a compressor is also achievable for simple, non process gas compressor units. The solution is easy and cost effective and may be used for all versions of a compressor.

Complex solutions, including expensive instruments and control valves will have a market for sophisticated units in the field of oil and gas as well as chemical processes. Simpler contracts in any field of operation may get a technically comparable solution as far as environment advantages are considered. The decision, how to design the condensate drain will be different from contract to contract and will depend on the specification and all negotiations between customer and manufacturer.

Dynamic design of the foundation of reciprocating machines for offshore installations – case study

by:

Dr.-Ing. Jan Steinhausen

KÖTTER Consulting Engineers KG

Rheine, Germany

**5th Conference of the EFRC
March 21-23, 2007
Prague, Czech Republic**

Abstract:

The installation of large and heavy reciprocating machines on offshore constructions demands specific requirements in the design of the foundation with respect to vibrations. Because the use of those piston engines implies high dynamic loads at the substructure of offshore systems, special measures are required. This paper shows how problems can be avoided by applying a detailed vibration engineering design. An offshore project in the German North Sea involving the installation of three heavy reciprocating mud pumps is taken as an example. It is demonstrated how vibration engineering aspects can be considered within a project at the very beginning. The developed installation concept and its specific technical implementation at the construction are part of this paper.

1 Introduction

For the foundation of heavy reciprocating machines at offshore platforms one has to keep an particular eye on the dynamic loads which will be induced into the substructure below the installation. Normally, block foundations made of concrete cannot be used because of their heavy weight and shortage of space on site. This paper presents the vibration engineering design for the example of the foundation of three reciprocating mud pumps on an offshore platform.

On “Mittelplate” (see figure 1), the artificial platform for drilling and mining of petroleum in the German wadden sea, a new drilling rig for increasing the exploration capacity has been planned since 2003. The drilling rig of type T150 has been built upon the existing skidding beams (of the former drilling rig) since August 2005 and has been set into operation in December 2005.



Figure 1: The drilling and mining platform „Mittelplate” in the state with the old drilling rig

The studies in the run-up to the project resulted in minimizing the weight of the drilling rig which moves on the skidding beams, see figure 3. For that reason, the idea was born to relocate the mud tanks, the pump installation, the silos for auxiliary flushing and parts of the electrical installation (SCR-unit) above the area of the “Fangedamm”. The “Fangedamm” is placed in the west of the platform. Its task is to absorb the water wave energy during heavy weather and to protect the “Mittelplate”. For the relocation of these units the “Fangedamm” should be covered with a concrete slab founded with piles into the wadden sea. Figure 2 presents the planned installation with the pump house in the middle of the slab above the “Fangedamm”. In order to minimize the transmission of vibrations due to the operation of the three mud pumps (power 2,200 hp each) to other units and especially to the sensitive SCR-unit, the vibration engineering aspects have been considered from the very beginning of the construction.

2 Feasibility analysis

For the basic design in the run-up to the project in 2003 first computations should investigate the basic vibration behaviour of the pump installation.

2.1 Modelling

For the setup of the computational model (Finite-element-method) the new platform construction (slab) above the „Fangedamm“ has been considered as a plane construction consisting of prefabricated elements of reinforced concrete. The inter-connections between the elements are considered as monolithic (rigid). The concrete slab is founded with steel piles into the ground of the wadden sea. Figure 3 shows the design of the slab and the pile foundation with the positions of the piles below the slab. The basic concept of the vibration insulation of the pump house provides a decoupling of the platform areas in the north and in the south. This decoupling is obtained by slits in the slab, see figure 9. Hence, the area of the pump house foundation can be treated separately. Therefore, the installation of the reciprocating machines has been modelled for eight rows of the piles between the axes C and F, see figure 4.

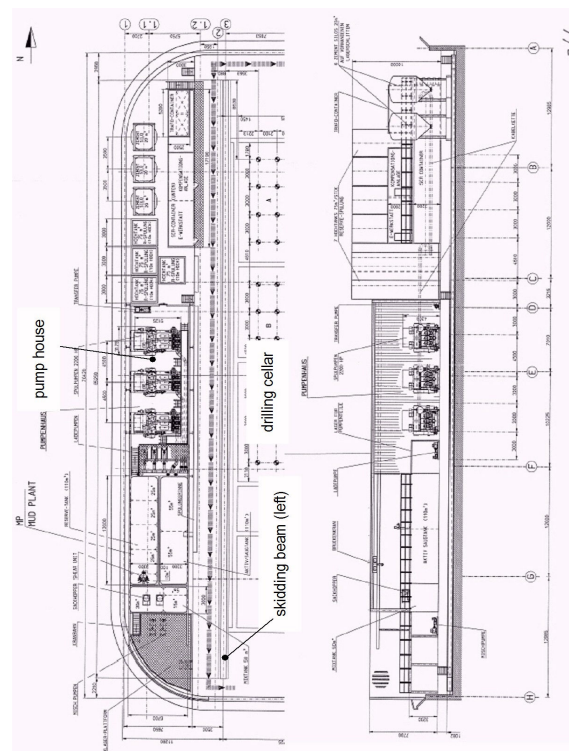


Figure 2: Application areas of the new platform above the „Fangedamm“, left: plan, right: side view

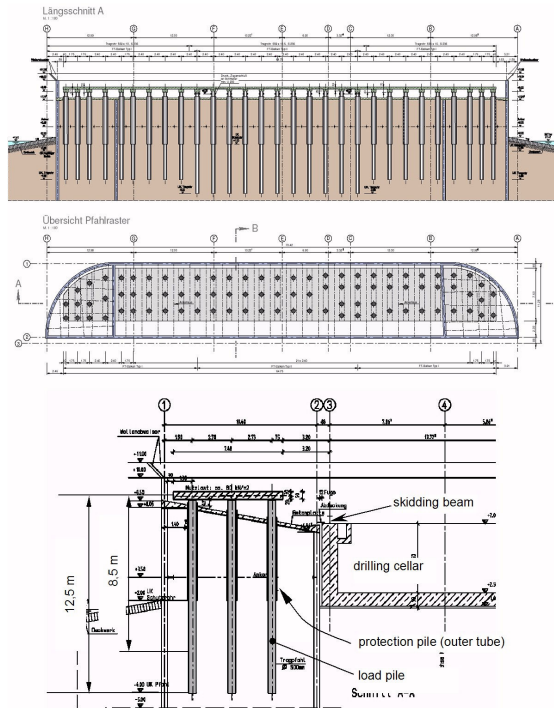


Figure 3: Pile foundation design for the new platform above the “Fangedamm”, top: section in north-south direction, middle: top view of slab (grey) with pile grid, bottom: section (in east-west direction) of the slab and pile foundation

For a first design of the pile foundation steel pipes with a diameter of 500 mm, a thickness of 10 mm and a length of 12.5 m have been considered. The outer piles (protection piles, diameter 700 mm) should protect the inner piles – the load piles – against the wave impact on the “Fangedamm”. They do not have any contact to the load piles. Therefore, they are not involved in the considerations here.

For a first evaluation of the foundation the (elastic) bedding of the piles has been substituted by a fixed length of 8.5 m from the top to the foot of the pile, see figure 3. There are three piles planned in a row in east-west direction. Each pile foot is considered as totally fixed.

The mud pumps are triplex-type reciprocating pumps, type 7.5”x14” / 2200 HP, manufactured by WIRTH. The weight mass of 46 tons of each machine has been distributed (lumped mass) according the fixation positions of the skid onto the slab of the FEM-model. The speed of the pumps is within the range from 0 rpm to 110 rpm.

The maximum dynamic load reactions arise at the 1st order due to the free mass moments of the machines (1st order: 0 – 1.83 Hz).

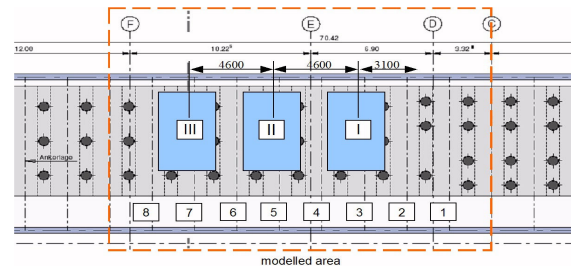


Figure 4: Positions of the mud pumps and alignment of the piles, first design

2.2 Modal analysis

A modal analysis has been carried out for a primary assessment of the dynamic behaviour of the first construction design. The results indicate the three lowest natural frequencies are within the 1st order frequency range (0 – 1.83 Hz), thus in the range of the largest reaction load. Figure 5 presents the natural mode shapes up to about 20 Hz. The 1st and 2nd mode shape indicate each primarily a translation of the concrete slab, the 3rd indicates a torsional movement (with vertical axis). The 4th mode shape indicates a deformation of the concrete slab itself.

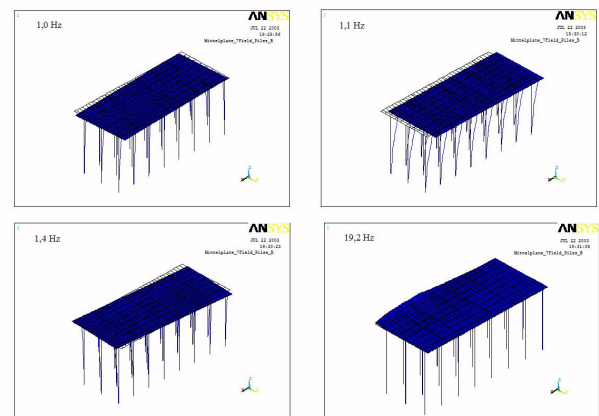


Figure 5: Natural mode shapes of the first design of the pump installation, undeformed: unfilled grid, deformed: filled grid

2.3 Response analysis at operating conditions

For a first assessment of the forced vibration level during operation of the pumps the exciting mass moments within the 1st order frequency range have been obtained from the data specified by the manufacturer. The exciting moments are applied on the model with respect to the location of the crank shaft of each pump, see figure 6.

The oscillating moments represent a harmonic excitation with direction normal to the slab. The direction of the rotating moments rotates with the rotating frequency in the y-z plane. All moments are acting synchronously (no phase shift). Thus, the worst case is considered, when all pumps are in operation. The critical damping ratio is set to 0.025 for the complete frequency range. The simulated results show that the vibration velocity on the concrete slab achieves in case of resonance up to 70 mm/s (target is: 3 mm/s rms) in horizontal direction.

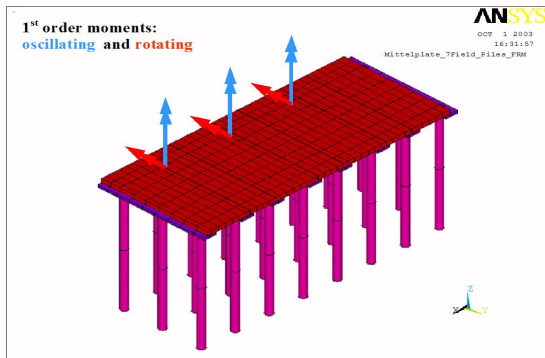


Figure 6: Applied moments for first response analysis

In order to avoid exceeding resonance vibrations within the frequency range of the 1st order, the target has been to shift the 1st (lowest) natural frequency of the complete construction above 3 Hz. Therefore, the slab of the pump house should be connected with a steel-framework to the massive drilling cellar (reinforced concrete), see figure 7. First calculations for this 2nd design indicated the lowest natural frequency far above the critical exciting range of the 1st order of the pump speed. Thus, exceeding resonance vibrations are eliminated within this frequency range.

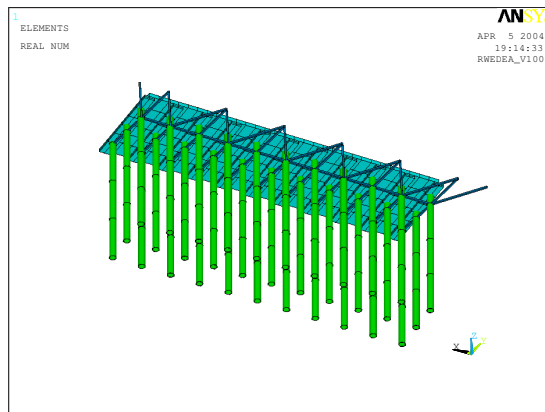


Figure 7: FEM-model of the 2nd design of reciprocating pump foundation, connection of the slab of the pump house to the massive drilling cellar by framework construction

However, the natural frequencies of the construction (2nd design) will be excited by the load reactions of the 2nd, 3rd and other higher orders. For a more accurate estimation of the expected vibration level (during operation of the pumps) the exciting reaction forces have been determined by measurements on the test bench at the manufacturer. For this, a single of the reciprocating pump has been set up on especially prepared steel profiles (beams) on which strain-gauges have been applied. The forces transmitted to the ground have been measured at selected locations of the skid. The forces have been determined in x-, y- and z-direction. The maximum forces have been detected at 110 rpm with maximum load (pressure). For example, figure 8 presents the time-frequency spectrum of the force in y-direction at a selected position on the skid during run up (0 – 110 rpm), steady state (110 rpm) and run down (110 – 0 rpm). Local resonances of the test bench setup can be seen here, too. The relevant frequency range goes up to about 30 Hz. From the measured forces (at different locations) the exciting forces and moments of the reciprocating machine for the further calculations have been derived.

The reaction forces and moments have been applied to the FEM-model of the 2nd design. The results of the response analysis show that even by the higher order forces (moments) exceeding vibrations of the slab can be excited (resonance cases). To take this into account, the resonance vibrations should be decreased by special damper elements and should be integrated in the framework design, see figure 11. The selected dampers are acting as viscous dampers [3].

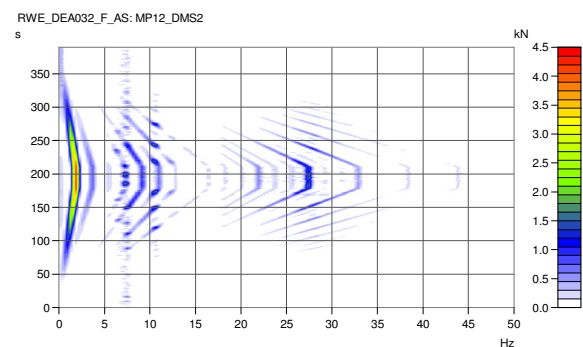


Figure 8: Time-frequency spectrum, example of force in y-direction (at a selected position) during variation of the pump speed: 0 - 110 - 0 rpm

2.4 Result of the feasibility analysis

The basic computations for the mud pump foundation reveal that the critical exciting frequency can be shifted above the critical exciting frequency range (1st order) by stiffening the structure with a steel-framework connected to the drilling cellar.

The damping of the expected higher frequency vibrations (structural resonances) will be provided by special dampers. All in all, from the vibration point of view the installation of the reciprocating pumps on the slab above the “Fangedamm” is feasible.

3 Detailed layout – Structural dynamic calculations

The feasibility study was followed by the detailed design of the framework and the damping elements. After completion of the work in the underground at the construction side, the following changes have been found compared to the existing (fundamentals of the calculation) model:

1. Strongly varying lengths of the piles and thus of the penetration depths into the supporting (ground) layer.
2. A change in bedding functions¹⁾ depending on the penetration depth of the piles.
3. A change in position of several rows of pillars made the pillar distance no longer equidistant in north-south direction.

3.1 Measurements to obtain the properties of the construction

To verify the model for the bedding function of the pile foundation, dynamic measurements of the construction properties have been carried out after completion of the bare concrete platform for the pumps (i.e. without the pumps and other constructions on the platform). Following the measurements, the calculation model has been adapted.

Preceding calculations with the original assumptions for the bedding functions have showed that the lower three mode shapes of the concrete platform (placed on piles) can be expected in the frequency range between 2.5 and 3 Hz. Because of this a special unbalance exciter was used during the measurements that excited with an adequate force at frequencies as low as 1 Hz. The filled slits for vibration decoupling at the north and south edge of the concrete platform for the pumps (see figure 9) were emptied. No contact bridges existed with adjoining platforms in the north and the south. The slab for the pumps could thus move freely in horizontal plane.

The FEM-model has been adapted to the measured natural frequencies and damping. Apart from the individual lengths of the piles and their penetration

¹⁾ bedding function = change of the modulus of elasticity of the soil-layer with depth

depths, the framework under the concrete platform has also been considered in this adaptation. The adaptation of the bedding function has been carried out on the following parameters:

1. dynamic bedding modulus, $K_{S, dyn}$
2. depth of (the top of) the supporting ground layer, h_{BA}
3. damping in the bedding function, D_S

For the location of the natural frequencies primarily the first two parameters are of importance.

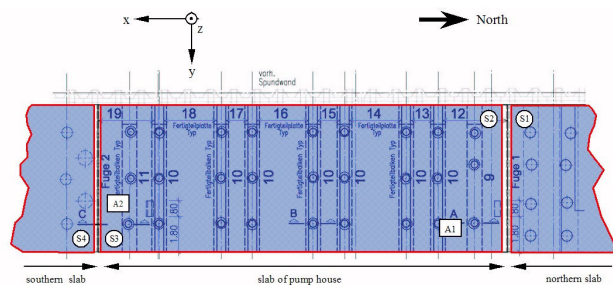


Figure 9: Location of the measurement points S1 to S4 and the locations of the unbalance exciter A1 and A2 (top view of the concrete platform).

3.2 FEM-model of the foundation

For the final model of the construction above the „Fangedamm“ in the vicinity of the pumps eight rows of piles in north-south direction have been taken into account (see figure 10). The concrete plate has been assumed to be monolithic, i.e. with rigid interconnections. The connection of the steel pile heads to the concrete slab has also been assumed to be rigid. The masses of the three Triplex reciprocating pumps have been distributed as four masses per pump (so in total 12 masses) at a height equal to the centre of gravity of the pumps, i.e. at 1.25 m above the centre of gravity plane of the concrete platform (thickness 30 cm).

Figure 10 shows the optimized FEM-model for the pump house including the framework connecting to the drilling cellar and the trusses for the implementation of the dampers. The framework that is connected to the construction above the drilling cellar has been adapted to the real north-south orientation of the pile rows. From several calculations, it has been found that the most favourable position for damping, i.e. the dampers, is under the overhang of the concrete platform.

3.3 Optimization of the framework

To reduce the resonances of the components above the 1st order of the pump speed, dampers have been implemented with almost viscous damping properties. From parameter studies followed a damping specification for the dampers of $d = 500 \text{ kNs/m}$ at 16 Hz.

Within the scope of optimizing the framework several configurations with different stiffness of the framework and number of dampers have been investigated. It has generally shown that for a framework with a higher stiffness the resonance amplitudes have been smaller compared to that of a framework with less stiffness with the same amount of dampers.

The implementation of 8 dampers has been favourable for obtaining a targeted maximum vibration velocity amplitude of 3 mm/s (rms) at the concrete surface under operating conditions. The calculated mode shapes of the optimized installation are depicted in figure 13. The 1st mode shape can be seen primarily as a movement of the concrete platform in x-direction parallel to the drilling cellar. The 2nd mode shape is a rocking and translational mode of the concrete platform into the drilling cellar. The 3rd mode shape is more a torsion mode of the concrete platform. The higher mode shapes are vibrations of the framework.

The results of the vibrational analysis at the operating conditions have showed that with three pumps operating in parallel the targeted vibration velocity of 3 mm/s (rms) is reached. As an example, figure 11 shows the time-frequency-amplitude spectra of the calculated vibrational velocity in y-direction at node 244 (location, see figure 10), where the highest vibration level occurs. The figure shows a resonance at 13 Hz that occurred at a simulated sweep of pump rotation speed up to 110 rpm.

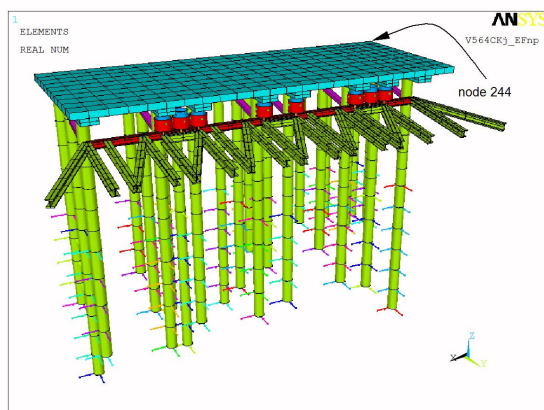


Figure 10: FEM-model of the optimized and realised framework with the 8 damping elements under the concrete platform (slab).

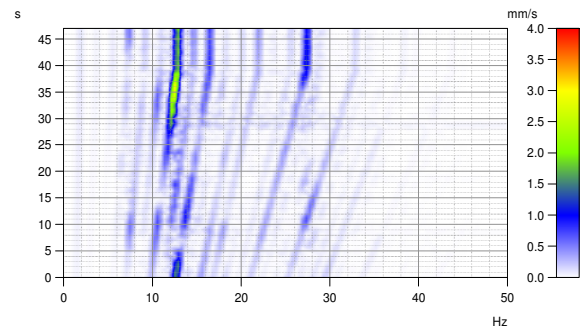


Figure 11: Time-frequency-amplitude spectrum of the calculated vibrational velocity in y-direction at node 244 (max. 3.1 mm/s rms) excitation in y-direction, rotational sweep 90 – 110 rpm.

4 Verification measurements

After completion and start-up of the new drilling rig, the vibrational situation during operation of the pumps was checked by measurements. The vibrations of the construction were measured at several locations at the slab of the pump house and at the neighbouring slabs (north: container, south: tanks). The measurements have showed that the structural vibrations (movements of the slabs) are within the limit of 3 mm/s rms at all operating conditions of the pumps. The slabs north and south of the pump house showed a significantly lower vibration level compared to the slab of the pump house. An excitation of higher resonances at neighbouring slabs could not be identified. Thus, the slits (with filling) are sufficient as vibrational decoupling. All in all, the function of the framework with dampers proved to be very satisfying.



Figure 12: Framework after completion.

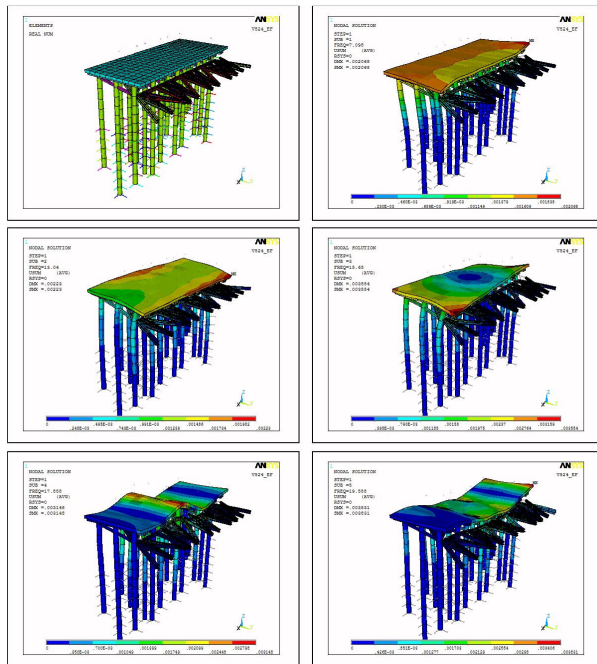


Figure 13: Undeformed model (top left side) and natural mode shapes, minimum displacement: blue, maximum displacement: red, natural frequencies (from left to right and from top to bottom) 7.1 Hz (top right), 13.0 Hz, 15.7 Hz, 17.8 Hz, 19.6 Hz.

5 References

- [1] Riehwein, W.; Lesny, K.; Wiemann, J.: „Nachweise und Sicherheitskonzepte für die Gründung von Offshore-Windenergieanlagen in der Deutschen Bucht“, 2. Symposium Offshore-Windenergie, Bau- und umwelttechnische Aspekte, September 2002, Hannover
- [2] Schaumann, P.; Seidel, M.: „Eigenschwingverhalten von Windenergieanlagen – Berechnungen und Messungen“, Vortrag zur DEWEK 2000, Wilhelmshaven
- [3] Gerb Schwingungsisolierungen, 11. Auflage, Berlin, 2002

Modelling Fluid Dynamics, Heat Transfer and Valve Dynamics in a Reciprocating Compressor

by:

Roland Aigner and Herbert Steinrück
Institute of Fluid Dynamics and Heat Transfer
Vienna University of Technology
Vienna
Austria
roland.aigner@tuwien.ac.at

5th Conference of the EFRC
March 21-23, 2007
Prague, Czech Republic

Abstract:

In the present study one- and two-dimensional numerical models are proposed for calculating gas flow and valve dynamics in a reciprocating compressor. It turns out that they are capable of capturing the most important physical effects during a compression cycle, namely the interaction between pressure waves inside the cylinder and valve dynamics. In order to model the heat transfer from the gas to the cylinder full three-dimensional simulations have been carried out. Inspecting the results a reconstruction of the heat flux depending only on few dimensionless numbers has been derived. The reconstructed heat fluxes have been incorporated into the simplified one dimensional compressor model allowing a heat transfer analysis of a compression cycle. Comparisons with measurements and full three-dimensional simulations of different types of compressors show good agreement.

1 Introduction

Full three-dimensional simulations of reciprocating compressors with present commercial CFD-programs are state of the art. They produce accurate and reliable results regarding valve motion, fluid dynamics and heat transfer. But, they cannot meet the demands of engineers for usability and short computation times. For example the average computation time for one compression cycle inside the cylinder can exceed 2 days¹.

At first glance calculating the gas flow in a compressor seems to be a complicated task and a full three-dimensional simulation unavoidable. However, it turns out that a quasi one-dimensional model for the gas flow coupled to a simple valve model is sufficient to describe the main effects in case of barrel design compressors with two valves. Compressors with more than two valves require a quasi two-dimensional approach in order to account for the multiple valve pockets, where the gas enters and leaves the cylinder. Apart from the fact that both the quasi one-dimensional model and the quasi two-dimensional model need remarkable less computation time than the full simulation, only the main features of the compressor geometry have to be specified.

Considering heat transfer one can perform on one hand a full three-dimensional numerical simulation including the heat transfer analysis of the mechanical structure, the exchange of heat with the environment and heat transfer processes in the compressor as well. The disadvantages of such an approach are stated above. On the other hand one can use some empirical estimates of the heat transfer from the gas to the compressor. These formulas are naturally very crude since they cannot be expected to capture the heat transfer process within the cylinder which depends on complex flow processes. Therefore the following approach combining both methods will be used. By means of well proven commercial CFD codes the heat transfer is determined for a wide range of compressor types and operating parameters. Inspecting the results and furthermore identifying the major physical effects of the heat transfer leads to reconstructed heat fluxes, whereas the reconstruction is based on a few dimensionless numbers and some process quantities such as gas temperature inside the cylinder and mass flow.

First we introduce the quasi one-dimensional and two-dimensional flow model. Since the quasi one-dimensional model was presented in detail in 2005 at the 4th EFRC conference² this paper focuses on the two-dimensional approach and compares simulation results with measurements. Then the heat transfer reconstruction method will be derived. And finally we present an extension of the well-proven one-dimensional simulation tool for two-dimensional geometries and heat transfer analysis.

2 Modelling of the Gas Flow and Valve Dynamics

2.1 Geometry

2.1.1 Three-dimensional

Half of the interior of a reciprocating compressor is displayed schematically in figure 1. The piston is shown at an intermediate position, where it does not mask the valve pockets. The valves are adjacent to the circular lateral surfaces of the valve pockets.

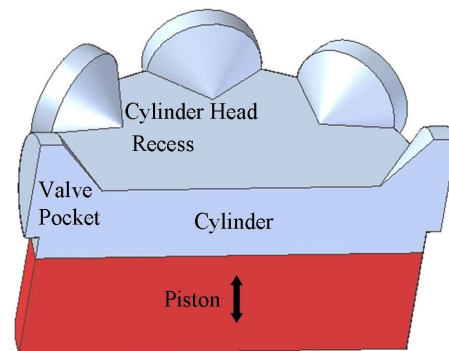


Figure 1: Geometry of compressor with more than two valves

2.1.2 One-dimensional

In the quasi 1-d model the wave propagation along the diameter (x -axis) of the cylinder from the suction to the pressure valve is considered. The equations of motion (Euler equations) are integrated over a cross section $A(x,t)$ perpendicular to the x -axis. The effective cross sections of the quasi one-dimensional model are displayed schematically in figure 2.

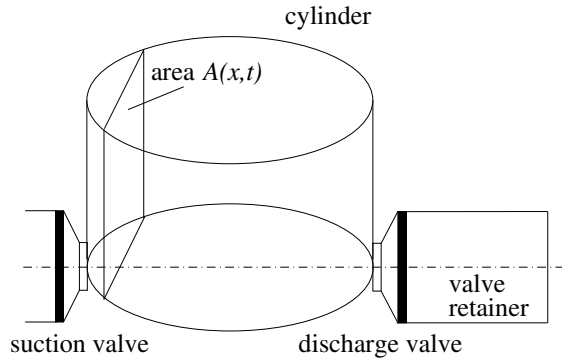


Figure 2: Schema of the one-dimensional model

2.1.3 Two-dimensional

The two-dimensional model takes the wave propagation in a plane parallel to the cylinder head (x,y -plane) into account. The equations of motion (Euler equations) are integrated over the height $h(x,y,t)$ of the cylinder. In terms of the compressor the height is the distance between the piston and the cylinder head. The two-dimensional computational domain is displayed schematically in figure 3.

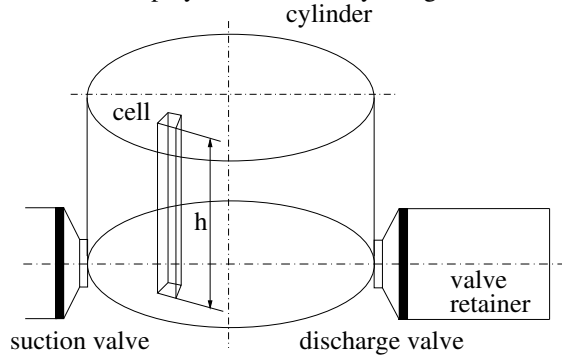


Figure 3: Schema of two-dimensional model

In order to keep the model as simple as possible and hence least time consuming (in terms of computational time) a one-dimensional approach is used for the valve pockets and valve retainers. A typical grid for a compressor with eight valves is shown in figure 4.

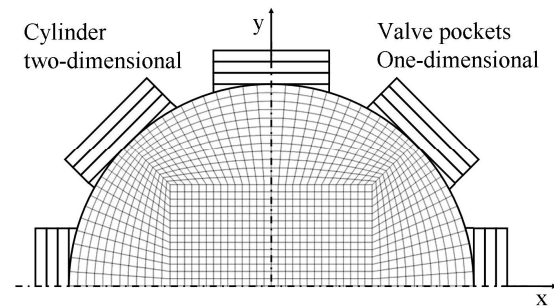


Figure 4: Combined two-dimensional one-dimensional grid

2.2 Governing Equations

2.2.1 Piston Motion

The distance between piston and cylinder head h depending on time t can be determined using the properties of the crank mechanism. We use the length of the crank lever r , the length of the piston rod l , the smallest distance between piston and cylinder top h_0 and the present angle of the crankshaft φ to obtain

$$h = r + l + h_0 - r \cos \varphi - l \sqrt{1 - \left(\frac{r}{l}\right)^2 \sin^2 \varphi}, \quad (1)$$

where $\varphi = 2\pi n t$. Here, n denotes the speed of the crankshaft.

2.2.2 Flow Field

The governing equations for the flow of gas are obtained by taking the mass and momentum balance over a cell. The variables ρ , u , v , p have their usual meaning, density, velocity in x -direction, velocity in y -direction and pressure, respectively.

$$\frac{\partial \rho h}{\partial t} + \frac{\partial \rho u h}{\partial x} + \frac{\partial \rho v h}{\partial y} = 0, \quad (2)$$

$$\frac{\partial \rho u h}{\partial t} + \frac{\partial (\rho u^2 h + p h)}{\partial x} + \frac{\partial (\rho v u)}{\partial y} = p \frac{\partial h}{\partial x}, \quad (3)$$

$$\frac{\partial \rho v h}{\partial t} + \frac{\partial (\rho v^2 h + p h)}{\partial y} + \frac{\partial (\rho v u)}{\partial x} = p \frac{\partial h}{\partial y}. \quad (4)$$

Assuming isentropic flow conditions we replace the energy equation with

$$p \rho^{-\gamma} = \text{const}, \quad (5)$$

where γ denotes the ratio of specific heat capacities. Note that equations (3) and (4) are not of conservation form. The right hand terms constitute a momentum source of the flow due to a variation of the height inside the cylinder. However, only smooth cylinder head recesses can be considered since the gradients of h become very large in case of sharp changes.

The governing equations (2)-(4) reduce to the one-dimensional model equations by replacing the height h with the cross-section A and setting the velocity in y -direction v to zero.

2.2.3 Valve Dynamics

The treatment of valve motion follows the well known Costagliola³ theory. The state of a valve is specified by the distance between valve plate and seating (valve lift) x_v . The motion of the valve plate is determined by the forces acting on it. We consider the following three contributions to the resulting force: the pressure difference across the valve acting on an effective force area A_v of the valve plate, the springing and thirdly a contribution due to viscous forces in the initial stages of valve opening. Denoting the pressure in front of the valve p_1 and behind the valve p_2 we obtain the equation of motion for the valve plate

$$m_v \ddot{x}_v = (p_1 - p_2)A_v - k(x_v + l_1) - F_{adh}. \quad (6)$$

Here m_v stands for the mass of the valve plate. The constants k and l_1 denote stiffness of springing and initial deflection of the springs. An initial sticking effect is modelled by the force F_{adh} . It is caused by the viscosity of the gas in the valve gap resulting in a small time delay when the valve is opening. It reads as follows (Flade⁴)

$$F_{adh} = f_1 \frac{\dot{x}_v}{x_v^3}. \quad (7)$$

The factor f_1 depends on geometric features of the valve and properties of the gas. It also takes lubrication oil at the valve plate into account.

2.2.4 Flow through the valve

The flow through the valve is considered as the (quasi stationary) outflow of a gas from a pressurized vessel through a convergent nozzle. The mass flow through the valves is given by St.Venant and Wantzell⁴,

$$\dot{m} = \phi \rho_1^0 \left(\frac{p_2}{p_1^0} \right)^{\frac{1}{\kappa}} \sqrt{\frac{2\kappa}{\kappa-1} \frac{p_1^0}{\rho_1^0} \left(1 - \left(\frac{p_2}{p_1^0} \right)^{\frac{\kappa-1}{\kappa}} \right)}. \quad (8)$$

where p_1^0 is the total pressure before and p_2 is the pressures after the valve, respectively.

The effective flow cross section ϕ of the valve is assumed to be a function of the position of the valve plate x_v only. It has to be determined empirically.

2.3 Numerical Solution

2.3.1 Finite Volume Method

For the numerical analysis it is useful to write the continuity equation (2) and both equations of motion (3), (4) in following form:

$$\frac{\partial \mathbf{u}}{\partial t} + \frac{\partial \mathbf{f}(\mathbf{u}, x)}{\partial x} = \mathbf{s}, \quad (9)$$

with the state vector $\mathbf{u} = (\rho A, u \rho A, v \rho A)^T$. $\mathbf{f}(\mathbf{u}, x)$ and \mathbf{s} denote flux functions and source functions, respectively. In case of the one-dimensional approach the state vector \mathbf{u} is reduced to $(\rho A, u \rho A)^T$ and appropriate flux functions and source functions are used.

The system of equations (9) can be solved by different finite volume schemes. The f-wave algorithm by Leveque⁵ and the Lax-Wendroff⁶ scheme can be applied to the one-dimensional approach and the two-dimensional method, respectively.

2.3.2 Boundary and Interface Conditions

The finite volume scheme has to be supplied with appropriate boundary conditions. If the valves are closed, they are described as a fixed wall, by setting $u=0$. If the valve is open the mass flow is prescribed. It is obtained by equation (8) as a function of the total pressures before and after the valve and the valve plate position. The pressure outside the suction valves is kept constant. To determine the pressure after the discharge valves wave propagation in the valve retainers are computed using the finite volume scheme. At the end of the valve retainer the pressure is prescribed. The equation of motion (6) of the valve plate is solved simultaneously by an explicit second order scheme.

Every opening or closing valve initiates a wave. Thus, in case of compressors with more than two valves two-dimensional wave patterns occur, which cannot be approximated by plane waves. Extending the model for the numerical simulation inside the cylinder to two dimensions resolves this problem. However interface conditions must be set for the transition from the one-dimensional domain to the two-dimensional domain.

Regarding our model the interfaces are located between the valve pockets and the cylinder.

2.3.3 Time step

The time step Δt of the numerical integration has to be chosen such that the stability conditions of the numerical schemes are satisfied. In case of the one-dimensional approach the CFL condition $\Delta t < \Delta x / (c + |u|)$ has to hold, where Δx is the interval length of the spatial discretization and c is the velocity of sound. In the two-dimensional case we limit the time step by $\Delta t < \Delta x / (c + |u| + |v|)$. Using an explicit scheme for the valve dynamics the numerical stability condition $\Delta t < m_v/k$ must be satisfied.

2.4 Comparison of the Numerical Solution with measured Data

2.4.1 Compressor with 2 valves

A double acting, 2 cylinders, barrel design reciprocating compressor was tested at Burckhardt Compression, Switzerland. The main specifications of the compressor can be found in table 1. Pressure sensors inside the cylinder (see figure 5) record the pressure at different locations. The relative pressures in the diagrams are referred to an ambient pressure of 0.97 bar.

Type of compressor	Burckhardt Compression 2K90-1A: 2 cylinders, double acting
Bore diameter	0.22 m
Stroke	0.09 m
Speed of Crankshaft	980 ÷ 990 rpm
Gas	Air
Number of Valves	2
Pressure Ratio	1/2 and 1/5

Table 1: Main specifications of the Burckhardt test compressor

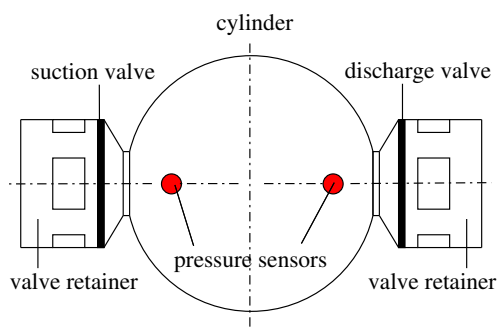


Figure 5: Position of pressure sensors

In figure 6 comparisons of the measured pressures at two positions with the numerical solution of the quasi one-dimensional model for discharge pressures of 5 bar and 2 bar are given. Figure 7 shows the appropriate comparison of the valve motion. Since the pressure distribution and valve motion are in a very good agreement with measurements we expect that the bulk temperature inside the cylinder and mass flow are also well represented. For more details of the flow behaviour we refer to ².

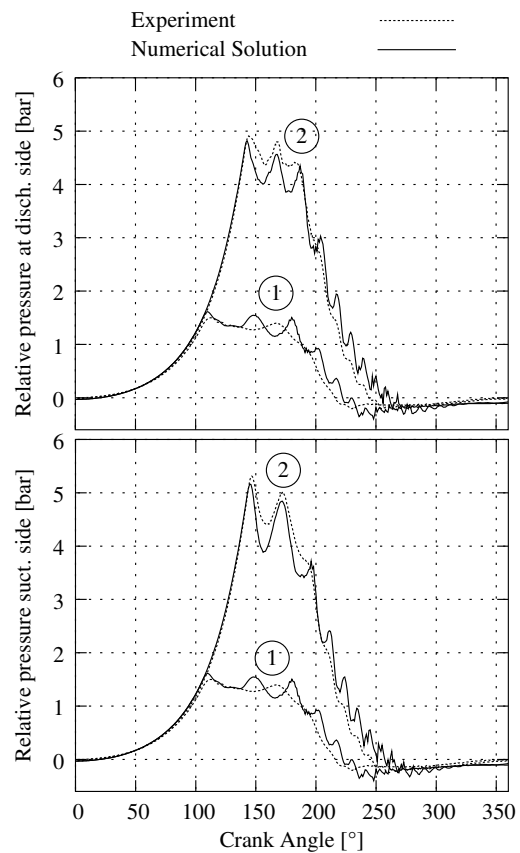


Figure 6: Comparison of the numerical solution of quasi one-dimensional model and measurements, a) pressure at discharge valve, b) pressure at suction valve for discharge pressures of 2 bar (curves 1) and 5 bar (curves 2)

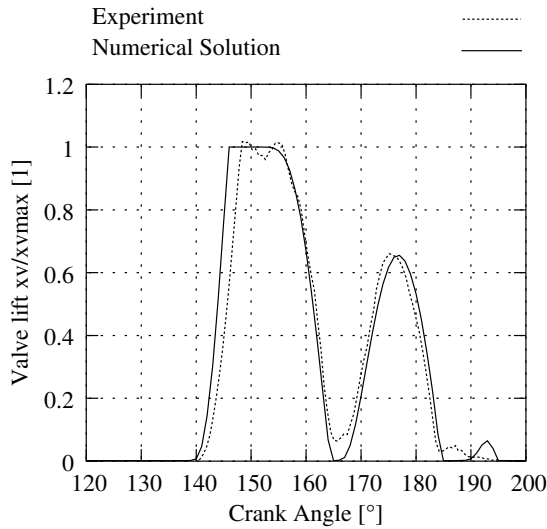


Figure 7: Comparison of the numerical solution of the quasi one-dimensional model and measurements; valve lift for discharge pressures of 5 bar

2.4.2 Compressor with 8 valves

The main specifications of the Ariel JGD 26.5 – test compressor can be found in table 2. The location of pressure sensors are marked in figure 8.

Type of compressor	Ariel JGD 26.5
Bore diameter	0.673 m
Stroke	0.14 m
Speed of Crankshaft	1182 rpm
Gas	Nitrogen
Number of Valves	8
Pressure Ratio	2.2/6.4

Table 2: Main specifications of the Ariel test compressor

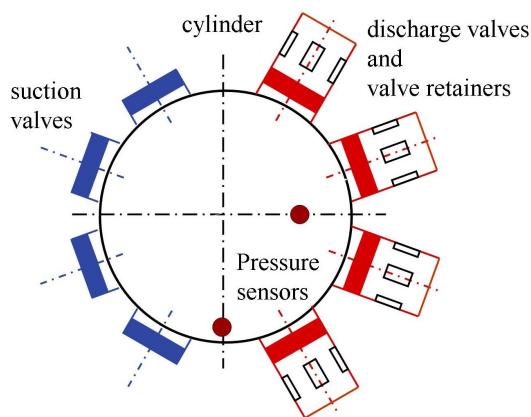


Figure 8: Position of pressure sensors

Figure 9 shows the pressure at the two locations inside the cylinder during a working cycle. Comparing measurements with numerical data shows a very good agreement.

The pressure distribution inside the cylinder shortly after the discharge valves has opened is displayed in figure 10. Since the wave fronts strongly deviate from plane waves a two-dimensional approach is necessary.

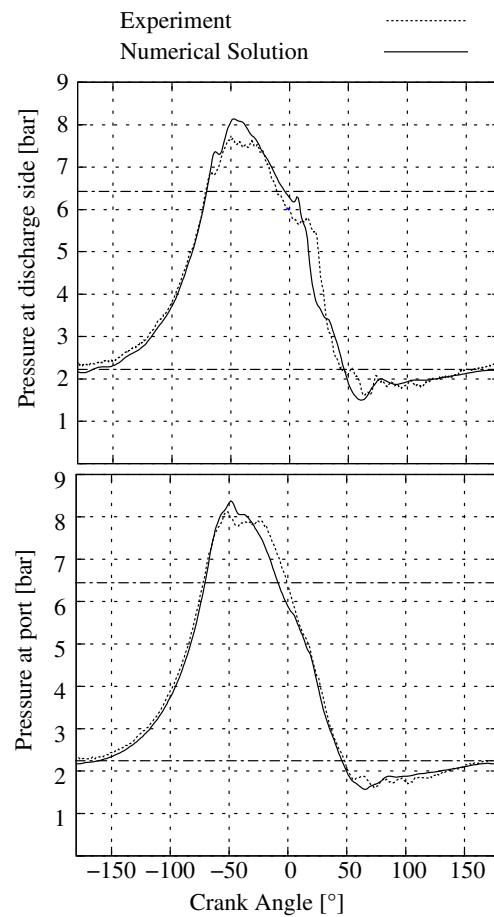


Figure 9: Comparison of the numerical solution of the quasi 2-d model and experiment, a) pressure at discharge side, b) pressure between discharge and suction side. Dash-dotted lines represent suction and discharge pressure, respectively

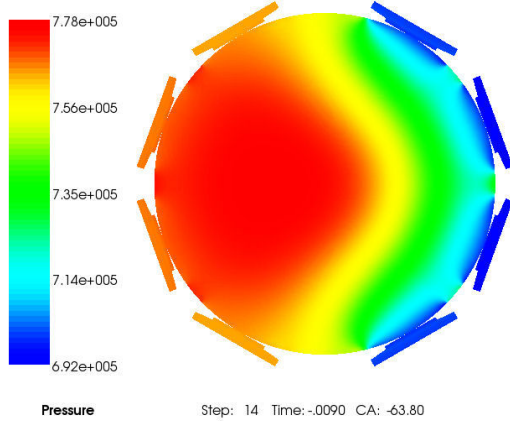


Figure 10: Pressure distribution inside cylinder shortly after opening of discharge valves (Screenshot of Compressor2d)

3 Modelling of the Heat Transfer

The essential part of the heat supply to the compressor is due to the temperature rise of the compressed gas during compression. Thus the main contribution to the heat balance of a reciprocating compressor is the heat transfer from the gas to the mechanical structure, e.g. the cylinder shell, the piston, the cylinder head and piston rod to name the most prominent surfaces of the compression chamber. It is essential to find the heat fluxes for the individual surfaces of the compression chamber.

3.1 Method

First the heat fluxes and heat transfer coefficients from the gas to the compressor have been determined for a sufficient number of cases by means of full three-dimensional numerical simulations. Next the heat fluxes through the individual faces are reconstructed by an ansatz which depends only on few dimensionless parameters. Finally correlations between these dimensionless parameters and the process parameters have been established.

3.2 Reconstruction

The basic idea of the reconstruction is to relate the local heat flux density \dot{q} to a sum of weighted reference enthalpy flux densities $\dot{h}_{ref,i}$. It is defined by

$$\dot{q} = \sum_i St_i \dot{h}_{ref,i} = \sum_i St_i c_p \rho_{ref,i} u_{ref,i} \Delta T, \quad (10)$$

where St_i can be interpreted as Stanton numbers and ΔT is a characteristic temperature difference. c_p stands for specific heat capacity at constant pressure. The reference value for the flow velocity $u_{ref,i}$ and the reference value for the density $\rho_{ref,i}$ depend on the physical effect i which contributes to the heat flux density. An educated understanding of the flow behaviour is essential in order to set suitable reference values. In terms of heat transfer three different phases during one working cycle can be distinguished; Inflow, Outflow and Compression/ Expansion.

3.2.1 Inflow

The gas enters through the suction valve. We expect a jet of cold gas emanating at the suction valve and impinging onto the piston rod or surfaces adjacent to the suction valve. We extract the reference velocity from the inlet mass flow \dot{m}_{in} through the suction valve:

$$u_{ref,in} = \dot{m}_{in} / \rho_{in} A_{cross}, \quad (11)$$

where A_{cross} is the cross section of the compression chamber along the piston rod. The density ρ_{in} is the density of the thermodynamic state of the gas at inflow. The heat transfer will be affected only after some retardation time t_0 since it takes some time that the cold gas impinges at the surfaces of the compression chamber. Thus the associated heat flux through a surface of area $A(t)$ of the compression chamber as a function of the time t takes the form

$$\dot{Q}_{in}(t) = St_{in} c_p (T_w - T_{gas}) \frac{A(t)}{A_{cross}(t)} \dot{m}_{in}(t - t_0). \quad (12)$$

3.2.2 Outflow

During outflow we expect that the flow is dominated by the outflow of the gas. Similar to the inflow phase we approximate the heat flux by

$$\dot{Q}_{out}(t) = St_{out} c_p (T_w - T_{gas}) \frac{A(t)}{A_{cross}(t)} \dot{m}_{out}(t). \quad (13)$$

For the outflow no retardation is necessary since the information that the valve is open spreads with the velocity of sound which is considerable large compared to the actual flow velocity.

3.2.2 Compression / Expansion

In the compression phase a natural reference velocity is the actual velocity of the piston $u_p(t)$. However, at the turning points of the piston motion it is zero but the heat flux density will not vanish. Thus we use the mean piston velocity u_m as reference velocity during that phase. As reference density we use the density $\rho_{isen}(T)$ which results from an isentropic change of state from the inflow condition (ρ_{in}, T_{in}) to the actual gas temperature T_{gas} in the compressor. The corresponding component of the heat flux can be written as

$$\dot{Q}_{ce}(t) = (St_p u_p(t) + St_m u_m) \rho_{isen}(T_{gas}) c_p (T_w - T_{gas}) A(t) \quad (14)$$

3.3 Reconstructed Heat Flux and Heat Flux Coefficient

Adding all components the total reconstructed heat flux is given by

$$\dot{Q}_{rec} = \dot{Q}_{in} + \dot{Q}_{out} + \dot{Q}_{ce},$$

and the corresponding reconstructed heat transfer coefficient can be obtained from

$$\alpha = \frac{\dot{Q}_{rec}}{(T_w - T_{gas}) A(t)}. \quad (15)$$

In this study the main surfaces of the compression chamber are considered, namely the piston, the cylinder head, piston rod and the cylinder shell. All other surfaces can be added to one of these.

3.4 Matching the nondimensional numbers $St_{in}, St_{out}, St_p, St_m$

The unknown dimensionless numbers $St_{in}, St_{out}, St_p, St_m$ are chosen such that for a given set of process parameters the reconstructed heat flux approximates the numerically computed heat flux best. Thus we minimize a functional which measures the distance between \dot{Q}_{num} and \dot{Q}_{rec} .

3.5 Example

In this section the results of a heat transfer calculation are discussed. The input data and specifications for the calculation are taken from the two valve test case (table 1) using a simplified valve model; when the valve has opened completely it is kept open until the piston reaches the dead centre (see section 2.4.1).

The full three-dimensional calculation has been performed and the reconstructed heat fluxes have been derived. Figure 11 shows all components of the heat flux through the cylinder head. \dot{Q}_{in} , \dot{Q}_{out} , \dot{Q}_p and \dot{Q}_m contribute 3%, 16%, 18% and 63% to the total heat flux. In figure 12a the reconstructed heat flux through the cylinder head is compared to the numerical one. In figure 12b this comparison is shown for the heat transfer coefficient as well. As usual we choose the sign of the heat flux to be negative, if the heat flux vector is pointing out of the compression chamber.

Figures 11 and 12 show that at the beginning of the compression phase the heat flows from the surrounding material to the gas. From 640 °CA on the wall temperature is lower than the gas temperature and heat flows from the gas to the wall. During discharge phase (675 – 720°CA) the heat coefficient is increased due to higher velocities in the cylinder and therefore the negative heat flux is rising simultaneously. When the valve is closed, the velocity in the cylinder becomes very low and the heat transfer coefficient drops to the lower level again. Not until the suction valve opens the heat transfer coefficient will not increase. Due to expansion the gas is cooler than the wall from 750°CA on and the wall heats up the gas again. During suction phase the velocity inside the cylinder is smaller than the velocity during discharge phase. However a slight increase in heat flux coefficient and thus a rise in the heat flux are recognized.

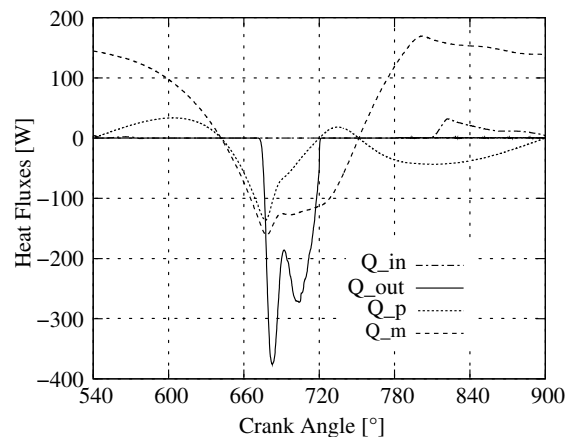


Figure 11: Heat flux through the cylinder head. Contributing components of reconstructed heat flux

In figure 13 the reconstructed heat flux through the side wall of the compressor is compared to the full three-dimensional data. Similar to figure 12 the heat fluxes or heat transfer coefficients are very well represented by the reconstructed ones. The area of the cylinder shell changes with time. When the piston approaches the dead centre high heat flux densities (due to high temperatures and heat transfer coefficients) meet only a small area and therefore the overall heat flux through the cylinder shell is only a fraction of the heat exchange at the cylinder head.

In general all statements for the cylinder head and the cylinder shell can be applied to the piston and the piston rod, respectively.

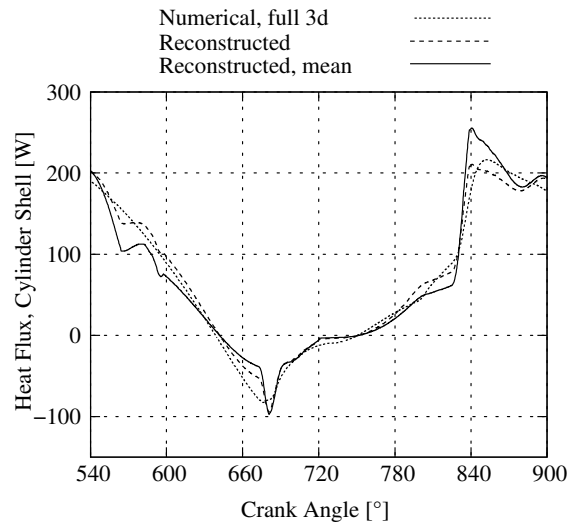


Figure 13: Heat flux through side wall of cylinder

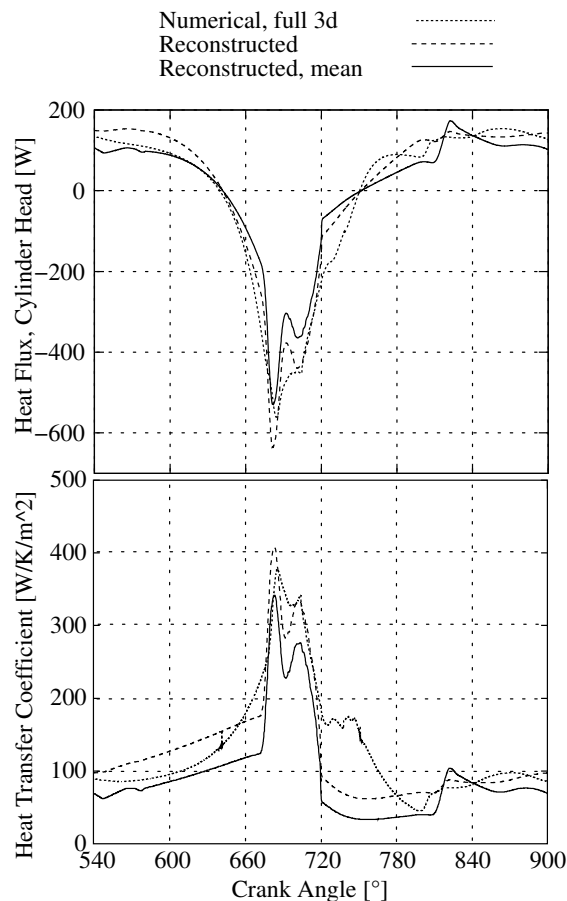


Figure 12: Heat flux through cylinder head (a) and associated heat transfer coefficient (b)

3.6 Correlation between Reconstructed Heat Flux and Process Parameters

Reconstruction of the heat flux and determination of the Stanton numbers were conducted in more than 24 cases. Figure 13 displays St_m for the cylinder head over the Reynolds number $Re = u_m \rho_{in} D / \mu$. It turns out that suitable average values of the Stanton numbers give very good results for the heat fluxes (figure 12 and 13; reconstructed mean). Thus universal Stanton numbers were found minimizing the functional which measures the distance between \dot{Q}_{num} and \dot{Q}_{rec} for all the simulated cases simultaneously.

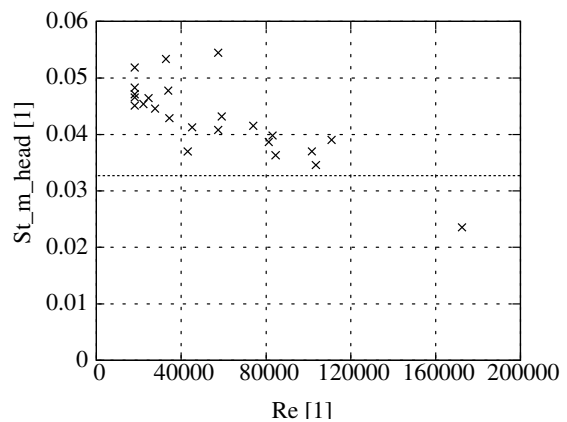


Figure 14: Stanton number St_m for the cylinder head for 24 different cases. Mean value of St_m is represented by dotted line

4 Simulation Tool

The one-dimensional and two-dimensional flow models which describe the pressure waves inside the cylinder and their interaction with the valve dynamics are incorporated in two user-friendly programs called Compressor1d and Compressor2d.

In order to determine the heat transfer coefficients besides the thermodynamic properties of the gas and the geometric description of the compressor, the mass flow and the gas temperature in the compressor has to be known. This data is provided by Compressor1d and Compressor2d. In addition, if the wall temperatures are specified the total heat fluxes can be calculated.

The comparisons between Compressor1d and full three dimensional solutions can be found in figure 15.

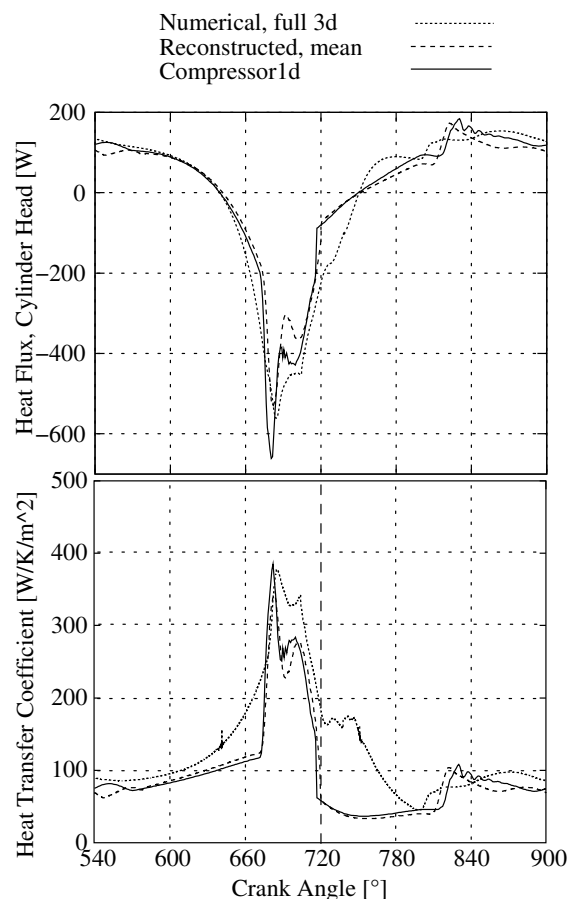


Figure 15: Heat flux and corresponding heat flux coefficient for the cylinder head

5 Conclusion

In the project ‘Modelling Fluid Dynamics, Heat Transfer and Valve Dynamics in a Reciprocating Compressor’ sponsored by the EFRC a one-dimensional and a two-dimensional gas flow model and a simplified heat transfer calculation are introduced. It turns out that these models are sufficient to capture the main characteristics of the compressor.

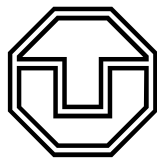
Future research will include expanding the range of validity of the heat transfer model to different compressor types. In addition we will conduct measurements of heat fluxes on a test compressor.

6 Acknowledgements

The research is financed by the European Forum for Reciprocating Compressors. The authors want to thank F. Newman (Ariel), G. Machu and P. Steinrück (Hoerbiger) and G. Samland and D. Sauter (Burckhardt Compression) for many fruitful discussions.

References

- ¹ Meyer, G. (2004): Simulation der Strömung in einem Kolbenverdichter. Diplomarbeit, TU-Wien.
- ² Aigner, R. Meyer, G., Steinrück H. (2005): Valve Dynamics and Internal Waves in a Reciprocating Compressor. 4th EFRC-Conference, 169-178.
- ³ Costagliola, M. (1950): The Theory for Spring Loaded Valves for Reciprocating Compressors. J. Appl. Mech, 415-420.
- ⁴ Zierep, J. (1997): Grundzüge der Strömungslehre. Springer Berlin Heidelberg.
- ⁵ Leveque, R. (2004): Finite Volume Methods for Hyperbolic Problems. Cambridge University Press.
- ⁶ Lax, P. D., Wendroff, B. (1960): System of Conservation Laws. Comp. Pure and Appl. Math., 13, 217-237.



**TECHNISCHE
UNIVERSITÄT
DRESDEN**

Model Based Diagnostics of Reciprocating Compressors

by:

Matthias Huschenbett / Prof. Gotthard Will

Technische Universität Dresden

Dresden

Germany

m.huschenbett@web.de

**5th Conference of the EFRC
March 21-23, 2007
Prague, Czech Republic**

Abstract:

Smart monitoring systems are key to condition based maintenance. Furthermore they can be used for the judgement of compressor health, allowing manually derived recommendations in regard to the efficient, reliable and safe compressor operation. The next higher level, a diagnostic system, supports automatic failure analysis. Core of such a diagnostic system could be either a data based or first principle based model of the real compressor application.

The aim of this EFRC Joint Research project was to explore the feasibility of a diagnostic approach based on the thermodynamic state behaviour of a reciprocating compressor. The developed simulation system introduced at the EFRC Conference 2005 has been tested and improved to meet main demands of advanced compressor simulation and to serve as base for diagnostics of reciprocating compressors.

This paper will describe some key elements of the developed compressor simulation and demonstrate the feasibility of parameter estimation by means of this simulation system.

1 Introduction

Modern monitoring systems record amongst others suction, discharge and indicator pressures, valve cage temperatures as well as vibration signals. Such systems enable already a high level judgement of the compressor state due to evaluation of these signals considering predefined warning or alarm thresholds.

However, the definition of the alarm thresholds demands specific knowledge of the respective compressor. Setting of vibration limits based on recording an initial trace demands an expert's judgement to verify the initially assumed faultless condition.

State of the art thermodynamic analyses provide useful information covering indicated power and estimated flow and energy losses. A correlation between a few measurements of process values such as temperature, line and interstage pressure on the one hand and specific malfunctions on the other hand is rather difficult. In particular dynamic effects make it almost impossible to track individual faults by just looking to said process values. This fact can either be resolved by utilization of a multitude of sensors or an investigation and interpretation of the recorded signals by an experienced engineer. E.g. the measurement of all valve cage temperatures allows a fault detection and identification of valve defects.

Despite the fact that state of the art monitoring systems provide much more than just "monitoring" they are far from being a diagnostic system. The missing part is an integrated expert system applicable to an individual reciprocating compressor.

Such an expert system could be realized using a data based model that can be trained by measurements. However, this model has to cover a complete map of all dynamic states, various operating conditions and all possible failures. Thus, to achieve such a system using real data is practically impossible, at least for customized products like custom-built reciprocating compressors.

The aim of this EFRC Joint Research projects was a feasibility study exploring the potential of an approach based on first principles. A comprehensive simulation system was developed in order to train a model (expert system) for specific reciprocating compressor.

2 Reciprocating Compressor Simulation

The created simulation system consists of a library called "Recip Toolbox" which can be used in the software environment Matlab/Simulink. It was introduced at the EFRC Conference 2005. The following chapters describe the development history and give an update on latest improvements.

2.1 Development History of the RecipToolbox

The initially simplified simulation model based on first principles created in 2003 considered the transient thermal behaviour neglecting gas dynamic effects. A theoretical investigation of a two stage air compressor was done in order to judge the reactions of possible defects on valves, rings or packing. Only a few special damages and controls were examined at this time. Nevertheless this investigation supported the assumption that temperature and pressure changes point to specific failure modes and thus fault detection should be possible.

In order to verify the required complexity and exactness of the compressor model an investigation on another two stage lab compressor was carried out. The simulation of this compressor was done with a steady flow model for the pipes and cooler.

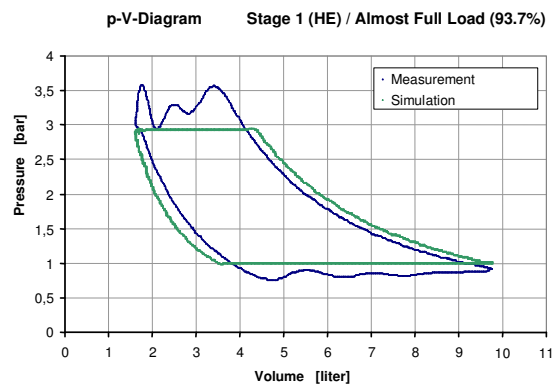


Figure 1: Measurement vs. simulation (simplified model)

The simulated pressure inside the HE cylinder chamber (see Figure 1) indicates that such a simplified model can't be used as base for thermodynamic diagnostics. Neither compression- and expansion - lines nor the intermediate pressure and consequently the temperatures match the measured data (Figure 1).

The observed differences are caused by neglecting valve and gas dynamics. The evaluation of stationary pressure and temperature measurements of the test compressor with a simplified model would lead to a wrong judgement of compressor condition.

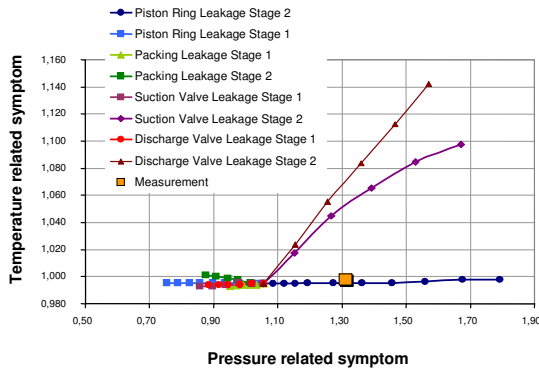


Figure 2: Diagnostic evaluation of test compressor based on stationary average data

As shown in Figure 2 – using a diagnostic model based on purely thermodynamic correlations - leaking piston rings would have been detected, despite the fact that the compressor was in a good condition. The real pressure ratio inside the cylinder chamber was calculated too low since the theoretical model strongly underestimated the losses due to valve restriction and pulsations. Hence, the simulated intermediate pressure was lower than the measured one and consequently a damage in the second stage would have been concluded.

These findings should not lead to the conclusion that cylinder pressure measurements are unavoidable. Regarding the requirements on the simulation this example proves the necessity to consider gas and valve dynamics as well as transient thermal effects.

Investigations on a lab compressor at the Dresden University revealed similar observations. The results of an improved simulation including pulsation and valve dynamic show a sufficient match between measured and predicted results. (Figure 3 and Figure 4).

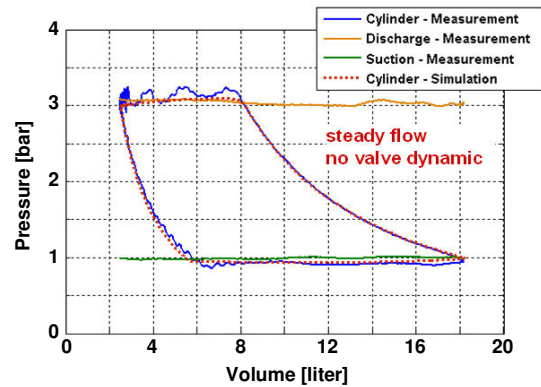


Figure 3: Measurement vs. simplified simulation

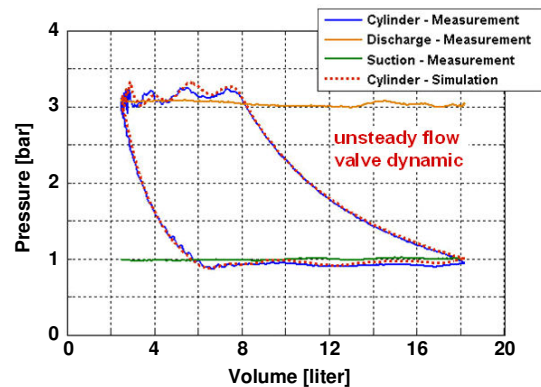


Figure 4: Measurement vs. dynamic simulation

The transient flow model used for the piping as well as for the intercooler considers pulsations in a simplified, but for this purpose sufficiently exact way. The applied method is definitely not suitable for pulsation studies.

2.2 Gas flow through cylinder

A challenging question was the judgement regarding effects along the flow through the cylinder. Various approaches have been tested in the course of the simulation development in order to determine considerable or rather negligible impacts.

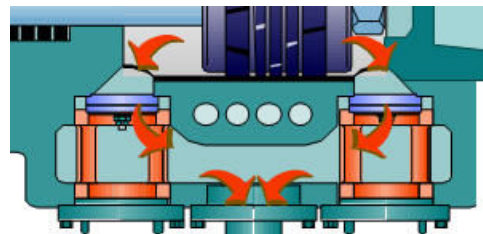


Figure 5: Flow pass through cylinder – discharge

Figure 5 shows the discharge flow from the compression chamber to the adjoining discharge piping.

Starting with this sketch the following separated simulation modules were developed:

Discharge chamber:

In this regard the discharge chamber is defined by the room around all valve cages. Heat transfer with cylinder wall has been account for. Mass flows from the cages and to the discharge pipe are given at each time step from these adjoining modules. The states inside the discharge chamber can be calculated by mass and energy balance.

Discharge valve cage:

Initially the valve cage was considered as separate element to evaluate the temperature changes directly behind the valve in case of a valve defect. It turned out that this approach is advantageous for the inclusion of gas dynamics as well.

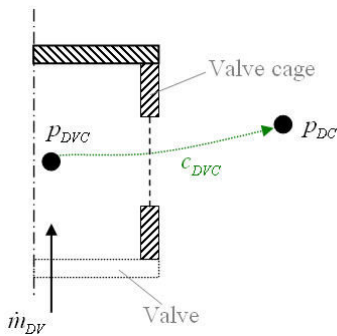


Figure 6: Gas flow – cage to discharge chamber

According to Figure 6 the non steady flow calculation takes into account the flow restriction of the cage ports and the inertia along the flow pass (DVC → DC).

Discharge valve:

The simulation of the flow through the valve includes the valve dynamic as well as the consideration of the compressibility. The later one requires neglecting the non steady flow term. This assumption is valid from the thermodynamic perspective since the flow distance is rather small. However, this approach together with the design of the entire simulation system may cause an instable behaviour. As mentioned before the compressor model calculates the state behaviour in separate blocks. Iteration within one time step including several blocks is not possible. The calculated mass flow through a valve affects the pressures inside the adjoining chambers.

However, the resulting pressure change influences the mass flow just at the next time step. This fact can finally lead to a repeating flow reversal at each time step if the pressure ratio over the valve amounts to nearly 1.

Such an effect is inconsistent to all physical laws and can be considered as numerical instability (Figure 7).

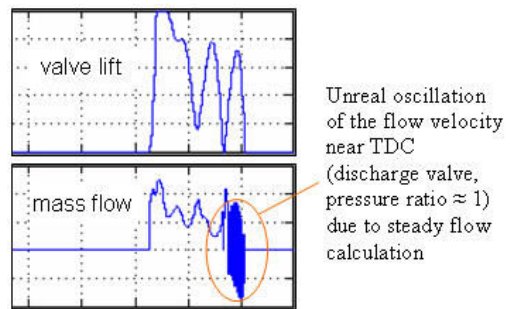


Figure 7: Instable valve flow simulation

The oscillating mass flow shown in Figure 7 excites the gas dynamic of the following modules. Therefore it can't be neglected. This behaviour happens at a pressure ratio close to 1 which doesn't require the consideration of compressibility. This problem has been overcome by switching the calculus to a non-steady incompressible model whenever there repetitive flow reversal occurs. As demonstrated in Figure 8 this approach avoids such numeric instability.

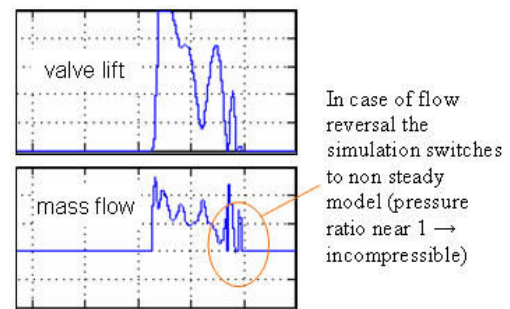


Figure 8: Improved valve flow simulation

Valve pocket – Piston masking of pocket port:

The standard cylinder design is characterized by valve pockets placed laterally at the cylinder chamber. A compact design and aspired optimized clearance volume lead very often to a partly masked pocket port when the piston approaches the top dead centre position. This was neglected in the simulation till a member of the EFRC Joint Research Group recently included that effect.

The open modular simulation architecture allows easily adding such a module. To separate this impact from the valve calculation is quite meaningful since the valve dynamic determines the valve flow area dependent on the pressure difference and piston masking is just a function of the crank angle.

2.3 Comparison measurement and simulation

In order to validate the described calculation of the flow from the compression chamber to the discharge pipe flange a simulation of an air compressor was done¹. The measured pressure traces at the suction and discharge pipe flange were set as boundary condition of the simulation.

Figure 9 displays the results of the simulation with and without the piston masking effect. It is obvious that considering the pocket port restriction enables a far better understanding of the cylinder performance. In particular at top dead centre position, i.e. at a maximum flow restriction, this effect couldn't be taken into account by an addition valve loss factor appropriately.

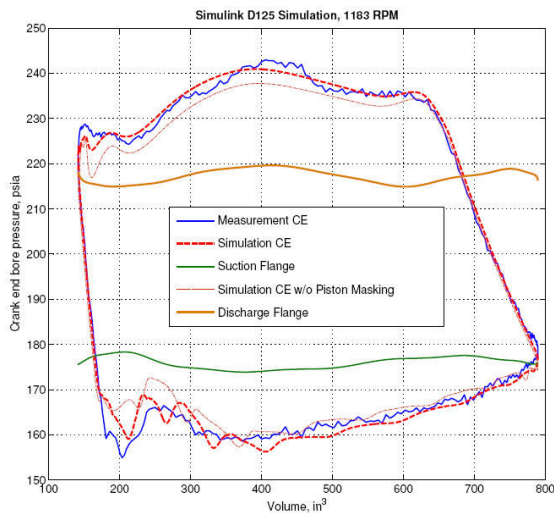


Figure 9: Comparison simulation vs. measurement lab compressor¹⁾ (Air, 1183RPM)

The simulation of the mass flow through valve and valve cage exhibits a quite good conformity with the measurements. This demonstrates that the developed models enable precise calculation of the flow pass through the cylinder even with these zero – and partly one dimensional models.

Furthermore this investigation proves the general nature of this model based diagnostic approach. All predefined parameters were set in the same range as done at different applications before. This allows the assumption that with the existing simulation model it should be possible to identify the initial condition of a reciprocating compressor. The required measurements for this purpose could be done with a state of the art monitoring system.

With help of some basic measurements the simulation model could be trained. With the basic parameters set in such a way the model allows the prediction of the entire operating map and possible damages on valves, rings and packing

2.4 Real gas behaviour

The validation so far could prove a sufficient accuracy of the developed simulation model, however, these tests have been done on compressor application with gases following ideal gas behaviour. In order to allow usage of the model for process applications demanding the consideration of real gas behaviour the entire simulation system was redesigned accordingly.

As an adequate approximation the *Redlich-Kwong* equation of state has been used. The required gas properties (triple point data, etc.) are stored for approximately 100 gases enabling the definition of all common gas mixtures. Figure 10 shows the test result for ethylene compared with a proven chart.

Ethylene - Simulation vs. Chart

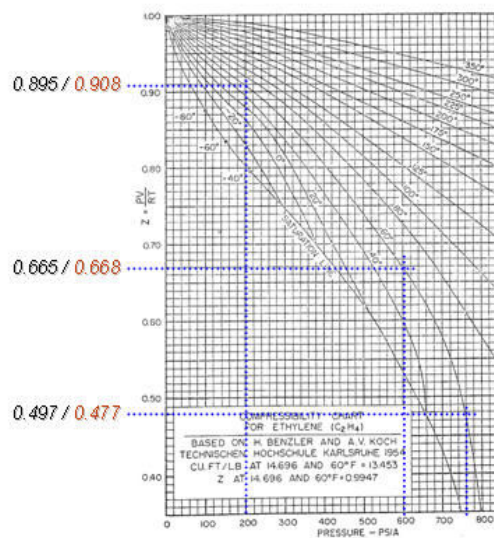


Figure 10: Calculated real gas behaviour of ethylene compared to a chart

¹ Courtesy of Ariel Inc.

3 Parameter estimation

Once a simulation model for a specific reciprocating compressor was created with the mentioned toolbox the initial state has to be determined by comparison with measurements. Regarding gas dynamics this procedure must be done manually due to the limited accuracy of the simplified theoretical calculations. However, this effort seems to be acceptable since minor changes of the parameters in a reasonable range enable a quick fit of the gas dynamic simulation to the measurements.

The determination of parameters describing the thermal behavior can be done by parameter estimation. For this purpose the simulation model runs several calculations with varied values of the unknown parameters. The results of the simulation and the measurements will then be evaluated by means of classifiers. In the following paragraph this procedure is explained demonstrating the determination of unknown constants for the heat transfer calculation in the cylinder.

A general approximation of the Nusselt number $Nu = C_1 \cdot Re^{C_2} \cdot Pr^{C_3}$ as function of Reynolds and Prandtl number is assumed for the calculation of heat-transfer coefficient $\alpha = f(Nu)$ in the cylinder chamber. These constants $C_{1,2,3}$ are predefined by expert knowledge and varied in a reasonable range.

In the discharge and suction chamber a proven equation for channel flow can be used.

$$Nu = A \cdot 0.0235 \cdot (Re^{0.8} - 230) \cdot (1.8 \cdot Pr^{0.3} - 0.8)$$

This function for the Nusselt number reduces the amount of unknown parameters to one constant (A).

The geometric cylinder model for the heat transfer calculation consists of approximately 100 discrete volume elements. A huge amount of calculations have been carried out in order to determine the constants $C_{1,2,3}$ as well as the constants A for the discharge and suction chamber. For this purpose the compiled simulation model was included in a parameter estimation software environment which changes the unknown parameters, runs all calculations and finally determines the values matching to the measurements. This evaluation of the initial state is the same task as the fault detection and identification.

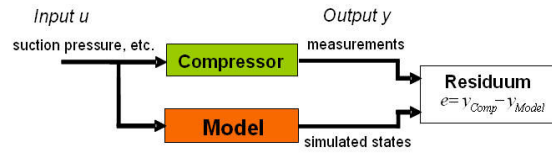


Figure 11: Basic approach of parameter estimation

As shown in Figure 11 the measurements y_{Comp} and simulated states y_{Model} define the residuum e which describes the deviation of simulation and measurement. Hence the parameters of the model correspond to the real compressor state if the residuum amounts to a minimum, i.e. to zero ideally. For the current task the residuum e for one measured operating point $X=1$ were evaluated by $N=243$ different simulations considering 3 different values for each of the $M=5$ parameters (parameter variation). These N simulations train the classifiers.

Residuum Vector:
$$e_n^T = \underline{y}_X^T - \underline{y}_n^T \quad n = 1..N$$

A relative residuum considers the fact that the thermodynamic states or extracted symptoms differ in magnitude.

Rel. Residuum:
$$e_{n,rel} = \frac{y_X - y_n}{y_0} \quad y_0 = y_{max} \text{ or } y_X$$

The calculation of the similarity J enables determination of simulation parameters. Weighting matrices enable a correction of the impact of several classifiers.

Similarity Vector:
$$\underline{J}_n = \underline{e}_{n,rel}^T \underline{\underline{W}}_m \underline{\underline{W}}_n \underline{e}_{n,rel}$$

Finally $\min(J)$ defines the value of the classifiers and consequently parameters matching to the measured state of the compressor.

The above mentioned evaluation concerning the unknown heat transfer coefficients led to the following results:

Cylinder chamber: $C_1=0.67 \quad C_2=0.78 \quad C_3=0.59$

Suction chamber: $A_S=1.01$

Discharge chamber: $A_D=0.95$

With the determination of the unknown parameters the simulation model is matched to the initial state condition of the reciprocating compressor.

The same approach by means of classifiers is applied for the purpose of fault detection and identification since the model contains parameters considering defects on valves, rings and packing as well.

Following steps are required for the creation of an expert system, i.e. classifiers, as base for diagnostics:

1. Creation of the simulation model based on experience and expertise
2. Compilation of the simulation
3. Integration of the compiled model in a diagnostic evaluation system
4. Calculation of classifiers for the determination of the initial condition
5. Connection of the evaluation system to the data acquisition system
6. Data collection on the compressor (several operating conditions)
7. Automatic determination of initial parameters
8. Recalculation of classifiers
9. On/Offline operation of diagnostic system

4 Conclusion

The developed simulation system was improved to cover gas dynamic effects as well as real gas behaviour. Tests on various compressors show a quite good conformity with the measurements. The element wise separation enables the consideration of specific effects.

The validation of the flow through the cylinder has shown the necessity to take into account piston masking as well as restriction due to valve cage. The fact that the simulation corresponds to the reality using parameters taken from the expertise strengthens the statement that a precise theoretical model meets the demands of a model based

diagnostic system. Such effects can hardly be identified by a measured data based model.

Parameter estimation is possible by means of classifiers. However, this procedure demands a huge amount of computing time. If once the classifiers are trained, a fast on line diagnostics can be done including fault detection and identification.



Identification of noise sources in reciprocating compressors

Leonard van Lier
Department of Flow and Structural Dynamics
TNO science & Industry
Delft
The Netherlands
Leonard.vanlier@tno.nl

5th Conference of the EFRC
March 21-23, 2007
Prague, Czech Republic

Abstract:

From a HSE (Health, Safety & Environment) perspective, a trend toward stricter legislation on noise emission is observed. Compressor manufacturers are regularly confronted with noise targets, also on a contractual level. For prediction and control of noise levels emitted by reciprocating fluid machinery, more accurate prediction models and design tools are required. Funded by the EFRC research budget, TNO has performed a survey on noise generating mechanisms, typical for reciprocating machinery. The dominant noise sources and noise transfer paths are discussed, and the relevant design parameters are illustrated. An overview on available numerical tools (for future, detailed modeling) and experimental techniques (allowing for source identification and model validation) was given. In support of the conclusions from this theoretical study, an experimental survey at an on-shore compression station has been executed. Various experimental techniques have been applied: in-line pulsation measurements, noise and vibration measurements and intensity scanning, yielding a valuable database of noise and vibration results. The main conclusions from this experimental survey will be discussed.

1 Introduction

Noise is becoming an increasingly important aspect of compression system design. Both the noise emission to the environment and the noise exposure of personnel deploying the compression machinery are regulated by guidelines and legislation. Compliance with these guidelines is becoming more and more important, before permits are allowed for site constructions or extensions. The new European Noise Directive for outdoor equipment is a good illustration of this trend. From January 1st 2006, stricter emission values are applicable to outdoor equipment, which includes for example small compressor machinery (< 350 kW).

On the other hand, also the noise sources in fluid machinery tend to become stronger. This is related to a trend to higher speed machinery, which shifts the sources to higher frequencies. Furthermore, reverse-flow capacity control systems lead to steeper pulse shapes of the pulsations. This implies inevitably stronger higher harmonics in the pipe system. Combined with the fact that pipe walls are relatively transparent for high-frequency noise, these developments lead to larger noise radiation from the installation and the attached piping.

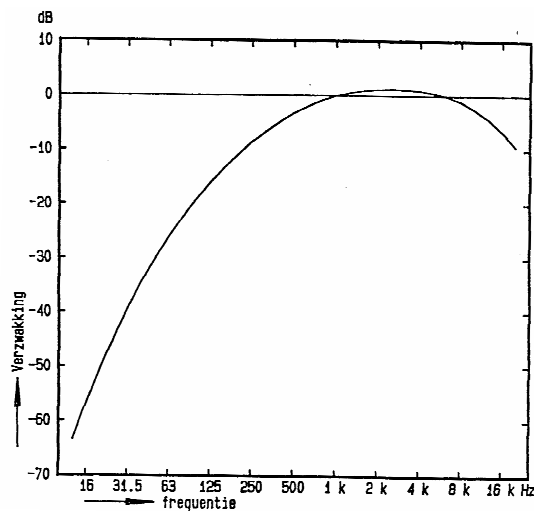


Figure 1. A-weighting curve, illustrating the strong suppression of low-frequent components in the total dB(A)-level

This is a very important observation, since environmental and occupational noise exposure guidelines are based on A-weighted noise levels.

This is done to account for the sensitivity of the human ear. In practice, it means that only noise generated at higher frequencies (from 500 Hz to 8 kHz) contributes significantly to the total level. The A-weighting filter is illustrated in figure 1.

Currently, only limited information is available on the details of the noise generating mechanisms and noise transfer paths in reciprocating machinery. Some guidelines are available for global noise prognosis [1], but these are entirely empirical in nature, and do not provide any insight in mechanisms, nor lead to low-noise design strategies. Therefore, in this research project, funded by the EFRC, goal is to identify and prioritize noise generating mechanisms and noise transfer paths in reciprocating compressors. This research has been based on available literature and existing knowledge within TNO. Available noise reduction measures are discussed, and experimental and numerical tools are formulated, that may be fruitfully used in future research. As a next step the noise mechanisms are prioritized [2]. Finally, a survey to experimental techniques to identify noise generating mechanisms in reciprocating machinery is performed, in a realistic compression station [3].

This research project was concluded with an outlook for a modelling framework that can be conveniently used to achieve more quantitative noise prediction of compressor equipment, which will be the focus of the next project phase.

2 Noise generating mechanisms

The first step in low-noise design is the noise source – transfer path diagram. This diagram allows for a very instructive representation of the acoustic system, and directly indicates that not only noise sources need to be considered, but that also the noise transfer paths need to be taken into account, for effective noise reductions. Furthermore, it indicates that tackling a single noise source – transfer path combination will generally not lead to significant noise reductions, if other noise transfer paths exist. Then all noise sources-transfer paths need to be taken into consideration. In this paper, we will refer to noise sources as Noise Generating Mechanisms (NGMs). Based on literature search, 3 contributions are identified: pressure pulsations due to piston movement, valve impact noise, and flow noise in valve throat. According to [4], these noise generating mechanisms can be prioritized as ordered below:

2.1 Periodic pressure pulsations due to piston movement

This is the most intrinsic noise generating mechanism in reciprocating fluid machinery, and difficult to control, by its very nature. The periodic compression and expansion of the gas in the cylinder, caused by the piston movement, yields strong pulsations in acoustic pressure and velocity. The pressure pulsations are generated in the cylinders, and generally strongly suppressed in the pulsation dampers, limiting the transfer of the pulsations to the upstream and downstream piping. The pressure pulsations in the cylinder however, remain extremely high, and can be responsible for significant noise radiation from the compressor installation.

The pressure pulsations are typically air-borne or fluid-borne noise generating mechanisms, exciting directly the surrounding medium.

Quantification of this source is relatively straightforward. From the mechanical system parameters (rpm, crank-rod ratio, stroke) the piston movement as a function of time is given (approximately sinusoidal). During the compression cycle, the laws of thermodynamics can be used to derive the pressure as function of time. The pressure ratio over the valve and the valve parameters (stiffness of springs) determine the valve dynamic behaviour, yielding the amplitude and shape of the pressure pulse. For example in TNO's PULSIM software, the pressure pulse, taking into account the geometrical and valve parameters, can be predicted accurately.

An experimental example is shown in figure 2, illustrating that the pressure pulse is not perfectly sinusoidal. This implies that not only the lowest harmonic (rpm) will be present in the frequency signal, but also higher harmonics. For noise prediction and compliancy with noise regulation, it is very important to have an accurate prediction of these higher frequencies. This implies that special care should be taken to predict the high-frequency content in the pulsation spectrum, in contrast to the low-frequency content that is important for structural integrity issues.

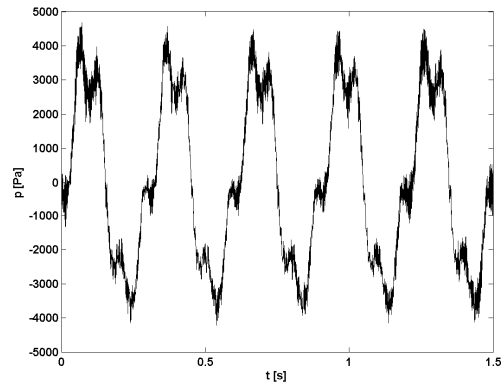


Figure 2: Example of measured in-line noise signal in suction line

In the narrow-band spectrum, the individual lower harmonics, related the compressor rpm are very strongly present (figure 3).

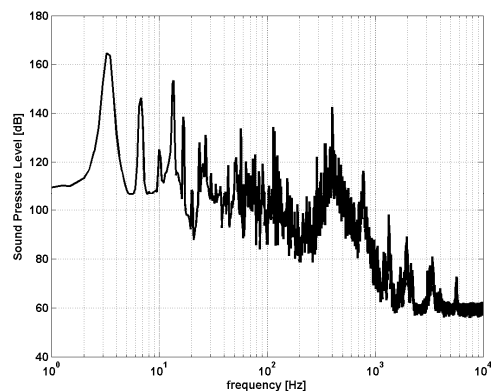


Figure 3: Narrow-band noise spectrum

However, when the results are converted to broader frequency bands, and A-weighted, the emphasis shifts to a very different frequency regime, near $f \sim 500$ Hz (figure 4).

The actual radiated noise from the compressor casing and pipes will depend on the interaction with pulsation source strength and acoustic resonances in the system, and by the properties of the noise transfer through the structure.

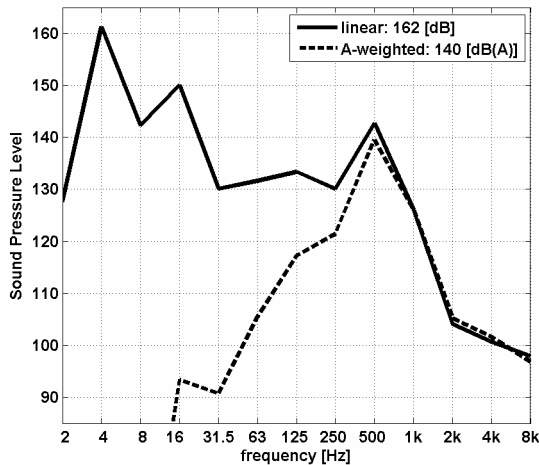


Figure 4: Octave-band noise spectra of in-line pulsations, (linear and A-weighted)

Within the EFRC research, more advanced modelling approaches are being developed, that may increase the accuracy of the high-frequency prediction. One of these is the advanced numerical modelling of propagation effects in the cylinder [5], in 1D and 2D. Another important aspect that affects the high-frequency content of in-line pulsation is the application of reverse-flow capacity control. TNO’s PULSIM software is capable of including the effect of capacity control application on the pressure pulses accurately [6].

2.2 Valve impact noise

Another important noise generating mechanism is the mechanical impact of the valve plates on the seating. Contrary to the in-line pressure pulsations, this is a structure-borne noise generating mechanism, directly exciting the structure. In order to predict this noise generating mechanism quantitatively, the impact force function is needed, during impact. This is a phenomenon that is not easily simulated nor measured. Numerical analysis would need the initial impact velocity (typically 5 m/s) and valve plate mass (~0.1 kg) as input, and uses the dynamic mechanical properties of the valve plate and the seating. If the impact force signal $F(t)$ is known, the excitation spectrum can be calculated, and used as a starting point for further structure-borne noise transfer calculations [7]. In general, short impact leads to high-frequency excitation, and slow impact leads to low-frequency excitation, as illustrated in figures 5 and 6. The excitation force spectrum due to mechanical impact is broadband in nature.

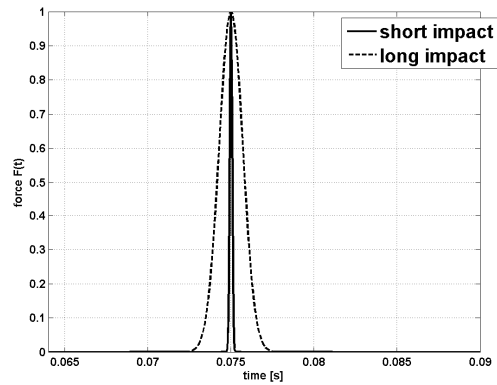


Figure 5: Example of short and long impact forces

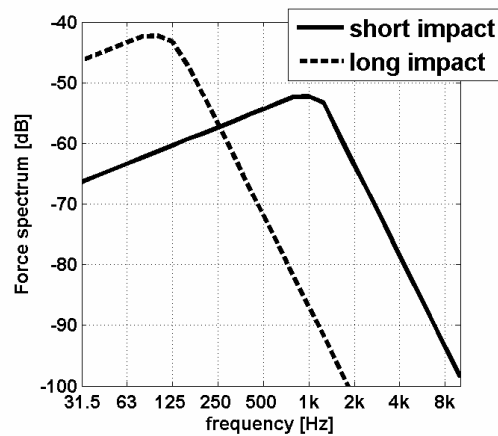


Figure 6: Corresponding structure-borne noise excitation spectra

2.3 Flow noise in valve throat

A third noise generating mechanism is the flow-induced noise due to the passage of the compressed gas through the valve throttle. This flow-induced noise is very similar in nature to the turbulent flow through a diaphragm or a control valve. The flow contracts and accelerates in the throat of the valve opening. When large Mach numbers occur in the throat, significant noise production will be observed. This noise generating mechanism is airborne in nature, since it excites directly the surrounding medium.

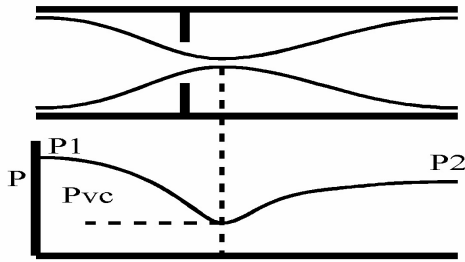


Figure 7: Schematic representation of a flow accelerating in a constriction, and illustration of pressure recovery

A general layout is illustrated in figure 7. The flow accelerates and the highest velocity (and the lowest pressure) is encountered in the vena contracta. After this contraction, the flow decelerates, and pressure is (partly) recovered. An important parameter for flow noise prediction is the pressure recovery coefficient, that describes the pressure recovery behaviour in the valve:

$$F_L = \frac{P_1 - P_2}{P_1 - P_{vc}} \quad (1)$$

Various engineering models exist for prediction of noise generation in control valves [8],[9]. Reethof [9] discriminates between different pressure ratio regimes over the valve. For compressor valves, the pressure ratio is generally close to unity, and in this region, the generated acoustic power scales with the 6th power of the Mach number in the vena contracta. The generated acoustic power is distributed in the frequency domain, with a maximum noise emission, at the frequency f_p associated with the Strouhal number in the jet (flow speed in vena contracta V_{vc} , and jet diameter D_j):

$$f_p = 0.2 \frac{V_{vc}}{D_j} \quad (2)$$

An illustration of the model prediction is given in figure 8. The valve noise spectrum is broadband in nature. These models indicate, that for prediction and reduction of valve noise, it is important to consider local effects (speed in vena contracta and pressure recovery coefficient), rather than global effects (overall pressure loss of the valve). For example by applying many small constrictions instead of a single large constriction, the pressure recovery decreases, which implies a lower effective speed in the contractions. Furthermore, the peak frequency shifts to higher frequencies (equation

(2)). This can be favourable, when the A-weighting curve is applied, or the frequencies can be even shifted to the ultrasonic frequency range, which is clearly beneficial for the occupational noise exposure.

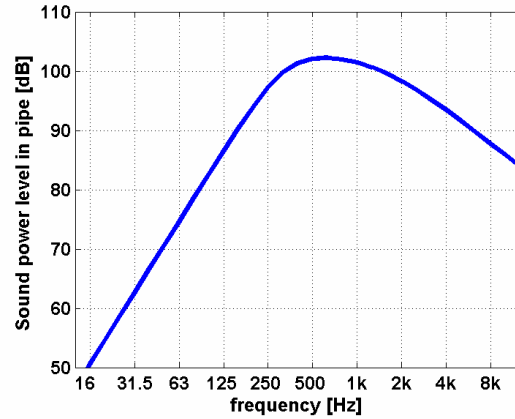


Figure 8. Example of a valve noise in-line spectrum. $V_{vc}=114$ m/s and $D_j=0.032$, yielding a peak frequency f_p near 712 Hz.

Since the geometry of compressor valves is more complex than geometry of control valves or restriction orifices, advanced tools are needed to estimate the input parameters for the prediction model accurately. This holds especially for the pressure recovery coefficient F_L and the speed in the vena contracta V_{vc} . CFD analysis can be a powerful tool to achieve this purpose.

Furthermore, the flow through compressor valves is not stationary. Therefore the models mentioned above are not directly applicable. Instead, an effective acoustic power level over 1 compression cycle should be used, applying an acoustic average procedure.

3 Noise transfer paths

Two major transfer paths can be identified in compression system: air-borne noise transfer and structure-borne noise transfer.

3.1 Air-borne noise transfer

The concept and the prediction models for air-borne noise transfer are relatively straightforward. The noise transmission takes places through air or another gas. The source is radiating acoustic energy into the gas, with the receiver or receiving structure at another location in the gas. There is a direct connection between source and receiver.

In environmental noise emission, the dominant noise transfer path is air-borne noise transmission through the atmosphere.

A simple example of air-borne noise transfer of a point source with sound power level L_w , in a reflection-free environment:

$$L_p = L_w + 10 \log \left[\frac{Q}{4\pi R^2} \right] \quad (3)$$

L_p is the sound pressure level at the receiver location, and R is the distance between source and receiver. Q is the directivity factor ($Q=1$ in free field conditions, $Q=2$ for noise propagation over a flat reflecting surface).

For noise propagation indoors, or in strongly reflecting environments, the following generalization must be applied:

$$L_p = L_w + 10 \log \left[\frac{Q}{4\pi R^2} + \frac{4}{A} \right] \quad (4)$$

Here, in addition to the direct acoustic field, a reverberant field is added. This reverberant field is independent of the distance between source and receiver, and depends only on the absorption A in the reverberating environment. Equations (3) and (4) are illustrated in figure 9.

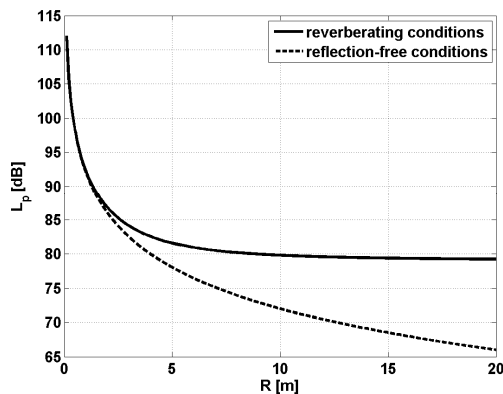


Figure 9. Illustration of air-borne noise transfer in free-field and reverberant conditions

3.2 Structure-borne noise transfer

For occupational noise exposure, the noise radiation in the vicinity of the compressor is most relevant.

For prediction of noise levels due to the noise generating mechanisms discussed in section 2, a description of the structure-borne noise transfer path is required. This includes the excitation and response of the structure, noise propagation within the structure and radiation from the casing of the compressor.

To illustrate the various steps in the structure-borne noise transfer modelling approach, see figure 10.

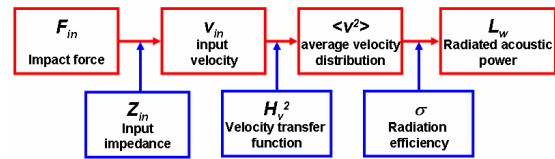


Figure 10. Typical modelling approach of structure-borne noise transfer.

Starting from a force excitation F_{in} (for example valve impact, figure 6), the structure will respond with forced vibrations. The relation between the excitation F_{in} and input velocity v_{in} of the structure is the input impedance Z_{in} .

$$Z_{in} = \frac{F_{in}}{V_{in}} \quad (5)$$

The input impedance of many simple geometrical elements (plates, beams, masses, springs) is described in standard textbooks [7]. In general, it depends on geometrical parameters (thickness, dimensions), mass of the receiving structure, the location of the excitation and the position of reinforcing elements. The input impedance is a frequency-dependent function $Z_{in}(f)$.

The next modelling step is the transfer of vibration energy through the structure. The relation between the input velocity and the averaged squared velocity $\langle v^2 \rangle$ over another part of the structure is described by the velocity transfer function H_v^2 :

$$H_v^2 = \frac{\langle v^2 \rangle}{v_{in}^2} \quad (6)$$

This velocity transfer function depends on the geometrical parameters (mass, dimensions), but also on the damping in the structure. Generally, it is a function of frequency: analytic expressions for simple elements are given in [7].

Finally, the average velocity distribution $\langle v^2 \rangle$ over the structure and the acoustic power W_{rad} radiated from the structure, are related by the radiation efficiency σ :

$$\sigma = \frac{W_{rad}}{\rho_0 c_0 A \langle v^2 \rangle} \quad (7)$$

A is the area of the radiating surface, and $\rho_0 c_0$ is the specific acoustic impedance of the surrounding air. The radiation efficiency is a frequency-dependent function that has low values for low frequencies, and approaches unity for higher frequencies. For simple elements (spheres, plates, beams and cylinders) analytical expressions for the radiation efficiency are available [7]. For more complex systems, Boundary Element Methods may be used to evaluate σ .

In standard textbooks for structure-borne noise transfer, analytical models are given for the quantities shown in the lower part of figure 10, for a large variety of simple elements. These models approximate the behaviour at higher frequencies, where broad frequency bands (e.g. 1/3 octave bands) contain many individual structural resonances. This is a very relevant and powerful approach, in the higher frequency range, which is relevant for noise radiation (> 500 Hz). For this reason, numerical deterministic tools, like Finite Element Methods, are not very appropriate nor convenient for this analysis. A global analysis in broad frequency bands yields the most realistic results. An illustration of this approach is given in figure 11. This example is based on a flat plate of 0.5×0.5 m². In a realistic compressor, the modal density will be even much higher in the 1 kHz region, than illustrated in figure 11.

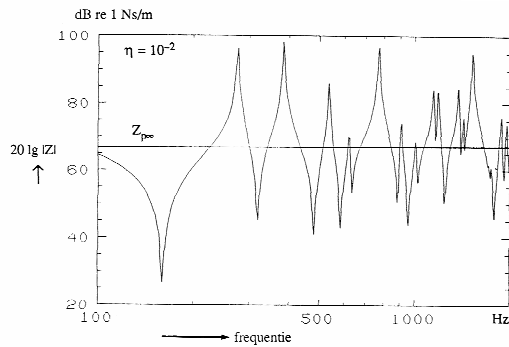


Figure 11. Input impedance Z_{in} for a flat plate: analytical approximate solution and numerical deterministic solution (FEM)

3.3 Empirical model for noise transfer of in-line noise

A useful example where both structure and airborne noise transfer are encountered is presented in [11]. An empirical model is presented for the transfer of in-line noise to noise radiated from a pipe. This includes an important interface between fluid and structure, commonly referred to as fluid-structure interaction. Accurate modelling of fluid-structure interaction is a highly complex task, and an vivid topic of research. The implementation in [11] is straightforward, and may be a convenient starting point for modelling the more complex transfer from pressure pulsations in a compressor cylinder to the noise radiated to the environment.

The model is applicable for a uniform pipe, and quantifies the transmission loss (TL) between the acoustic power in the pipe and the power radiated from the pipe wall. This transmission loss depends on properties of the pipe wall and the fluid contained inside (densities, speed of sound). The transmission loss displays a strong frequency-dependent behaviour. Finally, it depends on installation details, for example the presence of bends and flanges.

$$TL = 10 \log \left[\frac{c_p \rho_p h}{c_f \rho_f D_i} \right] + A(f) + C \quad (8)$$

The properties of the pipe are c_p (speed of sound in pipe material), ρ_p (density of pipe material), h (pipe wall thickness) and D_i (internal pipe diameter). The fluid properties are c_f (speed of sound in fluid), ρ_f (density of fluid). The first term in equation (8) is constant. The second term describes the frequency-behaviour:

$$A(f) = 30 \log \left[\frac{f}{f_r} \right] \quad f < f_r \quad (9a)$$

$$A(f) = 20 \log \left[\frac{f_r}{f} \right] \quad f > f_r \quad (9b)$$

The minimum of the function $A(f)$ occurs at the ring frequency of the pipe $f_r = c/\pi D_i$. At this frequency, coincidence with the first circumferential eigenmode occurs.

The third term C depends on the geometrical layout: relative location of the pipe section to bends,

flanges and valves. For a welded pipe with an average of 1 bend per $20 \cdot D_i$ length, $C=6$ dB.

Figure 12 illustrates that a pipe is shielding the lower frequencies very effectively, but that it is relatively transparent for higher frequencies. The minimum transmission loss occurs at relatively high frequencies, depending on the pipe diameter. For large pipes, the transmission loss at low frequencies is relatively low, compared to small pipes, due to the limited stiffness of the pipe.

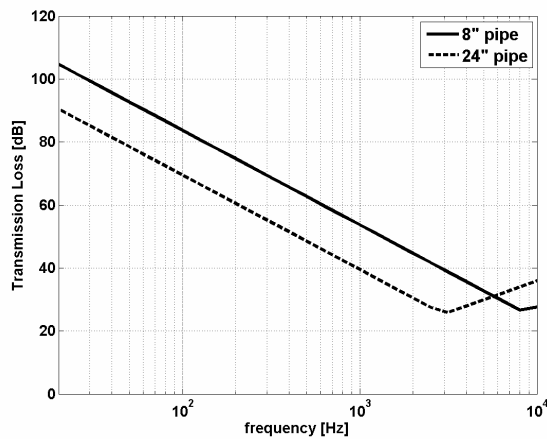


Figure 12. Typical transmission loss for small and large pipe (8" and 24", schedule 80)

4 Initial experiment in realistic environment

The last task in this research project to noise generation in reciprocating compressors, was an initial experiment in a realistic environment. Aim is to quantify the amplitude of occupational noise exposure effects and determine the contribution of various parts of the system. Furthermore, the experimental tools are validated on their merits for further detailed noise identification, and low-noise design.

The installation that was evaluated was a compressor station, with a 2-stage, variable speed, double acting reciprocating compressor, driven by an E-motor. The installation was mounted indoors, in a building of $16.5 \cdot 10 \cdot 6$ m³.

4.1 Measurement techniques

By synchronizing the system clocks between the analyzer and the operating support system, the instantaneous noise levels can be compared with operating conditions. This is a valuable tool for determination of correlations.

The most robust way however, is to monitor the compressor rpm, by fourier analysis of the in-line pulsation signals. This requires a low-frequent resolution ($df \sim 0.1$ Hz). For the noise radiation, the high-frequent part is also recorded, up to 12 kHz.

With a portable 1-channel noise analyzer, a quick survey of the noise levels in the installation can be performed. This gives a very global indication of the occupational noise exposure and the distribution within the installation. Furthermore, it will also indicate the dominant frequency bands in the spectra (in 1/3 octaves bands). However, it will not give any information on which are dominant sources in the installation, because the total noise level due to all sources is obtained. Furthermore, it contains no narrow-band information, so relating the noise levels to fluctuations in operating conditions (rpm) is not possible. This limits the possibilities of the use of portable equipment for noise source identification and recommendation of noise mitigation measures.

For noise source identification, more advanced measurement techniques are needed. Especially narrow band information, over a large frequency range, is very important. Therefore narrow band measurements were performed, using a multichannel data-acquisition system. Pulsation levels were monitored using 4 recording points in the upstream, interstage and downstream piping. Vibration levels were recorded in the upstream (3 locations) and downstream (2 locations) piping system. Portable vibration recordings were made at various parts of the installation. Noise levels were monitored at a location close to the second stage cylinder. Because all these quantities were recorded synchronously, many important cross-correlations can be studied. For example, the pulsation recordings allow for an accurate determination of the compressor rpm, and for the existence of higher-order harmonics in the in-line pulsations. Vibration measurements allow for identification of the dominant radiating surfaces of the installation. The narrow-band noise spectra can be correlated with compressor rpm and the in-line pulsation spectra. By monitoring the in-line pulsations, the wall vibrations and the radiated noise levels, the noise transfer path, described in section 3.3 can be validated.

The most advanced technique applied during the measurements was intensity scanning. The acoustic intensity is the product of p (acoustic pressure) and u (acoustic particle velocity).

The intensity is a vector quantity: it is an (acoustic) energy flow and has consequently a direction. Integrating the normal component of the intensity over a scanning surface yields the radiated acoustic power, through that surface. By evaluating the sign of the acoustic energy flow, it is possible to determine whether an important frequency component is located inside or outside an enclosed surface. During this initial measurement, a $p-u$ intensity probe was applied, that uses direct measurement technique to determine both p and u [12]. All important parts of the installation were scanned, while synchronously monitoring the noise levels and the in-line pulsation levels. In this way, a full qualitative survey was made of the installation (compressor, E-motor, lube-oil skid, cooling water-skid).

The intensity scanning method can also be used, for quantitative determination of sound power levels of parts of the installation. In that case, it should be applied over closed surfaces that contain no significant absorption inside. The first condition is in practice limited by accessibility of the installations. The second condition is generally met in process installation. A final condition is that during scanning of the individual surfaces, enclosing the source, the source remains constant. This is a critical requirement, since in this installation the rpm of the machine fluctuated constantly, over a time scale smaller than the time needed to scan the installation. Therefore, the typical cancellation effects applied in the determination of the absolute sound power levels, fails if applied in narrow frequency bands. Therefore, a dedicated analysis in broader frequency bands is needed.

4.2 Typical results

The noise levels in the actual installation are between 80-90 dB(A). The noise levels does not depend very strongly on the position within the building, which is an indication of the reverberant conditions in the building (homogeneous acoustic field). The largest value is encountered at a location close to the 2nd stage cylinder and the E-motor body. At this location (and moment in time), the noise is dominated in the 1 and 3.2 kHz frequency band.

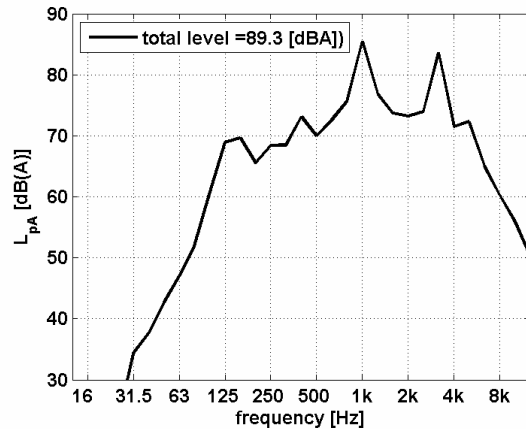


Figure 13. 1/3 octave band spectrum close to compressor and E-motor

The scatter in time of the noise levels at a fixed observation point, during regular operation is considerable, and is due to changing operating conditions (rpm fluctuations). It amounts to 8 dB(A). This large fluctuation stresses the importance of long-term average measurements, for realistic HSE compliancy.

In general, the noise radiation is homogeneous in the sense that adjacent scanning surfaces have comparable noise radiation properties. For example the noise radiation from the cylinder and the crank case does not differ by more than 10 dB, and the general shape of the curves is similar. The cylinders radiate more high-frequent noise. However, the compressor rpm was changing during the scanning of the surfaces. Thus, the changing effect of resonant amplification is also included in figure 12.

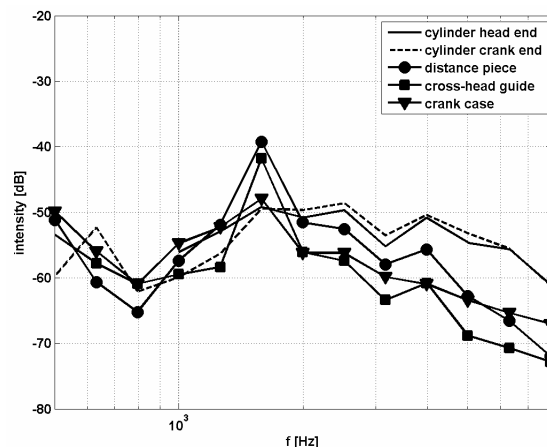


Figure 14. Illustration of acoustic intensity, radiated from various part of the compressor

The similar radiation behaviour of the various parts of the construction is not surprising, given the very

tight couplings, and low damping. In practice this means that, for example enclosing the cylinders only, will have very limited effect on the occupational noise exposure.

However, fluctuations in the compressor speed during scanning, led to considerable differences in radiated noise. This is confirmed by comparing the acoustic intensity taken at different instants in time. The amplitude of individual peaks changes significantly, but also a shift in frequency is observed. This strongly suggests that a resonance phenomenon occurs at higher multiples of the first harmonic. This is confirmed by the observation that, upon resonance, these tones are also present in the in-line pulsation spectrum. They are much weaker than the first harmonic, but for noise emission, very relevant (see also figure 12).

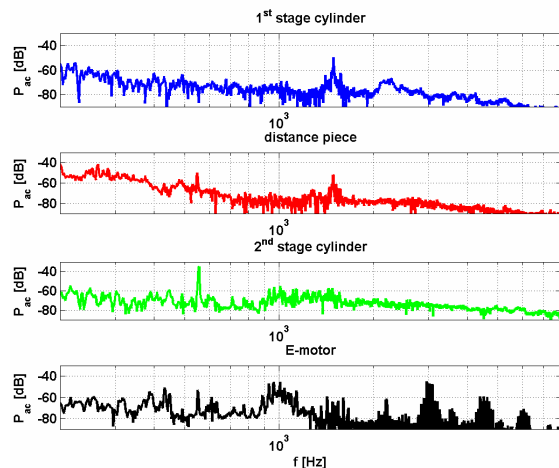


Figure 15. Radiated power of various parts in the installation: 1st stage cylinder, distance piece, 2nd stage cylinder and E-motor

During the scanning cycle (~1 hour), the compressor rpm changes, which led to different resonance conditions. In the upper figure (1st stage cylinder), a resonance near 1500 Hz is observed. In the second figure (distance piece), the resonance shifts toward 450 Hz. In the third figure (2nd stage cylinder), this 450 Hz resonance becomes very strong. The fourth figure illustrates the noise radiation from the E-motor, which is dominant near 1 kHz, 3 kHz and higher frequencies.

The E-motor induces strong tonal noise at frequencies that weigh heavily in the total dB(A) level. This is confirmed both by vibration measurements and intensity scanning measurements. The tentative assumption, formulated in [2] that drivers are insignificant in the total noise emission, is contradicted by the experimental results from this installation.

The lube oil skid and the cooling water skid do not contribute significantly to the total radiated noise.

The noise radiated from the compressor casing is very strongly tonal in character. This, combined with the observation that the peaks shift with changing rpm, suggests that resonance phenomena occur, with a high quality factor. This strongly suggests that in-line pressure pulsations are responsible for the radiated noise. It is less likely that this is due to valve impact noise or valve flow noise, which are more broadband in character. Furthermore, at these high frequencies, structural resonances have a large modal density, which conflicts with the very discrete behaviour of the resonances. However, these two mechanisms do contribute to the broadband noise radiation.

5 Acknowledgements

The measurement results described in section 4, were obtained by kind permission of NAM Nederlandse Aardolie Maatschappij B.V.

6 References

- [1] VDI 3731 – Emissionskennwerte technischer schallquellen – Kompressoren, 1982.
- [2] L. van Lier, “Survey on reciprocating compressor noise”, EFRC report, September 2006.
- [3] L. van Lier, “Evaluation of experimental techniques for identification of noise radiation in reciprocating compressor installations”, EFRC report, January 2007.
- [4] VDI 3735 – Arbeitsblätter Lärmquellen Prozesshubkolbenverdichter, 1972.
- [5] G.Will, G.Flader and M.Gehlert, “Calculation of fluid flow in the cylinder of a reciprocating compressor”, EFRC report 2003.
- [6] H.Korst and W.Brocatus: “Noise reduction at a NAM-compressor station”, 4th EFRC conference, Antwerp, June 2005.
- [7] L. Cremer, M.Heckl and E.Ungar, “Structure-borne sound”, 2nd Edition, Springer Verlag, 1988.

- [8] VDMA 24422 – Richtlinien für die Geräuschberechnung regel- und Absperrarmaturen, 1989.
- [9] IEC 534:8:3 – Control valve aerodynamic noise prediction method, 1995.
- [10] G.Reethof and W.Ward, “A theoretically based valve noise prediction method for compressible fluids”, *Journal for Vibration, Acoustics, Stress and Reliability in design*, 1986.
- [11] VDI 3733 – Noise at pipes, 1996
- [12] F.Jacobsen and H. de Bree, “A comparison of two different sound intensity measurement principles”, *Journal of the Acoustical Society of America*, 188(3), 2005.

RWE Energy – Westfalen-Weser-EMS Netzservice

Overhaul of a 8-Cylinder Ingersoll Rand compressor for a liquefaction process

by:

**Dr. Burkhard Katzenbach
Management Underground Storages
RWE Energy - WWE
Dortmund
Germany
Burkhard.katzenbach@rwe.com**

**5th Conference of the EFRC
March 21-23, 2007
Prague, Czech Republic**

Abstract:

RWE operates the Liquid Natural Gas–Storage (LNG-Tank) in Nievenheim near Düsseldorf. As the liquefaction is done on site a complex plant is necessary, the heart of this plant is a reciprocating compressor.

In spite of the exotic range of use and the associated irregular load, the compressor was not in a perfect, but in a repairable state, even after 30 years of operation including a two year period of shutdown.

It was revealed that slow running piston compressors are able to cope quite well with this extraordinary operation profile due to their extended range of characteristics, and obviously have considerable reserves during their service life.

1 Introduction

Description C21601, liquefaction compressor

The compressor used for the liquefaction process was first started by Dresser Rand in 1975. The unit type is "HHE VG". The compressor has 8 cylinders and 8 cranks. It is driven by an electric motor with fixed speed. The electric motor has 1.91 MW and 10 KV; the speed is 331 rpm. A 10 KV start-up throttle is interconnected during the start-up process.

A *single cycle process* is used for liquefaction. In this process, two material flows are relevant. The first one is the coolant circuit. The second one is the generative gas flow.

The coolant is a mixture of propane and methane and is called MRL (mixed refrigerant liquid) it can be used throughout the entire relevant temperature range (approx. +100 °C to -150°C). In a first step, the gas is compressed to approx. 2 bar in 2 parallel cylinders (temperature approx. 70 °C), then it is further compressed successively in two cylinders until it reaches approx. 39 bar (92 °C). the hot gas is cooled to approx. +20 °C (approximate ambient temperature) by means of an air cooler and then further cooled down to approx. -20 °C via a bypass in the cool box. The subsequent expansion (Joul Thompson) to approx. 0 bar cools the gas flow down to approx. -150 °C. This cold gas flows the cold box, in a counterflow to the clean gas, and is then again added to the 2 first cylinders.

Initially, the regeneration gas to be compressed consists of the low-temperature cooled clean gas for liquefaction (only approx. 30% is liquefied after pressure expansion during the feeding into the tank). This deeply cooled gas is channelled through the cold box to support the deep cooling process. In the course of this process, its temperature rises from -164 °C to approx. +20 °C. Then it enters the compressor and is compressed from approx. 1 bar (atmospheric pressure) to approx. 22 bar in three stages and at the same time heated to approx. +100 °C. Subsequently, it is heated further to approx. 280 °C via a thermal oil plant and added to the absorbers for regeneration. After flowing through the absorbers, the gas including the additives is cooled to 20 °C in air cooler and compressed to a level slightly above the system design pressure (approx. 64 bar) in the fourth stage of the compressor, and then fed into the high-pressure gas network.

This small gas flow (approx. 7,000 cbm/h) mixes with the main flow of the gas network (> 50.000 cbm/h).

Both material flows are compressed at the same time. The throughput amounts can only be controlled manually by changing the exhaust chambers.

Following a period of two years, in which the compressor was not used, and a previous operating period of approx. 4,000 hours, an overhaul of the compressor was necessary.

2 Overhauling the compressor

First of all, all valves were removed and various reference dimensions recorded. Then the cylinder caps were dismantled and the pistons removed.

The condition of the valves was in line with the operating periods. Only normal repair work was necessary, such as a change of the spring and the plate.

The pistons and cylinders were dimensioned and adjudged. The result was that all cylinder dimensions were beyond the tolerance range. Consequently, the cylinders were drilled to a larger size and honed.

The old coating of the plungers did not have sufficient adhesive strength. Therefore, the plungers were renewed.

The pistons of the individual stages had been equipped with piston saddles up to the fourth stage of regeneration gas. On the MRL side, all pistons had been equipped with PTFE saddles up to stage 1a, which was equipped with white alloy saddles. It is assumed that the plan was to gain experience with different materials.

Jointly with the operator, it was decided to equip all pistons with PTFE guide rings in order to make future repair work, a replacement of the guidance, easier and less expensive in future.

The inspection of the crank drive and of the bearings revealed damage on the main bearings. Dimensioning revealed that these dimensions were also beyond the tolerance range. In addition, strong grooving had developed on the bearing surface. This resulted in the decision to exchange all main bearing shelves. The crank shaft showed minor running tracks on the bearing points. It was possible to remove this by polishing.

The connections between the crank case and the oil level indicators were so dirty that it was probably impossible to see the actual oil level. The operating staff could assume that the oil level in the power unit was normal. Consequently, the compressor was probably operated with an insufficient amount of oil at times. This led to the bearing damage described above. It was decided to not only renew the existing oil level indicator but to install a radar level gauge in addition.

The temperature measurements on the main bearings were all renewed and newly installed in the drive unit tunnel.

The crossheads showed minor discolouring, possibly caused by temperature influences. Polishing was sufficient, the material was not damaged, the discolouring was only on the surface.

3 Conclusion

In spite of the exotic range of use and the associated irregular load, the compressor was not in a perfect, but in a repairable state, even after 30 years of operation including a two year period of shutdown.

It was revealed that slow running piston compressors are able to cope quite well with this extraordinary operation profile due to their extended range of characteristics, and obviously have considerable reserves during their service life.



Online Condition Monitoring of LNG boil-off gas compressors

by:

Josu Elorza Etxebarria
Bahia de Bizkaia Gas
Bizkaia, Zierbena
Spain
jelorza@bbe-bbg.com

Thorsten Bickmann
PROGNOST Systems GmbH
Rheine
Germany
thorsten.bickmann@prognost.com

5th Conference of the EFRC
March 21-23, 2007
Prague, Czech Republic

Abstract:

Bahía de Bizkaia Gas operates a LNG regasification terminal at Bizkaia in the north of Spain. Two 2-stage vertical laby piston compressors are in service to recompress boil-off gas.

In the recent years, LNG became more and more relevant as a clean fuel and as a feedstock for petrochemicals, agricultural chemicals and plastics. To comply with the demand and consequently the increase of ship unloadings and storages of LNG in tanks, Bahía de Bizkaia Gas installed an online condition monitoring system for reciprocating compressors to increase the reliability and safety protection for their compressors.

Low temperature applications such as LNG have always been difficult as standard vibration and pressure sensors are limited in low temperature environments. With special modifications applied to the compressors, standard sensors can be used on LNG compressors and provide reliable readings and useful information for the operator.

The paper describes the LNG process and how an existing LNG compressor has been modified mechanically to install an online condition monitoring system with standard acceleration and pressure sensors. Plots of crosshead slide and cylinder vibration as well as pV-diagrams are discussed with their low temperature specialities. The typical LNG boil-off gas-compressor operation scheme with its frequent starts and stops and its influence on the compressor condition is presented and discussed.

1 Introduction

The Bahía de Bizkaia project as a whole is headed by four equal partners, all top companies in the energy sector, such as: BP, Iberdrola, Repsol-YPF and Ente Vasco de Energía (the Basque Country's Regional Energy Agency). They are firmly committed to bringing about this key strategic project, which will secure and guarantee sufficient high-quality Natural Gas-based energy supplies transported by sea, and will make industry more competitive in energy terms by bringing energy production closer to the point of consumption.

1.2 Project history

Bahía de Bizkaia as a Project involves the construction and Commercial Operations of an LNG Regasification Plant (Bahía de Bizkaia Gas), which will have an annual regasification capacity of 800000 Nm³/h, and an 800 megawatt Combined Cycle Power Plant (Bahía de Bizkaia Electricidad).



Figure 1: BBG land facilities and maritime terminal

The starting point for Bahía de Bizkaia lies within the Energy Strategy devised by the Basque Government, which has been brought about by means of several energy plans. The Basque Country is located in the north of Spain, and is characterised by a high demand for energy, as it is a highly industrialised area. Such Energy Strategy had at its basis during the 1980s the premises of energy efficiency, diversification, and the promotion of renewable energy sources, apart from guaranteeing energy supply for the area.

One of the first actions resulting from the aforementioned diversification policy was the lying out of the gas network in the Basque Country, which allowed for a decrease in oil reliance, apart from reducing the environmental impact associated to energy usage.

Bahía de Bizkaia Gas should be regarded as a further step within such diversification policy, as it will help guarantee gas supply for the Basque Country, as well as reinforce the Spanish Gas System.

On the other hand, the liberalisation of the Electricity Market paved the way for another project: the construction of a Combined Cycle Power Plant (Bahía de Bizkaia Electricidad). This was intended to make the most of the possibilities offered by the Regasification Plant, as well as benefit from the different synergies between both projects, and help correct the shortage of power production in an area which, as mentioned above, has a great demand for such kind of energy, but not enough generation capacity.

The total investment for the Project amounts to 655 million Euro; 338 million Euros have been invested on the Power Plant (Bahía de Bizkaia Electricidad), and the remaining 317 million Euros have been invested on the Regasification Plant (Bahía de Bizkaia Gas).

The construction of both Plants has had a relevant and very positive effect on local construction and capital goods companies, apart from helping revitalise the industrial and economic network in the surrounding area.

	2004	2005	2006
Gas tankers unloaded	37	45	59
LNG Quantity (10⁶ m³ LNG)	4,32	5,65	7,58
Annual Production (GWh)	30.000	34.000	51.000
Number of trucks loaded	1.178	1.950	2.098
Power factor (%)	36	45	61
Ships coming from(%):			
▪ Nigeria	75	81	57
▪ Algeria	22	14	2
▪ Trinidad - Tobago	----	----	22
▪ Qatar	----	----	19
▪ Others	3	5	----

Figure 2: Operations data 2004 – 2005 - 2006

This chart (Figure 2) reflects the current trend towards a continuous increase in gas consumption & production.

2 Description of Plant and Process

The LNG Terminal and associated Regasification Plant owned by Bahía de Bizkaia Gas, S. L. is located in land owned by the Port Authority of Bilbao, in the town of Zierbena, Bizkaia.

Liquefied natural gas (LNG) is natural gas that has been chilled to a liquid state at -161°C . In its liquid state, natural gas takes up just 1/600th (about 0.17%) of the amount of space required in its gaseous form. This size efficiency renders LNG extremely practical for transport and storage.

LNG is stored in two tanks, with a capacity of 150.000 m^3 each. These tanks are cylindrical in shape and aerial, as per the UNE-EN-1473 standard for full containment tanks.

The overall maximum LNG send-out rate from the time of commissioning is $800.000\text{ Nm}^3/\text{h}$, which means an annual dispatch of 7 bcm. Furthermore, the Plant could even increase its capacity up to 9 bcm in the future. Send-out pressure stands at 72 bar g for the gas intended to be sent to the Gas pipeline and 36 bar g for gas intended for the nearby Combined Cycle Power Plant.

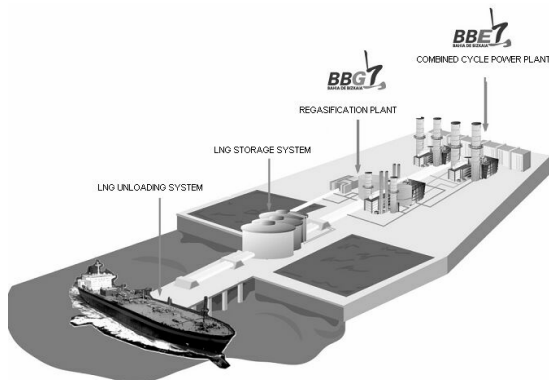


Figure 3: General layout of Bahía de Bizkaia facilities

LNG is delivered by means of methane carriers, which berth at a Jetty devised exclusively for that same purpose. The front of the Jetty area is located at a distance of 200 metres from the front of the processing and storage area.

2.1 LNG unloading system

The main components of the LNG unloading system are the following: unloading arms, unloading pipelines, vapour return and re-circulation lines, and a tank used to separate the pipe from the vapour return system.

LNG unloading from the methane carriers is done by means of cryogenic pumps located on board. Three 16" unloading arms, located on the Jetty, dispatch LNG to the discharge manifold, which is 42" wide, and which in turn directs LNG as far as storage tanks.

There is a fourth 16" unloading arm, used to connect with the 30" wide vapour return line, and which serves the purpose of supplying the vessel with the required amount of LNG to replace the volume of LNG unloaded, thus avoiding either a situation of low pressure or even vacuum within its storage tanks. Gas to be returned to the vessel is filtered at a tank (FA-103), where all potential liquid is eliminated.

The maximum LNG unloading capacity of the aforementioned unloading system is $12.000\text{ m}^3/\text{hour}$, that is to say, $4.000\text{ m}^3/\text{h}$ per unloading arm.

Unloading arms are drained after each unloading operation by sending LNG down to the discharge line by means of nitrogen.

During the period between unloading operations, a flow of LNG is sent down the 6" re-circulation line from the tanks. A part of the LNG pumped by the primary pumps located inside the tanks is used for this purpose, and then returns via the 42" discharge line, thus keeping the pipelines cool.

2.2 LNG storage system

The LNG storage system is made up of two LNG tanks (FB-101 and FB-102) with a capacity of 150.000 m^3 each, as well as LNG tank pipelines and four primary LNG pumps per tank, two of them with a capacity of $265\text{ m}^3/\text{h}$, and two more with a capacity of $485\text{ m}^3/\text{h}$ (identified as GA-101 A/B/C/D y GA-102 A/B/C/D respectively). These pumps are located in their pits inside the LNG tanks.

These tanks are cylindrical in shape and aerial, as per the UNE-EN-1473 standard for full containment tanks. They have a design pressure of 290 mbar g, and an operating temperature of approximately -163°C . Their main components can be detailed as follows:

1. An inner tank devised to hold LNG, whose walls and bottom are made of steel plate at 9% Ni, and a suspended steel roof.
2. An external reinforced concrete tank, with carbon steel lining (as per ASTM A516).
3. A secondary container built in steel plates at 9% Ni, aimed at withholding potential LNG leakages from the inner tank, thus avoiding any impact on the external reinforced concrete tank.

An isolation system has been fitted between the concrete slab and the bottom part of the inner tank, which holds the LNG. Such system is made up of dry sand layers and foam glass block layers.

The remaining space between both containers has been filled with isolating elements such as a resilient insulation blanket, which has been attached to the inner tank, and expanded perlite. Foam glass has been located over the steel lining of the inner tank.

All pipes come into the tanks through the roof, thus avoiding emptying the tanks by accident on account of a breakage on one of the pipelines.

Provisions have been made according to the expected responses to seismic conditions in the area, as per Spanish norm NCSE-94, as well as UNE-EN-1463 and operations' status, pneumatic test and hydraulic test, together with the required safety coefficient standards (EHE, Euro-code 2, UNE-EN-1473, BS-7777).

Further provisions include:

- Fire resistance with no collapse, by which the tank keeps its functions fully in the following situations: fire in one of the safety valves, fire in the spillage tray and fire on the roof of the tank. Each of these situations would create a heat flow of 32 kW/m² at least for 6 hours.
- Resistance to external impact of a solid element of 110 kg at a speed of 160 m/s on wall surfaces and external tank roof with no loss of integrity of the primary container.
- Resistance against explosions, with a suction of -0,15 bar in 0,45 seconds, and an immediate over-pressure of 0,15 bar in 0,15 seconds.
- Evacuation to flare of all gas discharges carried out at safety valves on account of overpressure. There is also a second level of safety valves that would, if necessary, discharge directly to the atmosphere.
- LNG level sensors fitted with pre-alarm, alarm and unloading operations stoppage systems as a result of an excessive level of LNG storage.
- Surveillance of variations in LNG density as per its depth inside the tank, so as to be able to detect a potential stratification and thus proceed to homogenize tank contents.
- An LNG spillage tray with a capacity of 401 m³ has been built on site in order to contain a potential LNG spillage.

- Fire-fighting systems have been fitted in process platforms (operated with seawater), as well as a Chemical Dry Dust System for safety valves fitted for a potential discharge to the atmosphere.

2.3 LNG regasification plant

A regasification plant in itself, with a regasification capacity of 800.000 Nm³/h. The regasification process is done by means of 4 seawater vaporisers that make use of water previously used in the Power Plant to cool off the Condenser.

Seven secondary pumps are used to supply the vaporizers; four of them have a capacity of 256 m³/h, while the other three have a capacity of 385 m³/h. Secondary pumps have a submerged engine, and are protected by means of minimum flow re-circulation, gas venting and a safety valve in the container.

The vaporizing system consists of four seawater vaporizers, with an operating capacity of 200.000 Nm³/h each and another submerged combustion vaporizer, with an operating capacity of 200.000 Nm³/h. Seawater vaporizers are used for normal operations, while the submerged combustion vaporizer is to replace the others whenever they are offline on account of maintenance tasks. This system guarantees the availability of Natural Gas supply to the send-out lines. The minimum gas temperature upon exiting this system is approximately 0°C.

From the vaporizers, Natural Gas is then measured at the Metering Station and odorised, to be sent later to the gas pipeline at a maximum pressure of 72 bar.

Natural Gas aimed at supplying the Combined Cycle Power Plant is sent out at a maximum pressure of 36 bar. Such adjustment in pressure is carried out at the Metering and Regulation Station, with a send-out capacity of 133.000 Nm³/h. There are two Natural Gas heating systems which ensure a minimum temperature of 0 °C after being regulated for send-out to the Combined Cycle Power Plant. The first system consists of a seawater heater, similar in design and operation to seawater vaporizers, while the second system, which comes into operation if seawater happens to be cold, consists of a closed circuit with water on site, which is heated by means of boilers supplied with Natural Gas.

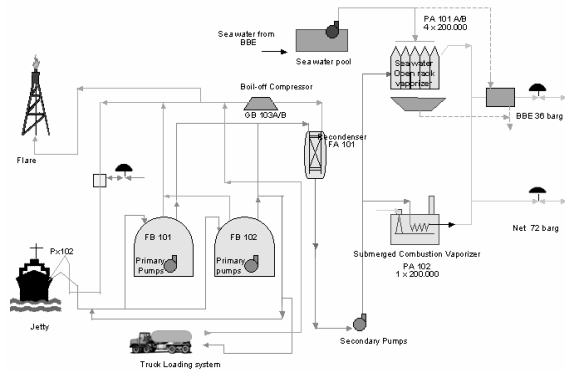


Figure 4: BBG flow chart

2.3.1 Boil-off gas recovery system

This system consists mainly of two gas recovery compressors (named GB-103 A/B), together with their associated pipeline. These two vertical 2-stage Laby compressors were built in 2001 by Burckhardt Compression Type 2D250B-2C_1. The compressors are operated at 496 rpm with a maximum flow of 2560 kg/h each, driven by induction motors with a power of 520 kW to recompress boil-off gas from the tanks.

The Capacity is controlled by unloading of suction valves and by switching fixed clearance pockets. The regulation allows the load steps of 100 %, 75 % (head end clearance pockets open at both stages), 50 % (crank end unloaded at both stages), 25 % (crank end unloaded, head end clearance pockets open at both stages) and 0 % for start up.

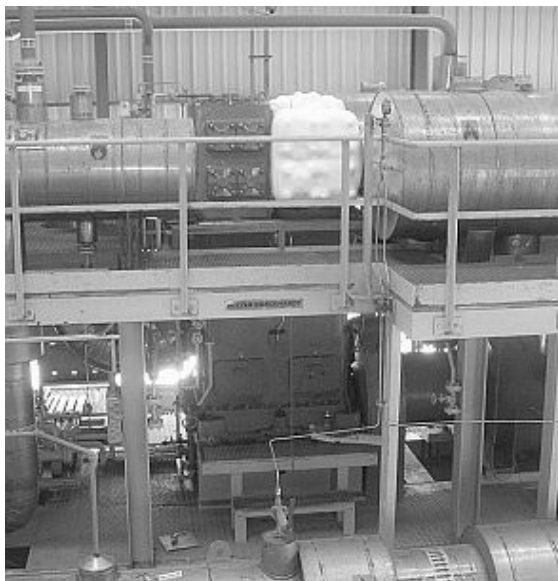


Figure 5: Burckhardt Compression Laby Compressor 2 stages

During normal operations, a single boil-off gas compressor at approximately 50% of its capacity is

used to deal with vapour originated as a result of heat in the tanks. Such vapour is then sent to a recondenser, which is able to handle the whole flow of vapour arisen in the terminal, thus keeping tank pressure under the maximum permitted values.

Upon LNG carrier unloading operations, a noticeable increase in the gas flow is generated in relation with gas produced during normal operations; therefore, both compressors are used, sending out to the vessel excess gas that has not been absorbed by gas tanks on board down to the recondenser. These two compressors have a capacity of 2.560 kg/h each.

Natural Gas propelled by compressors is sent to the recondenser where primary pumps on tanks liquefy it.

The re-liquefier houses an inner cylinder packed with stainless steel pall rings, which forms an annulus with the outer wall of the recondenser. Boil-off gas and LNG enter the inner cylinder from the top of the recondenser and are contacted in the packing. The annulus pressure and liquid level are controlled and this maintains a constant pressure at the suction to the send-out pumps (GA-104 A/B/C/D).

Pressure in the packed bed and annulus are individually controlled by splitting the flow of boil-off gas into each one of them. Regulating the LNG flow into the recondenser controls the volume of liquid in the vessel. The bed liquid level varies with pressure and vapour/liquid load on the recondenser.

Recondenser pressure is kept by passing a portion of boil-off gas from the compressors around the packed bed section of the recondenser. In the event that insufficient boil-off gas is available from the compressors, send-out gas taken upstream of the Metering Station will be used for recondenser pressure control.

The recondenser acts as well as a liquid buffer volume for the send out pumps (GA-104 A/B/C/D). It has been designed for the initial send-out rate of 400.000 Nm³/h (plus self-consumption) with all boil-off gas compressors in operation and a holding time of one minute at that send-out rate. Part of the LNG pumped by primary pumps in the tanks gets directly to secondary pumps (GA-104 E/F/G) with no processing through the recondenser.

2.4 Why install an online condition monitoring system?

In normal operation only one boil-off gas compressor is needed, usually. So one of them could be out of service, however both compressors are needed during ship unloading.

BBG guarantees to unload a ship within 36 hours which is the established lay-time. If this period is exceeded a significant penalty has to be paid.

In case only one compressor is available, the unloading of an LNG carrier will require two days or more.

The unloading time depends on the physical characteristic of gas unloaded from the ship and the time that is needed to achieve a homogeneous mixture between the gas inside the tank and the unloaded “new” gas from the carrier.

If every three days an LNG tanker is anchoring, both boil-off gas compressors will be in permanent operation.

In 2006 a total number of 59 ships were unloaded with an average of 6,2 days. (in practice that is three to seven days).

This proves that the compressors are critical because any shutdown that requires more than two days might impact the unloading of the next LNG carrier.

Based on the above requirements for the availability of the boil-off gas compressors BBG decided to install an online condition monitoring system with the following objectives:

- 100% availability of both compressors during ship unloading to guarantee unloadings in time.
- Safety protection to avoid mechanical damages and consequential machinery shutdowns.
- Early failure detection of gas leakages and in the running gear in an increasing stage.
- Extending the predictive maintenance philosophy that is applied at BBG to all rotating equipment.
- Precise maintenance and component replacements without overhauling the whole compressor.
- Accelerate the process of gathering information about the “new” compressors.
- Maintain the efficiency of compressors.

- Increase MTBM.
- By using the condition monitoring system BBG is relying on hard fact data to make sensitive maintenance decisions.

3 Online Condition Monitoring for Boil-off Gas Compressors

3.1 Demands

To ensure the safety and availability of the plant, continuous operational condition monitoring, data on a machine’s condition, must be permanently collected and assessed. The focus lies on data that indicate a rapid change in the condition of the machine, e.g. vibrations by segmented analyses or operating condition dependent warning threshold checks. This gives early warnings and minimises possible consequential damages and related high costs.

In condition-based maintenance, machines are only shut down if their condition requires it. Parts are only changed if a damage criteria is reached. In this way the maximum lifetime of spares and wear reserves should be exploited and above all a reduction in material costs is realised. This is only possible if the operator has a precise knowledge of the machine condition. First and foremost the existing wear potential in “traditional” wear parts, e.g. valves or packings, can be exploited and thus optimise machine operating life and availability.

3.2 Description of the Installation

The mechanical safety of both stages is monitored by acceleration sensors, which are mounted on the outer frame close to the support, which connect each crosshead slide with the frame. Thereby the operator receives detailed information of the condition of each stage.

SPECIAL TOPIC: LNG

Online Condition Monitoring of LNG Boil Gas Compressors, *Josu Elorza Etxebarria; BAHIA BISCAYA GAS*
Thorsten Bickmann; PROGNOST SYSTEMS

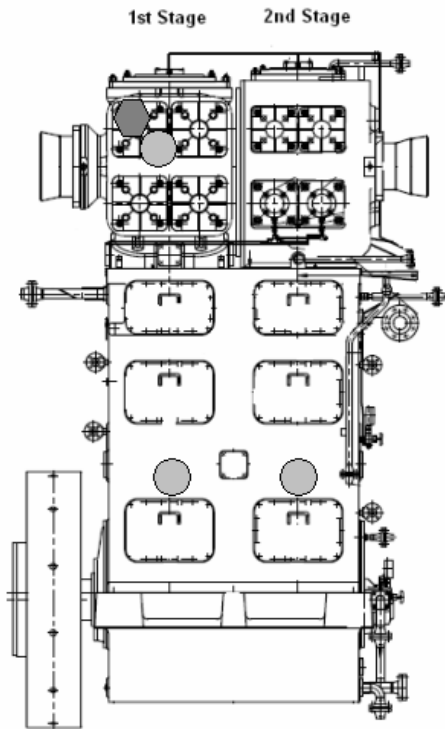


Figure 6: Burckhardt Compression Laby Compressor 2 stages with measuring points

Due to this low temperature specialities, the accelerometer and dynamic pressure sensor needs to be located outside the cylinder ice cover. Thus the dynamic pressure sensor is attached to a drilled valve cover and the acceleration sensor is attached to the elongated valve cover bolt (Figure 8).

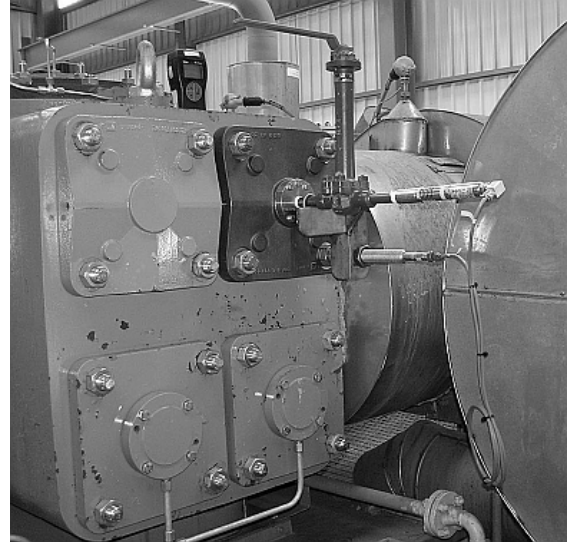


Figure 8: special apparatus for cylinder vibrations and pressure head end 1st stage

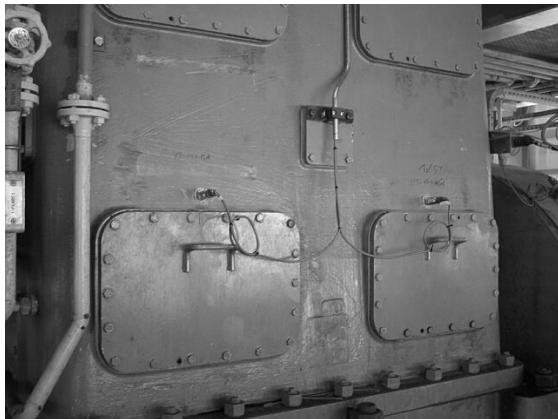


Figure 7: Accelerometers close to the Crosshead slide

Specific modifications have to be made during the installation of the pressure sensor and vibration sensor at the cylinder.

The pressure sensor measures the indicated dynamic pressure in the compression chamber and the acceleration sensor the cylinder vibration.

The suction temperature of the first stage is around $-140\text{ }^{\circ}\text{C}$. The low gas temperature causes an ice coating of up to 100 mm around the cylinder.

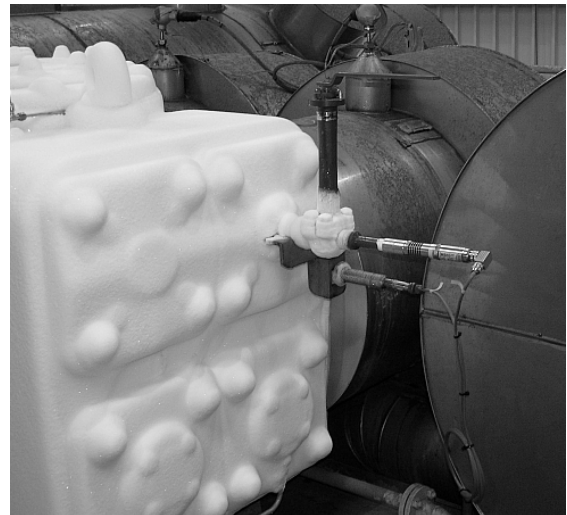


Figure 9: Ice coating with measuring equipment during operation

3.3 Condition Monitoring

Continuous monitoring of the accelerations at the crosshead slides and the continuous comparison with individual warning thresholds for each load step is necessary to detect failures in the drive trains. Damages or clearances in the drive train, e.g. a loose crosshead – piston rod connection result in higher vibrations in certain parts of the stroke.

For every revolution, the crosshead slide vibration signal is subdivided into 36 segments and the RMS values are calculated for each segment and compared to the safety limit for each segment. Thus the safety protection is given for the compressor and the plant.

Figure 10 displays a waterfall diagram of 1st and 2nd stage crosshead slide vibrations after the start up. The change in vibration is visible when the load is shifted from 75 % to 50 %.

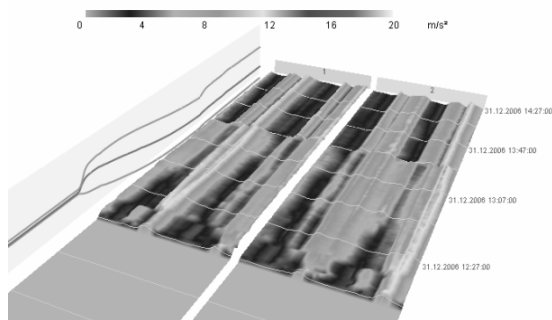


Figure 10: waterfall diagram of both crosshead slide vibrations for a period of three hours showing the start up process and a 75 % to 50 % load change

When compressors are operated with several load steps, an effective monitoring is only given, if individual operating conditions with individual warning thresholds for each analysis can be defined.

The following online signals display the indicated dynamic pressure at the head end and the crosshead slide vibration (upper part of the figure) with the 36-segmented analysis (bottom) for the loads at 50 %, 75 % and 100 % for one revolution. Indeed, it is visible, that each segment has a different RMS value for each load step.

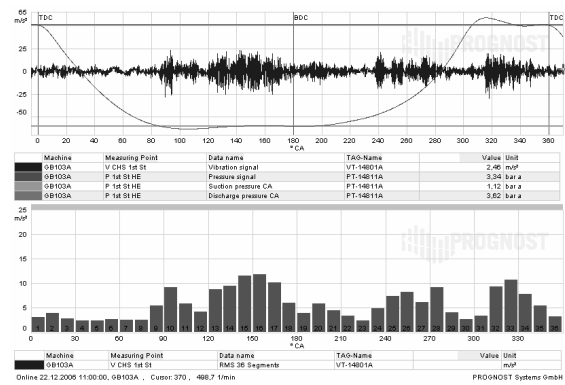


Figure 11: Segmented RMS values of crosshead slide vibration at 50 % load for one revolution

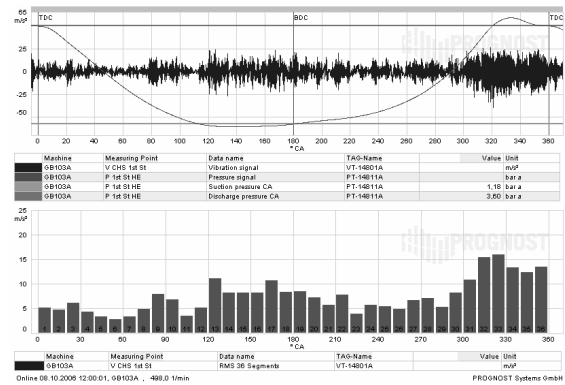


Figure 12: Segmented RMS values of crosshead slide vibration at 75 % load for one revolution

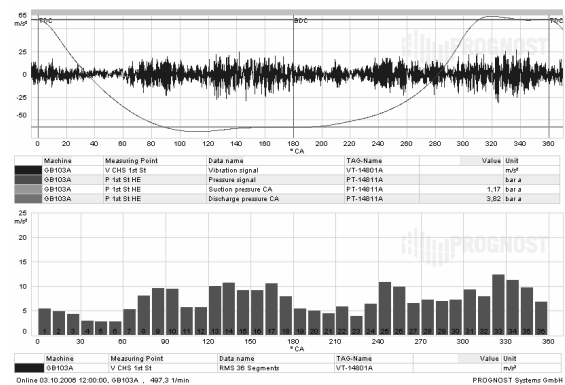


Figure 13: Segmented RMS values of crosshead slide vibration at 100 % load for one revolution

These changes in amplitude are due to different rod loads and are not related to damages. Failure detection of the running gear during operation in several load steps and therefore continuous changes in the vibration level, is not possible if there is only one overall value defined for every operating condition.

SPECIAL TOPIC: LNG

Online Condition Monitoring of LNG Boil Gas Compressors, *Josu Elorza Etxebarria; BAHIA BISCAYA GAS*
Thorsten Bickmann; PROGNOST SYSTEMS

Individual operating conditions with individual warning thresholds have an advantage. In Figure 14, the RMS value of segment 8 is drawn in a reading of two days. Due to the load change from 50 % to 75 %, the strength of the vibration is doubled. Individual warning thresholds for load step 50 % and load step 75 % display no violation in this usual change.

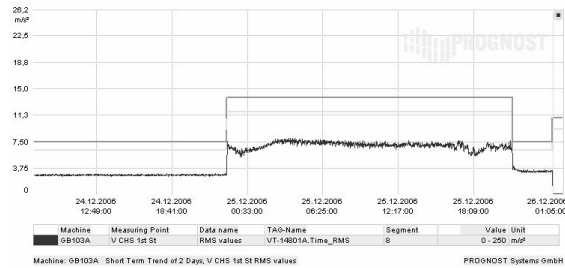


Figure 14: Trend of two days of CHS RMS segment 8 with individual warning thresholds at load change from 50 % to 75 % and back to 50 % load

During the same load change, segment 10 decreased in comparison to segment 8. Also individual warning thresholds are used to monitor and detect unexpected failures at an early stage.

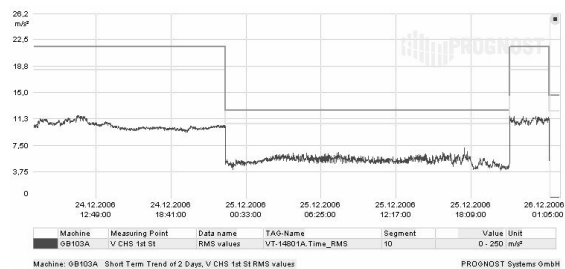


Figure 15: Trend of two days of CHS RMS segment 10 with individual warning thresholds at load change from 50 % to 75 % and back to 50 % load

The condition of the suction and discharge valves is monitored with the help of the indicated pressure and the pV-diagram analysis. For this, special pressure sensors with a high frequency sensitivity are installed. Additional conclusions can be made with regard to the sealing elements such as packing and rider rings (in this case, the condition of the labyrinth skirt and liner). Further on, the effective function monitoring of the control devices (suction valve unloaders, clearance pocket unloaders) is possible with the continuous pV-diagram analysis.

Both boil-off gas compressors are regulated via suction valve unloaders and clearance pockets. The following Figure 16 shows the pV-diagram at 100% load.

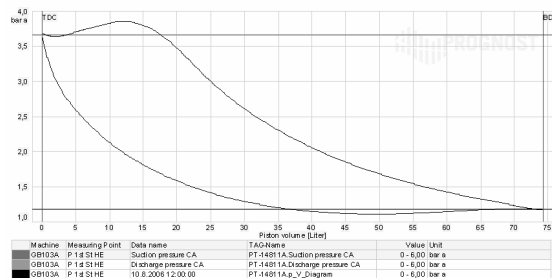


Figure 16: pV-diagram 1st stage head end (100%)

The flow regulation via additional clearance pockets is displayed in the pV-diagram of Figure 17.

The clearance pocket adds fixed clearance to the cylinder and enables additional capacity control that cannot be achieved through cylinder end unloading. When clearance is added to the cylinder, the throughput of the cylinder and engine performance is decreased.

During compression stroke, the clearance volume must be filled before the gas reaches discharge pressure and opens the discharge valve, so less gas is discharged. This also leaves extra gas at discharge pressure trapped in the clearance pocket, which expands during the suction stroke and delays the opening of the suction valve.

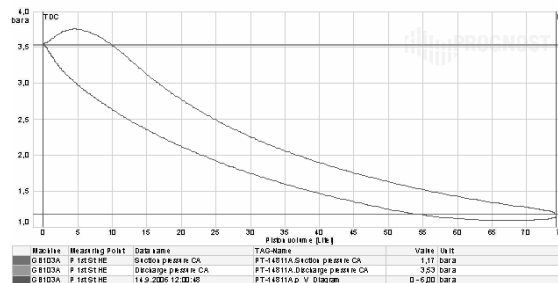


Figure 17: pV-diagram 1st stage head end (clearance pockets active, 50% Load)

The energy used for the compression process can be read directly from the area of the measured p-V diagram. The trend of three weeks displays the indicated energy and thereby the frequency of regulation by adding the clearance pocket.

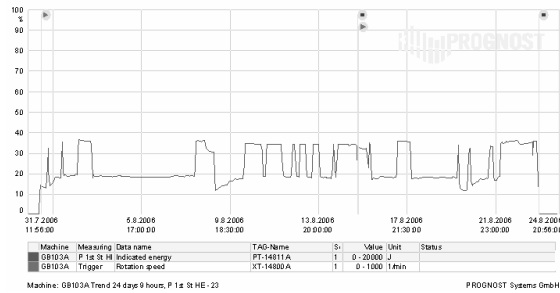


Figure 18: Trend of the indicated energy 1st stage HE shows the frequentness of regulation by adding the clearance pocket

The pV-diagram analysis is one of the most important methods for valve condition monitoring. The analysis of a recorded signal allows to draw conclusions on conditions of the seal elements in the cylinder area. Damage to valves that result in leaks cause characteristic changes in the dynamic pressure curve.

The measured pressure flow is converted into a pressure - volume diagram for which characteristic values are calculated at certain fixed points. These values, e.g. valve losses, polytropic exponents or crank angle at which the suction pressure is reached, are subject to an automatic warning threshold monitoring in order to identify defective suction or discharge valves.

In order to take account of the various compressor operations and to differentiate between operational-dependent and leakage-dependent changes in data, individual warning thresholds for each load are configured. Figure 19 displays the polytropic exponent 1, an important value for the detection of leakages at sealing elements, with individual upper and lower warning thresholds for the loads of 50 % and 75 %.

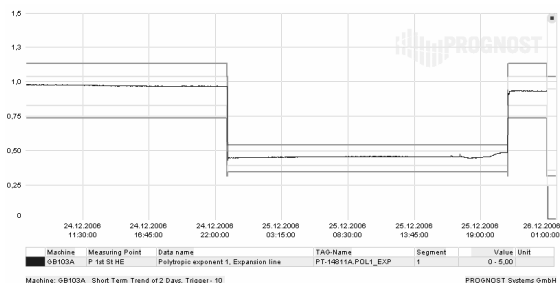


Figure 19: Trend of two days of Polytropic exponent 1 with individual upper and lower warning thresholds at load change from 50 % to 75% and back to 50 % load

Without operating condition dependent warning thresholds a valve failure cannot be detected.

The vibration accelerations measured at the cylinder provide additional information on valve condition. Valve impacts can be recognized and broken valve plates or loose valve cages can be detected. This involves installing accelerometers on the cylinders, which cover a high frequency range.

The opening and closing events of the suction and discharge valves are visible in the following online signal over one revolution. The impact at 120 °CA belongs to the opening slug of the suction valve head end. The discharge valve crank end opens with a visible peak at 140 °CA. The impacts around 270 °CA are due to the opening of the crank end suction valve. At 330 °CA the discharge valve head end opens conspicuously by the high vibration amplitude.

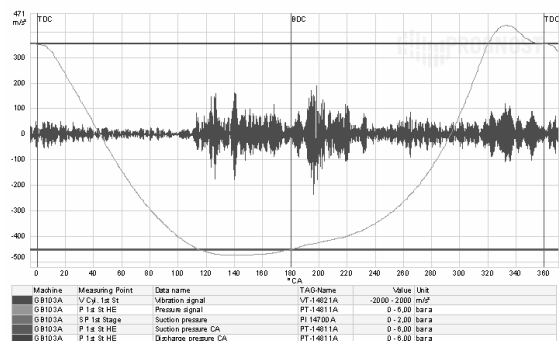


Figure 20: cylinder vibrations and pressure head end 1st stage for one revolution

In future the apparatus and the position of the accelerometer will be approved with the objective of receiving clearer opening and closing impacts.

Process data like suction and discharge pressures, gas temperatures before and after the compression, winding temperatures, load steps and frame vibrations are integrated into the monitoring system and can be displayed in a trend. The possibility of comparing correlations of the measured vibrations and process data is given.

The following trend view of four hours shows the suction, interstage and discharge temperatures, when a ship is unloading and the compressor is started.

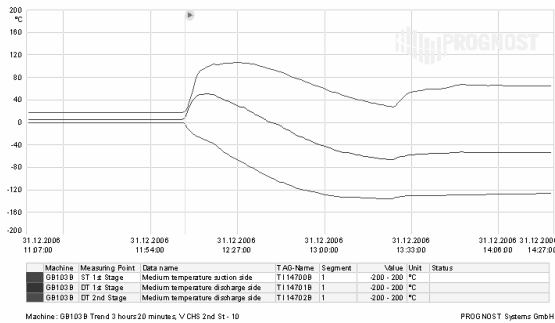


Figure 21: Gas temperatures after start up

During the cool down of the arms, the gas that is going through is directly from ship manifold and is usually a warm gas. This gas has to be tempered with pure LNG spray to achieve a lower inlet gas temperature. But when the ship lines are getting colder the gas coming through is colder and the climate system has to be stopped.

4 Conclusion

Previously, the condition monitoring systems ensured the flawless, safe and reliable operation of both reciprocating boil-off gas compressors. Hence, the operator could count on 100% services.

Due to the increasing LNG traffic at the BBG terminal (see Figure 2) and a higher capacity utilisation, the two boil-off gas compressors have completed 6350 operating hours since the installation of the PROGNOST-NT System in May 2006 (GB103A 2686 h, 46 %, GB103B 3664 h, 62 % in operation).

This growth in business has turned the boil-off gas compressors into critical equipment and qualifies them for protection and online condition monitoring. The growth in LNG business will continue and therefore turn more and more boil-off gas compressors into critical equipment, that previously were not considered critical and have not been equipped with a specialised protection, performance and condition monitoring system.

This is especially valid for terminals with onshore storage tanks that will require almost a permanent compressor operation - not only during offloading. Hence the level of protection and monitoring needs to be evaluated and questioned in many cases to ensure the mechanical safety, minimize the duration of shutdowns and improve the overall level of availability and reliability.

This paper shows that boil-off gas compressors can be equipped with monitoring sensors using special modifications at the machine to receive qualified readings for the condition evaluation.

In order to consider of the various compressor operating conditions and to differentiate between operational-dependent and failure-dependent changes in data, individual warning thresholds for each load step need to be available. This helps the operator to detect failures at an early stage and avoids false and unplanned shutdowns.

Therefore, the monitoring system is an important tool to reach the goal of unloading three LNG carriers per week.



MACHINERY ANALYSIS

Dynamic Analysis of Reciprocating Compressors on FPSO Topside Modules

by:

Eberle, Kelly and Harper, Chris

Engineering Design

Beta Machinery Analysis

Calgary

Canada

keberle@betamachinery.com charper@betamachinery.com

**5th Conference of the EFRC
March 21-23, 2007
Prague, Czech Republic**

Abstract:

A growing number of reciprocating compressors are being used on Floating Production Storage and Offloading vessels (FPSO) for many applications. These compressors are significant sources of vibratory forces and can cause high vibrations of the compressors and FPSO module, resulting in costly and premature machine failures as well as safety concerns to operators in work areas. Owners and engineering companies often require a dynamic analysis of the production structure when high horsepower reciprocating compressors are employed to mitigate these issues.

Based on our experience with over 60 offshore reciprocating projects, this paper discusses new analysis techniques to calculate the amplitude and location of high vibrations on the module deck and to optimize the topside module design. An example is included that reviews an integrated design approach, combining the topside module structural model with the mechanical model of the compressor packages. A summary of the recommended specifications for performing dynamic analysis studies is included. This paper includes examples from recent projects, including a large FPSO project where three compressor packages were mounted on the topside module.



1 Introduction

Reciprocating compressors serve a number of purposes on offshore petroleum facilities, such as Floating Production Shipping and Offloading (FPSO) vessels. These compressors range from small vapour recovery compressors – typically 500 HP (370 kW) – to large, multi-stage compressors used in high pressure injection service that can be over 3000 HP (2240 kW). The reciprocating compressor, driver (engine or motor), piping, scrubbers, and pulsation bottles are packaged as a unit and loaded onto the FPSO. While this paper highlights FPSOs, the principles discussed apply equally to other floating and fixed offshore installations.

Reciprocating compressors generate high dynamic forces due to the motion of the mechanical components inside the compressor during delivery of gas to the system.

The dynamic forces, as shown in Figure 1, include:

- pressure pulsation induced forces
- mass unbalance
- crosshead forces
- gas force inside the compressor cylinder causing cylinder motion (cylinder stretch)
- misalignment

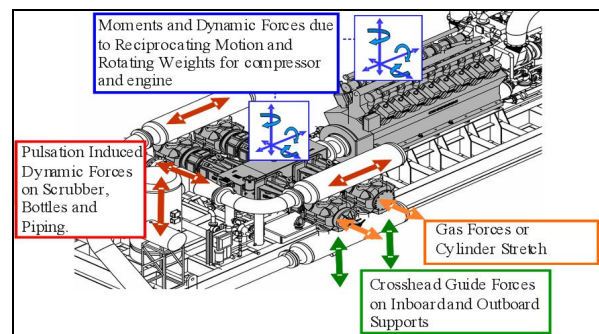


Figure 1: Dynamic Forces on Reciprocating Compressors

These forces can generate excessive vibrations on the piping, scrubbers, compressor frame, small bore attachments, compressor skid, and FPSO topside structure. Excessive vibration is the major cause of mechanical failures on reciprocating compressors.

Failures are costly and create safety concerns for operators. The offshore environment creates two other challenges for owners and operators:

- Repair and downtime costs have been estimated to be 4 to 5 times higher in offshore applications than most land based applications. This is due to the significant travel and logistic requirements. End users demand high reliability applications and can't afford vibration related problems.

- Space is at a premium on an FPSO or any offshore installation. The limited space requires a compact mechanical design for the piping, vessels, and heat exchangers. A compact design places more components close to the compressor. This means the layout is often complex and, therefore, compromises must be made between the support requirements, process requirements, access, and maintenance. As illustrated in Figure 2, this often results in a design that is more susceptible to vibration.

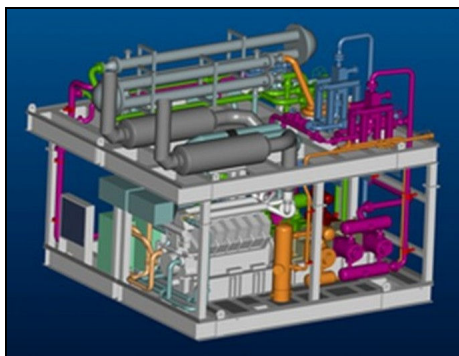


Figure 2: Compressor Module with Limited Space Results in Challenging Vibration Issues. (Courtesy of Universal Compression, Mustang, Chevron)

The purpose of this paper is to:

- Discuss what is included in a dynamic analysis and when it should be performed.
- Use actual case studies to illustrate methods that integrate the dynamic analysis with other project requirements to ensure the most cost effective solution.
- Describe challenges with vibration guidelines for offshore applications
- Give recommendations for specifying dynamic analysis studies

2 Dynamic Structural Analysis - Overview

Owners, engineering companies, and compressor packagers contract machinery consultants to perform studies on the reciprocating compressor package to mitigate vibration issues. A summary of the typical design studies is given in Figure 3.

Some studies are recommended in API 618 4th edition (and the upcoming 5th edition) and are designated below by their “M” nomenclature. Others are specific to the package and its application.

Design Studies For Reciprocating Compressor Packages on FPSO and Offshore Platforms

- **Pulsation Analysis (M2):** assesses pulsations and unbalanced forces. Recommends solutions to control pulsation induced forces.
- **Compressor Performance Analysis (M3):** determines performance, pressure drop, and capacity, for the recommended pulsation control design.
- **Mechanical Analysis (M4, M5, M6, M7, M8):** calculates Mechanical Natural Frequency (MNF) of piping and cylinders, detunes mechanical design to avoid resonance, predicts vibration and stress in critical areas of piping, cylinders, and bottle internals. Gives recommendations to avoid vibration on the compressor package.
- **Piping Flexibility (M11):** determines piping system flexibility for cooler nozzle loads and piping stress due to thermal cycles, pipe weights, and bolt up strain effects (for coolers mounted off skid). *Note: API 5th edition will require the same consulting firm to complete both the Mechanical Analysis and Piping Flexibility studies.*
- **Torsional Vibration Analysis:** assesses crankshaft and coupling design, evaluates torsional stress for all operating conditions.
- **Skid Analysis:** consists of two components: (1) lifting and design review; (2) quasi-static analysis to assess loads due to transportation, ship motion, and wind during normal operation, storm condition, and blast conditions.
- **Dynamic Structural Analysis:** analysis of the topside structure or production deck structure with the reciprocating compressor package compressor structure to identify areas of high vibration due to dynamic loads from the reciprocating compressor.

Figure 3: Design Studies For Reciprocating Compressor Packages on FPSO and Offshore Platforms

A Dynamic Structural Analysis study (last study listed in Figure 3) is not unique to offshore applications and is sometimes conducted for land based systems. The scope of the analysis is somewhat different for land based systems as compared to an offshore unit, however the principles of the design process are similar.

Reciprocating compressors are mounted on a network of trusses and beams, called topside structures, deck structure, module, or “pancake” on FPSOs and platforms. These structures can be designed by the structural engineer to withstand the static and quasi-static loads using common practices.

Designing the structure to withstand dynamic loads requires special consideration. The dynamic analysis must accurately determine if there are any structural resonances and calculate the expected vibrations. Resonance occurs when a Mechanical Natural Frequency (MNF) of the structure occurs at the same frequency as the dynamic forces described earlier.

The goal of this analysis is to evaluate the response of the skid and the topside structure to the equipment’s dynamic loads and provide recommendations to ensure vibrations are below guidelines.

The Dynamic Structural Analysis also includes:

- Evaluation of dynamic forces for all planned operating conditions. Note that focusing on the *perceived* worst case conditions is a short-cut that can miss actual worst case conditions. The changes in force amplitude and phase at different frequencies must be evaluated.
- Assessment of the interaction between multiple compressor units. The model should assess if the compressor units amplify the vibrations under specific conditions.
- Consideration of the FPSO deck dynamic stiffness at each module mounting location (stabbing point).
- Expanding the scope to include evaluations of the driver dynamic loads. The dynamic loads from a motor are typically low and can be ignored. The dynamic loads from any engine may be sufficient to cause vibration which, when added to the response from the compressor, could be over guideline.

3 Who Specifies a Dynamic Analysis? When is it Required?

Engineering consultants are typically responsible for design of the topside structure. The design often includes consideration of the static and quasi-static loads imposed on the structure by equipment

mounted on the structure. The supply and design of this equipment is typically contracted to other parties by the engineering consultant doing the topside structure design.

The reciprocating compressor package is typically contracted to a provider of gas compression equipment that designs and constructs a unit to meet the required performance. The compressor packager is often held responsible for ensuring the dynamic response of the compressor package is acceptable. Holding the compressor packager up to this responsibility is, in many ways, unrealistic.

Typically, the reciprocating compressor package, such as seen in Figure 4, is designed to ensure that dynamic forces and the resulting response will be controlled to some reasonable level assuming that the package support (or foundation) will provide some restraint. It is possible to design a very robust reciprocating compressor package that requires minimal support from the topside structure, however the design of the compressor package may be very costly. The connections between the compressor package and the topside structure will still have some effect on the package response that could make the robust design ineffective. Alternatively, the compressor packager could design a relatively light-weight package that would require a stiff topside structure to control the dynamic response. The technically correct approach, and often most cost effective approach, for conducting the structural dynamic analysis is to conduct an overall or combined dynamic analysis of the compressor package dynamics and topside structure dynamics.



Figure 4: Example of Reciprocating Compressor on FPSO. Dynamic analysis of compressor forces on FPSO structure requires coordination between Machinery Consultant, Packager, and Engineering Consultant

A third party Machinery Consultant is often contracted to conduct this overall dynamic analysis and make recommendations for the reciprocating compressor package design, topside structure design, and the connection between the two components. The dynamic analysis requires an intimate understanding of the reciprocating compressor dynamic loads that the topside structure Engineering Consultant and/or Compressor Packager generally do not have. Specialized modelling techniques are also required to accurately calculate the dynamic response.

The dynamic analysis of the reciprocating compressor package involves simulation of a lot of details in the compressor package design. The loads in the compressor must be calculated for a range of operating conditions.

The forces acting on pulsation bottles and scrubbers from pressure pulsations must be calculated. The mechanical characteristics of the compressor frame, cylinders, pulsation bottles, scrubbers and other equipment must be included. All of these details will be, or may already have been, included in the mechanical study of the compressor package (API 618 studies). There are technical and commercial benefits to the owner, or end user, and engineering consultant from having one machinery engineering firm complete all dynamic analysis and pulsation studies on the reciprocating compressor package. It is beneficial to contract the dynamic analysis to a machinery engineering firm that specializes in dynamic analysis, which is typically the same firm that assesses the pulsation and dynamic analysis for compressor package (API 618) and skid design.

The decision to specify a dynamic analysis is ultimately based on a risk assessment of the application. The following attributes are useful for quantifying the risk:

- How critical is the application? What are the consequences (costs) associated with downtime and field modifications to the structural elements in an FPSO or platform?
- What is the size of the reciprocating compressor? Generally the larger the power requirement per compressor throw, the higher the dynamic forces will be:
 - 500 HP (370 kW) per throw is a high risk
 - < 200 HP (150 kW) per throw is a low risk

- How many reciprocating compressors are on each module?
 - 1 unit: low to moderate risk
 - >1 unit: high risk
- Is the reciprocating compressor fixed speed or variable speed? If the compressor operates at a single speed it is easier to detune structural MNFs away from resonance. Variable speed packages are a much higher concern for vibration due to risk of resonance.

4 Vibration Guidelines for Structural Dynamic Analysis

One basic criterion to assess the acceptability of the structural dynamics is vibration. Guidelines have been developed by many different organizations to ensure the health and safety of personnel as well as protect equipment from premature failure. Health and Safety Executive Offshore Technology Report 2001-068⁽¹⁾ gives general vibration guidelines for machinery and personnel. Other organizations such as ISO, DNV, ABS also have guidelines for vibration.

All reciprocating compressor manufacturers, motor manufacturers, and engine manufacturers have vibration guidelines, or vibration limits, to protect their equipment. Typical guidelines include a vibration amplitude specified at the crankshaft centerline in the horizontal, and sometimes vertical, direction. Some engine manufacturers include overall vibration guidelines in addition to frequency based guidelines. Note that vibration limits for shut-down of equipment that are specified by manufacturers should not be used as design guidelines.

Owners, operators, and engineering consultants may have their own vibration guidelines based upon their experience and specific requirements. Beta Machinery Analysis (Beta) has developed vibration guidelines for all aspects of evaluating reciprocating compressor installations. Figure 5 shows Beta's guidelines for piping, vessels, and compressor cylinders.

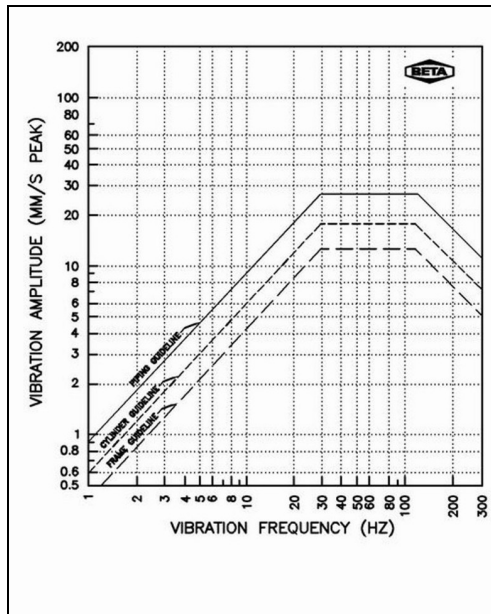


Figure 5: Vibration Guideline Chart for High Speed Reciprocating Compressors

A vibration guideline should be used as a guide to assess a design regardless of what vibration guideline is specified. The vibration guideline may be too stringent in some specific applications and it is acceptable to exceed the guidelines. In other cases, vibrations may be within guidelines but the resulting design is not able to tolerate the vibration. Vibrations should be used as a screening tool to assess the design; and closer inspection of the operating deflected shape should be done to determine if the vibrations are acceptable or not.

Consider the example shown in Figure 6. The figure shows a simplified cross-section of a compressor frame and skid. A typical vibration guideline for a high speed reciprocating compressor is 0.5 ips pk (13 mm/s pk) at the crankshaft centreline. A typical vibration guideline for skid vibration is 0.1 ips pk (2.5 mm/s pk). The vibrations shown in Cases 1 and 2 are within guidelines. Inspection of the direction of the vibration (or operating deflected shape) shows that the vibrations are in-phase for Case 1 and out-of-phase for Case 2.

The vibrations for Case 2 are judged to be excessive and corrective actions are required.

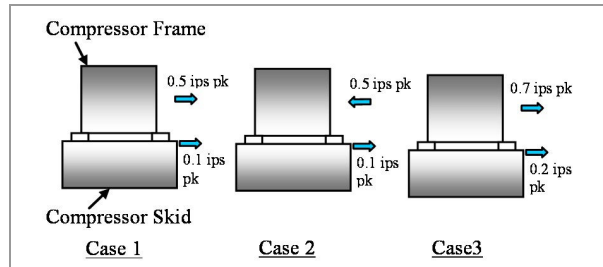


Figure 6: Schematic of Compressor Frame and Skid Operating Deflected Shapes

The vibration shown in Case 3 may, on first inspection, obviously require corrective actions. However as is shown by the operating deflected shape, the relative vibration between the base and centreline of the compressor frame is 0.5 ips pk (13 mm/s pk), which is within guideline. The skid vibration exceeds the design guideline of 0.1 ips pk (2.5 mm/s pk) and further analysis may be required to determine if the skid vibration is acceptable.

The issue of vibration guidelines gets more complex when there are multiple compressors on a common topside structure and the compressors are close to each other, such as the installation shown in Figure 7.



Figure 7: FPSO Design for Two 1000HP (746kW) Compressor Units on a Common Topside Structure

The vibrations from multiple units in close proximity will interact with other. The phase relationship between the two (or more) units will change with each start-up in the case of synchronous motor drive compressors, or be continuously varying in the case of induction motor drive or engine drive systems.

A single forced response assuming a fixed phase relationship between the compressors may not necessarily determine the worst case condition. The conservative design approach is to conduct a separate analysis for each compressor package assuming it is the only unit operating and calculate a scalar addition of the vibrations from the separate simulations. An alternative approach for synchronous motor drive systems is varying the phase angle between the units in fixed increments and calculating the vector addition of vibrations at all locations to determine the worst case phase relationship. This step-wise analysis may need to be repeated if structural modifications are made to the module as modifications will change how the vibrations from the multiple units will add.

As with all engineering decisions, there are trade-offs to be made for selecting one guideline over another. A more stringent guideline will generally require more design effort, higher capital cost for material and labour to install additional structural components, and increased weight which can be a significant factor in some offshore applications. A too lenient vibration guideline could result in excessive maintenance due to premature failure of running components. Careful evaluation of the results from the dynamic analysis is necessary to balance these issues along with the vibration guideline.

There are other guidelines that can be specified for the dynamic analysis of reciprocating compressor installations on FPSOs or platforms. There are guidelines to avoid resonance which specify an interval between structural MNFs and frequencies of dynamic loads, typically 10% to 25%. A dynamic analysis and vibration guideline supersede this resonance guideline as the dynamic analysis calculates the vibration at resonance.

Stress guidelines and fatigue can sometimes be expressed as a design consideration for reciprocating compressor installations. API 618 Analysis M6 addresses dynamic stress from the dynamic loads that cause vibration of piping and vessels. Dynamic stress and fatigue in the topside structure are not typically an issue. The dynamic stress in the topside structural members is typically very small if the vibration guideline is met. The dynamic stress is typically well below fatigue criterion as specified by Maddox² and others.

5 Modelling Recommendations

The dynamic analysis of the compressor package and topside structure is done using finite element analysis (FEA). The accuracy of the FEA depends in large part on the accuracy of the finite element model. Accuracy of the model refers to not only dimensional accuracy but also using the proper mathematical formulations to accurately simulate the physical behaviour. Accurately simulating the dynamic response of a reciprocating compressor package and topside structure requires different modelling techniques than are typically used for static and quasi-static simulations.

5.1 Model Mesh Size

FEA involves breaking a structure into a series of smaller pieces (called elements) that can be mathematically solved to determine the overall structural response. The number and distribution of elements is referred to as the mesh size. It is typical for the engineering company conducting the structural analysis to evaluate the quasi-static response using a structural analysis program (STAAD, SACS, others). The structural model uses beam-type elements to model the structure using a single element between joints or connections within the structure, a mesh size of 1. This mesh size will give accurate results for static loads and deflections however a finer mesh (more elements) are required to accurately calculate the dynamic response. Typically a mesh size of 2 to 4 is recommended to accurately calculate the dynamic response, particularly for higher order modes. Figure 8 shows images of a portal frame finite element model showing different element meshes.

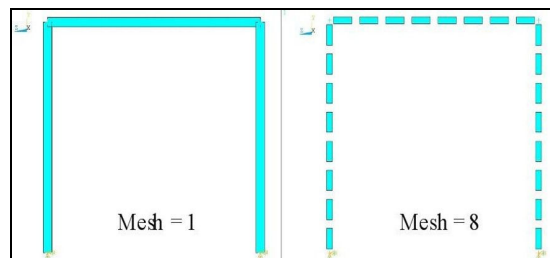


Figure 8: Finite Element Model of a Portal Frame

5.2 Mass Model

The way that the element mass is represented can also have a significant effect on the dynamic analysis results whereas the static results analysis results are typically not as sensitive to the element mass representation. Many finite element codes use a lumped mass approximation to simulate the beam weight. This means that the element weight is treated as 2 lumped weights at the ends of the beam. This can be an over-simplified model of the element mass, particularly for dynamic studies, that can introduce errors into the simulation results. Other finite element codes have an option to use a distributed mass element model. The distributed mass model is generally more accurate for dynamic analysis with a coarser mesh size compared to a lumped mass model.

Figure 9 and 10 show the effects of the mesh size and element mass properties on the calculated modal response and static response for the simple portal frame model shown in Figure 8.

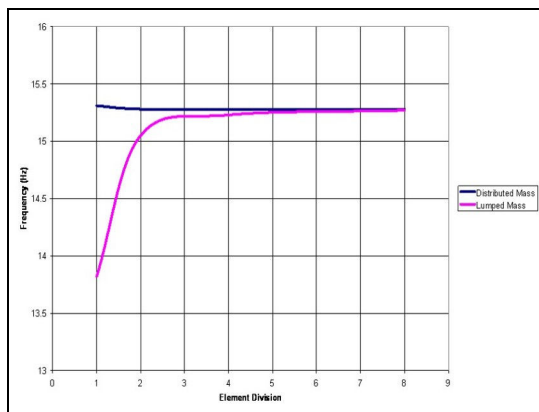


Figure 9: Effect of Mesh Size and Element Mass Formulation on the Calculated Mechanical Natural Frequency of a Portal Frame

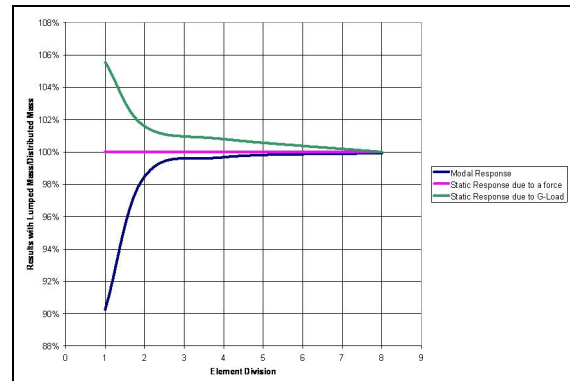


Figure 10: Effect of Mesh Size and Element Formulation Considering Different Loads and Analysis Types

5.3 Beam Element Warping

Another limitation in some finite element codes is that the beam elements do not have a warping degree-of-freedom. The warping degree-of-freedom controls the torsional response of the beams. A common method of modelling additional weight on a structure is to add several point masses on the deck beams. The point masses on the deck beams can result in spurious modes of the structure if the warping degree of freedom is not taken into account.

5.4 Reciprocating Compressor Package Model

The reciprocating compressor package must be modelled in sufficient detail so that the dynamic characteristics of the package are captured. The compressor package is sometimes represented as a single plate element or a simple frame of beam elements. These models are an overly simplistic model of the compressor package. The stiffness and mass characteristics of the package must be modelled so that the bending mode(s) of the compressor skid will be accurately calculated. The distributed weight effect of the compressor skid must also be included.

Many different methods can be used for connecting the reciprocating compressor package to the deck as long as proper analysis and design is done to ensure the dynamic response will be acceptable. The most common method of connection is welding the compressor skid to the deck beams. However, other methods such as antivibration mounts, gimbels, or stiff weldments at specific locations have also been used depending upon the application.

Accurate modelling of the connection is key to calculating accurate results. Modelling a rigid point-to-point link between the compressor skid and the deck can, in some cases, concentrate loads when in reality the loads will be dispersed. Also, the connection model can add stiffness to the structure that will not in reality be there.

Accurate simulation of the compressor package and topside structure requires that the mass of the components mounted on the module are included. One method of simulating the effect of these components is by using a point mass at the centre of gravity of the component. This model of the component weight will accurately simulate the translational inertia effects of the component. There are often dynamic motions of the compressor package or topside structure that involve a strong rotational response of the component. Therefore, the rotational inertia of large components must be included. The rotational inertia can be included by specifying the properties in the point mass properties at the centre of gravity, or simulating the mass distribution of the component. One challenge to the analyst is estimating the rotational inertia as this data may not be available from the manufacturer. Testing can be done on components in the compressor packager's fabrication facility to estimate the rotational inertia.

Some of the highest loads in a typical reciprocating compressor are unbalanced forces and couples from the reciprocating and rotating components in the compressor. These forces and couples are caused by the offset between the opposed compressor throws and the fact that the opposed throws are never perfectly balanced. One perceived advantage of 6 throw compressors is that because of the phase difference between the throws, the residual unbalanced forces and couples from each throw cancel and the resulting unbalance is very low. This cancellation of forces is based on the assumption that the compressor frame and crankshaft are rigid. Detailed finite element modelling of the reciprocating compressor shows that the compressor frame is not rigid (see Figure 11). The compressor frame deflection due to the loads within the compressor frame can have a significant effect on the dynamic response of the compressor package and topside structure. A detailed model of the reciprocating compressor, be it a 2 throw, 4 throw, or 6 throw, may be necessary to conduct an accurate dynamic analysis.

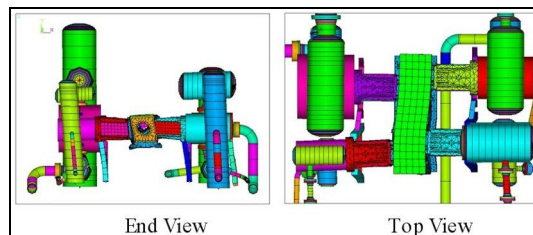


Figure 11: Four Throw Reciprocating Compressor Showing Frame Distortion Due to Normal Compressor Dynamic Loads

6. Case Study

The following is a case study that illustrates the example of the dynamic analysis of reciprocating compressors on a FPSO.

The dynamic analysis included simulation of a single module on which three reciprocating compressors are mounted. The reciprocating compressors include:

- Two x MP compressors, 6 throw, four stage operation, 9.3 bar to 208 bar, 4815 HP (3590 kW), 718 RPM
- One x HP compressor, 2 throw, single stage operating, 205 bar to 286 bar, 915 HP (680 kW), 890 RPM

The three compressor packages were mounted on one module to allow for fabrication of the module and installation of the compressors on the dockside. The compressor packages and module were then lifted and installed as a single unit on the ship. The module also includes a central pipe rack and several process vessels.

A finite element model of the reciprocating compressor packages and topside structure was created with a commercial FEA program called ANSYS. The structural components were simulated in most part with beam elements. Shell elements were used for plate structures. The engineering consultant provided the model of the topside structure that was used for the quasi-static and lifting analysis. The model was created using the STAAD structural analysis software and converted to an ANSYS format by a custom translator created by the authors' company. Figure 12 shows plots of the finite element model of the module and reciprocating compressor packages.

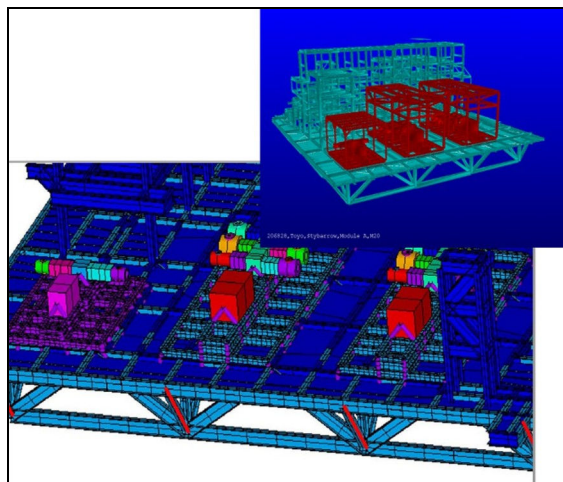


Figure 12: Images of the Module Finite Element Model

The dynamic loads in the reciprocating compressor as well as the unbalanced forces from pressure pulsations in the piping and vessels were calculated and applied to the finite element model. Post-processing software routines were used to extract and interpret results from the simulations.

Results from the dynamic analysis showed several areas with vibrations over the design guideline. Figure 13 illustrates typical results of the module dynamic analysis highlighting areas of high vibration. The module deck vibration design guideline was a particularly restrictive guideline, approximately 50% of Beta's standard guideline. Three different modifications were proposed to reduce vibrations to acceptable level.

- Diagonal bracing to stiffen the cantilevered edge around module.
- Diagonal bracing to stiffen the top deck underneath the compressor.
- Increased beam sizes in selected locations (near edges of compressor).

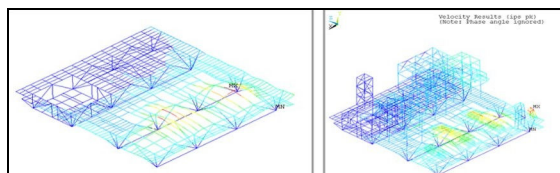


Figure 13: Dynamic Analysis Results for a Module Supporting Multiple Compressor Packages. Areas of yellow and red indicate marginal to high (over guideline) vibration.

The final design included a combination of the various modifications. Also, although the module deck vibration guideline could not be met in all locations, the design was considered acceptable. The dynamic stress was found to be well within guidelines and the areas with vibrations over the design guideline were restricted to a very small area of the module and were not significant. The calculated vibration was a conservative estimate, as the vibration from all units were combined in a worst case. Vibrations will likely be lower for much of the compressor operation. It should be noted that some compromise between the module design and the vibration guidelines is sometimes necessary because of the limitations in the modifications that can be made to the module. Input by the engineering consultant doing the dynamic analysis early in the project is key to minimizing vibrations.

Some basic considerations such as location of the reciprocating compressor packages relative to the module main structural members and support columns to the ship web frame can have a significant impact on the dynamic response. Often these design decisions are made at an early stage before the machinery consultant is involved.

7. Recommendations for Specifying Dynamic Analysis Studies

The following recommendations are made for specifying dynamic analysis studies of reciprocating compressor on FPSO topside modules:

- The dynamic analysis must be conducted by an engineering firm with specialized knowledge of the reciprocating compressor dynamics. The analysis must include detailed dynamic simulation of the reciprocating compressor and the topside module.
- It is important for stakeholders to meet and agree on scope, methodology, and guidelines early in the design process. Stakeholders include owner, engineering consultant(s), and compressor packager.
- The design of the reciprocating compressor package and the topside structure should be conducted in parallel so that an optimal design can be determined to minimize the dynamic response.

- We recommend that the engineering firm that conducts the topside dynamic analysis also conducts the detailed reciprocating compressor dynamic studies that are applicable (API 618 studies). This approach will minimize engineering time and avoid conflicts in the compressor package design, vibration limits, and design recommendations.
- The engineering consultant conducting the detailed design of the topside structure for static and quasi-static loads should supply the computer model to the consultant conducting the dynamic analysis. This significantly reduces the amount of work and end user costs for the dynamic analysis.
- Details of the dynamic analysis must include:
 - The dynamic loads that include the unbalanced forces and moments, crosshead guide forces, gas rod load forces, pulsation induced forces in key piping and vessels, and unbalanced forces in the motor or engine.
 - Simulation results at the first and second orders of compressor speed as dynamic loads are the highest at these frequencies. Analysis at higher orders of compressor speed may be necessary in some cases such as an engine drive or where significant acoustical forces exist.
 - Calculated vibration on the structure, compressor skid, and major components mounted on the compressor package such as the compressor frame, compressor cylinder, drive, and major vessels. The calculated vibrations will be compared to industry guidelines for the different components.
 - A topside finite element model that includes a representative stiffness for the ship deck and web frame at the topside structure's stabbing points.
 - A final report that includes recommendations for the reciprocating compressor package design and/or topside structure design as well as a summary of the applied loads and results (calculated mode shapes, mechanical natural frequencies and vibration amplitudes).

8 Summary

A growing number of reciprocating compressors are being installed in offshore applications. Owners and engineering companies should consider a dynamic analysis of the production structure when high power reciprocating compressors are employed (i.e., over 500 HP (370 kW)). The paper outlines recommended specifications to include in tender documents and other tips to improve the design, construction, and long term operation of reciprocating compressor packages for offshore applications.

References

1. Safety Executive Offshore Technology Report 2001-068, pp 10-13
2. Maddox, S.J.: 'Fatigue Strength of Welded Structures' 2nd Edition, Abington Publishing, Cambridge, 1991



LARGE RECIPROCATING COMPRESSORS ON FPSO's

by:

Graham Gilkison
Director – Mechanical Engineering
ITL
New Plymouth
New Zealand
graham@itnz.co.nz

Stephen Rowntree
Director – Compression Technology
Flotech
Stockholm
Sweden
steve.rowntree@flotech.com

5th Conference of the EFRC
March 21-23, 2007
Prague, Czech Republic

Abstract

This paper reviews aspects of design and operation specific to Floating Production Storage and Offloading (FPSO) applications.

A comparison is made with the performance of centrifugal compressors for this application.

The dynamics of the marketplace are discussed, and this is referenced to current trends in specification for reciprocating compressor packages.

The purpose of this paper is to identify specific areas where improvements are needed by the reciprocating compressor industry.

1.0 Introduction

FPSO's have become a preferred solution for offshore oil and gas developments over the last decade. FPSO's are a cost effective alternative to offshore fixed platforms, particularly when the oil-field is a long way from shore. Problems have been experienced with the operation and maintenance of large reciprocating compressors on FPSO's. The cost to fix problems is high due to the remote location and due to the impact of production.

Lower life cycle costs occur with improved reliability.

This paper attempts to provide an upper level guide to good practices for the facilities design of large reciprocating compressors on FPSO's.

2.0 Overview

2.1 Why are FPSO's Different?

FPSO's are floating, and therefore are subjected to wave motion and hull deflections.

Gas flows and pressures on FPSO's are typically very high, and the application normally pushes the limits of commercially available compressor frames, which are typically multi-unit applications.

The compressors are typically mounted within a processing module, which is positioned above and is connected to the deck of the ship. Stiffness of the supporting structure becomes critical. Vibration control is difficult due to elevated equipment and multi-levels.

Contained gas volumes are very small and therefore operating transients occur very quickly. The discharge pressure is typically in the range of 150 – 300 barg.

2.2 Centrifugal versus Reciprocating Compressors for FPSO's

FPSO's have large areas available for processing equipment and can accommodate large weights. (By comparison, reciprocating compressors are uncommon on fixed platforms due to the very high costs of space and weight.)

Reciprocating compressors:

- Typically less than 5 MW per unit.
- Often requires multi-units.
- Large and heavy.
- Vibration and pulsation control are critical.
- Good with variable molecular weights.
- Good where operating conditions may vary and turndown is required. (The oil production wells always behave differently than predicted.)
- Installed cost of reciprocating compressors is typically 75% of centrifugal compressors.

Centrifugal compressors:

- Economic centrifugals start at ~ 3MW, and get bigger from there.
- Requires single unit only.
- Compact and light weight.
- Noise contained within an acoustic box.
- The life life cycle cost is often lower due to higher availability and reliability.
- Centrifugal compressors are less tolerant to wave motion and bending of the support skid.
- Poor operational flexibility

Reciprocating compressors are often selected over centrifugal compressors on a cost basis.

2.3 Key Selection Parameters for FPSO's

The FPSO compressor duty commonly exceed the maximum power rating of a single reciprocating compressor.

A significant selection parameter is the number of compressors required for the duty, and the sparing philosophy of the Client.

There is an economic driver to select compressors that approach the manufacturer's design limit, where key design parameters are:

- Speed - There is acceptance in the industry that the lower the speed, the longer the compressor can operate between services. However, there is no definitive document that stipulates the allowable rotational or piston speed for a desired reliability. Instead, responsibility lies with the compressor manufacturer, where experience and a proven track record become the key factors.

SPECIAL TOPIC: FPSO

Large Reciprocating Compressor Packages on FPSOs, *Graham Gilkison, Stephen Rowntree; INDEPENDENT TECHNOLOGY*

- Rod Loading - Should be calculated for expected upset conditions, and must be within the manufacturer's rating.
- Frame Power Rating - not to exceed manufacturer's rating.
- Design Pressure - PSV set pressure not to exceed the manufacturer's cylinder pressure rating.
- Design Temperature - not to exceed manufacturer's rating.

The view of the writers is that safety margins should apply on all the key parameters mentioned above, and instances of non-compliance should be evaluated and agreed with the Client and the FPSO Owner.

Competitive tenders (without specific guidance within the tender documents) will lead to compressor selections with smaller (or non-existent) safety margins.

2.4 Reciprocating Compressor Codes

Two styles of code are used by the oil and gas industry:

- Moderate to low speed in critical service, designed and constructed for a minimum service life of 20 years and at least 3 years of uninterrupted operation (interruptions for the replacement of wearing parts that have exceeded their lifetime are exempted.) Refer to API 618 and ISO 13707.
- High speed compressors. Refer API 11P (withdrawn) and ISO 13631. Most compressors are supplied to this less demanding standard.

The codes were originally put in place so that:

- Compressors would not break

- Compressors would perform, without excessive shutdowns or vibration.

Since those early days, compressor manufacturers have implemented their own design features and taken advantage of technology advances and as a consequence are now departing from the historical codes. In the view of the writers, the codes have not kept up with the advances in the industry.

The industry however, continues to use these codes for strict compliance, without due consideration of the original intent of the codes or of technological advances.

2.5 Specifications

Typically one of two approaches are adopted by the Client:

- i) Very detailed specifications, processes, and procedures, or
- ii) Fit for purpose approach – typical where the Client does not wish to impose his very time-consuming and costly systems.

The industry tends to operate in one of these two ways. The writers believe that high quality, fit for purpose, and timely facility design and build can be achieved with an approach somewhere between these two approaches.

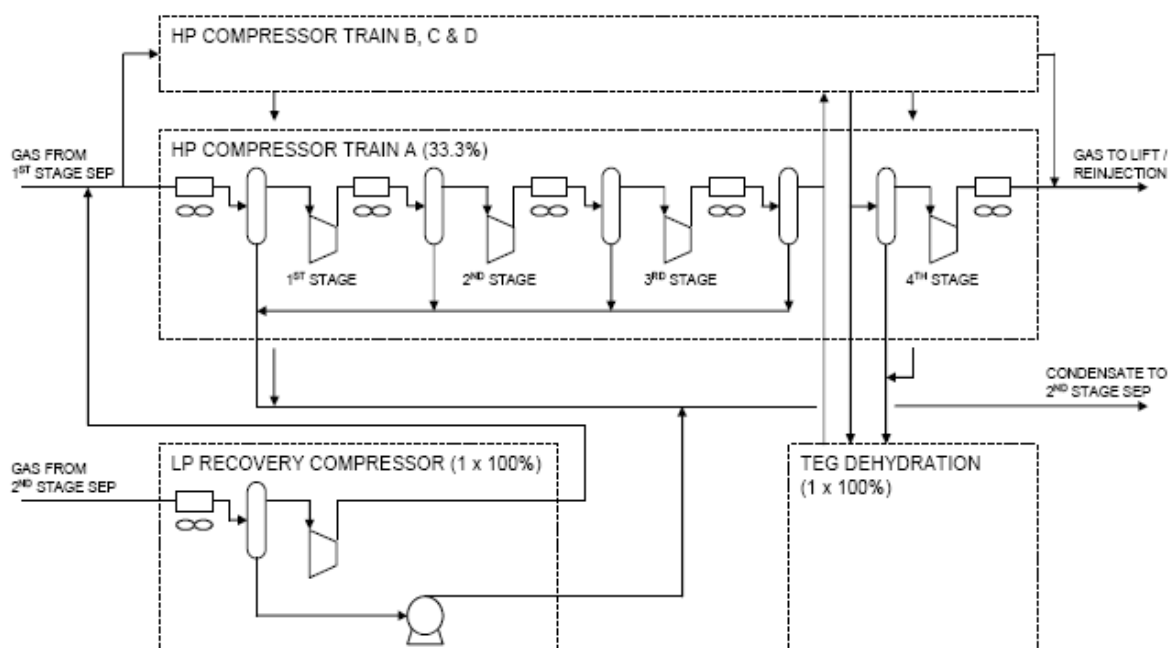
The writers support a collaborative approach between the Client, FPSO Owner, and the compressor packager/designer in order to tailor the equipment selection and specifications for each application.

3.0 FPSO Process Design

FPSO compressor applications tend to be very similar.

SPECIAL TOPIC: FPSO

Large Reciprocating Compressor Packages on FPSOs, *Graham Gilkison; INDEPENDENT TECHNOLOGY*



Typical Flow Diagram for Gas Lift / Reinjection Compression System

Gas flows from the production/test separators through to the compressor inlet. Outlet gas is typically for gaslift and/or reinjection.

Gas processing is provided at an interstage, common to all units. (Gas conditioning is often water removal only. ie. No hydrocarbon dew point control.)

The compressors must integrate into the overall process design.

4.0 Design Issues

4.1 Ship Integration

Single deck (pancake) or separate module.

The deck and connection stiffness needs to be designed to suit the dynamic requirements of the compressor skids.

Separate compressor modules simplify the dynamic design required of reciprocating compressors. Separate compressor modules allow the compressor packager to include the structural steel to the deck connections within their scope.

Separate compressor modules allow the compressor skid main structural steel to be integrated into the module design.

Pancake design allows the complete module to be built in the fabricators yard, and minimizes tie-ins.

The lift of the pancake onto the ship requires cranes with high lifting capacity.



Typical pancake design under Construction

Three point mount.

The purpose of a three point mount is to prevent bending and torsional stresses induced due to deck movement, and is typically a requirement of centrifugal compressors (which operate at high

speeds, have small tolerances, and can tolerate little bending).

In reciprocating service, three point mounts make vibration control very difficult and are therefore not recommended.

Equipment shaft orientation

Transverse mounting reduces stresses due to ship deflections.

Transverse mounting allows convenient piping tie-ins, with the pipe rack running lengthwise on the ship.

Lengthwise mounting reduces dynamic loads due to ship movement and minimises special motor and crankshaft bearing design. (Transverse movement is typically much less than longitudinal.)

Wave motion – liquid issues

Level instruments positioned in the bow-stern axis.

Liquid level measurement positions to allow for bow-stern movement.

Scrubbers to allow for transverse wave motion.

4.2 Compressor and Process Issues

Capacity control and recycle valve philosophy.

Is the compressor permitted to float on the inlet pressure?

How tightly must interstage pressures be contained?
Are recycle lines required around each stage?

Are separate startup and recycle valves required due to turndown?

Control valve sensitivity given the small gas volumes on FPSO's, and hence fast occurrence of transients.

Possible hydrate formation downstream of recycle valves.

Are the recycle valves fail open or fail closed?
If fail open, what is the settleout pressure, and what is the blowdown philosophy?

If fail closed, what is the blowdown capacity to prevent overpressure?

Integration of inlet separation, gas processing, gaslift, reinjection, flare system, and utilities.

Transient management.

PSV selection

Set point for overpressure and rod loading protection. Spring or pilot?

If pilot, regulating or snap?

Low temperature material selection?

4.3 Vibration and Pulsation Control

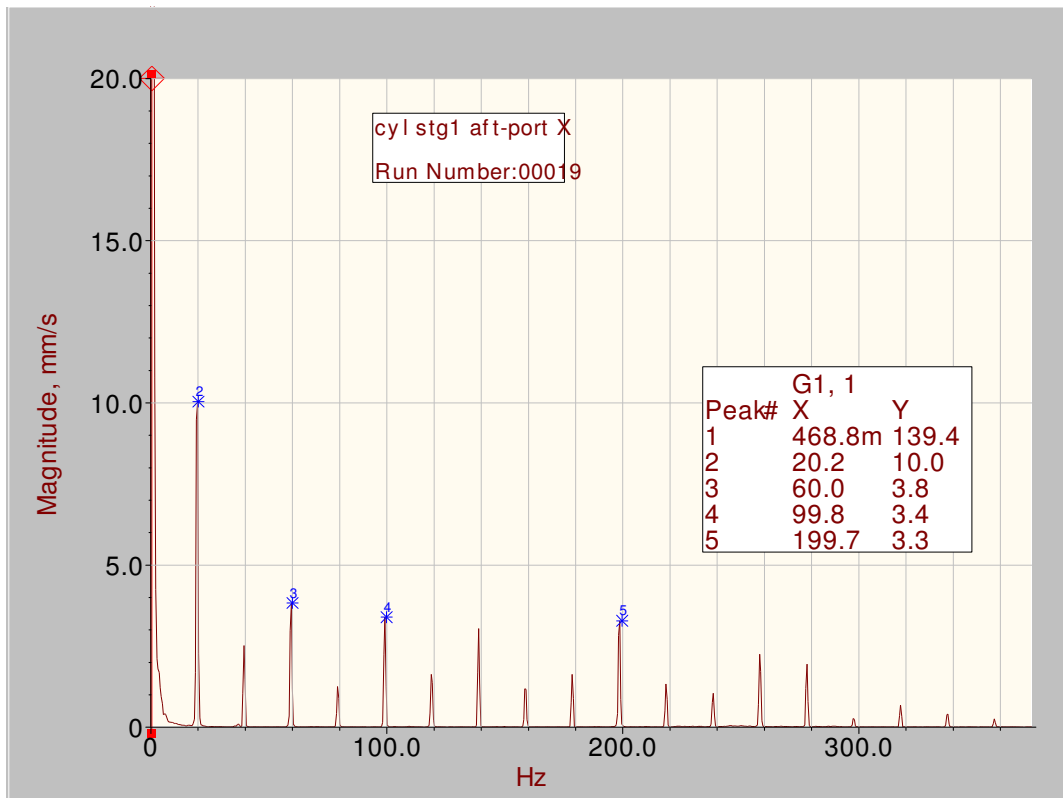
Small bore fittings.

One of the most common causes of piping failure is associated with vibrations on small bore fitting, and is an increased risk in FPSO applications.

High frequency excitation occurs at run speeds and multiples of runspeed due to gas loads. (Which is seen as movement at the end of the cylinder.)

The compression power of each cylinder in FPSO duty is high, and is typically 0.5 – 1.0 MW/cylinder.

The corresponding cylinder stretch occurs at runspeed and multiples of runspeed, with significant excitation at frequencies as high as 300 Hz.



Typical Cylinder Vibrations at Cylinder Outer-End - in direction of piston motion. (Vertical scale mm/s pk)

Separation of mechanical natural frequencies of small bore fitting from their excitation frequencies becomes difficult if not impossible as the frequency increases.

The excitation is localized to the suction and discharge bottles and the suction and discharge piping close to the bottles.

Small bore fittings should be avoided where possible in these vibration prone locations.

Where that is not possible, small bore fittings should be robust with minimum weight. (Consider monoflanges.)

Temperature transmitters should be located remote from the device to minimize weight.

Where risk exists that small bore fittings may have high vibrations, consider installing bracket connection points from the run pipe for future bracing.

Pulsation control strategy

Pulsation control should target less than half of API618 guideline levels on common piping systems.

This is because pulsations from several units feed into the common pipework and that the pipework itself is very difficult to support robustly due to the multi-levels.

Substantial pulsation control is also needed to cater for the unavoidable deadlegs created by recycle lines and PSV's. (Where the outlet of PSV's typically is required to slope into the flare header.) The deadleg length should also be set to avoid coincidence with excitation frequencies - but this is not always possible.

The pulsation control should reduce shaking forces in bottles and piping to low levels.

The typical European solution to dampener bottle design is to have no internals. The typical American solution is to apply acoustical filters. (Choke tubes.) The writers believe that properly sized and designed acoustical filters lead to superior pulsation control for high speed applications. (ie. Greater than 900 rpm.)

Vibration Control

Excitation is due to:

- Pulsation induced shaking forces. (These can be kept to very low levels by design.)
- Primary and secondary forces and moments. (These can be reduced to low levels by using 6-throw compressors or by using a fully balanced design.)
- Gas loads causing cylinder stretch.
- Gas loads causing vertical forces at the crosshead guide.

The significant and unavoidable excitation is gas-load related.

The dampener bottles are to be designed to avoid coincidence with runspeed and twice runspeed.

Given the need to reduce pulsations to very low levels, suction and discharge bottles are sometimes very large and require special supporting.

Cylinders also need to be well supported, and outboard cylinder supports should be considered.

A FEA analysis is required of the compressor skid including structural connections to the deck, as well as to the upper level(s). The FEA analysis should encompass mechanical natural frequency estimations, and once corrections have been made, excitations applied and vibration and stress amplitudes estimated.

Industry guidance should be provided in the way that FEA analyses are conducted. Many issues surround the FEA analyses:

- How accurate are boundary conditions required to be?
- When can boundary condition simplifications be made without substantially compromising the results?
- Is a manifold study required, and if so, to what level of detail?

The current situation is that specialists guard their modeling techniques on the basis of their methods being proprietary.

4.4 Liquid Issues

Water saturated gas through to gas conditioning. This is an issue for many compressors and not just FPSO's. The primary concern is the elimination of large liquid slugs to the cylinder. Secondary issues are corrosion and erosion control.

- The inlet gas should be cooled to ~30 degrees celsius or less in order to reduce the water holding capacity of the gas and to minimize condensation of the gas from ambient temperatures.
- The suction bottle should be designed for controlled low volume flow of liquid into the cylinder. (Note that liquid related failures typically occur during operation, not during startup.)
- API 618 requires the water temperature of water cooled cylinders to be above the inlet temperature of the gas – in order to prevent condensation.
- Consider pre-heating the gas downstream of separation. (This is not a common solution).
- Consider insulation and heat-trace of piping downstream of separation, for heat maintenance when the unit is off. (This is not a common requirement.)
- Piping to slope towards the 1st stage scrubber. (no pockets.) This is a common industry solution. However, if the pipe from scrubber to suction bottle is short, is most likely unnecessary.
- Where there are multi-units, inlet scrubbers should be sized for a liquid slug going to just one of the scrubbers.
- Line from cooler to next stage scrubber to be sloped. (no pockets).
- Recycle line to slope away from the valve on both inlet and outlet sides. Connection to run pipe to be off the top.
- Consider CFD analysis of scrubbers to minimize the risk of liquid bypass.

5.0 Conclusion

The reliability and availability of large reciprocating compressors on Floating Production, Storage, and Offloading facilities (FPSO's) is currently in need of improvement.

The reciprocating compression industry should consider producing a guideline document specifically for FPSO applications.

With careful selection and design higher reliability and operability can be achieved, while remaining competitive with centrifugal compressors.



Optimized MTBM with Model Based Online Diagnostics

by:

**Christian Koers
PROGNOST Systems GmbH
Rheine, Germany**

**5th Conference of the EFRC
March 21-23, 2007
Prague, Czech Republic**

Abstract:

Monitoring systems based on empirical or mathematical models have recently gained much popularity due to the ever increasing availability of computing power. Unlike traditional monitoring systems, that monitor the violation of some warning or alarm limits, such systems enable the detection of smallest deviations from a reference condition. Hence they are the ideal tool for wear monitoring and predictive maintenance. Other advantages are robustness under varying or transient operating conditions and virtually no limits on technical processes suited for monitoring. Drawbacks of monitoring systems based on empirical models are the need of a large number of measurements required for model training and the lack of quantitative information about ongoing wear processes. To overcome these disadvantages, empirical and conventional thermodynamic compressor modelling technologies have been merged. This results in a diagnostic system, that provides accurate information about the severity of a worn compared to a fully functional component and which is operational after just a short training period.

1 Introduction

Operators of rotating equipment are facing increasing cost pressure to produce efficiently and stay competitive. A key area where significant savings can be generated is by optimizing the meantime between maintenance (MTBM) of machinery. This is based on the principal that machinery operation time can be increased by utilizing current spare parts or by sourcing improved components. Successfully applying this strategy could lead to an increase of MTBM e.g. from 12 to 24 months. In any case the longest operating time between maintenance is determined by the component with the shortest lifecycle. In many cases, great improvements in terms of reliability have been achieved and the number of unscheduled shutdowns has been decreased. In most cases the applied maintenance interval of a machine depends only on a small number of components. Those components are mainly the cylinder sealing components e.g. suction/discharge valves, packings and piston rings. Hence, a precise and reliable online diagnosis of these components is a key element in assessing safe maximization of operating time.

2 Challenges in maintenance planning

The major prerequisite for accurate maintenance planning is a repeatable operating life of each relevant wear component. However, recent surveys show that only 11% of complex industrial machinery have a predictable lifecycle. 89% have an unpredictable MTBF behavior with the risk of random failures leading to unscheduled shutdowns increasing towards the end of the component lifecycle (see [MOU97]).

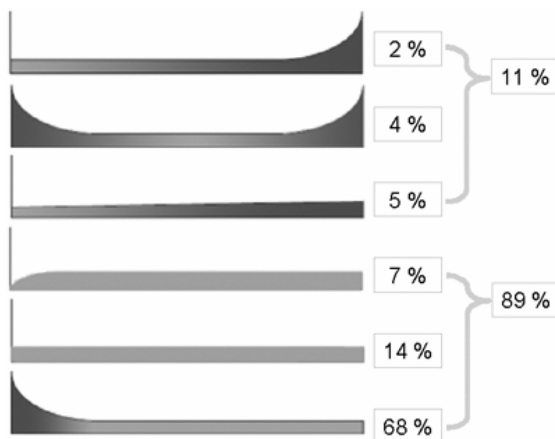


Figure 1: Failure Patterns

Until today, operators managed this inconstancy with mostly preventive maintenance routines selecting a conservative time between overhauls. However, the time based preventive exchange of components has its downsides leaving the potential lifecycle of the components unused and bearing the risk of "infant mortality".

3 Predictive maintenance

Hence it is very helpful to enable the maintenance personnel to predict the lifetime of the components. Prerequisite for predictive maintenance is the knowledge about the condition of the components, that are inaccessible under operation. Mobray [MOU97] describes, how the development strategies changed from "Reactive" via "Preventive" to "Predictive" within the last century. Today "Condition based maintenance" is supported by "On-line diagnosis". This makes the prediction of component damages much easier than in the past.

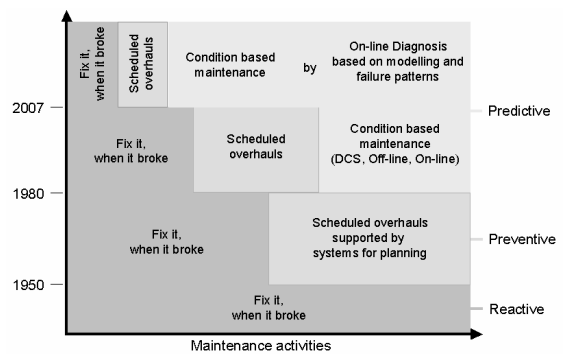


Figure 2: Maintenance Strategies

4 Monitoring of sealing elements

The majority of all machine stops are caused by the sealing elements like packings, valves and piston sealing rings. Consequently, it can be stated that these components have a strong influence on planning maintenance intervals. Failures of mechanical components e.g. crosshead or piston/rod-connections cause higher consequential costs and maintenance resources, but the probability of failures of these mechanical parts is comparatively low. If the operator's goal is an efficient increase of meantime between maintenance (MTBM), the monitoring of the above listed sealing elements is a promising way to go.

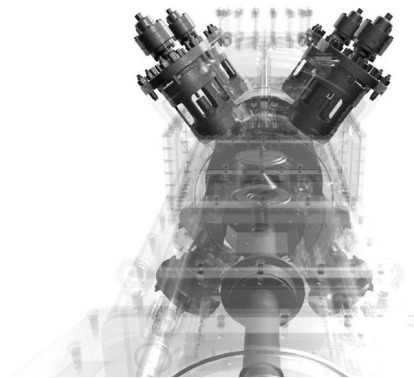


Figure 3: Sealing elements

5 Model Based Monitoring

The classic method of monitoring sealing elements consists of examining the measured signals by means of threshold monitoring for the presence of a damage. The threshold values are generally set in a way that false warnings are avoided as far as possible. As the signals vary considerably even in good condition as a result of changing operating conditions, the threshold values are usually set at some considerable distance from the actually measured values. It is known from sensitivity analyses, which have been carried out with compressor simulation models, that leaks, that cause the loss of several percent of the discharge flow, do only cause slight deviations in the temperatures and pressures typically measured at the compressor (see fig. 4). Consequently it is as a rule not possible to achieve the early detection of damages for predictive maintenance with classic threshold monitoring, while avoiding false alarms.

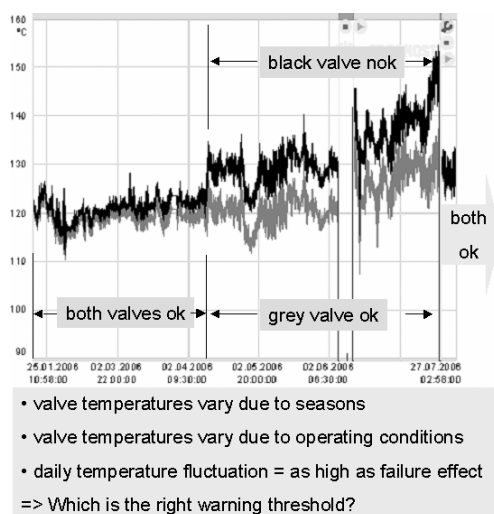


Figure 4: Valve temperatures of two discharge valves acting in the same stage

It is also well known in practice, when sealing elements leak there are almost always deviations in the remaining compressor stages, too. If there is no measurement of the indicated pressure available, the diagnosis of damage to sealing elements demands multivariate analysis, which includes the information from all the sensors for the purpose of diagnosis.

6 The use of process models

A significant improvement in the early detection of damages can be obtained by using a mathematical compressor model. Depending on operating conditions, the compressor model reflects the entire process in its reference state, which ideally represents the good condition of the compressor.

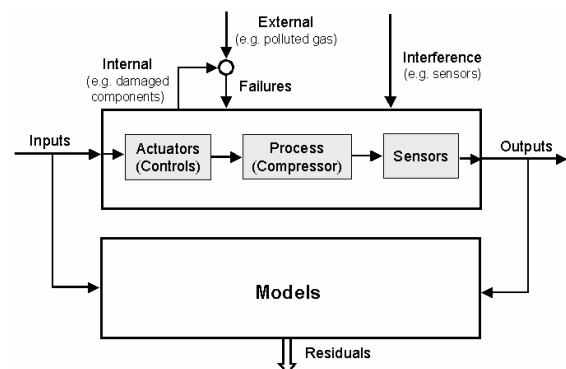


Figure 5: Principle of model based monitoring with a process model

If a damage occurs in the case of an adaptive model, the currently calculated model parameters deviate from the reference parameters ("parameter estimation method", [ISR94]). Disadvantages of this version include a lack of robustness under industrial conditions and long reaction times. If, on the other hand, a model is used that does not change over time, it is possible to derive a statement about the status of the compressor from the difference between measured and modeled output signals, known as residuals. This method, also called "parity equations", is robust and can be implemented with various types of process models. A few examples worth mentioning are:

Empirical, data-based models:

- Statistical, non-parametric: look-up tables, kernel regression
- Linear, dynamic, parametric: ARX, OE, ARMAX etc. (see [LJU99]), PCA
- Non linear, dynamic, parametric: Piecewise linear models, neural networks, neuro-fuzzy etc. (see [NEL00])

Theoretical models:

- Dynamic, parametric, linear: process transfer function
- Dynamic, non-linear: complex process simulation

If we disregard parameter adaptation, theoretical models offer the advantage of being able to detect damage immediately on startup. On the other hand it takes a lot of time and effort to model the entire process, including the actuators (e.g. by-passes, valve lifters) and the sensors, each of which represents a dynamic subsystem in itself, with adequate precision. In order to avoid having to go to this great effort, the concept presented in this article is based on empirical, data-supported models, i.e. process models calculated by means of system identification. In particular this approach can be used in order to represent the transient behavior of a compressor and of its sensors in a simple manner, by selecting a dynamic model type.

7 Combined application of an empirical process model with a thermodynamic model

Known disadvantages of empirical models include the high demand for training data and hence a long period of model training and the risk of "overfitting", particularly when applying complex model types (such as feed-forward networks). This phenomenon occurs when there is an inadequate volume of training data in comparison with the model parameters to be determined, or inadequate stimulation of the model as a result of too little variation in the operating condition. Overfitting can lead to faulty setpoint calculation when applied outside the learned operating range (extrapolation). In order to avoid these drawbacks, empirical modeling is supported by a theoretical compressor model, which is also used in diagnosis. As a first step, setpoints Y_{TM} are calculated for the measured signal by means of the theoretical compressor model.

Only the difference e_{TM} , which includes non-modeled components such as the influence of transient operation and, as a rule, an offset, is represented by the empirical model. The residual e is calculated from the difference between e_{TM} and \hat{e}_{TM} , and used for diagnosis.

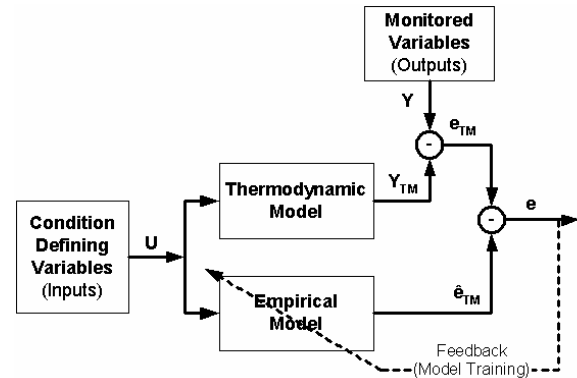


Figure 6: Combined application of a thermodynamical and an empirical process model for residual calculation

This preliminary use of the thermodynamic model permits the use of simpler model types with few free parameters, and thus shortens the period of training from several months to a few days or weeks.

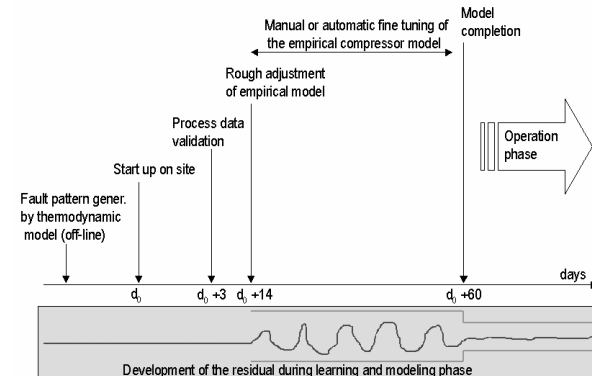


Figure 7: Learning and modeling phase

Modeling a compressor thermodynamically and empirically requires the following sensor signals:

Process data	Required per...
Condition defining values	
Suction gas temperature 1st stage	Machine (Process)
Gas cooler / Ambient temperature	Machine
Suction pressure 1st stage	Machine (Process)
Discharge pressure last stage	Machine (Process)
HydroCOM - regulation signal	Stage
Bypass regulation	Stage
Valve unloader	Compression chamber
Speed	Machine
Clearance pockets	Compression chamber
Gas side stream (inlet / outlet)	Stage
Gas composition	Process
Monitoring Values	
Valve temperatures	Valve
Interstage pressures	Stage

Figure 8: Mandatory field sensors

8 Fault pattern database

The residuals represent a multivariate set of diagnostic signals. If damages occur, just as in the case of the signal pattern shown in section (9), a residual pattern which is characteristic of the damage class and the severity of the damage, made up positive and negative values, becomes apparent. So the task in diagnosis is to deduce the damage from a given pattern. One very common option is to set up a fault pattern database by means of tests and/or damages that occurred previously, and to use this in operation. As a result of the very large number of wear components and the fact that crosshead compressors are usually one-off items, the use of the thermodynamic compressor model leads significantly more quickly to the establishment of the fault pattern database. The operating parameters are varied step by step, leaks in sealing elements are simulated for each set of operating parameters, and the calculated fault patterns are stored in a database. For performance reasons this is carried out once before startup of the diagnostic system. In routine operation the fault patterns are simply matched to the current operating condition by means of an efficient mathematical operation.

9 Diagnosis

To avoid false alarms, the residuals are not checked by means of a single threshold violation but by means of a sequential, statistical test concerning the threshold violations. If the threshold is exceeded for at least one of the residuals, the current values of all residuals are read out and passed on to the pattern-matching module.

Here a geometric/algebraic process is first used to determine a combination of individual faults from the faults database, which best matches the given residual pattern, either individually or in combination.

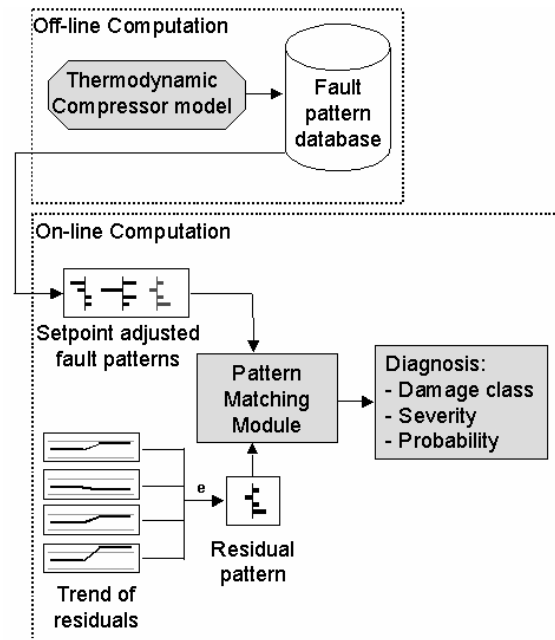


Figure 9: Setpoint adjusted fault patterns and computed residuals are compared. In case of a statistical match the fault is diagnosed

A statistical χ^2 test is used in a second step to examine the significance of the match. If the match is too poor, the output of the diagnosis is suppressed. This represents an additional mechanism to prevent false diagnoses.

10 Calculation of the damage severity

The severity of a diagnosed fault (S_{Fault}) is determined by the ratio of the calculated gas flow under standardized ambient conditions with and without a fault at the appropriate operating condition:

$$S_{Fault} = \left(1 - \frac{Q_{Fault}}{Q_{Ref}} \right) * 100\%$$

This standardization enables the operator to compare different fault classes with each other and to make decisions for maintenance.

The compressors modeled to date have shown that valve and gas cooler faults can be reliably diagnosed from a degree of 0.5 %, piston ring damage from approx. 1.5 % and packing damage from approx. 3 %. The latter damage can be diagnosed earlier by means of measurement and modeling of the leakage gas temperature.

11 Case study

The system was installed at 4 recip of a refinery in Germany in March 2006. The case study shows, how the failures of two discharge valves of the same stage developed over a period of 5 month. The machine compresses hydrogen in two stages and is driven by a speed controlled steam turbine. The following parameters are integrated through DCS link:

- all suction/discharge valve pocket temperatures
- all suction and discharge pressures of each stage
- suction and discharge gas temperatures of each stage
- cooling water / ambient temperature

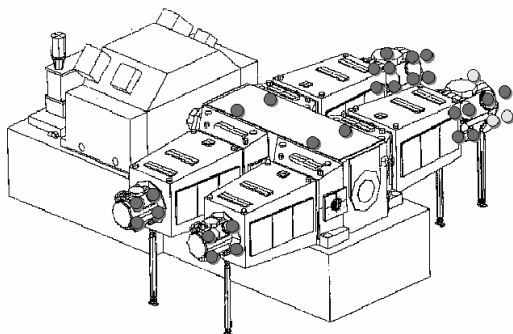


Figure 10: 4 cylinder hydrogen compressor

After a while the system indicated a problem at the discharge valves of the 1st stage west, head-end.

Diagnosis Status

Damage class detected

Current Damage Message

Damage class	Cylinder	Sev...	Probability
Damaged Discharge Valve, Head end	1.St. West	1,93	94,82 %

Machine	Cylinder	Damage class	Severity
✓ G8-6702 A	1. Stufe West	Damaged Discharge Valve, Crank end	2,05
✓ G8-6702 A	1. Stufe West	Damaged Discharge Valve, Head end	4,14

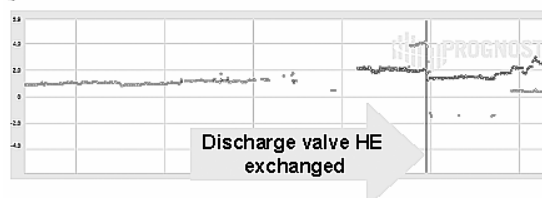


Figure 11: Severity trends of 1st stage west

The discharge valve was replaced end of June 2006. Later the severity of the discharge valve failure at the crank end increased to a level of 3% of the nominal gas flow, too. Both valves showed firmly bonded deposits and were not mechanically defective.

12 Conclusion and Summary

Model based monitoring becomes applicable for reciprocating compressors by combining thermodynamic and empiric models. This technology is different to traditional monitoring applications. Instead of monitoring single parameters such as temperature and pressure with absolute thresholds, the deviation of calculated setpoints and on-line measured values is determined.

The setpoints are provided on-line by a theoretical compressor model that continuously calculates the expected values for each parameter (e.g. suction/discharge pressures and temperatures) based on the operating condition. The deviation of both values, the so called “residual”, is monitored with a threshold.

Ideally, the value of the residual is zero, which means that the measured value is equal to the calculated setpoint. In case of an abnormal condition, e.g. a suction valve leakage, several residuals increase (e.g. stage pressures, valve temperatures) and violate their dedicated thresholds. The diagnosis module compares the pattern of the violated residual with a database that contains patterns of typical sealing components failures.

The database includes leakages of suction/discharge valves, piston rings, stuffing boxes and additionally, gas coolers. If the current pattern matches one in the database, a diagnostic clear text message is automatically generated. The diagnostic message includes information of the damage class, e.g. discharge valve failure, and a percentage value for the severity of the damage and the probability that the correct failure type has been diagnosed.

References

[MOU97] J.Moubray: Reliability-centered Maintenance

[ISR94] R. Isermann (Hrsg.): Überwachung und Fehlerdiagnose, VDI Verlag, 1994

[LJU99] L. Ljung: System Identification (second edition), Prentice Hall PTR, 1999

[NEL00] O. Nelles: Nonlinear System Identification, Springer, 2000

ETHYLENE BOIL OFF GAS COMPRESSOR IN PETROCHEMICAL PLANT AVAILABILITY AND RELIABILITY ENHANCEMENT

by:

Syed Fuad Abbas
Staff Engineer (Reciprocating & Screw Compressors)
P.O.Box 10002, Petrokemya
SABIC
Al-Jubail -31961
Saudi Arabia

abbassf@petrokemya.sabic.com

Mousa A. Al-Haijan
Manager Maintenance.
P.O.Box 10002, Petrokemya
SABIC
Al-Jubail -31961
Saudi Arabia

haijanma@petrokemya.sabic.com

Dr.-Ing. Klaus H. Hoff
Head of Central Division of Technology
NEUMAN & ESSER GmbH & Co KG
52531 Übach-Palenberg
Germany

Klaus.Hoff@neuman-esser.de

5th Conference of the EFRC
March 21-23, 2007
Prague, Czech Republic

Abstract:

In a petrochemical industry, an olefin plant uses reciprocating compressors to handle ethylene boil off gas from storage tank. The compressors take vapors and compress them back to the ethylene header, thus maintaining the vapor pressures of storage tank within operating limits.

These compressors operate at different load levels depending upon the vapor generation within the storage tank and having sub zero suction temperature of -80°C. So it is utmost important to have comprehensive and through selection and design process.

This paper discusses from Petrokemya's perspective the problems experienced during the startup, commissioning and during operation of 3-stage horizontal reciprocating compressors. The objective of this paper is to share experience and efforts, which were applied to enhance the reliability by continuous improvement in collaboration with the OEM.

1. Introduction

In our petrochemical complex, an additional Olefin plant was commissioned in January 2001. The main product is ethylene with name plate capacity of 800,000 TPY. The ethylene product from C2 splitter is split into the consumer header as a high pressure ethylene vapor while excess ethylene goes to liquid storage as a low temperature ethylene liquid, based on the consumer demand.

A double walled refrigerated ethylene storage tank having capacity 50,000 cum is used to store liquid ethylene. The boil off gas (BOG) is generated due to flash of rundown liquid and heat leak into the storage tank and associated piping.

The boil off gas from the refrigerated ethylene tank is compressed by ethylene BOG compressor and combined with the high pressure vapor ethylene to the consumer header.

Motor driven, double acting, three stages, four cylinders horizontal machines with non lubricated cylinders are used to perform the BOG compression function. Two compressors are installed with one in operation and second one as stand by. This compressor keeps the tank pressure within operating limits of 50 to 100 millibar by compressing the boil off gas to 45 barg. This machine can handle up to 3,494 kg/h of BOG.

The capacity of the BOG compressor can be controlled by the un-loader system at 0%, 25%, 50%, 75% and 100% depending upon the vapor generation within the tank. The jacket cooling water closed cycle system is provided for the 2nd and 3rd stage cylinders while 1st stage cylinders are cooled by silicone oil fluid PD5 through thermal siphon system, to remove heat of compression.

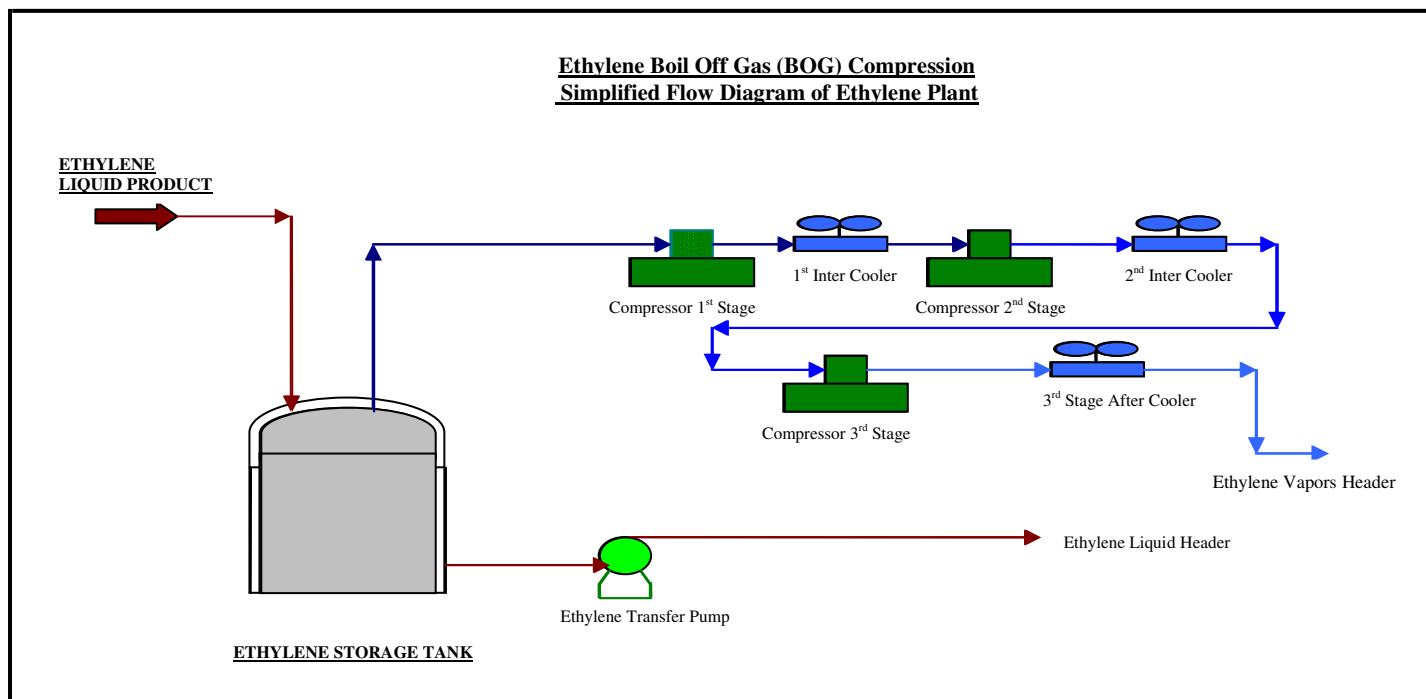


Fig 1: Simplified flow diagram of Ethylene Plant for Ethylene storage

2. Start up experiences

During the first 24 hours of operation, excessive noise and high vibrations were observed in the first stage cylinders of compressor 'S'. Upon dismantling, followings were the observations.

- Valve debris was found in 1st stage cylinder B on head end side. Head end discharge valves were found severely damaged with its lock nut broken, the stud came out and valves plates and valve seats got damage.
- Cylinder head cover and piston face towards head end received heavy impingement marks.
- 2nd stage Crank end Suction and discharge valve cages were both broken. While head end cage of suction valve had one pin loose. Valve seat also got damage.
- 3rd stage suction valve Crank end had spring missing with only one large spring intact. Rest of the valves was in good condition.



Fig 2: Cylinder Head Cover



Fig 3: Damage Valves and cage legs

2.1. 1st Stage suction loaders

During the initial months of operation (Feb and March 2001), it was observed that whenever the load of the compressor was reduced from 100% to 75% or from 75% to 50%, the suction loader got stuck at higher level of loading. This was due to the icing at the suction valves. The overhaul length of the loader stem from the valve cover was too short and complete loader was covered with ice. To overcome this problem, an in house temporary modification was carried out by inserting a plate of 10" diameter in between the valve cover and loader head. This had increased the surface area, thus preventing the ice formation to the top of loader actuator. A new design of loader valve is being recommended by Valve-OEM to resolve this problem on permanent basis.

2.2. 1st Stage Cylinder Liners

These compressors were supplied with a Ni-Resist (Cr-Ni alloyed cast iron) cylinder liners. During the initial inspections after few months of operation, cracks were observed at the bottom of the liner where the rider rings travels. The East side 1st stage cylinder liner has two radial cracks side by side in the middle at the bottom. While, the West side 1st stage cylinder liner has one small crack at same location as of east cylinder. The rider rings were being damaged due to these conditions.

2.3. Crankshaft main bearings

After six month of operation, excessive sound was observed in the crankcase area at the coupling end. Upon dismantling and inspection of bearings it was noticed that all main bearing and connecting rod big end



Fig 4: Cracks on the 1st stage cylinder liner



Fig 5: Cracks on the 1st stage cylinder liner

bearings had Babbitt material disassociated at loading area.



Fig 6: Material chipped off Main Bearing



Fig 7: Damaged Main Bearings

2.4. Crosshead pin and bearings

The crankcase inspection also revealed metals derbies around 3rd stage connecting rod and crosshead area. The crosshead was dismantled, the crosshead pin and its bearing was completely damage. Other stages crosshead and connecting rods were also removed and inspected. They were all in good condition and their dimensions were within allowable limits.



Fig 8: Crosshead Bearing damaged



Fig 9: Crosshead pin

2.5. Connecting rod

The 3rd stage connecting rod small end diameter was de-shaped and had become oval. The most damage was at the loading side of the bearing. While opposite to the loading side there was no damage.



Fig 10: Connecting rod small-end damage



Fig 11: Unloaded side remain intact

2.6. Distance piece to crankcase connecting bolts

During the replacement of main and connecting rod bearing on S compressor, it was observed that the main compressor ‘A’ which was running had excessive vibration on the distance piece. The compressor was stopped and inspected. It was noticed that one bolt was very loose. After opening the cover plate, it was found that four of the eight bolts were loose. Actually these bolts got sheared off. Broken pieces of the bolts were removed after drilling hole and then took them out by means of retractor tools. OEM recommended new design Neck Down bolts, which were installed after removing all existing 140 bolts for both the compressors.

2.7. 1st Stage piston and rider rings

The piston and rider rings of 1st stage had problem of material chipping off from side edges. The wear had not been the problem. The jamming of rider ring within the groove of the piston, due to initial dust carry over from the storage tank was the cause of the initial failures of the rings. While the piston ring got damage from the overlap portion. Later on the frequency of rider ring failure was increased when the cylinder linear problem appeared. Also when the cylinder linear material was changed, the rider rings started failing on faster rate. So material and design change was suggested to match the new cylinder linear.



Fig 13: Piston ring broke off from overlap portions



Fig 14: 1st Piston ring with one overlap portion intact



Fig 12: Chipped off material from Rider ring of 1st stage



Fig 15: Heated effected Rider Rings



Fig 16: Set of rider ring effected due to high temperature

2.8. 2nd and 3rd Stage piston and rider rings

The 2nd and 3rd stages piston ring usually broke off from the overlapped portion due to increased notch effect and brittleness of the used ring material. While on 3rd stage the failures of piston and rider rings in the form of broken pieces was also observed. So tangential cut design rings were supplied to overcome the breakage problem and the material of 3rd stage was change to overcome the brittle failure of rings. In these stages the wear of the rings was never been an issue.

2.9. Crankcase foundation bolts

During the bearing replacement of “S” compressor, increased vibration was observed on “A” compressor. On checking it was noticed that the foundation bolts of crankcase near the 3rd stage was loose. Tightening of bolt revealed that it was traveling upward, which meant that the engagement of tee head of the rod with bars is no more. That portion of the foundation was chipped off and tee head was engaged. Finally foundation was repaired with epoxy grout.

3. Design changes in the existing system.

To improve the compressor system from maintenance and reliability point, following changes were carried out. These changes resulted in enhanced maintainability and reliability of the machine.

3.1.1st Stage cylinder’s coolant piping system.

Piping modification for cooling system arrangement was carried out in February 2001. This was to facilitate the filling of coolant and avoiding the removal of piping connections each time for piston and rider rings inspection.

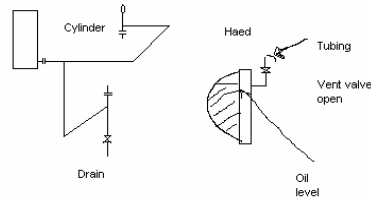


Fig 18: Modified Arrangement of cooling system for 1st stage cylinder

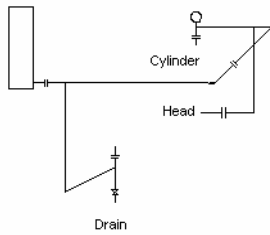


Fig 17: Existing Arrangement of cooling system for 1st stage cylinder

3.2.1st Stage cylinder liner

After OEM’s investigations it was found that residual stress in the liner—although it was annealed after pre-machining - in combination with the different thermal expansion of cylinder and liner caused the cracks. The Ni-Resist type which was used here tends to distort if the annealing is not done in a correct way. In the vertical plane the radial clearance was consumed by this compression. Now, the rider bands start to jam and to create frictional problem intensifies. The stresses in the liner material heat exceeding the tensile strength of the liner. By this heat the difference become so big that a crack was created.

To avoid the crack generation, OEM suggested the replacement of the Ni-Resist-linear with a Cast Iron liner. So on both cylinders the liner were replaced and for standby compressor also. Due to the new liner material the rider and piston rings material were also changed.

3.3.Crankcase lubricating oil

The failure of crankshaft and connecting rod bearings, prompted to reconsider the lubricating oil grade. It was calculated and recommendations by OEM was given to switchover the lubricating oil from ISO grade 100 to ISO grade 150, having the viscosity of 150 cst from 100 cst. Accordingly the lube oil for the compressor was changed.

3.4. Crankshaft and connecting rod bearings.

Crankshaft and connecting rod bearings failure has been solved by replacement of existing bearings with new “Galvanic” bearings. It was stated by OEM that old Babbitt type can have average load bearing capacity of 12 N/mm² while the new galvanized bearing have 17 N/mm². A slight overloading of the bearings was responsible for the main and crank pin bearing failures. This overloading was introduced by higher flow losses of the valves than designed.

The crosshead pin bearings for all the stages were just replaced by bearings of the original design since the failures were caused by the malfunction of the suction valve unloaders and the subsequent loss of rod load reversal.

The replacement of Galvanic bearings did prove to be successful and reliability of compressors had improved. However the 3rd stage crosshead pin bearing again got damaged in similar fashion for one of the compressor after many years of trouble-free operation. In house investigation looked into the operating condition, and did not find any parameter contributing to this failure. The details of the failure were given to OEM for investigation. The root cause of this damage is in progress.



Fig 19: Crosshead Bearings

3 5. 1st Stage piston and rider rings

The piston and rider rings of 1st stage went through different stages of failures. Initially the rider rings problem of chipping off from the edges and cracks in the middle of its width.

It has been finally solved with the installation of the cast iron linear and different material of rings as described before. Hereafter, we achieve considerable level of run length. But ultimately a different design of rings were recommended and installed with some minor changes to the piston. This design consist of rider rings in two parts, the lower part was having more thickness than normal while upper part with less thickness. The machining of piston grove to accommodate the increase width of rings and counter bore drilled for the stud, which will hold the rings.

This design was recommended because it seems that the clamping of the guide rings which was caused by temperatures, is giving all these problems to the rider rings. Now with the new design it create more cold gas passage too and through the guide rings so it will not see these extreme temp again. Now we had achieved a run length of about 7500 hrs.

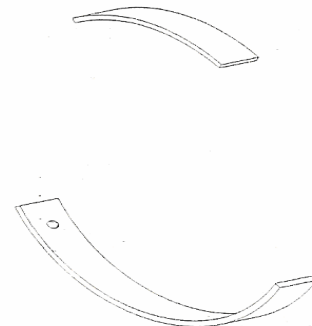


Fig 20: 1st Stage Rider Ring in two parts

4. Availability and reliability enhancement

Reliability of the reciprocating compressors is mainly depending on the wearing parts. That normally consists of piston and rider rings, suction and discharge valves, packing rings and oil scraping rings. On long term base the wearing parts consists of main bearings, connecting rod bearings, crosshead, piston rod and crankshaft web deflection.

The reliability aspect of the machine can be addressed at two stages, firstly at design stage and secondly during its operation period. Generally the reliability aspect of wearing parts at design stage, do not get fair consideration. At this stage the emphases is mostly on the

minimum requirement of API and contractual binding.

A comparison of the design data between the existing BOG compressors of different vendors at two other plant of petrokemya and the one being discussed is given in table 1.

Here we can see that the KW requirement of the subject compressor is higher than the existing compressors which are 525 KW verses 375 and 350KW. While the selection of frame rating is smaller then existing ones that is 668 BKW as compared to 1000 BKW of the existing compressors. Moreover if we consider the calculated gas loads, we note that it is much higher for this compressor as compared to existing compressors while the size of bearings and the crankshaft is smaller. Similarly the crosshead bearing is also smaller than the existing compressors.

This does not mean that the selection of the subject compressor was not right. However it can be that the existing compressors which had shown longer life of these wearing parts that is main bearings, connecting rod and crosshead bearings, may have the built in margins. This longer life could be attributed to OEM philosophy of having in built margins during designing stage.

BOG COMPRESSORS	OLEFIN - I	OLEFIN - II	OLEFIN - III
MAKE	VENDOR # 1	VENDOR # 2	VENDOR # 3
TYPE	Horizontal – 3 stage	Horizontal – 3 stage	Horizontal – 3 stage,
# OF CYLINDERS	3	3	4
FRAME RATING	1000 BKW	1000 BKW	668 BKW
RATED RPM	500	507	505
DRIVER KW	375	350	525
CAPACITY CuM/Hr 1 / 2 / 3 ST	1551 / 489 / 163	1440 / 449 / 138	2349 / 718 / 231
CYLINDER BORE mm	525 / 300 / 195	550 / 310 / 165	600 / 385 / 220
PISTON ROD DIA mm	70	60	70
CRANKSHAFT BRG DIA	190	160	130
CROSSHEAD BRG DIA	110	85	80
CALCULATED GAS LOAD KN in COMPRESSION	87.37 / 70.8 / 65.22	98 / 86 / 63	128.2 / 125.7 / 85.1
CALCULATED GAS LOAD KN in TENSION	85.8 / 64.03 / 64.43	96 / 80 / 47	125.5 / 116.6 / 61.4
Max. Allow. Cont. Rod Loading KN C	132.39	157	150
Max. Allow. Cont. Rod Loading KN T	137.29	157	150

Table 1: Design data comparison

Second aspect of reliability is during commissioning and under normal operation. This

part becomes more important if one encounter several problems in addition to routine commissioning ones. In our case it started with the day one of the operation.

It is to be mentioned here that most of the problems were shared by both compressors that is main “A” and stand by “S” compressor, except the 3rd stage crosshead bearing problem which was on “S” compressor only.

The trend of compressors availability data shows that it has improved from 2001 to 2006. The main cause was the resolutions of the problems. 240 hrs are for planned maintenance activities for each compressor per year.

Equipment	Year 2001	2002	2003	2004	2005	2006
Compressor A	7000	7200	7400	7650	7800	7650
Compressor S	6600	7000	7200	7600	8200	6600

Table 2: Compressors Availability in Hours (8760hrs per year)

Table 3 shows the maintenance history of the subject compressor.

The 1st stage rider rings are showing low run length. This had now improved by new design rings. Presently we had achieved run length for “S” compressor to 7500 hrs which is a satisfactory performance. While for 3rd stage rider rings, the material change will result in satisfactory run length. The packing and valves are showing better results.

5. Conclusion

An effective interaction between the end user and the original equipment manufacturing at earlier stage of the project can result in better selection of equipment. This can be achieved with sharing of end user experiences combined with the vendor’s knowledge of design and material.

Later on, an after sales service and technical support with prompt respond, provided by the vendors to the end user is key to success in enhancement of equipment reliability. The problem resolution with strong technical backup from the vendor helps the end user to maintain the equipment in good running condition thus achieving the set target of equipment availability and enhancing its reliability.

OPERATIONS & MAINTENANCE

Ethylene Boil Off Gas Compressor in Petrochemical Plant Availability Enhancement, *Syed Fuad Abbas, Mousa A. Al-Haijan; SABIC Klaus Hoff; NEUMAN & ESSER*

6. References

1. API Standard 618 “Reciprocating Compressors for the Petroleum, Chemical and Gas Industry Services”
2. OEM Reports, Correspondences and Equipment Manual
3. Equipments Maintenance History Records and Failures Analysis Reports.
4. Machinery Reliability Assessment. (2nd Edition) By Heinz P Bloch & Fred K. Geitner.

Equipment		Start-Up	Piston Ring	Rider Ring	Suction Valve	Dish Valve	Packing	Crank shaft	X-head	Piston Rod	Piston	Cylinder
Plant 3	1	Jan-01	4000	2400	6000	6000	12000	1	1	0	0	2
BOG-A	2		6000	6000	12000	8000	12000	1	1	0	0	0
	3		3500	2400	8000	6000	8000	1	1	0	0	0
	1	Jan-01	4000	3000	8000	8000	12000	2	2	0	0	2
BOG-S	2		8000	8000	12000	12000	12000	2	1	0	0	0
	3		4000	3500	8000	6000	12000	2	2	1	0	0

Table 3: Maintenance History of subject BOG compressor



NAM

THOMASSEN
COMPRESSION
SYSTEMS



Increased Availability and Reliability by OEM Maintenance Agreements

by:

Crena de Iongh, Rob

EPE-P-EL

NAM

RobCrenadeIongh@shell.com

Bongers, Hans

Maintenance Agreements

Thomassen Compression Systems

job@thomassen.com

**5th Conference of the EFRC
March 21-23, 2007
Prague, Czech Republic**

Abstract:

Reciprocating compressors for refinery and oil and gas services are designed to operate approximately 16,000 to 24,000 hours without maintenance. These expected running times are not always met in the field, having an adverse effect on the availability and/or reliability of compressors with as result unplanned shutdowns and deferment. A performance maintenance agreement is a tool to improve the reliability/availability and maintenance costs of compressors. You should not only be skilful technically but also know the parties involved in the maintenance and define goals and the maintenance organisation based on this. Key to success is condition-based maintenance built solidly on many years of experience of the OEM and continuous performance monitoring of the compressors. This results in a maintenance approach that is customised to criticality and the operating conditions of these machines. By applying value-driven techniques, technical and strategic improvements can be developed resulting in optimised availability and reliability and reduced maintenance costs. When considering whether these improvements should be applied sufficient certainty must be offered that the investment in the improvement will ultimately show a return on investment through a reduced Total Costs of Maintenance and, therefore, Total Costs of Ownership.

This paper describes a case history of the NAM – Thomassen performance maintenance agreement where all the above issues will be highlighted.

1 Introduction

Several parties are involved in the maintenance of compressors as is often the case when using and maintaining capital goods. The parties involved do not necessarily have the same business interests.

The easily recognised mutual interest for all parties with regard to maintenance is guaranteeing the availability and reliability of the machinery at issue while incurring acceptable costs. The opinions, regarding the required degree of availability, reliability and acceptable cost levels (and who should bear the costs), will often vary. Total Costs of Ownership and Total Costs of Maintenance are terms that can be easily confused. A saving on maintenance costs for one party can, after all, mean an increase in costs for the other party.

A successful partnership in compressor maintenance requires being aware of the individual and joint interests of all involved parties as well as having sound technical knowledge. Success can be brought about by organising maintenance based on this awareness.

The maintenance agreement that NAM concluded in 2001 for its installed base of critical compressors with compressor manufacturer Thomassen Compression Systems BV (Thomassen) has demonstrated that this can have good results in a customer - supplier relationship. The joint goal: maintaining the high availability and reliability while spending 20% less on maintenance costs.

2 Parties involved

Three parties are involved in the case under consideration: NAM, Thomassen and, to a lesser extent, also the Integrated Service Contractor (ISC).

2.1 NAM

NAM (Nederlandse Aardolie Maatschappij BV) is a subsidiary of Shell (51%) and Exxon/Mobil (49%). NAM's mission is to explore gas and oil fields and produce gas and oil in the Netherlands and the Dutch part of the continental shelf in a sustainable way. The Netherlands has 56% of all gas reserves in the European Union. NAM is responsible for 75% of the total Dutch gas production. Gas is supplied to the Gasunie, which is the main Gas trading company of the Netherlands.

Nowadays half of the produced gas comes from the Groningen gas field, the other half comes from smaller fields located elsewhere in the Netherlands and offshore. NAM has to, in particular, deal with changing conditions in these smaller fields such as fluctuating pressures and gas compositions. This is why NAM has 50 reciprocating compressors installed, of which 34 are deployed as depletion units.



Figure 1: Gas production/depletion in the Netherlands by NAM

The NAM Production organisation represents the realisation of the main goal of NAM: a reliable supply of gas. The gas must be delivered at the request of users with peak demands during the winter period. A guaranteed production capacity must, however, still be available when gas is less needed such as in the summer months.

The NAM maintenance organisation is responsible for the maintenance and management of the maintenance budgets. The NAM maintenance strategy can be summarised as follows:

- Apply one maintenance strategy per criticality category;
- Optimise availability/reliability of units based on production requirement;
- Optimise effectiveness of maintenance; and
- Improve supply chain performance.

NAM has outsourced agreements to various service companies and different manufacturers of critical machines (compressors, electromotors, gas turbines, coolers, etc.) to implement this strategy.

2.2 ISC

The present main ISC (Integrated Service Contractor) for NAM is OMC.

A holding company made up from several different contractors each with their own speciality. Main players are GTI, Tebodin and Imtech. This ISC contract was intended for all regular maintenance tasks, as well as breakdown and preventive maintenance. However, it has been recognised that OMC was not equipped to perform the maintenance tasks on more complex machines in accordance with the high standard NAM demands. Taking the high consequences of failure of these complex critical machines as well as the above statement into consideration, we have the main reasons why NAM decided to contract these machines out to the OEM (Original Equipment Manufacturers).

2.3 Thomassen

Thomassen is a compressor manufacturer with its main location in Rheden, the Netherlands, and a few service companies around the world. Thomassen has had NAM compressors under a maintenance agreement since 2001. This maintenance agreement has been extended to cover a total of 40 machines during the period from 2001 up to now. Compressors from various manufacturers are involved. Thomassen supplies the following within this agreement:

- Maintenance management (coordination, planning, work preparation, reporting, engineering feedback);
- Service personnel for the supervision of the planned and unplanned maintenance (carried out by the OMC);
- Troubleshooting;
- Component and spare part stocking;
- Repair services;
- Modification engineering;
- Product engineering;
- Training.

3 Goals and interests

All the abovementioned parties are involved in developing the NAM maintenance strategy for its installed base of depletion/production compressors.

We, naturally, have to deal with three companies that have their own business economics and commercial goals. These interests must be managed in the elaboration of the maintenance agreement. First, however, there must be clarity about the assessment that NAM has made in relation to availability, reliability and the cost level.

Several issues must be compared and considered with regard to this. The most important ones are listed below.

3.1 Maintainability

The maintainability of a unit is an aspect which is mainly determined during the engineering stage of a unit. Part of this is in the design of the unit itself and the selection of materials and a part is in the access to the areas where maintenance is required and the ergonomics of this access. It must also be determined whether adequately instrumented units will provide the best opportunity for effective maintenance.

The best design from a maintenance perspective may, however, not be the most inexpensive design with regard to purchase. A “saving” on the purchase of the new installation, ostensibly a saving for NAM, can result in higher maintenance costs and ultimately to higher Total Costs of Ownership for NAM.

3.2 Maintenance

Making savings when it comes to maintenance budgets might improve short-term company results, but they will have a long-term adverse effect on availability and reliability.

3.3 Assessment

Basically, most users of capital goods believe that the main objective for maintenance is the improvement of availability and reliability while incurring an acceptable investment or cost level from a business economics perspective. The improvement of availability and reliability will quickly contribute to more production efficiency for production-critical machines.

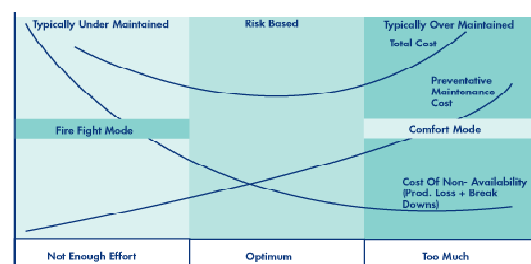


Figure 2: How to optimise Total Costs of Maintenance

NAM has decided to have a maintenance cost reduction of 20% as its goal while retaining the current high availability and reliability of the critical machines and, where possible, making improvements.

The challenge: to translate these goals into an approach and to define them in business and commercially solid agreements.

4 Approach

The performance maintenance agreement that was concluded in 2001 with Thomassen was a continuation of an existing agreement based on a new and jointly chosen approach. Thomassen is responsible within this context for maintaining the high availability and reliability of the compressors under consideration as well as for realising the required cost saving of 20%.

4.1 Economies of scale

A significant part of the cost saving could be achieved by using the principle of economies of scale. Thomassen had already 21 compressors in its maintenance programme by the end of 2004. NAM was satisfied about the provided services and wished to extend the existing maintenance agreement with an additional 19 machines in 2005. This meant that an important part, approximately half, of the contemplated savings could be brought about without there being any consequences that may affect availability and reliability. The economies of scale could be achieved by using the existing maintenance team, dedicated stocking and supply of spare parts and infrastructure of Thomassen. The extension of the agreement was in the interest of both NAM (cost saving through economies of scale) and Thomassen (additional business). A clear win-win deal.

4.2 Sophisticated service levels per machine category

A second part of the saving could be brought about by better harmonising service levels to machine categories. Two aspects played a role in this:

1. The criticality of a compressor function within the process installation.
2. The level of complexity and expertise required.

The first aspect is the easiest to determine and results in an obvious approach. Machines for which the availability in the production process is less critical, require a lower degree of maintenance investment.

The second aspect is more interesting. An intelligent service approach was defined for each machine category based on the knowledge, experience and history that were built up by NAM and Thomassen and through the Thomassen PPMO method.

PPMO stands for Pro-active Performance and Maintenance Optimiser and is the Thomassen's tool to implement a condition-based maintenance strategy on compression equipment. PPMO combines data that is collected during operation and performance inspections and during mechanical inspections. The purpose is to assess the condition of the units and to predict the lifetime of the critical parts, in order to execute maintenance before failures occur. The inspections are planned based on running time frequency, maintenance intervention frequency, together with the historical performances of the relevant machine.

In order to minimise the Total Cost of Maintenance of each unit while retaining the required reliability, a production criticality assessment has led to the definition of different service levels with connected work scopes.

Different service levels were determined to specify the most appropriate fit for purpose maintenance strategy, where:

- Service level A is a condition based maintenance strategy which is specified for units which are critical to NAM operations and which require high maintenance support.
- Service level B is a condition-based maintenance strategy which is specified for units which are critical to NAM operations and which require medium maintenance support.
- Service level C is a time-based maintenance strategy which is specified for units which are not critical to NAM operations and/or has specific reasons why a low maintenance support is required.

OPERATIONS & MAINTENANCE

Increased Availability and Reliability by OEM Maintenance Agreements, *Hans Bongers; THOMASSEN COMPRESSION SYSTEMS*
Rob Crena de Iongh ; NAM

- A separate service level 0 is defined for units which are being implemented for maintenance for one year. The scope will contain additional calibration of unit data, condition spare parts, history and behaviour.

Service Level	Description TCS	Description NAM	Stock Level	PPMO	Site Visit / Tech. Adv.	Cond. Mon.	Contract Mgt.	Report	Callout Planned	Callout Emergency	Engineering Back-up Included
0	Calibration Year		TBD	Full	Yes	Yes	Full	Quarterly + Field	Yes	Yes	Yes
A	PPMO Based	Critical with high support	Full	Full	Yes	Yes	Full	Quarterly + Field	Yes	Yes	Yes
B	Time Based with Cond. Mon.	Critical with no close support	Medium	Medium	Yes	Yes	Medium	Quarterly + Field	Yes	Yes	Yes
C	Time Based	Non Critical	Low	No	No	No	Low	Field	Yes	No	No
D	Break Down	Non Critical	None	No	No	No	No	Field	No	No	No

Figure 3: Service Levels for NAM compressors

The maintenance budgets consist mainly of costs for personnel, training, parts, tools, outsourcing and stocking. Savings could be realised by shorter turnaround times with regard to maintenance activities and stretching the time in-between maintenance interventions.

In stocking parts, mayor savings can be created by intelligent warehousing, logistics, insurances and the prevention of locking up capital.

Costs can also be controlled by clustering maintenance activities. The scope of a maintenance cluster is determined by a logical combination of maintainable parts having similar life span expectancies. For example: cluster valves that have compressor valves with O-rings and gaskets. Cluster stuffing boxes that have stuffing boxes, compartment seals, rider rings and piston rings with all necessary gaskets and small items.

Life span expectancy of every maintenance cluster can be monitored via inspections, job reporting and refurbishment reports. Life span increase for a complete cluster will both result in reduced maintenance costs and will improve availability.

Compressor / Serial No.	Cluster A	Cluster B	Cluster C	Cluster D
K-2101 / 1300	12.000	24.000	52.000	40.000
Fixed Date	18-01-2001	20-01-2003	18-01-2001	18-01-2001
K-2201 / 1409	16.000	24.000	52.000	40.000
Fixed Date	20-01-2003	20-01-2003	18-01-2001	18-01-2001
K-2202 / 1410	16.000	24.000	52.000	40.000
Fixed Date	20-01-2003	20-01-2003	18-01-2001	18-01-2001
K-8 / 1411	16.000	24.000	52.000	40.000
Fixed Date	13-07-2000	13-07-2000	21-05-2001	18-01-2001
K-9 / 1412	16.000	24.000	52.000	40.000
Fixed Date	21-10-2003	20-01-2003	18-01-2001	18-01-2001
K-602 / 11081/411	16.000	24.000	52.000	40.000
Fixed Date	18-01-2001	19-06-2001	18-01-2001	18-01-2001
K-9100 Den Helder Dresser	8.000	16.000	32.000	40.000
	26-01-2006	26-01-2006	26-01-2006	26-01-2006

Cluster A = Replace Valves
 Cluster B = Replace Compartment seals - Piston rings - Rider rings - Stuffingboxes
 Cluster C = Replace Piston rods
 Cluster D = Replace Crosspin bushings- Small-end bearings
 Cluster E = Replace Liners
 Cluster F = Replace Big-end bearings - Main bearings - Crosspins - Crosshead shoes
 Cluster Y = Performance Inspection, Pro-active Performance & Maintenance Optimizer
 Cluster Z = Mechanical Inspection, Pro-active Performance & Maintenance Optimizer

Figure 4: Clusters with life span

The remaining part of the saving could be achieved through the sophisticated service levels for each machine category and the definition of maintenance clusters.

4.3 Long-term vision

This maintenance concept only works if it is concluded for several years because then there are real opportunities to introduce improvements and to show their effect. Long-term commitment by both parties gives security and confidence to concentrate on joint interests.

The maintenance agreement between NAM and Thomassen was concluded for a period of 5 plus 5 years. The long-term horizon supports and promotes making improvement proposals. An example is the commitment of the maintenance team during the engineering phase of new machines to ensure that the correct choices can be made for the maintainability of the design for a new machine in consultation with NAM Production and any other involved parties (such as an engineering contracting company).

Improvements can also be initiated for machines with problems through methods such as RCM (Reliability Centred Maintenance), RCA (Root Cause Analyses) and FMEA (Failure Mode Effect Analyses). The important benefit of a long-term partnership for maintenance with a compressor manufacturer can be found herein. The compressor manufacturer, after all, has all the required competences to monitor, analyse and initiate technical improvements to the performance of the whole machine in the process.

An example. A sizeable 6-cylinder compressor was added in 2005 to the maintenance agreement as well as other compressors. This machine was classified in the highest service level. The machine history revealed five to seven valve failures each year as an average. Failures occurred randomly on suction and discharge. In spite of exchanging complete sets of suction or discharge valves at certain moments the, failure rates where staying the same.

An RCA study was performed together with operations, the valve vendor and maintenance engineering when maintenance started. The conclusion that was arrived at was that failures of the discharge valves were most likely caused by failing suction valves.

The allowable operating envelope of the compressor was modified to stay within the design parameters of the valves. The material selection of synchronous plates and rings was changed to minimise found extreme wear rates (thickness reduction of 1.9 mm was found). Also the guiding of synchronous plates and rings was adapted and is now implemented in the valve guard.

The proposed improvements on the suction valves from mid 2005 have been proven to increase the MTBF of these valves. However, it appeared that the discharge valves were now the Bad Actors of this compressor, i.e. the valve problems appear to have shifted.

A further RCA was conducted in April 2006 with the following results:

- Design issues on the design of the discharge valve rings;
- Sticking of the valve rings in the valves;
- Oil supply to the cylinders, including change of oil specifications.

It was then decided to conduct the following modifications in mid 2006:

- Change the thickness of the discharge valve rings from 6 mm to 8 mm (carbon filled PEEK) to withstand high impact forces as established during a conducted PV measurement on the compressor.
- The cylinder lube oil will be changed to ESSO Teresso L 100 and the quantity will be adjusted in accordance to Thomassen's advice.

Since the summer of 2006 no valve failures have occurred.

4.4 A dedicated organisation

Having a dedicated organisation, a transparent consultation and decision structure at all parties and allocated critical competences as well as having available a dedicated stock of critical parts supplemented with spare parts and repairs are essential to execute a performance maintenance agreement.

The maintenance organisation is based upon single vocal point approach from each party involved. This together with clearly described responsibilities will ensure proper communication.

The contract manager is the single contact related to agreement execution where the focus is on the implementation of agreements made in relation to maintenance execution. The contract manager reports to the agreement steering committee in which customer and supplier senior executives have seats. The contract manager will also regularly meet with his or her counterparts at the ISC to discuss policy and administration issues.

First line support for technical assessments of units is done by a technical advisor. The technical advisor is fully dedicated to manage the technical issues of the maintained units within the agreement. He or she is the Point of Contact for troubleshooting and (modification and product) engineering. The technical advisor is also responsible for providing feedback to engineering after maintenance intervention. Different improvement actions may follow from this. He or she will supervise the correct implementation of any technical modification during the following intervention.

Single point of contact during (planned or unplanned) maintenance intervention is offered by the service coordinator. During an intervention, the coordinator is responsible for the correct execution of the maintenance and for the preparation, communication and logistics. He or she is the person who ensures the coordination of actions and information streams between NAM, Thomassen and OMC are in place.

The field service engineer is an experienced and trained supervisor on compressor equipment.

Under his or her responsibility, the execution of the maintenance scope activities on the various units will be executed.

The service support departments are responsible for the realisation of engineering analysis and modifications. These consist of product and system engineering and repair departments.

4.5 Measure and reward performance

It may be very stimulating for the involved parties to keep going in the same direction when performance is transparently and regularly measured and discussed. This is certainly the case if the performance to be achieved, such as cost savings, are recognised as a joint interest and the achieved results will also benefit all involved parties.

The Plan, Do, Check and Act cycle can be completed with Key Performance Indicators (KPI's) to improve maintenance. The parties have agreed to different KPI's in this specific case. The most important KPI's are listed below.

4.5.1 HSEW

In order to implement maintenance based on requirement, it is essential that all HSEW (Health, Safety, Environment and Welfare) requirements are adhered to in order to ensure safe maintenance execution for personnel and environment. The target for this KPI is zero incidents.

4.5.2 Availability and reliability

The availability and reliability requirements are defined per unit and is related to the defined service level. The achieved figures have to be at least at the defined level. Deviations will immediately lead to analysis and action regarding which regular reporting will take place.

4.5.3 Maintenance cost control

Within the philosophy of condition-based maintenance there is a target towards under running the costs as has been defined at the start of maintenance. For each unit an initial variable cost budget has been calculated. These initial budgets are compared yearly with the actual spent values.

Other KPI's are related to the availability of critical competences, the level of spares in stock and the administrative performance of both parties, supplier (reporting, invoicing) and customer (payments). After all, the issue is to continue serving the interest of all the involved parties.

To conclude, the parties have agreed to a bonus structure to reward and stimulate achieved performance, savings and improvements. Realised cost-effective and efficient maintenance for the user must continue to be an interesting business proposition for the manufacturer. This will ensure that the partnership will offer prospects in the long-term for each party.

5 Conclusion

Maintenance of capital goods greatly influences the total costs of ownership.

It is essential that the required competences for maintenance, analysis of technical performance and improvement are available for the maintenance of complex machines such as depletion compressors. This can be assured in a maintenance agreement between the user and the manufacturer for critical machines such as compressors. This will ensure savings are made with regard to costs without effecting the availability and reliability of the machinery.

You can optimise maintenance if the interests of all involved parties are taken into account and they are professionally translated into an unambiguous approach that does justice to the position and interests of all involved parties. Parties who should agree on the joint goal and the organisation. The communication lines should be transparent and there should be sufficient prospects for all parties in the long-term.

It is important that the goals, approach, strategies, actions and results are known not only to the maintenance staff, but to all involved parties. Maintenance is, after all, an issue that effects all involved parties. Without this mindset, there is no chance of success.



Pros and Cons of Various Coupling Types for Reciprocating Compressor Installations

by:

Gerhard Knop

Dr. Klaus Hoff

Central Division of Technology

Neuman & Esser GmbH & Co. KG

Übach-Palenberg

Germany

gerhard.knop@neuman-esser.de

klaus.hoff@neuman-esser.de

5th Conference of the EFRC

March 21-23, 2007

Prague, Czech Republic

Abstract:

Various coupling types are used for reciprocating compressor installations like rubber-in-shear (high-flexible couplings), rubber-in-compression, metal-disc, diaphragm and rigid flange couplings. They all have their individual advantages - otherwise they would not exist - however, experience shows that some types bear much higher risks in terms of drive train vibration problems than others. This report compares common coupling types on the basis of many years of experience. It evaluates different aspects but has a special focus on torsional vibration issues like height of natural frequencies, reliability of stiffness values and load capacity.

1 Introduction

There are few parts within the reciprocating compressor and its drive train that show an equivalent design variety as the coupling. Apart from some exotic types like e.g. fluid couplings, all common kinds of couplings have been used in numerous applications. This fact already implies that there seems to be no coupling type which stands out from the others in terms of all relevant aspects. If this were the case, no other kind would exist.

However, a closer look at the experience gained after many years of drive train design, and a thorough analysis of the same shows, that there is indeed a quality unbalance when focusing the most important criteria. These criteria have to be defined and the different coupling types have to be evaluated accordingly. This is tried in this report.

Certainly, the ranking of the criteria is somewhat subjective, but the main focus is put on the reliability in operation where experience shows that this is usually considered to be the most important aspect. The reliability in operation is closely linked to the actual dynamic torque load in operation which strongly depends on the coupling torsional stiffness characteristics and also on the coupling dynamic torque load capacity.

2 Coupling types

In general, couplings can be categorized in flexible and rigid types. Flexible couplings are used in reciprocating compressor installations for the purpose of compensating shaft misalignment. The term ‘flexible’ in this context usually refers to the radial, axial and angular stiffness of the coupling but not to the torsional. As an example, all steel disc type couplings are referred to as flexible ones although their torsional stiffness is very high. Rigid flange type couplings do not compensate shaft misalignment. Below is a list of the most common coupling types used in reciprocating compressor installation. Within these groups there is an ample amount of different detail-designs but the basic items that are dealt with in this report can be covered by the chosen rough classification.

2.1 Rigid flange type couplings

These couplings are traditionally used for large compressor installations. As they are rigid in all directions, they do not compensate shaft misalignment. Therefore, most users require single bearing motors for the drive.

With this motor type, the rotor-flange is free to move in radial direction and shaft constraint is avoided.

There are also double bearing motors coupled by rigid flanges to the compressors and – despite no compensation of misalignment – show successful operation. However, there are general worries that the initial alignment could deteriorate in course of the time because of uneven foundation sag. The consequence could be bearing damage or even shaft fracture. This applies especially for large and therefore heavy machines because their foundation geometry is often very irregular which supports non-uniform foundation sag. Fig. 1 shows a typical design of rigid flange couplings.

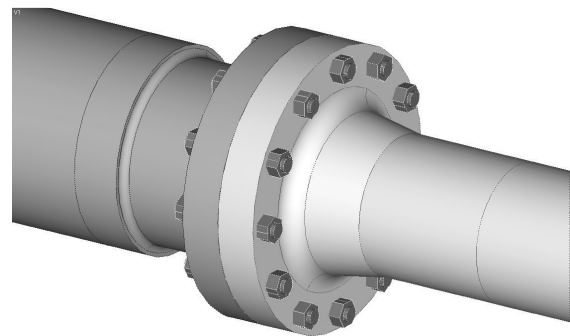


Fig. 1: Rigid flange type coupling

2.2 All-steel disc type couplings

Fig. 2 shows the typical appearance of an all-steel disc type coupling.

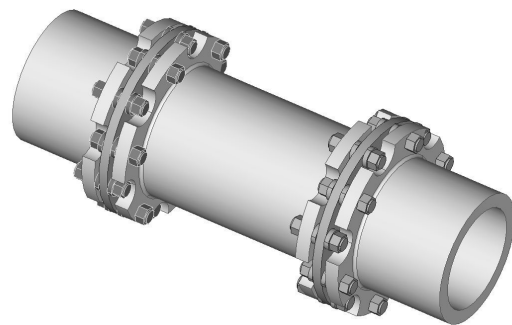


Fig. 2: All-steel disc type coupling

This coupling consists of two hubs (possibly only one if it is directly flanged to a flywheel), two plate packs and a spacer. The plate packs are made up of metal sheets and are alternately bolted to the hub and the spacer. They can be ring discs or bar type discs. The spacer is usually a tube. Sometimes a solid shaft is used to introduce some torsional softness.

Often, the spacer length – or better the distance between shaft ends (DBSE) – is specified to be in accordance with API 671 [2] (DBSE = 460mm) in order to allow dismantling the coupling without having to move motor or compressor. All-steel disc type couplings are torsionally rather rigid and flexible in radial, axial and angular direction.

Within this group, we can further distinguish between the so called 'turbo' couplings and the 'pump' couplings.

'Turbo couplings' are basically designed for high speed turbo compressors (speed range up to 20,000 rpm). Consequently they have the necessary features which are required for such an application like: small diameter, perfect balance and high static torque capacities. It is sometimes found that these couplings are also installed in reciprocation machinery, although this application is foreign to this coupling type.

'Pump couplings' are designed for low speed ranges and dynamic torque characteristics which are typical for recips. Therefore, they have rather large diameters to be robust enough for the dynamic torque load.

2.3 All steel diaphragm type couplings

These couplings compare to the all steel disc type couplings, only they have 2 diaphragms rather than metal sheet discs. This makes them very soft in axial direction. Diaphragm type couplings are to be allocated to the 'turbo coupling' group.

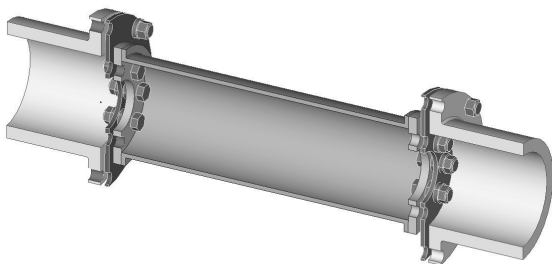


Fig. 3: All-steel diaphragm type coupling

2.4 Rubber-in-sheer couplings

These couplings are also referred to as 'high-flexible' couplings because of their very low torsional stiffness. The rubber elements may have the shape of a disc or of a tire like illustrated in Fig. 4 and 5. Usually the manufactures supply different rubber materials which allow the tuning of the torsional natural frequencies. They can be fixed to the machinery by means of hubs or flanges. Usually it is also possible to remove the rubber elements without having to shift motor or compressor. The flexible coupling elements represent the predetermined breaking point of the drive train in order to protect motor and compressor.

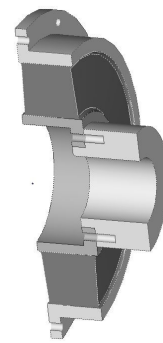


Fig. 4: Rubber-in-sheer coupling (disc type)

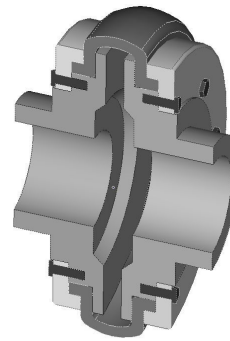


Fig. 5: Rubber-in-sheer coupling (tire type)

2.5 Rubber-in-compression couplings

These couplings have cylindrical or block type rubber elements which transfer the torque by compression (see Fig. 6).

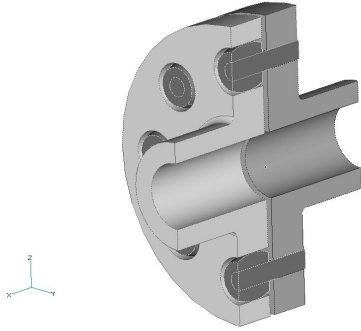


Fig. 6: Rubber-in-compression coupling

Like the rubber-in-shear couplings, different rubber materials are available to adjust the torsional natural frequencies. Sometimes the flywheel is utilized to be part of the coupling, so only one coupling-half is required.

3 Selection criteria and evaluation of the coupling types

3.1 Compensation of shaft misalignment

Experience shows, that the extent of shaft misalignment is rather low. Only the combination of *rigid flange couplings* and double-bearing motor leaves the possibility of bearing or shaft damages caused by heavy uneven foundation sag or non-uniform thermal vertical expansion of motor and compressor. Studies [4] report the former event to be the most frequent cause of crankshaft fractures. It is therefore advised to plan regular inspections of the alignment when double bearing motors are coupled by rigid flanges.

The basic function of *flexible couplings* is the compensation of shaft misalignment. Although the amount of possible shaft misalignment compensation differs to some extent within the different flexible coupling types, it can be generalized that they all serve this aspect more than sufficiently.

3.2 Height and characteristic of torsional stiffness

The height of the torsional stiffness is certainly the most decisive parameter for the dynamic drive train behavior. It determines the position of the lowest torsional natural frequency (TNF) relative to the speed harmonics which may drive destructive torsional vibrations. Tab. 1 gives an overview of typical positions for the different coupling types.

Considering that the highest torque amplitudes of reciprocating compressors are usually around the 1st to the ≈5th harmonic, Tab. 1 shows that *rigid flange coupling* installations with single bearing motors are usually well above that range. This means, that they are far off dominant excitation, but pass the high torque variations, coming from the compressor, on to the motor without any reduction.

Coupling type	Typical position of TNF in terms of speed harmonics
Rigid flange Single bearing motor	8th to 16th
Rigid flange Double bearing motor	4th to 8th
All-steel disc	3rd to 5th
All-steel diaphragm	3rd to 5th
Rubber-in-shear	< 1st
Rubber-in-compression	1st to 4th

Tab. 1: Typical position of the lowest torsional natural frequency (TNF) relative to the speed harmonics

There is often a high frequent torque variation superimposed because with harmonics higher than the ≈10th, it is hard to avoid resonances (→ the relative margin is always below 5% above the 10th harmonic).

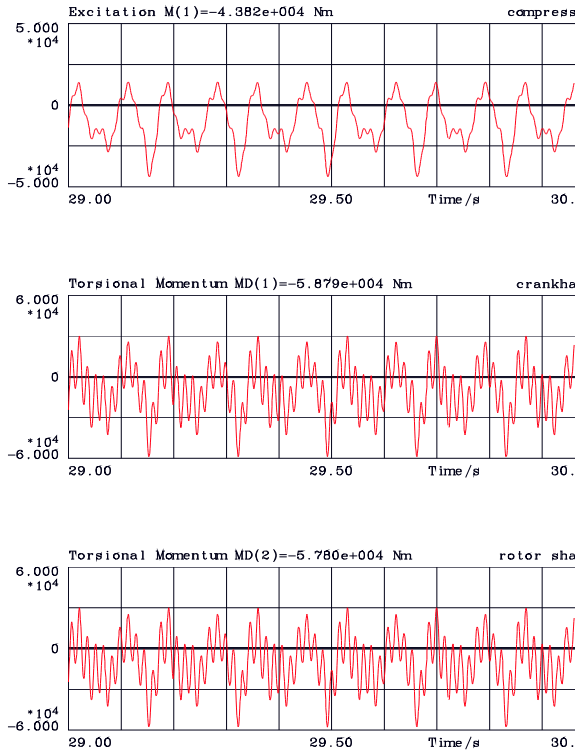


Fig. 7: Typical torque curves for rigid flange couplings at single-bearing motors showing the usual high frequent superimposed torque at crankshaft and rotor shaft

To sum it up, it can be said that all issues mentioned can be handled, but require close investigations.

Double-bearing motors flanged to the compressor crankshaft result in much lower TNF and are therefore much more critical.

All-steel couplings fall within the dominant compressor excitation harmonics (1st to ≈5th) regarding their TNF. This can be managed as long as the torsional stiffness characteristics are sufficiently known. Tests [5,6,7] show, that for some all-steel couplings, especially ‘turbo’ type couplings, the torsional stiffness value may differ by up to 100% from the value given on the coupling drawing (see Fig. 8).

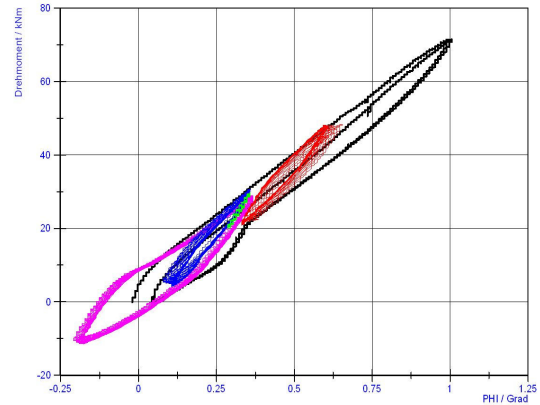


Fig. 8: Example of a torque-angle diagram for different load situations measured at a ‘turbo coupling’ (torque vs. torsional angle)

The torsional stiffness may be much load and frequency dependant. This fact makes it nearly impossible to design a drive train without the risk of a failure. Only a clear knowledge of the real torsional stiffness characteristic allows a save and secure dynamical design of the drive train.

Their low torsional stiffness is the main property of *rubber-in-shear couplings*. It is usually possible to find a coupling that produces a TNF below the 1st speed harmonic. The resulting low-pass filter effect almost eliminates all torque variations coming from the compressor. Consequently, the following motor also sees very little dynamic torque load and the electrical power fluctuations mostly come down to a negligible height. Fig. 9 compares crankshaft torque, coupling torque and rotor shaft torque for a torsionally rigid all-steel coupling and a soft rubber-in-shear coupling.

The outstanding torque reduction is also effective at all transient events like motor start, terminal short circuit, system transfer or re-connection of the power supply after a voltage drop. Only when using a frequency converter, care has to be taken at the motor start that the initial supply frequency does not fall in the range of the TNF.

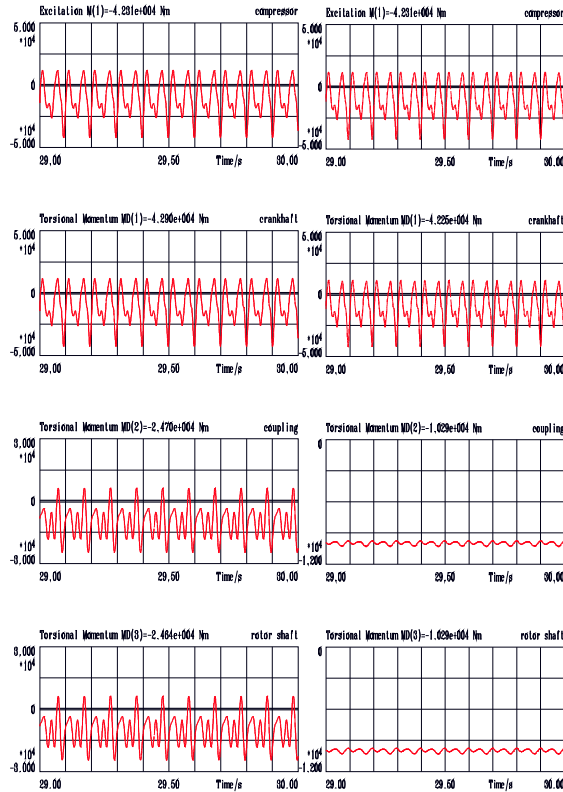


Fig. 9: Typical torque curves for rigid all-steel couplings (left) compared to rubber-in-sheer couplings (right)

Another advantage of the coupling's torsional softness compared to other parts of the drive train is illustrated in Fig. 10. At the bottom is a typical view of a rigid all-steel-coupling compared to a soft rubber-in-sheer coupling on top.

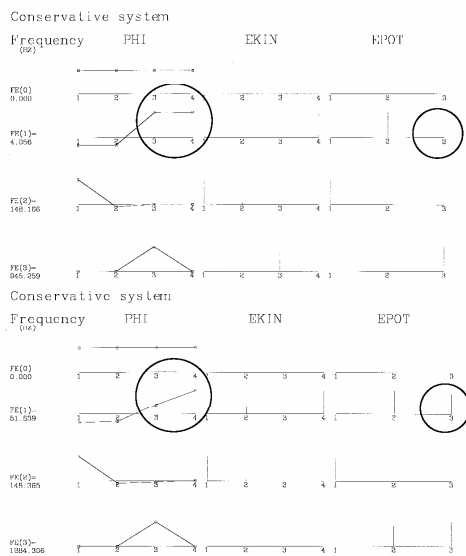


Fig. 10: Typical Eigenvalue-analyses for rigid all-steel couplings (bottom) compared to rubber-in-sheer couplings (top) → differences are marked by circles

It can be seen from the mode shape and the height of the potential vibration energy (EPOT), that for the rubber-in-sheer coupling the 1st TNF is only determined by the coupling (shaft #2) and not by the motor shaft stiffness (shaft #3) → circled. This means that all possible errors of the motor-shaft stiffness have no effect. (Experience shows that the correctness and accuracy of the motor-shaft stiffness has sometimes – depending on the motor manufacturer's calculation approach, the ratio of shaft diameter in the pole area to the drive end area and the fixation method of the poles to the shaft – to be questioned.)

A further benefit of the torsional softness of *rubber-in-sheer couplings* is the low number of required information needed from the motor manufacturer to design the drive train. Actually only the rotor inertia, the nominal power and the shaft drive end diameter is needed to select a suitable coupling. This allows the final selection of coupling and flywheel at a very early stage, a fact that is liked a lot by the people who have to design foundation and general arrangement.

The torsional stiffness of *rubber-in-sheer couplings* is usually considered to be constant within the torsional simulation. Actually this is not quite correct. Fig. 11 shows the dependence of the torsional stiffness by the torque amplitude for an example coupling at certain conditions.

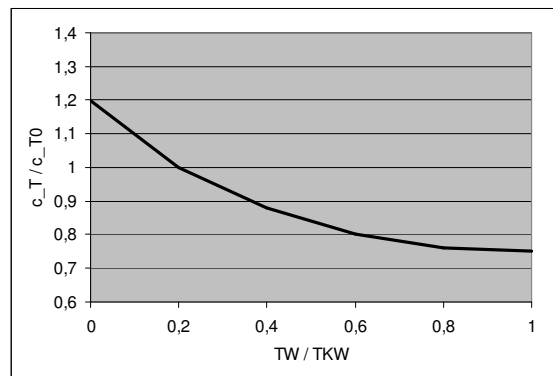


Fig. 11: Torque amplitude dependence of the torsional stiffness for a rubber-in-sheer coupling (example)

Further influences are mean torque, load frequency and temperature. There are simulation models for the coupling that try to cover these dependencies like [3], where the coupling is modeled as 7 Coulomb-Maxwell lines with non-linear friction and a non-linear spring in parallel. However, by keeping sufficient safety margins it is also possible to have a safe drive train using a constant stiffness value for the simulation.

Therefore the effort to find (by measurement) all required parameters for the more sophisticated coupling simulation model is usually not taken.

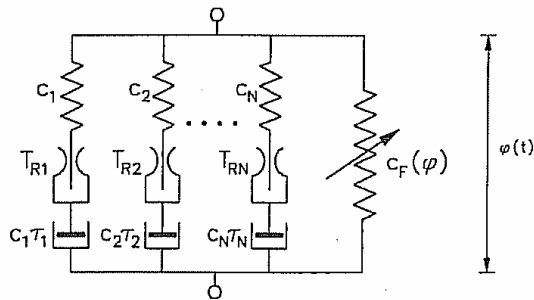


Fig. 12: Rheological model for elastomeric couplings [3]

Rubber-in-compression couplings, same as all steel couplings, end up in the dominant compressor excitation harmonic range. The manufacturers of these couplings give a non-linear torsional stiffness characteristic which makes it a bit more complicated to tune the drive train than having a constant stiffness value. Experience shows the given stiffness curves to be correct as there are not many coupling damages reported. The high damping of the rubber may have contributed to that. Summarizing: although it seems to be a bit tricky to have the TNF near the dominant harmonics, experience shows that this is feasible. But careful design of the drive train is required.

3.3 Maintenance

Flange couplings and all-steel flexible couplings have an unlimited life time and require no regular inspection unless they are exposed to aggressive atmosphere.

All *rubber type couplings* need examination of the rubber elements on a regular basis. This is because all rubber materials change their characteristics in course of the time. When asked for, the manufacturers of rubber couplings usually cannot guaranty life time because they do not know about the real dynamic operation load of the couplings. The service life however depends to a great deal on the dynamic torque loading. Coming back to experience, some typical numbers can still be given. If the drive train is well tuned in terms of torsional vibrations, the life span of a rubber-in compression coupling should be around 3 to 7 years and for rubber-in-shear 5 to 10 years. The longer time of rubber-in-shear compared to rubber-in-compression can be explained by the very low dynamic torque load as a result of the low torsional stiffness.

The rubber quality can be examined by checking the amount of small cracks and permanent deformation of the rubber. As all reciprocating compressors require maintenance stops after typically 6 to 12 months, these stops can also be used for checking the rubber elements. Therefore, the need for regular inspection of rubber element couplings can be considered to be a rather minor disadvantage.

Most rubber couplings allow the exchange of the elements without having to shift motor or compressor. Therefore, the effort of an exchange during a regular stop is rather low. When putting rubber spare elements on store, the shell life is a point of consideration. By proper preservation, the shell life should be around 10 years.

3.4 Dynamic torque load capacity

High torque variation, which is a typical feature of reciprocating compressors, has to be either reduced or sustained by the coupling. As explained above, only the high *flexible rubber-in-shear couplings* are able to filter out the high torque pulsations introduced by the compressor. All other coupling types have - more or less - to deal with these dynamic torque loadings.

For *rigid flange type couplings*, torque capacity is usually not much of an aspect at steady state operation. Only the transient torque at the beginning of a direct on line start (DOL) can be critical if a torsional natural frequency (TNF) is in the range of the power supply frequency. Then the torque peaks right after switching on the motor can be very high. The flange bolts have to be sufficient in number and preload to transfer these torque peaks by friction. The flange load is getting higher, if more inertia is put between the flanges in form of a flywheel. This is because the height of the torque peaks is - next to the distance to the TNF - directly related to the ratio of flywheel inertia to overall drive train inertia.

The manufacturers of *all-steel disc type couplings* often provide fatigue load diagrams where the admissible torque amplitude is given as a function of the mean torque. Fig. 13 shows an example.

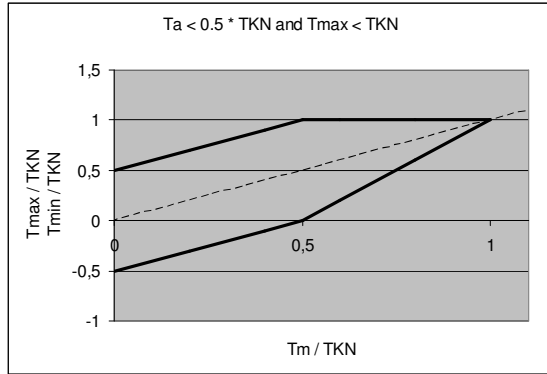


Fig. 13: Example of a fatigue torque load diagram of an all-steel disc coupling

Other manufacturers still use a service factor to evaluate the coupling strength. This method goes back to the time when it was not possible to quantify the dynamic torque load by means of simulation. The mean service torque T_m (derived from power and speed) was multiplied by a machinery type specific service factor “s” and the resulting value was compared to the nominal coupling torque T_{KN} .

$$T_m \cdot s < T_{KN}$$

The selected service factor “s” should cover the unknown torque variations at steady state operation and the peak torques during transient events. Today, this approach has to be considered as very rough. As experience shows that it is not even conservative, it should no longer be used.

The dynamic load capacity of the large and robust ‘pump couplings’ are usually relatively high. However, as described in the previous chapter, their torsional stiffness does not contribute to the reduction of torque variations coming from compressor and motor. Therefore their strength is often utilized to the limit.

The small ‘turbo-couplings’ are rather restricted in terms of fatigue strength. This is because their primary application is the high speed turbo compressor service where no dynamic torque load exists during steady state operation. Probably this is the reason why most turbo coupling manufacturers have not even tested the dynamic load limits of their couplings.

Rubber type coupling manufacturers give their strength limits dependent on temperature and load frequency. Often they follow the nomenclature of the former DIN 740-2. In addition, the coupling damping work is sometimes used for the dynamic load evaluation.

Rubber-in-compression type couplings, same as the all-steel disc couplings, are often fully utilizing the dynamic load capacity as they cannot provide sufficient reduction of the compressor torque.

High flexible *rubber-in-sheer couplings* usually ‘see’ only a very small fraction of the allowable torque amplitudes because of their low-pass filter effect. That is why the amount of strength utilization is normally no issue for this coupling type. Only if the natural frequency cannot be placed below the operational speed because of unusually low rotor inertia or low speed, this is a point that needs closer verification. However, this is rare. Sometimes, even when shifted into resonance within the simulation, the torque load remains uncritical.

3.5 Costs

For the purpose of assessing the costs for flexible couplings, a cost index can be defined as the ratio of price and nominal coupling torque. This evaluation seems to be reasonable because the required coupling size is closely related to its nominal torque. When proceeding like that, a cost index of 15 to 30 c/Nm (Euro-Cent per Newton-Meter) can be found for all types of flexible couplings. The price variation is rather high but there seems to be no coupling type that drops out of this range much in neither direction. Only some *diaphragm type couplings* may exceed this area a lot.

Spare part costs are also a point for *rubber type couplings*, but considering the long service span of the elements, this is not that much of an aspect.

Comparing *rigid flange type couplings* and *flexible couplings* in terms of costs cannot be done without considering the costs for flywheel and motor. Flange couplings in combination with single bearing motors often can do without flywheel so this money is saved. On the other hand, the expenses for single bearing motors are mostly high compared to double bearing motors. So, overall this can be considered to be the more expensive solution.

4 Overview of the coupling type evaluation

Tab. 2 summarizes the previous chapter.

	Compensation of shaft misalignment	Height and characteristic of torsional stiffness	Maintenance	Dynamic torque load capacity	Cost
Rigid flange coupl. Single bearing motor	0	+	+	+	-
Rigid flange coupl. Double bearing motor	-	-	+	+	+
All-steel disc coupling 'pump type'	+	-	+	0	+
All-steel disc coupling 'turbo type'	+	--	+	--	+
All-steel diaphragm coupling	+	--	+	--	0
Rubber-in-sheer coupling	+	++	0	+	+
Rubber-in-compression coupl.	+	0	0	+	+

Tab. 2: Overview

5 Guide lines and specifications

5.1 API 618

API 618 [1] p. 3.2.1.2 references API 671 [2] to be considered if specified. The coupling type shall be agreed on by purchaser and vendor of driver and driven equipment.

5.2 API 671

API 671 [2] generalizes all kind of coupling applications without clearly distinguishing between the different requirements of high-speed constant-torque machinery like turbo compressors and low-speed dynamic-torque machinery like reciprocating compressors. This makes it sometimes difficult to filter out what is really important for the given application.

Paragraph 1.1.3 names the coupling types which are covered in this standard and in appendix B.1 the use of torsional damping and resilient couplings is advised for trains in which potentially harmful torsional excitations occur during transient or continuous operation. Motor driven reciprocating compressors certainly belong to this kind. Therefore, whenever API 671 is specified, rubber type couplings are advised to be used.

6 Conclusion

A closer look to the pros and cons of different coupling types in reciprocating compressor installations allows the evaluation of the suitability in a more comprehensive way.

Rigid flange couplings at single bearing motors are free of technical disadvantages as long as they include most of the overall inertia within the motor. In commercial terms, these motors are situated on the more expensive side.

Rigid flange couplings at double bearing motors can be critical in the dynamic drive train design because of the slim motor shaft. The TNF usually ends up within the range of the dominant excitation harmonics. Furthermore, there is always the 'shadow' of possibly deteriorating alignment.

The 'pump type' *all-steel disc couplings* may be uncertain as to the height of their torsional stiffness and the TNF cannot be shifted out of the range of dominant excitation. Both could cause destructive resonances. This point is also supported by the fact that many operators put spare discs on store although this coupling type is considered to be free of maintenance → meaning bad experience exists.

The 'turbo type' *couplings, both disc and diaphragm*, are not suitable for reciprocating machinery because they fail in the two most important aspects for this application: certainty of torsional stiffness and dynamic torque load capacity.

The *rubber-in-sheer coupling* type without a major disadvantage and the outstanding benefits caused by its low torsional stiffness has to be considered to be the best suitable coupling for the reciprocating compressor application.

Rubber-in-compression couplings serve all criteria well, only the fact that the TNF is always near the dominant compressor harmonics leaves an unpleasant taste. However, careful drive train design makes this feasible.

7 References

- [1] API Standard 618, Reciprocating compressors for Petroleum, Chemical and Gas Industry Services, Fourth Edition, June 1995
- [2] API Standard 671, Special-Purpose Couplings for Petroleum, Chemical and Gas Industry Services, Third Edition, October 1998
- [3] FVA Forschungsheft Nr. 450, Forschungsvorhaben Nr. 139/III, 1995, Kupplungskennwerte - Standardisierte Kennwertermittlung für Elastomer-Kupplungen
- [4] Harrell, J.P., Smalley, A.J., Southwest Research Institute, San Antonio, Texas, Foundation Health and Compressor Reliability, issued at the EFRC Conference 1999 in Dresden
- [5] Confidential report: Measurements of torsional stiffness characteristics at an all-steel-disc type 'turbo' coupling, manufacturer "A"
- [6] Confidential report: Measurements of torsional stiffness characteristics at an all-steel-diaphragm type 'turbo' coupling, manufacturer "B"
- [7] Confidential report: Measurements of torsional stiffness characteristics at an all-steel-disc type 'pump' coupling, manufacturer "C"
- [8] FVA Forschungsheft Nr. 538, Forschungsvorhaben Nr. 263, 1997, Ganzstahlkupplungen – Berechnungsverfahren zum dynamischen Verhalten von Ringscheiben- und Laschenkupplungen



Torsional Design Considerations for Reciprocating Compressors

by:

Thomas J. Stephens, P.E.
Technical Services Department
Ariel Corporation
Mt Vernon, Ohio
United States of America
tstephens@arielcorp.com

**5th Conference of the EFRC
March 21-23, 2007
Prague, Czech Republic**

Abstract:

Torsional vibration is a very important consideration when designing reciprocating compressor machinery. Inherent vibratory torque produced from reciprocating machinery can result in catastrophic failure of crankshafts, motor shafts, couplings and auxiliary equipment if a system is improperly designed. Quite often, a torsional analysis has incorrect assumptions that may jeopardize the system design. This paper identifies the critical components and common shortcomings of torsional analyses.

Topics discussed: Mass Elastic Properties, Torque Excitation (including Load Step Selection & Optimization), Resonance Management, Speed Restrictions, Fatigue Analysis, and Field Testing.

1 Introduction

A torsional vibration analysis is a study of a mechanical system and how it responds to the vibratory torque that is inherently produced by the machinery and/or process. A thorough torsional vibration analysis entails several critical components as listed below.

Torsional models reduce the mechanical properties of a drive system into inertia and stiffness in order to calculate natural frequencies and mode shapes. These modes are then plotted against orders of run speed on an interference diagram (Campbell Diagram) to show where resonance interaction will occur between system natural frequencies and orders of excitation. For some low risk, constant speed applications, this may be sufficient to ensure the machinery is not operating at resonance or near electrical line frequency, but most applications with reciprocating compressors require a forced response analysis.

To perform a forced response analysis, the vibratory torque amplitudes must be predicted for the driver and compressor. Vibratory torque is produced from both inertial loads (reciprocating weight and speed) and gas pressure loads (operating pressures and cylinder configurations). All pertinent operating conditions should be evaluated, including partial loading and off design conditions (idle, misfire, valve failure).

A forced response of the system throughout the entire speed range is determined in a computer model. Amplitudes at resonance are determined by excitation amplitudes and system damping. Significant amplification of vibratory torque and angular deflection occur in most systems, which causes high stress levels, potential fatigue failures, and auxiliary end equipment drive problems. Viscous dampers and rubber couplings may add damping to the system and reduce amplification, but they will overheat and fail if overworked.

The end goal in a torsional analysis is to ensure all drive line components will operate safely at all pertinent loads and speeds. Predicted vibratory stresses are determined from the forced response analysis in order to conduct a fatigue analysis on driver and compressor shafting, ensuring a conservative design factor is applied. Damper and rubber coupling heat dissipation limits, and free-end angular deflections should all be within OEM limits. The coupling selection must also be confirmed.

There are several torsional design references available to mechanical designers. Material that is specifically recommended for review regarding the torsional design of reciprocating equipment includes technical papers by SWRI [1], EDI [3], the ANSI/ASME B106.1M standard [5], and the comprehensive works of Kerr Wilson [13] and B.I.C.E.R.A. [12]. This paper expands upon some of the topics discussed in the references noted above.

2 System Mechanical Properties

A torsional analysis begins with a mass-elastic model of the equipment to be analyzed. This is a reduction of the specific geometries and materials of the equipment to values of inertia, stiffness, and length. The mass elastic data is analyzed to determine the Torsional Natural Frequencies (TNF) of the system and their mode shapes. This data is usually available from the equipment manufactures, but should also be verified when possible.

2.1 Mass Elastic Variability

Mass elastic data has inherent variability due to tolerances, materials, and calculation variances that can lead to mass elastic differences. Significant errors in natural frequency calculations may occur, which can be particularly critical if a design depends on the placement of the systems natural frequency to occur in between orders of run speed to avoid excitation.

Two methods are common to deal with the variability of mass elastic data. One approach used by some analysts is to compute a lower and upper tolerance band for each component in the model and analyze a range of mass elastic parameters. The final system design can often be made to accommodate a range of possible natural frequencies for each mode, instead of exact values. An alternate method to account for input variability is to extend the speed range of the analysis and keep dangerous responses as far away from the active speed range as possible.

2.2 Motors

While reciprocating machinery is designed to accommodate high levels of alternating torque, this may be somewhat of a unique application for electric motors.

On reciprocating compressors, the mean nominal shaft stress calculated from the rated HP is a low percentage of material ultimate strength, typically only on the order of 1-3% per throw. Motor shafts are more commonly optimized for high mean torque applications with relatively low vibratory torque levels. Motor application engineers may not be familiar with the high vibratory torque levels associated with reciprocating equipment which is why a common recommendation from the compressor manufactures is to have the minimum motor shaft diameter to be equal to or larger than the compressor stub shaft diameter

Motor rotors are often over simplified and modeled as a lump sum inertia and stiffness; however, breaking apart the rotor shaft into different elements based on diameter changes offers some advantages. Modeling motor rotors with multiple stiffness and inertias allows for increased accuracy of the mode shape representation, stress and fatigue calculation capability at each location along the rotor, and it can be used to verify the manufactures stiffness and inertia calculations. Several resonance issues have developed because the rotor mass/elastic properties were different than what was calculated by the manufacturer.

Another factor in modeling rotors is the influence of the core and spider bars on rotor stiffness. A way to evaluate these effects is to model the rotor with both a rigid and soft core assumption to determine if these variances in stiffness will appreciably affect the design. A Finite Element Analysis (FEA) of the rotor assembly is another more advanced technique that may provide better results.

2.3 Engines

Engine mass/elastic data is typically provided by the manufacturer. They have significant counter weights to consider and free end dampers are typically installed to help protect the engine gear trains. Damper inertia is typically calculated by adding 1/2 of the inner disk inertia to the damper outer housing inertia. Some engines use multiple dampers on reciprocating applications.

Engines typically have a large drive end fly wheel which helps to isolate the equipment, making separable natural gas engines more benign than motors for reciprocating packages. In addition, the power cylinders also tend to add system damping.

2.4 Drive End Flywheels

Compressor drive end flywheels are common on separable reciprocating compressor and provide several benefits. Flywheels can be sized to tune the system natural frequency in between orders; however, if a flywheel exists at a node, then increasing the size will not reduce the frequency of the mode. Large inertias tend to dominate mode shapes and can be accurately predicted, increasing modeling accuracy. Drive end compressor flywheels, due to their high inertia, significantly reduce the alternating torque transmitted to the coupling and driver by the compressor.

2.5 Couplings

Typically, disk-pack couplings are installed on compressor applications that do not require soft coupling isolation. Disk pack couplings are considered torsionally rigid and are preferred from a maintenance and cost standpoint if they can be made to work. When selecting a disk-pack coupling, one should use a service factor of 3 or higher. Published coupling stiffness values may not be exact and actual values may vary by more than +/- 20%. Another common mistake is related to how the stiffness data is published. Coupling stiffness may be given with, or without, 1/3 shaft penetration included which can vary the results considerably. Some analysts have found using a 2/9 penetration factor leads to more accurate stiffness calculations

Torsionally soft couplings can effectively isolate the compressor from the driver, but they have many design challenges and maintenance draw backs that need to be addressed. With rubber couplings, the 1st TNF (system or coupling mode) is usually placed well below the fundamental run speed to avoid excitation of this mode. On occasion, this mode has been placed between the 1st and 2nd order when appropriate. Because this design technique places the 1st mode TNF so close to the fundamental operating frequency, the first mode is often influenced by the 1X torque vibration, which can be substantial when single acting load steps are utilized. Coupling heat loads must be calculated at part load operating conditions (i.e. single acting cylinders) to ensure a reliable design.

Some soft couplings are designed with a continuous oil supply which allows for higher heat rejection and increased damping.

These types of coupling can offer a significant amount of damping and may allow for operation at resonance. Oil is usually supplied from the engine crankshaft and oil viscosity is a key factor that determines the couplings effective damping. Predicted oil viscosity at operating temperature should be confirmed in the design phase by the engine manufacturer. Most other soft couplings have to reject heat by convection and are limited as to the amount of angular displacement they can handle without overheating.

Rubber couplings are either designed for loading in shear or compression. Couplings designed to operate in compression complicate the design because the stiffness of the coupling is not linear. As mean torque (power) increases, the coupling stiffness also increases as the rubber is compressed. Although the design is complicated, the bonding is less apt to “shear” in these types of couplings and some analysts consider them more industrial. For either style rubber coupling, the designer should specify a service factor of 5-6 (2X catalog rating with a SF of 3) to ensure maximum reliability. Some coupling vendors, if requested, can test and match individual elements to guarantee initial coupling stiffness.

All rubber is subject to stiffness variations as the rubber changes temperature or ages. These effects must be considered in the design.

2.6 Compressors

Compressor mass/elastic data is provided by the manufacturer and is usually calculated with modern design software. Reciprocating throw inertia can be different for every compressor configuration and must be included. Counter weights, if applicable, are also included.

As an aid in detuning resonance, crankshaft detuning disks or internal flywheels may be available. Detuners are inertial clamps that can be clamped to the spreader section of a crankshaft to lower system natural frequencies. These clamps also can slightly change the stiffness in the same way a hub does on a stub shaft and the stiffness effects may need to be considered in certain applications.

Care should be taken to ensure that any additional tuning inertia attached to the drive train is properly modeled on the correct element in the mass-elastic system. Auxiliary end flywheels may not be automatically attached to the end element.

Review the mode shape to ensure the model is correct as any mechanically attached inertial device should not have high deviations across a single station.

3 Torque Effort

Proper interpretation of the dynamic loads of the system is critical to achieve a safe, reliable system. With some extra effort, the torsional design can also be optimized by loading the unit in the most torsional friendly method.

3.1 Vibratory Torque

Vibratory torque from a compressor or engine is created by two components: Gas Torque (internal bore pressure on the pistons), and Inertial Torque (reciprocating weight). Gas torque depends mainly on compressor loading, and is relatively consistent over speed. Inertial torque is a function of speed (squared). Some analysts prefer to receive only the gas torque effort coefficients and calculate inertial torque in their software. This makes automating runs for a given speed range much easier.

Compressors are capable of a wide range of loading techniques, which considerably impact the torsional design. To reduce capacity and load, cylinders can change clearance volume or deactivated ends in a multitude of ways. Separable compressors also come in a multitude of configurations, consisting of a wide range of bore sizes, reciprocating inertia, and multiple throws (opposed 2, 4 & 6 throws are common on separable compressors). This creates a wide array of loading and vibratory torque signatures.

Typically, the torque effort curve is calculated from compressor prediction software in the time domain. This curve is evaluated in frequency with a FFT, and the frequency coefficients (up to the 24 order) are computed for use in a forced response computer model.

3.2 Load Step Selection/Optimization

One of the most critical aspects of a successful torsional analysis is to determine which load steps need to be analyzed and what load sequence should be implemented. Often, the compressor manufacturer is willing to help with this process.

DRIVE TRAIN

Torsional Design Considerations for Reciprocating Compressors, *Thomas Stephens; ARIEL CORPORATION*

As a general concept, it is favorable to minimize vibratory torque at the free end of the compressor because most mode shapes have the highest amplitude deflection at the free end. It is also favorable to have symmetrical loading, when possible. If asymmetric loading is required (i.e. end deactivation), it should be done gradually up the side of the compressor so each pair of throws share the unbalance. Two throws deactivated side by side can reduce peak to peak vibratory torque 25% or more compared to deactivating opposing cylinders.

As an example (Figure 3.2.1): a six throw, single stage compressor with end deactivation should be loaded such that the deactivation starts at the drive end, and continues up one side and back down the other. This will generally produce the lowest vibratory torque amplitudes. While this may be the friendliest way to load the unit torsionally, it may not be the best way to load it acoustically and the design engineer must determine which way the system should be optimized. Acoustical, mechanical, and torsional studies rarely interact in the design phase, which is recommended for complete system optimization.

Torque Effort Coefficients for Various Unloader Configurations (6throw, single stage compressor)

Load Configuration	1x	2x	3x	4x	5x	6x	7x	8x	9x
No Single acting	0	0	119397	0	0	30796	0	0	12767
SACE Throw 1	47439	48795	106084	2968	6271	26678	588	2015	11432
SACE Throw 1 & 2	94877	97591	93341	5936	12541	22664	1176	4029	10127
SACE Throw 1 & 3	47439	48795	93341	2968	6271	22664	588	2015	10127
SACE Throw 1, 3, & 5	0	0	85238	0	0	18757	0	0	8863

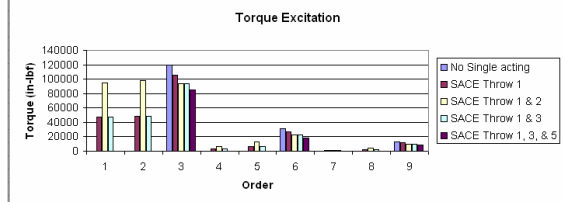


Figure 3.2.1

A secondary example (Figure 3.2.2) involves the placement of second stage cylinders. A 4-2 opposed (four first stage cylinders with 2 opposed 2nd stage cylinders) generates higher vibratory torque than a 4-2 aside configuration. A 3x3 (3-1st stage cylinder on one side and 3-2nd stage cylinders on the other side) generates even less vibratory torque.

Torque Effort Coefficients for Various Stage Configurations (6throw, two stage compressor)

Load Configuration	1x	2x	3x	4x	5x	6x	7x	8x	9x
4-2 opposed	46642	60382	97186	4912	5896	24867	5707	4506	5033
4-2 aside	39308	31204	99440	5930	3010	24867	4080	1926	5033
3-3 Symmetric	27234	26996	87006	2032	2820	20921	1184	891	4354

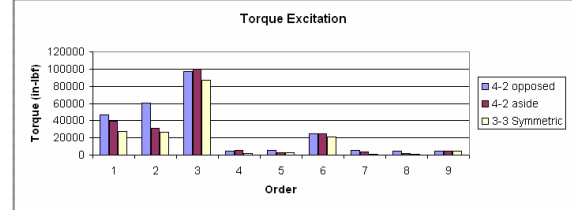


Figure 3.2.2

3.3 Engine Excitation

Engine torques are done in a similar fashion as compressors, but 4-cycle engines take two revolutions to complete a cycle so 1/2 orders also have to be computed and analyzed. Engine torque coefficients are sometimes published as a function of BMEP (0% and 100%) so part load excitations can be interpolated. Care must be taken as to the sign convention used as engines produce drive torque, while compressor torque is driven.

Engines typically have a 25% turn down, so resonance issues will exist. It is not practical to assume that an engine will only operate at a single speed throughout its life and leave critical resonances within the operational speed range (from idle speed to rated speed). Engines also require some operation at idle for warm-up or cool-down which needs to be considered in the analysis. Operating at resonance, even at idle, can cause severe damage.

Miss-fire conditions are real load conditions that should be considered. Typically, a misfire on the #1 cylinder will cause the highest torque fluctuations critical to the engine, but other cylinders operating under misfire may be important to higher modes and create unfavorable system responses.

Engines have a "Roll Torque" associated with them that can vary with engine design. Roll torque is a result of the phasing between cylinder compression cycles and counterweights, which results in angular speed fluctuations, especially at low speeds. Roll torque effects can easily be felt when barring an engine over by hand. Engine manufacturers can provide more information upon request

Another unique aspect about engine/compressor combinations is that they can be affected by coupling phasing. Some harmonics produced by the engine may match up with compressor harmonics (i.e. 6th order in a 12 cylinder engine and a 6 throw compressor). The effects of these harmonics can be influenced by the phasing of the engine to compressor. One field study noted a 50% reduction in angular deflection of the compressor free end when the coupling was shifted one bolt hole out of a 12 bolt flywheel adaptor. Very few torsional providers consider phasing between components on a regular basis.

3.4 Motor/VFD Excitation

The main torsional problem associated with Variable Frequency Drives (VFD) is the fact that a VFD will operate over a wide speed range (typically 50% turndown or better), inevitably allowing operation at multiple points of resonance. Often, speed restrictions will be required to prevent operation at resonance, and a soft coupling may be needed to isolate the compressor from the driver. Drive manufacturers usually have the ability to programmatically omit certain speeds from operation due to resonances. Resonance management is difficult and somewhat risky as many factors of the design are estimations at best, such as true torque excitation and system damping. End users who wish to utilize VFD's in reciprocating compressor applications should be made aware upfront that some speed restriction within their desired operating range may be required.

Motors and VFD's rarely generate any torque excitations of interest. VFD's produce some high frequency excitation at electrical switching frequencies, but they are usually too high in frequency to stimulate the mechanical drive train. Drive manufacturers can be consulted to estimate torque pulsations by simulating current or voltage wave forms produced by the drive at multiple speed points.

Another rare issue with variable speed drives can occur when the drive is set up to control the torque or speed of a motor at a frequency that coincides with a system natural frequency. The drive can effectively function as an instable control loop and create severe torque fluctuations. This problem is very difficult to prevent before hand, but it can usually be solved by changing some of the control parameters in the VFD software.

3.5 Other Torque Excitations

Cardan Joints (U-Joints) create speed fluctuations at two times run speed. The effect can be canceled if two joints are used in parallel with phased yokes (i.e. CV Joints), but compound angles or out of phase yokes aggravate the speed fluctuation. These are sometimes used to drive cooler fans and can be the cause of chronic blade failures.

Infinite step unloaders also produce unique torque signatures in the drive train. The infinite step valve unloader forces reverse flow through the suction valve for part of the cycle before allowing the suction valve to close. The process produces an impact-like torque pulse in the drive train on high speed compressors that can damage soft couplings.

4 Forced Response & Resonance

Torsional resonance occurs when a vibratory torque at some harmonic of run speed occurs at the same frequency as one of the system torsional natural frequencies. This condition amplifies the response of the system by a factor of 10 to 100 on most applications.

The initial design goal of a torsional study is typically resonance avoidance. If an application requires variations in speed to control flow and power, the goal changes from resonance avoidance to resonance management as the ability to avoid all resonant interferences for all modes become impractical. Often, speed segments within the operational speed range will require avoidance to prevent torsional problems from occurring.

4.1 Damping

The amplification response at resonance depends on system damping. Damping transforms motion into heat from either fluid shear (Viscous Damping), or from structural deflection (Hysteresis Damping). Compressors achieve a small amount of viscous damping from the oil in the journal bearings. Viscous dampers can also be attached to the drive train to increase system damping. Rubber couplings have significant hysteresis damping due to the flexing of the elements.

From experience and measurement, reciprocating machinery with rigid couplings have critical damping ratios near 2% for smaller frames and closer to 1% for larger frames (crankshafts over 6 inches or 150 mm in diameter). Soft coupling applications have modes that are dominated by hysteresis damping. The percentage of damping varies depending on what couplings are utilized.

4.2 Non Resonant Response

Although resonant amplification is usually the main design concern, the vibratory torque levels in some application can be so severe that shaft integrity may be a concern in non-resonant conditions. Two throw compressors generate very large vibratory torque demand. If fatigue calculations show low design factors for these applications, larger shafting, bigger couplings, and/or flywheels may be required to ensure a safe design.

5 Fatigue Analysis

In North America, shaft fatigue analysis in torsion usually incorporates a Stress-Life design as industrial compressor applications must be designed for infinite life; as apposed to the Strain-Life method which typically is used for finite life applications. The Stress-Life fatigue design method is associated with work done by Marin and is commonly referenced in most machine design text books, including the popular Shigley reference [2]. The design process is somewhat complex, and often factors are misinterpreted or omitted, resulting in incorrect design safety factors. Two other references that thoroughly describe this method of fatigue design for shafting include the ANSI/ASME B106.1M 1985 [5] document on Transmission Shafting Design, and a SWRI document presented at the 2005 GMRC [1]

Fatigue analysis starts with the determination of critical locations in the drive train, which is dependant on shaft geometry, loading, and mode shapes. Some designers compute design factors at all locations in the model and report worst case. The key components that determine critical crankshaft locations include diameter, stress concentration factor, and the size factor. Diameter is the most important variable as the influence it has on shear stress is to the 3rd power:

One major factor that is sometimes overlooked is the effect of intensified stress due to geometrical stress concentration factors inherent in every component of complex geometry. Nominal torque applied to a straight shaft will have increased stress in location of geometrical changes, such as U-grooves, counterweight webs, pin webs, and oil holes.

Intensified alternating stresses must be compared to the material endurance limit to determine a design factor of safety. The material endurance limit is corrected for a multitude of factors, called Marin factors or modifying factors. These include surface finish, size, loading, temperature, reliability, and miscellaneous effect.

In the final determination of the design safety factor, the magnitude of alternating intensified stress ratio to endurance limit and the un-intensified mean stress ratio to yield or ultimate strength must be considered. Several failure criterion relationships have been developed with the Modified Goodman being the most widely used.

5.1 Shear Stress vs. Von Mises Stress

Torsional vibration results in shear stress on the drive shafting. To calculate shear stress from vibratory torque, the peak vibratory torque (T), calculated from the wave form [(peak-peak)/2] or [(Max-Min)/2], is utilized in the following equation (D=shaft diameter):

$$5.1.1 \quad \tau = \frac{16 \times T}{\pi \times D^3}$$

Although torsional vibration produces shear stress, it simplifies some of the stress concentration calculations, and provides flexibility for complex loading, if an effective equivalent stress is considered in the analysis instead of shear stress. Effective equivalent stress is commonly called Von Mises stress named after Dr. Von Mises who contributed to the theory. For pure torsion, the Von Mises equivalent stress is obtained from the following relationship:

$$5.1.2 \quad \sigma = \sqrt{3 \times \tau^2}$$

A common error in torsional fatigue analysis involves the endurance limit modifying factor Kc or the load factor. If the analysis is done in shear stress, then this factor is applied at .577 for torsional loading; however, if stresses are converted to Von Mises first, this factor remains at one (1).

5.2 Stress Concentration

Stress concentration factors (SCF) can realistically be as high as a factor of 3. These values can be accurately calculated with FEA analysis, which is becoming a very common tool for most designers. One can obtain a SCF from FEA by creating a finite element model with a fine mesh around the geometry trait of interest, and then apply a nominal torque to the model. The ratio between the peak stress in the area of interest and the nominal stress can be considered the stress concentration factor (SCF).

Other Popular sources for determining stress concentration factor are from well known references such as Peterson [7], and empirical curve fits to the Peterson plots by Roark & Young [4, 10]. This is a critical part of the calculation, and has been an oversight in many problematic applications.

5.3 Endurance Limit

The endurance limit as described by Marin and Shigley [2] consists of a rotary beam endurance limit (S_e') multiplied by several modifying factors to apply that limit to a real life geometry.

5.3.1.1 $S_e = S_e' * K_a * K_b * K_c * K_d * K_e * K_f$

The various K factors correct for surface finish, size, loading, temperature, reliability, and miscellaneous effects.

5.3.2 Rotary beam Endurance - S_e'

Material endurance limits have been determined for most steels by rotary beam fatigue testing of .3" R. R. Moore specimen. Typically for steel, the fatigue endurance limit in bending for rotary beam test specimen averages to be 1/2 of the ultimate strength. Mischke [6] determined this factor to be .49 to .504 from some Naval Weapons test data. An independent analysis on the data confirmed that a .5 factor represented the data with a standard deviation of seven (7) percent.

5.3.3 Surface Factor - K_a

Surface factors can be determined by empirical equations or plots. They are typically grouped into four categories: "Ground", "Machined", "Hot Rolled", and "As Forged". Modern day crankshafts and motor rotors can usually be considered "Ground" or "Machined".

Equation 5.3.3.1 shows the surface finish factor for ground material as referenced by Shigley [2].

$$\begin{aligned}
 \text{5.3.3.1} \quad K_a &= a S_{ULX}^b \\
 a &= 1.34 \left[S_{ULX} \text{ KPSI} \right] \\
 a &= 1.58 \left[S_{ULX} \text{ MPA} \right] \\
 b &= -.085
 \end{aligned}$$

5.3.4 Size Factor - K_b

The size factor is an attempt to correct for the differences in fatigue strength that is evident from a standard .3 in (7.62 mm) diameter fatigue test sample to that of a large diameter shaft under similar stress levels. The factor has been derived from a limited amount of large diameter shaft fatigue test data documented over the last 60 years. It is the Author's opinion that this factor has been applied in an overly conservative manner for torsional applications in most modern day references.

Common Size Factor Equations

$$\text{Shigley7th: } K_b = \left(\frac{D}{.3} \right)^{-1.07} \quad (D < 2 \text{ inches})$$

$$\text{Shigley7th: } K_b = .91 * (D)^{-1.57} \quad (D > 2 \text{ inches})$$

$$\text{B106.1M: } K_b = \left(\frac{D}{.3} \right)^{-0.68} \quad (D < 2 \text{ inches})$$

$$\text{B106.1M: } K_b = (D)^{-1.19} \quad (D > 2 \text{ inches})$$

$$\text{Mischke: } K_b = \left(\frac{D}{.3} \right)^{-1.133} \quad (D = \text{inches})$$

Figure 5.3.4.1 - D =Diameter (inches)

A historical review was conducted in attempts to understand the origin of the size factor, with some interesting results. A publication in 1952 [14] documented fatigue test results on rail road axles, which appears to be the general basis for the size effect. The test shafts were contoured to maximize stress over a large area with little to no stress intensification.

DRIVE TRAIN

Torsional Design Considerations for Reciprocating Compressors, *Thomas Stephens; ARIEL CORPORATION*

Testing results showed that these shafts typically broke at about 65% of the stress level that was required to break R. R. Moore standard fatigue test samples of the same material which are only .3” (7.62 mm) diameter. These results manifested themselves into a size factor that was typically noted as a function of diameter. Of interest to note was that all fractures occurred within a specific 21” span (533 mm) designed to be at 96% or higher stress level.

Another interesting reference by Kuguel [8] noted that these effects could be better explained if they were referenced to a stress volume level instead of a diameter. Kuguel [8] analyzed a multitude of samples with different sizes, materials, and geometries (including notched specimen). He plotted the results against a predicted 95% stress volume (on log scale) and was able to show that all the data fell within 10% tolerance bands except for 2 data points. The exponential slope for all materials and geometries remain constant at -.034.

Some FEA work was done to confirm 95% stressed volume levels of the fatigue samples documented in a multitude of historic papers. The standard R.R. Moore sample have a 95% stressed volume of .00117 cu in (19 mm³), while the 6” rail road axle specimen had over 25 cu in (409 cu cm) 95% stressed volume. Utilizing the volume relationship to a standard R. R. Moore sample (of which there is a large population of statistical fatigue data), the following size factor relationship was developed by Hope, C. W. at Ariel:

$$5.3.4.1 \quad K_b = \left(\frac{V}{.00117(in^3)} \right)^{-0.34}$$

$$K_b = \left(\frac{V}{19.173(mm^3)} \right)^{-0.34}$$

This equation directly reproduces the diameter based size factors for rotating bending test results in all references (Shigley [2], Mischke [6], and ANSI B106.1M [5]). Where the diameter based size factor becomes overly conservative in torsional applications become apparent when one looks into the volume of material that the typical stressed to 95% from torsional loading. Drive shaft designs usually have considerable stress intensification due to geometrical characteristics, yet the volume associated with the high stress is very small. Stress concentration and stressed volume are inversely related. Applying both a large SCF and a large size factor (inappropriately based on diameter), results in is overly conservative design.

Both the Shigley [2] and ANSI B106.1M [5] reference the work by Kuguel [8], but they incorrectly reduced the work of Kuguel [8] into an effective diameter, not volume.

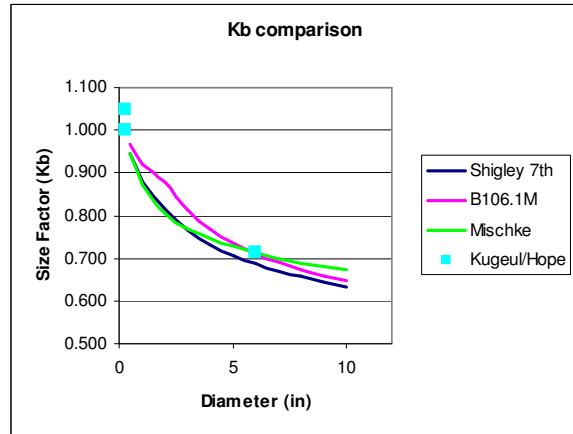


Figure 5.3.4.2

Per FEA analysis, Ariel has determined some simple, conservative, 95% stressed volume calculations for typical crankshaft geometries (Figure 5.3.4.3).

95% Stresses Volume for Size Factor Calculations

U Groove	L=PI*D (Circumference)	W=Radius	D=.015” (.318 mm)	V=L*W*D
Counter Weight Groove	L=PI*D/2 (Circumference/2)	W=Radius	D=.015” (.318 mm)	V=L*W*D
Pin Web	L=PI*D/3 (Circumference/3)	W=Radius	D=.015” (.318 mm)	V=L*W*D
Oil Hole	Diameter = .150” (3.81 mm)	Qty = 2	D=.015” (.318 mm)	V=PI(Diam ² /2)/4*D*2

Figure 5.3.4.3

5.3.5 Load Factor – Kc

As discussed earlier in the paper, this factor should be 1 if Von Mises stresses are used in the analysis, and .577 if shear stresses are used.

5.3.6 Temperature Factor - Kd

The temperature factor is not significant unless the steel is operating over 250 degrees C (~500 Deg F). A factor of 1 can usually be assume, but a detailed table of factors can be found in Shigley [2].

5.3.7 Reliability Factor - Ke

The reliability factor accounts for the statistical deviation of the rotating beam endurance test data. A standard deviation is typically less than 8 percent. If a reliability of 90 percent is desired, which relates to 90 percent of the test data not failing, one can determine a Transformation Variate (Za) of 1.288. The reliability factor of 90% can be determined by equation 5.3.7.1 (Shigley [2]).

5.3.7.1 Ke = 1-.08*Za

Common reliability factors are listed in fig. 5.3.7.2:

%	Za	Ke
50	0	1
90	1.288	0.897
95	1.645	0.868
99	2.326	0.814

5.3.7.2

5.3.8 Miscellaneous Factor – Kf

This factor is typically applied as 1, but may be another value if electro plating, corrosion, residual stress, metal spray, or other unusual factors are documented to somehow reduce or improve the material endurance limit.

5.4 Failure Criterion

To evaluate a design in fatigue, a failure criterion calculation is used to develop a design factor of safety. A minimum acceptable design factor for compressor shaft fatigue should be held to 1.5 or higher if the analyst has confidence in the input data. If data is suspect or a project demands conservatism (critical machinery, unknown loading, remote location, etc), design factors of two (2) or higher may be more appropriate. Motors design factors should be 2 or higher to ensure long term acceptability, especially if the rotor has any welded components.

As stated earlier, the Modified Goodman approach is one of the most widely used formulae in fatigue evaluation. A diagram of this approach, along with other approaches, is listed in the appendix (Figure 5.4.1.1 and 5.4.1.2). All failure criterion equations evaluate (in various ways) the intensified alternating stress ratio to the material endurance limit stress, and the un-intensified mean stress level ratio to the yield or tensile material limit.

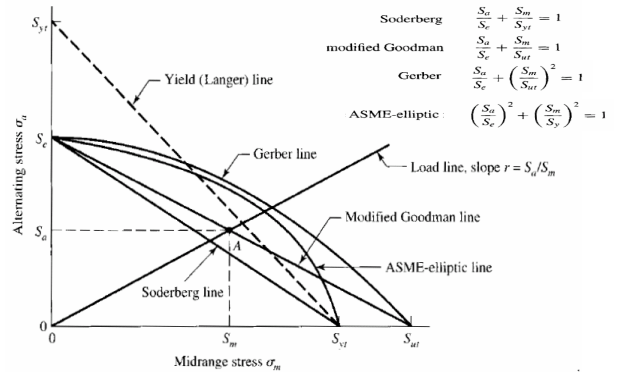


Figure 5.4.1.1

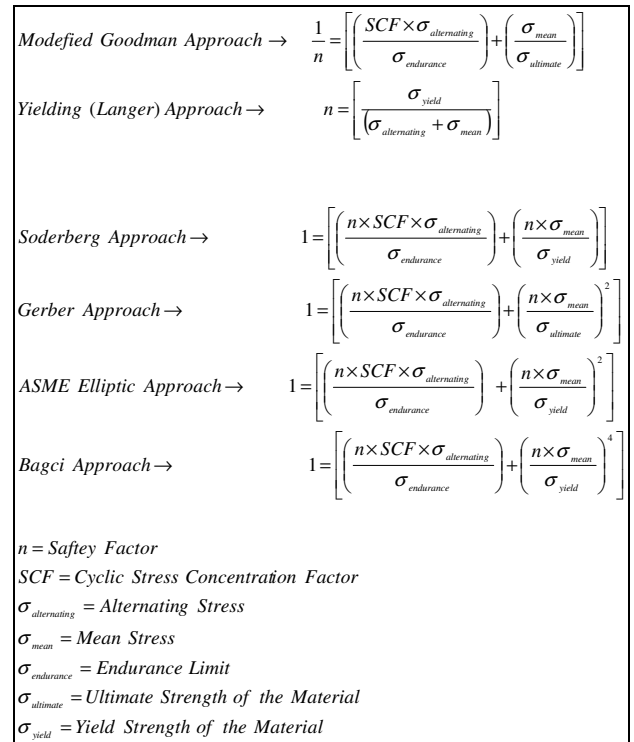


Figure 5.4.1.2

For torsion, the mean torque does not have a very significant contribution to fatigue failures in shear, so the preferred approach (in this author's opinion) is the ASME elliptic or Gerber approach. Both of these approaches discount the mean torque in the safety factor calculation by taking the ratio of the mean torque to the ultimate (or Yield) strength squared. The B106.1M [5] standard prefers the ASME Elliptic approach.

In addition to fatigue concerns, the peak stress (vibratory stress + mean stress) should be checked against the yield strength of the material to ensure acceptability from a yield stand point; although, this is rarely a problem for torsional applications with relatively low mean torque levels.

6 Field Testing

Angular deflection measurements can be obtained at multiple locations in the drive train and amplitude data can be used to confirm forced response predictions. Encoders can usually be installed at the free ends of the machinery, which is where the highest mode shape deflections typically occur. Any rotating gear with equally spaced teeth can be used to measure angular displacement. Doppler Laser equipment is also available for angular displacement measurements. Strain gauges and telemetry devices can be installed on straight shafting or coupling inner members to measure and confirm vibratory torque levels. Angular displacement and/or strain measurements can be used to determine system natural frequencies during start up or coast down transients.

7 Conclusions

Many factors go into a torsional analysis to ensure a safe design. Variability in mass elastic data, torque effort prediction, and system properties such as damping and material endurance limits, leave this key part of the design process open to interpretation and error. Field testing is recommended for critical machinery in order to verify the analysis.

8 Acknowledgements

I would like to thank D. McCoy, K. McDonald and others at Ariel Corporation for supporting the effort to better inform the compression industry about torsional vibration analysis. I would also like to thank the numerous consultant companies that I have had the privilege to work with on the subject, including RBTS, EDI, BMA, ARLA, SWRI, IDC, CAT, WED and others.

References:

1. SWRI/GMRC, "*Recommended Practice for Control of Torsional Vibrations for High Speed Separable Reciprocating Compressors*", GMRC, 2005
2. SHIGLEY, J. E., MISCHKE, C. R., and BUDYNAS, R. G., "*Mechanical Engineering Design*", 7th ed., McGraw-Hill, New York, 2004
3. FEESE, T. D. & HILL, C., "*Guidelines for Improving the Reliability of Reciprocating Machinery by Avoiding Torsional Vibrations Problems*", EDI/GMRC, 2001
4. YOUNG, W. C., "*Roark's Formulas for Stress and Strain*", 6th ed., McGraw-Hill, New York, 1989
5. ANSI/ASME B106.1M-1985, "*Design of Transmission Shafting*", ASME, 1985
6. MISCHKE, C. R., "*Prediction of Stochastic Endurance Strength*", Trans. of ASME, Journal of Vibrations, Acoustics, Stress, and Reliability in Design, Vol. 109, no. 1, January 1987, pp. 113-122
7. PETERSON, R. E., "*Stress Concentration Factors*", John Wiley & Sons Inc., 1974
8. KUGUEL, R., "*A Relationship Between Theoretical Stress Concentration Factor and Fatigue Notch Factor Deduced From the Concept of Highly Stressed Volume*", Proceedings of ASTM, Vol. 61, 1969, pp. 732-748
9. JUVINALL, R. C., "*Engineering Considerations of Stress, Strain, and Strength*", McGraw-Hill, New York, 1967
10. ROARK, R. J., "*Formulas for Stress and Strain*", 4th ed., McGraw-Hill, New York, 1965
11. HEYWOOD, R. B., "*Designing Against Fatigue*", Chapman and Hall LTD. London, 1962
12. NESTORIDES, E. J., "*A Handbook on Torsional Vibrations*", British Internal Combustion Engine Research Association (B.I.C.E.R.A.), 1958
13. WILSON, W. K., "*Practical Solutions of Torsional Vibration Problems*", John Wiley & Sons Inc., New York, 1956
14. HORGER, O. J. and NEIFERT, H. R., "*Fatigue Properties of Large Specimens with Relative Size and Statistical Effects*", Symposium on Fatigue with Emphasis on Statistical Approach, Special Technical Publication No. 137, ASTM, 1952
15. MOORE, H. F., "*A Study on Size Effect and Notch Sensitivity in Fatigue Tests on Steel*", Proceedings of ASTM, Vol. 45, 1947, p. 507



Optimisation of Reciprocating Compressor Plants by using Flexible Couplings supported by Advanced Engineering Methods

by:

Dr.-Ing. Andreas Laschet

Managing Director

ARLA Maschinentechnik GmbH

Hansestraße 2

D-51688 Wipperfürth

Germany

E-mail: a.laschet@arla.de

Dr.-Ing. Michael Matzkeit

Test Department

VULKAN Kupplungs- und Getriebbau

B. Hackforth GmbH & Co. KG

Heerstraße 66

D-44653 Herne

Germany

E-mail: michael.matzkeit@vulkan24.com

**5th Conference of the EFRC
March 21-23, 2007
Prague, Czech Republic**

Abstract

An important aspect of reciprocating compressor plant engineering is the torsional vibration calculation in order to identify sources of critical vibrations, which may lead to damage of the rotating elements. Besides geometrical boundary conditions, the operating parameters and load conditions of the compressor influence the unit behaviour with respect to the occurrence of vibrations. The paper presents advanced computer-based engineering methods helping to predict critical vibrations, taking into account the whole range of the possible operating parameters of the plant. With a view to maximum energy efficiency, this is important for both full load and especially partial load conditions. It was found that the use of flexible couplings with natural rubber elements, which are state-of-the-art in a wide industrial field, often gives advantages over stiff steel couplings when considering variable operating speed ranges. With flexible couplings the torsional system can be easily tuned, i.e. the natural frequencies can be shifted so that the required operating speed range is no longer critical. Thus, the compressor can be operated without restrictions within the whole operating speed range.

1 Introduction

Reciprocating compressor plants usually consist of the compressor unit itself and a power-supplying drive unit, which in most cases is either an electric motor (constant speed or VFD), a Diesel or gas engine. The coupling transfers the power between both devices (**Figure 1**). An important aspect of reciprocating compressor plant engineering is the torsional vibration calculation (TVC)¹. The aim is to identify and to evaluate sources of critical vibrations, which may lead to magnifying response torques within the driveline or even lead to damages of the rotating elements. It is necessary to detect these critical speed ranges in advance by using suitable calculation methods.

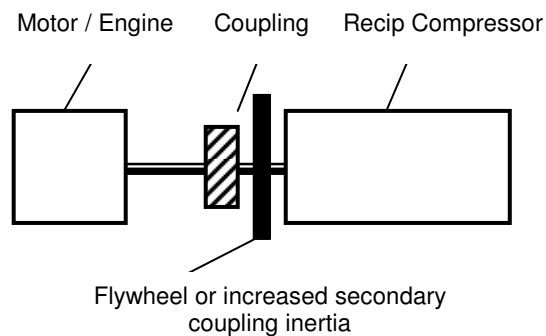


Figure 1: Drive system structure of a reciprocating compressor plant

Advanced computer-based engineering and evaluation methods help to predict critical vibrations, taking into account the whole range of the possible operating parameters of the plant. The use of flexible couplings with natural rubber elements, which are state-of-the-art in a wide industrial field (like ship propulsion systems and electric power generation sets), often shows significant advantages compared to stiff steel couplings considering variable operating speed ranges (particularly in VFD systems).

This paper shows how flexible couplings - configured with the support of advanced engineering methods - help to operate the compressor within a wide range of parameters, giving maximum energy efficiency at any specific load condition.

2 Basic requirements for couplings

The main task of couplings in general is the torque and power transmission. In the case of Diesel and gas engines or reciprocating compressors, the torque is angle-dependent due to the fluctuating combustion and compression process, respectively. Thus, the periodical torque signal can be described as a summation of the nominal torque and a superimposed vibratory torque.

Another important aspect is the compensation of shaft displacements and misalignments between the drive side and the driven side². Shaft displacements can either be axial, radial, or angular. Often, the displacement changes during operation due to transient load conditions, start or stop procedures, or clutching and declutching processes.

A third aspect is the tuning of the system natural frequencies and thus occurring torsional vibrations by choosing the coupling parameters like damping and stiffness. The aim is to cut out critical speeds due to excited natural frequencies from the operational speed range, so that no dangerous resonance phenomena occur during system operation.

3 Engineering process

Reciprocating compressor plants are usually designed in the following way:

- choice of the compressor type and size according to the requirements,
- selection of a suitable drive unit (motor or engine),
- finding the optimum coupling configuration in order to meet all requirements.

Since the coupling usually is the "weakest" part inside the driveline, it corresponds to the lowest natural frequencies and can be effectively used to shift resonance speeds out of the operating speed range.

The recommended procedure of the torsional vibration calculation is shown in **Figure 2**¹.

The first step of a TVC is to create a practice-oriented simulation model, which is not too complex but straightforward with reference to the engineering task, the reasonable model size, and the computation time.

The following computation steps are important and to be respected^{3,4}:

- formulation with respect to the planned model
- determination of the model limits
- model generation using reduction rules
- analysis of the linear model (natural behaviour)
- analysis of excitability (i.e. interpretation of all natural frequencies and the corresponding modes)
- 1st model validation
- model extension (excitations, non-linearities if applicable)
- test calculations, qualitative evaluations (concerning comprehensibility of the model)
- model reduction or extension and 2nd model validation
- model refinement, quantitative evaluation, final validation of the computer results
- discussing the model sensitivity concerning data uncertainties or parameter variations to optimise the system

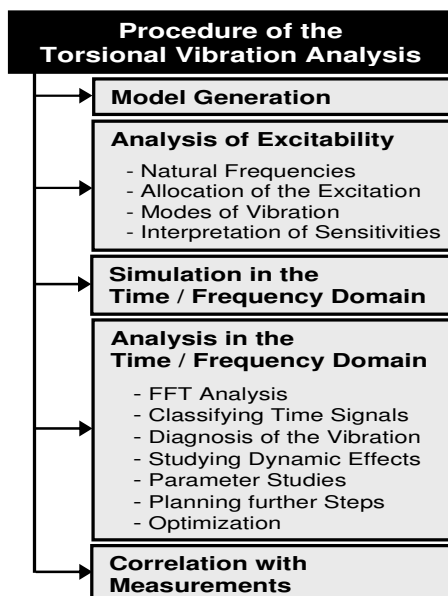


Figure 2: Procedure of the TVC¹

If non-linearities are not awaited in the system behaviour, the simulation methods, which are usually used, are based on steady-state simulation methods (i.e. simulation in the frequency domain).

Such methods are based on linear system characteristics with harmonic excitation torques. The flow chart showing the integration of the plant engineers in close cooperation with the coupling manufacturer is presented in **Figure 3**.

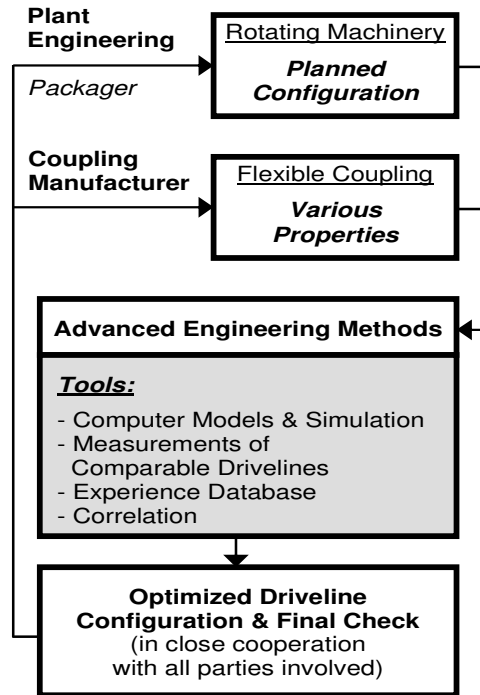


Figure 3: Advanced engineering methods integrated in the overall plant configuration process

The details how to apply the API standards^{5,6} and how to include the model generation and simulation methods in the overall engineering process is described in the literature^{1,3,4}. The essentials of advanced engineering methods refer to simulation techniques which cover the mechanical and possibly also the electrical influence in the overall dynamic behaviour including various speed-dependent load situations. Therefore, the standard steady-state simulation may be extended by time-transient calculations which could also embed even non-linear effects if such effects really occur. Furthermore the advanced computations contain an analysis of the parameter sensitivities in order to optimise the system configuration. This is crucial for the coupling selection because the coupling design has a major influence on the critical speeds and the magnitudes of the vibratory torques. Powerful simulation software packages⁷ support the engineering job.

4 Use of flexible couplings

The use of flexible couplings with natural rubber or silicone elements as shown in **Figure 4** is state-of-the-art in a wide field of industrial applications⁸.



*Figure 4: Typical flexible coupling⁸
(two rows with four elements each)*

These couplings have proven to be reliable for long service times and are also used in safety-critical applications. Well-known examples are compressor plants as shown in **Figure 5**, main and auxiliary drives in ships and boats (ranging from yachts to ocean liners) and trains as well as electric power generation sets.

However, a strict requirement for reliable coupling operation is the performance of TVCs to determine and to evaluate the occurrence of natural frequencies, resonance phenomena and vibrations.

Today, with computer-aided advanced engineering methods, TVCs can be carried out very detailed even for complex compressor plant layouts and a wide range of operational parameters. These calculations take also into account the effects of warm rubber conditions or small amplitude excitation, which influence the coupling behaviour.



Figure 5: Compressor plant to be equipped with flexible coupling

Due to many years of successful use of flexible couplings, very large knowledge and experience in TVC, rubber chemistry and coupling element production are available. Additionally, the span of material and product properties is checked for extensive testing during production process before delivering to the customer and also with destructive testing.

Although the material properties of natural rubber are time-dependent (unlike e.g. those of steel) they are not unpredictable, so a warranty of 30,000 hours (about 3.5 years of continuous operation) can be given in most cases.

If desired by the customer or required by naval classification societies, non-intrusive load and vibration measurements are performed for different load cases after installation of the coupling, to ensure that the actual values are within the limits of the TVC, guaranteeing safe plant operation^{9 10}.

In the case of ship main propulsion systems, it is a common practice to have these measurement devices permanently installed and working for each main engine. **Figure 6** shows a so-called continuous monitoring device which measures the coupling twist and vibratory angle and helps to detect engine problems like misfiring or governor hunting. In the case of abnormal coupling load detection, the measurements are logged automatically and an alarm in the engine control room is triggered.

All these testing result in very reliable couplings and well-tuned plants as required by TVC and thus ensure years of care-free plant operation.



Figure 6: Two continuous monitoring devices used for engine and flexible coupling control

5 Design of flexible couplings

In comparison with rigid and comparatively very stiff couplings the flexible coupling is usually soft and therefore tends to a lower 1st (basic) natural frequency. By changing the number of the rubber elements the dynamic system behaviour may easily be tuned without significantly changing higher natural frequency ranges. It is generally known that due to the material properties of rubber the dynamic torsional stiffness at low amplitudes is higher than the dynamic torsional stiffness at higher amplitudes. Therefore the coupling manufacturer recommends performing a calculation with the expected dynamic torsional stiffness of the coupling which is usually about 120 to 140 % of the nominal catalogue stiffness C_{Tdyn} . The torsional stiffness and relative damping of the coupling is primarily influenced by the level of thermal loading due to the ambient temperature and/or power loss inside the flexible elements. The calculation of the power loss and its comparison to a permissible value keeps the resulting temperature rise within a defined limit. The highest temperature is attained at the so-called core. The dependence of the dynamic torsional stiffness on the core-temperature is shown in Figure 7.

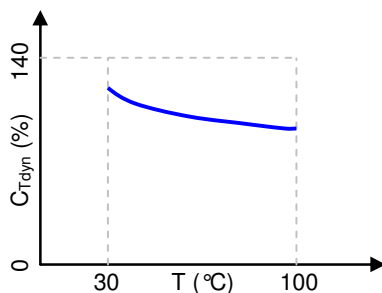


Figure 7: Temperature influence on the dynamic coupling stiffness

Due to this influence it is recommended to perform a calculation with 70% of the nominal stiffness C_{Tdyn} . The torsional stiffness C_{Tdyn} for the warm condition takes into account the influence of thermal load on the torsional stiffness and is therefore equivalent to 0.7 C_{Tdyn} . Depending on the process usually three different steady-state calculations have to be performed in order to predict a safe operation of the installation:

- a) Nominal Condition (100 % C_{Tdyn})
- b) Warm Condition (70 % C_{Tdyn})
- c) Small Amplitude Condition (120-140 % C_{Tdyn})

For the application of flexible couplings in the main driveline of a reciprocating compressor plant, the small amplitude conditions are usually not effective so that – considering the worst case scenario – the "warm" condition is the most important condition to design the coupling properly. The above mentioned percentages also refer to the damping properties so that the "warm" condition leads to higher amplitudes in comparison with the other mentioned conditions. There is another important aspect which is typical for the design of rubber couplings: the influence of non-linearities. It is often the case that rubber couplings show a typical progressive behaviour of the torque versus the difference angle (i.e. the angle between the primary and secondary coupling inertia) as shown in Figure 8.

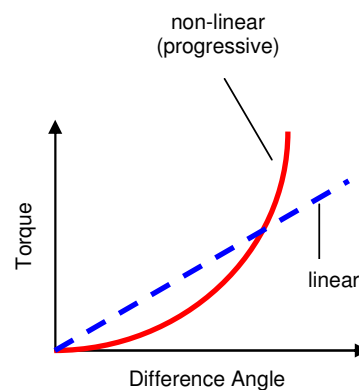


Figure 8: Non-linear and linear torque-angle curve of a flexible rubber coupling

On the one hand the torque amplitudes are low for small displacements, on the other hand the torque response may increase progressively while increasing the angular twist. This leads to a more or less limited difference angle but to comparatively high torque amplitudes. Thus, the coupling behaviour becomes load dependent.

That is why the selection of flexible couplings as presented in this paper show nearly an ideal linear behaviour so that the dynamic behaviour remains predictable and load independent which is a significant advantage for the coupling and driveline design. More detailed information on flexible couplings is found in the literature¹¹.

6 Comparison of calculation and measurement

The following example shows how calculation and measurement correlate with a very good quality.

Within the TVC for a reciprocating compressor plant, the natural frequency of the crankshaft was calculated to 84 Hz. In the Campbell diagram, where the natural frequency is plotted as a function of the rotational speed range (400...750 rpm in this case), it can be seen at which speeds the different orders cross the natural frequency. These speeds, where resonance phenomena and vibrations can be expected, are to be avoided during the compressor operation.

For the discussed case, the upper part of **Figure 9** shows the Campbell diagram. The horizontal line at 84 Hz indicates the calculated natural frequency.

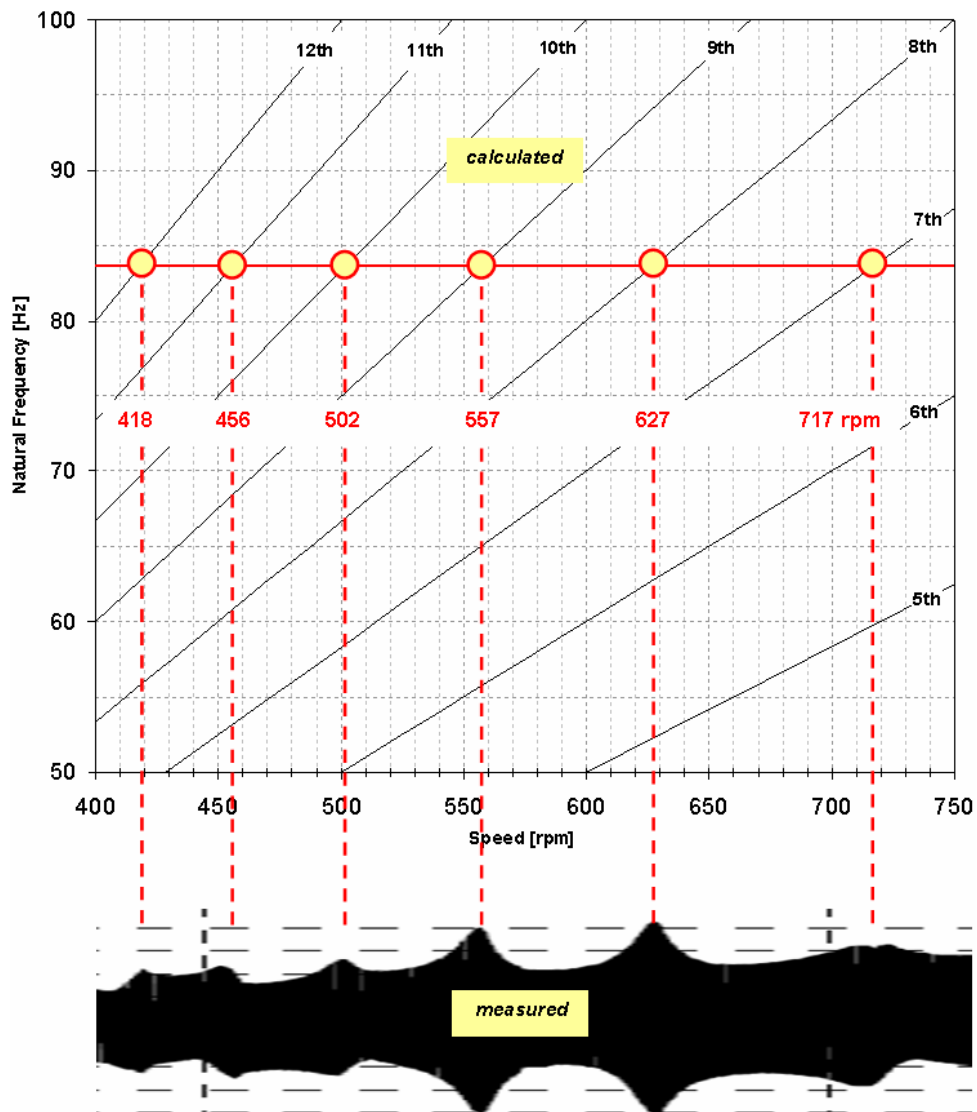


Figure 9: Comparison of results obtained for compressor crankshaft with TVC (top) and measurement (bottom)

The lower part of the figure shows the corresponding torque measurement results for the crankshaft. The dashed vertical lines connect the calculated intersections between the natural frequency and the different orders on the one hand with the measurement results on the other hand. A very good coincidence between TVC and measurement is obvious. The measured torque peaks correlate with the computation as well.

This confirms that the applied TVC method is a powerful and reliable tool to predict coupling and plant behaviour with respect to natural frequency occurrence and can thus be used for plant engineering using different case studies.

7 Strategy of an optimum drive system configuration

The values for inertia and stiffness for both engine and compressor are fixed in most cases by choosing the corresponding items. However, for the choice of the coupling a degree of freedom remains, which can be used to tune the system. The key for successful use and long service life of flexible couplings in compressor plants is the correct choice of the coupling type, size and design parameters (mainly stiffness and damping), respectively. To achieve this goal, detailed TVCs have to be performed and evaluated. As natural frequencies and resonance phenomena of a system are unavoidable, the strategy is not to ignore them but to actively control and shift them towards speed ranges which are outside of the operation speed range.

The TVC needs to be repeated for each different load case (e.g. varying rotational speed and number of active throws), which may well be around 30 variations or more. The outcome of these TVCs is then to be compared with the results of the calculations concerning power efficiency at the investigated parameters. By changing the coupling type, size and/or the used rubber grade (i.e. variation of material properties), the torsional system behaviour can be tuned and optimised with regard to the most power efficient set of operational parameters. Additionally, the system can be fine-tuned by adding modular flywheels, which is a relatively cheap solution.

As an example, possible coupling variations are shown in **Figure 10**. Due to the modular coupling design concept, even complex drive system configurations can be realised to optimise the torsional vibration behaviour.

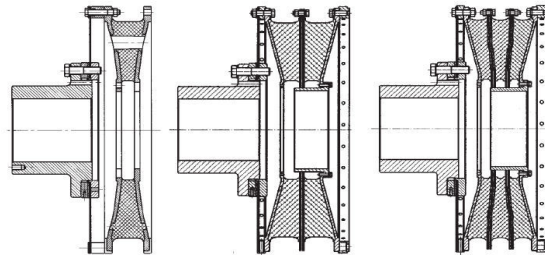


Figure 10: Modular coupling design concept

Figure 11 shows the TVC results obtained for a given compressor and VFD drive (electric motor) with a steel coupling installed. The figure shows the vibratory torque of the three "strongest" orders which have been calculated (9th, 7th and 6th in this sequence) and the synthesis value for all calculated 12 orders versus rotational speed. The possible operational speed range of the compressor is marked. It shows that especially for the 9th and 7th order high vibratory torques are expected in the possible speed range. The average vibratory torque value is relatively high, resulting in strong stress for the compressor crankshaft. It can be easily concluded that this steel coupling is not the optimum choice for the projected compressor plant, as rather wide parts of the possible range of operation cannot be used due to the occurring resonances.

In contrast, **Figure 12** shows the TVC results obtained for the same compressor and electric motor, however with a flexible coupling installed. In this case, the three strongest orders are the 3rd, 1st and 2nd and their vibratory torque level is significantly less than in the case of the steel coupling. The stress in the compressor crankshaft is also reduced. The natural frequencies have been shifted to lower values, so the complete required speed range of the compressor can be used for the operation of the plant. Crossing the natural frequencies during start up or shut down of the compressor plant does not damage the system, as these are passed in very short time.

DRIVE TRAIN

Optimisation of Reciprocating Compressor Plants by using Flexible Couplings supported by Advanced Engineering Methods

Andreas Laschet, ARLA MASCHINENTECHNIK

Michael Matzkeit, VULKAN KUPPLUNGS- UND GETRIEBEBAU B. HACKFORTH

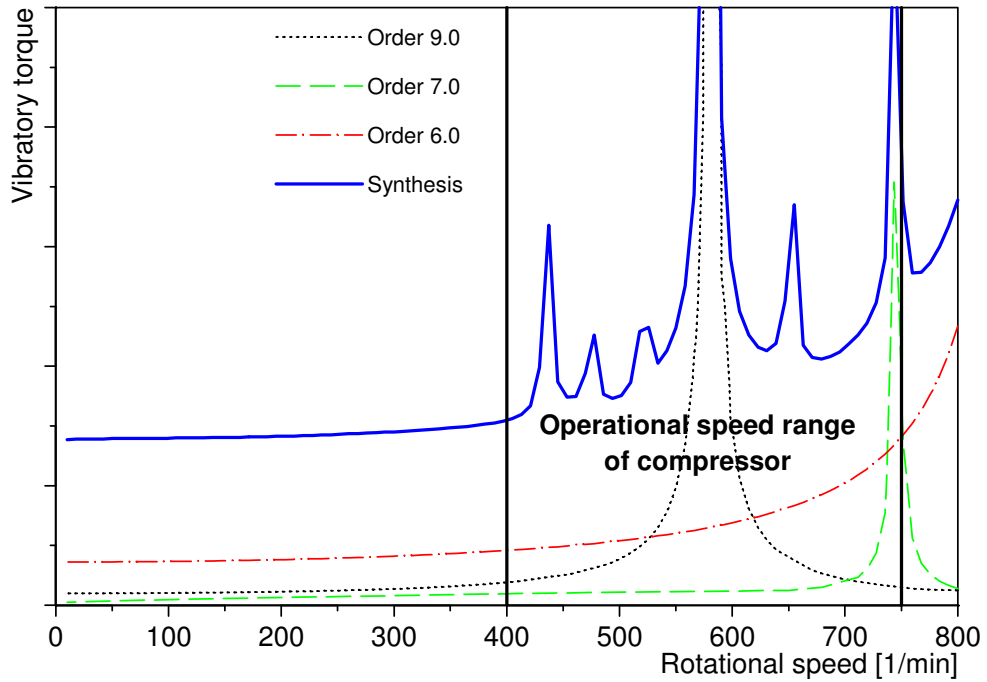


Figure 11: TVC results obtained for an electrically driven compressor plant using a steel coupling

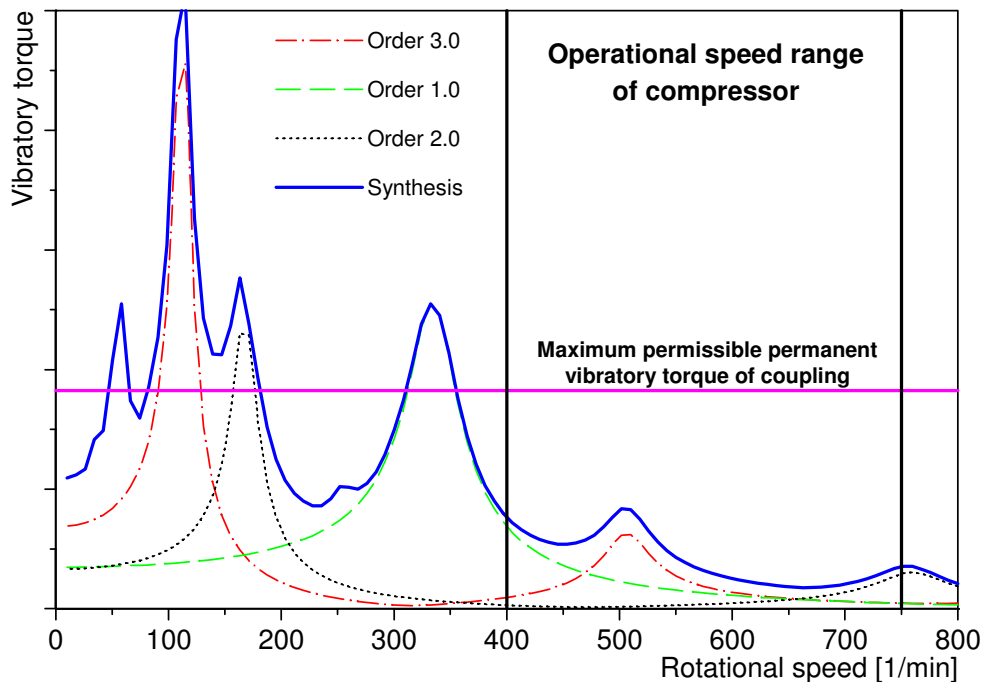


Figure 12: TVC results obtained for an electrically driven compressor plant using a flexible coupling

The decision, at which speeds the compressor is to be run at different load cases, can simply be made on the results of the power efficiency calculations, as there are no limitations concerning TVC and natural frequencies.

It shows, that advanced engineering methods play an important role in the choice of the right coupling for a compressor plant. Therefore, the solution is not only a product called "coupling element", but also the assistance in choice of the most suited solution, performance of TVC, measurement and judgement after installation, continuous monitoring during operation and finally life cycle service with provision of spare parts which meet the desired requirements in order to maintain trouble-free plant operation.

8 Conclusion

This paper shows how reciprocating compressor plants can be optimised by using flexible couplings and advanced engineering methods.

In the given example, the choice of the right coupling enabled the operating company to use the complete operational speed range of the compressor without any limitations with regard to natural frequencies or resonance phenomena. This results in significantly less energy consumption, as the optimum operational parameters corresponding to the actual compressor load situation can always be set.

References

¹ Laschet, A.: Analysis of Torsional Vibrations in Reciprocating Compressors driven by Electric Motors and Gas Engines, 4th EFRC Conference, Antwerp, 2005

² Neale, M.; Needham, P.; Horrell, R.: Couplings and Shaft Alignment. London: Professional Engineering Publishing 1998

³ Laschet, A.: Simulation von Antriebssystemen, Fachberichte Simulation Vol. 9. Berlin, Heidelberg, New York: Springer-Verlag 1988

⁴ Laschet, A.: Computer Simulation of Vibration in Rotating Machinery. Machine Vibration (1992) 1, pp. 42-51. London: Springer-Verlag 1992

⁵ API Standard 618: Reciprocating Compressors for Petroleum, Chemical, and Gas Industry Services, 4th Ed., American Petroleum Institute, June 1995

⁶ API Publication 684: Tutorial on the API Standard Paragraphs Covering Rotor Dynamics and Balancing: An Introduction to Lateral Critical and Train Torsional Analysis and Rotor Balancing, 1st Ed., American Petroleum Institute, February 1996

⁷ Various Software Packages: ITI-SIM, ITI-STAT, ARMD, ARLA-SIMUL, ARLA-SIMSTAT, special ARLA model building tools

⁸ VULKAN Kupplungs- und Getriebebau, B. Hackforth GmbH & Co. KG, Herne, Germany Couplings catalogue 2007

⁹ Dylla, M.; Büschges, H.: Verfahren zur Überwachung von hochelastischen Wellenkupplungen in Antriebsanlagen mit Großmotoren, VDI-Tagung Schwingungen in Antrieben, 2001

¹⁰ Gajetzki, M.; Dylla M.: Erfassung von Belastungsprofilen im Antriebsstrang und die Möglichkeit der Ferndiagnose, ISF Infotagung, 2006

¹¹ Peeken, H.; Troeder, C.: Elastische Kupplungen. Berlin, Heidelberg, New York: Springer-Verlag 1986



Utilization of Soft-Starter VFD in Compressor Applications

by:

Carsten Ritter, Heinz Kobi, Peter Morf

Medium Voltage Drives

ABB

Turgi

Switzerland

**carsten.ritter@ch.abb.com, heinz.kobi@ch.abb.com,
peter.morf@ch.abb.com**

**5th Conference of the EFRC
March 21-23, 2007
Prague, Czech Republic**

Abstract:

Polyethylene production requires high power multiple pole machines for ethylene gas compression. In most cases the machines are started DOL implying in high starting currents, additional mechanical stresses, influence on other loads, limitation of the number of consecutive starts and reduction of equipment's lifetime.

This paper introduces and compares the conventional DOL start with soft-starting alternatives, including the variable frequency drive. Advantages and disadvantages of using a drive are investigated. The importance of the design coordination between machinery and drive are addressed. Key points to specify a soft-starter, aspects to consider and pre-conditions of the installation are summarized. The possibility to start multiple machines is outlined and evaluated. Concluding the work, application case study results are presented and discussed.

2.4 Reactor/Capacitor Start

Reactor/capacitor start is used on networks with very low short circuit capacity. In this method a capacitor bank is energized during motor start in order to provide necessary reactive current to the motor.

During motor acceleration to rated speed, the capacitors are disconnected. If a large capacitor bank would remain permanently connected, the voltage could rise above motor's maximum allowed level. For this reason the grid voltage or motor speed need to be monitored and controlled in such a way to connect/disconnect complete or part of the capacitors to avoid overcompensation and overvoltages. If the motor voltage reaches an intolerable level or if the motor has not accelerated to a suitable speed, the controller must open the mains. Synchronous machines can also be designed to provide reactive power neutralizing the advantages of this method.

2.5 Voltage Regulator Soft-Starters

Voltage regulator soft-starters are based on a thyristor bridge with two anti-parallel coupled semiconductors in each phase. During the starting process, the soft-starter progressively increases the motor voltage from zero enabling the motor to accelerate the load to rated speed without causing torque or current peaks. The reduction of starting voltage also reduces the available torque to the driven load by the square of the voltage. Voltage regulator soft-starters can also be used to control the stopping of the machines.

2.6 Variable Frequency Drive Start

Although a static frequency converter is designed to continuous feed the machines, it can also be used exclusively for start-up². The variable frequency drive (VFD) enables low starting currents because the motor can produce exactly the required torque at rated current from zero to full speed. The VFD soft-start provides smooth, step-less acceleration of motor and load while controlling inrush current and starting torque. As the voltage regulator soft-starters they can be used to control the stopping of the process. One VFD can be used to start multiple machines.

This chapter presented various available starting methods. Not all starting methods are effective when starting large machines. The selection of one or another will depend on system topology, starting torque requirements, machine and supply network characteristics. Important aspects to take into account are the maximum allowed voltage drop in the supply network during start, start load torque and required starting time. Applications often require a less stressful and more controllable soft-start system. A commonly used method is with auto-transformer. The main disadvantage of this option is that with given network short circuit capacity it cannot be used. In this case a Static Frequency Converter turns into a very attractive solution, as will be outlined in the next chapter.

3 VFD Soft-Starting

Figure 2 illustrates a typical configuration and the main components of a VFD³. The synchronous machine (SM) with its main excitation and the running circuit breaker (RCB) are the components which are required to operate the load direct on line.

The task of the VFD is to accelerate the SM from zero up to nominal speed and synchronize it to the power supply system by closing the RCB, and optionally - after RCB has been opened - to decelerate the SM from nominal speed to standstill. Its main function is to control the energy exchange between the power system and the motor, which during acceleration and deceleration is operated at variable frequency and voltage

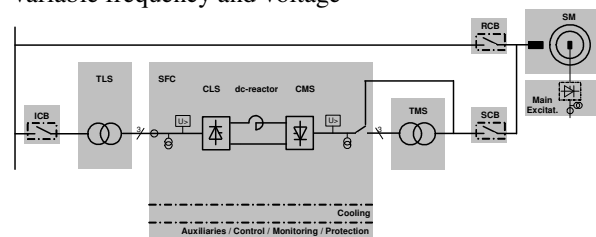


Figure 2: VFD soft-start with a 6/6 pulse converter.

The main components of the soft starting system are:

- Input circuit breaker (ICB) and starting circuit breaker (SCB)
- Input transformer (TLS) and output transformer (TMS) which match the supply voltage and the machine terminal voltage to the converter design voltage. For economic reasons the VFD is designed with a voltage which is lower than the rated supply and machine voltages.

The transformers also limit the fault current in the converter. With the presented configuration the TLS and TMS have the same design, avoiding the saturation of the TMS at low frequencies.

- The VFD is based on the LCI (Load Commutated Inverter) principle. It comprises the following main units: line converter (CLS), dc-link reactor, machine converter (CMS) and control unit with auxiliaries that is responsible for the control, monitoring and protection. The transformer bypass is used at very low machine frequencies, from speed zero up to approximately 10% of speed.

A brief summary of the function of the VFD follows.

- The line converter CLS is connected via the input transformer TLS to the power supply system. It is line commutated and operates at constant voltage and frequency. The machine converter CMS is connected to the machine. It is “load commutated” and is operated with variable voltage and frequency. Both converters are interconnected through the dc-reactor, which decouples the different frequencies of the converters.

- When the machine is operated as a motor (energy flow from power supply system to machine), the line converter acts as a rectifier providing current control and the machine converter acts as an inverter commutating the currents between the machine phases. Optionally the machine can also be operated in generator mode (energy flow from the machine to the power supply system; used for fast deceleration) without adding any extra equipment in the VFD, by simply controlling the machine converter as a rectifier and the line converter as an inverter.

- Speed and torque (equal current) can be controlled independently.

- The machine is self-controlled and hunting or loss of synchronization is not possible since the firing pulses of the machine converter are derived from the machine voltages and are therefore in phase relation with the angular position of the rotor.

4 Specifying the Soft-Starter VFD

Not always all parameters of the network, the compressor and the motor are known in an early phase of the project but the knowledge of the key data allows the adequate selection and design of the soft-starter equipment.

The power of the VFD is defined by the required starting torque of the compressor. Starting with an unloaded or partly-loaded compressor allows reducing the size of the frequency converter and the VFD transformers.

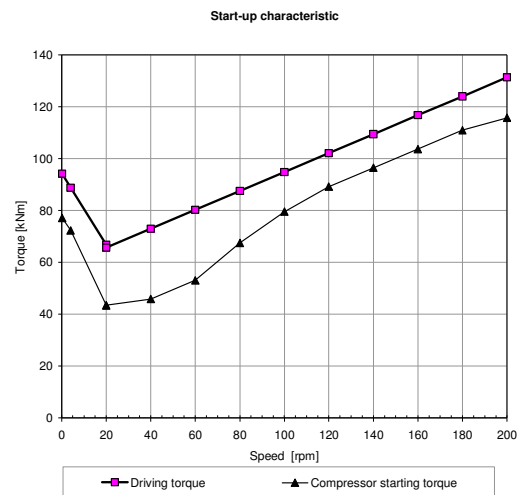


Figure 3: Typical starting characteristic curve

The driving torque of the motor is typically designed with a 10-15% margin above the required compressor torque over the entire speed range.

The starting torque – speed curve provided by the compressor vendor allows the VFD supplier to calculate the required VFD power. Together with the inertia of the rotating system (compressor, gearbox, motor) the expected starting time can be calculated. Any requirements for short starting time need to be specified since they can lead to an increased power requirement for the frequency converter and the VFD transformers.

In case the booster and hyper compressor are both synchronous machines one single soft-starter VFD can be used. Due to the rating of the smaller machine not always it's practical to invest on a synchronous machine and a DOL start could be more convenient. The proper selection depends on each case and should be evaluated.

4.1 Frequency converter

Frequency converters are available in different configurations and the selection is based on various parameters

- Required VFD power / starting power
- Short circuit capacity of the network (system fault level)
- Compliance with harmonic standards
- Availability of cooling medium

For smaller VFD powers (below 4000 – 5000kW) the selected configuration is a 06 / 06 pulse converter whereas for higher powers 12-06 or 12-12 pulse configurations are preferred. Higher pulse numbers allow reducing the harmonic impact the converter has on the feeding network (current and voltage harmonics) as well as on the mechanical system (pulsating torques).

Soft-starters are normally air cooled due to their short operation time. For high powers or in case of reduced availability of cooling air, water cooled converters might be preferred.

The control system of the frequency converter is designed for reliable protection of the motor during the starting of the compressor. It also communicates with the motor excitation system to adjust and monitor the motor voltage.

4.2 Transformers

The transformers at the in- and output of the frequency converter are required to match the network voltage and motor voltage to the permitted converter voltages. They reduce the harmonics injected into the network, limit the fault current inside the frequency converter and provide the required phase shifting in case of 12-pulse configurations. The design of these transformers is adapted to the parameters and requirements of the entire starting system.

For starting system, these transformers can be designed with a duty cycle (limited number of starts per hour) in order to reduce the size and investment costs for these components.

The transformers can either be dry type or oil immersed, depending on customers choice and environmental & installations conditions.

4.3 Motor

The electric motor design can theoretically be simplified when it is exclusively soft-started by a VFD and mechanical and thermal aspects of a DOL starts must not be considered in the motor design. However, such motors are frequently designed with DOL start capability as a back-up starting method.

The design of the VFD is adapted to match the given motor parameters; the motor parameters do not need to be changed to match the VFD design.

There is only one special requirement for motors started by a VFD and this is an excitation system that allows full excitation of the motor even at standstill. These are either DC excitation systems with brushes or brushless AC-AC excitation systems. For new projects, the AC-AC excitation is the preferred choice whereas DC excitation with brushes might be considered for installing a soft-starter VFD for an existing motor.

4.4 Harmonics

The operating time of the VFD soft-starter is small and the generated harmonics, even when higher than IEC and IEEE standards, are acceptable for the time duration. In case this is not accepted, a harmonic filter needs to be considered.

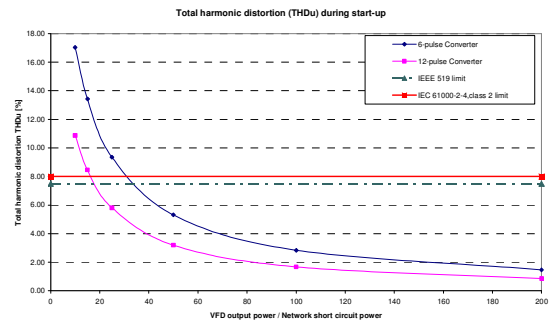


Figure 4: Harmonic distortion in the network.

Pulsating torques are not regarded as critical since the required starting torque is smaller than the nominal compressor torque and the starting is only a short and transient process. Mechanical resonances are not sufficiently excited by the generated pulsating torques to cause excessive mechanical stresses.

5 Case Studies: VFD starter for compressors

In the last 30 years several hundred starting systems in the power range of 1 – 20 MW converter power were installed in various applications (power, petrochemical, metals, research & testing)^{3, 4}. Two case studies are presented in this chapter.

5.1 VFD soft-starter for a reciprocating compressor

In 2003 a Company required a soft starter for a 27 MVA / 28-pole / 214 rpm synchronous motor driving a reciprocating compressor. The power supply voltage and the rated motor voltage were both 10 kV, the rated motor current was 1'571 A_{AC}.

The load torque of the unloaded compressor during the start required a 5.6 MW starting converter. With this power the resulting acceleration time was approximately 27 s (Figure 5).

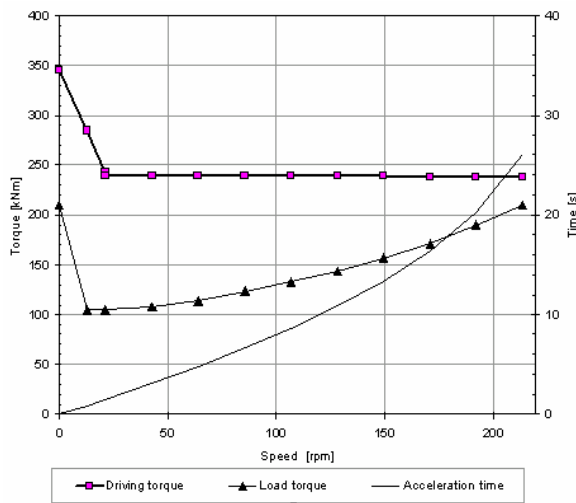


Figure 5: Design curves of 5.6MW starting system

An air cooled VFD with 12/12-pulse configuration was selected (Figures 6 and 7), with in- and output voltages of 2.1 kV and with a rated dc-current of 1'210 A_{DC}. Both 3-winding transformers are identical: 6.9 MVA rated power, Dd0y1 vector group and voltage ratio of 10 kV / 2x 2.1 kV.

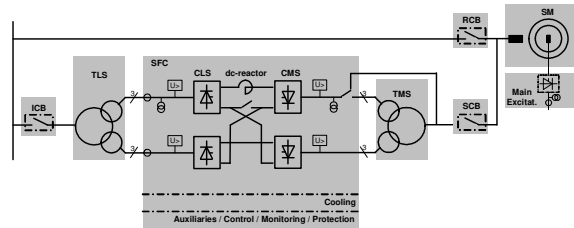


Figure 6: VFD soft starting with a 12/12-pulse LCI converter



Figure 7: 5.6 MW air-cooled LCI soft-starter

The electrical values of the motor during soft starting are shown in Figure 8. The motor voltage is controlled proportional to speed, from 0 V at standstill till 10 kV rated voltage at rated speed of 214 rpm, keeping nominal motor flux in whole speed range. The motor current during acceleration is controlled to a value equal or below 386 A, a value much lower than rated motor current of 1'571A.

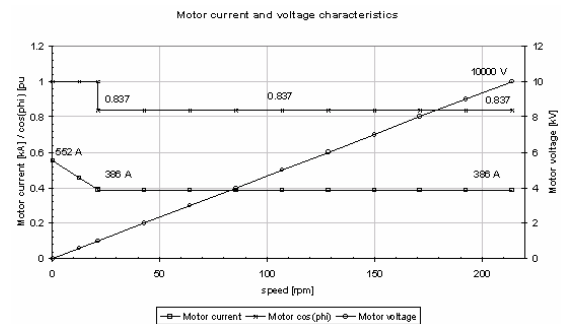


Figure 8: Motor electrical values during start.

5.2 VFD soft starter for two hydrogen compressors

In 1995 the owner of a refinery installed and commissioned two 5.4 MW synchronous motors aimed to operate two hydrogen compressors. Both motors were ordered and designed to start direct-on-line (DOL). At the beginning, each DOL-start produced troubles: loss of power supply in the whole refinery and, as a consequence, production stop. A palliative solution was then developed: every time one of the motors had to be started DOL, a team that included employees of the refinery and the power company was involved to stop production, in order to supply a power boost to be able to start and synchronize the motor DOL. This starting sequence was time consuming, inconvenient, expensive and did not satisfy the refinery owner.

The final solution was the installation of a 1.3 MW soft starting VFD. An air-cooled VFD with 6/6-pulse configuration was selected (Figure 9), that today starts the two motors sequentially, whenever required from the process.

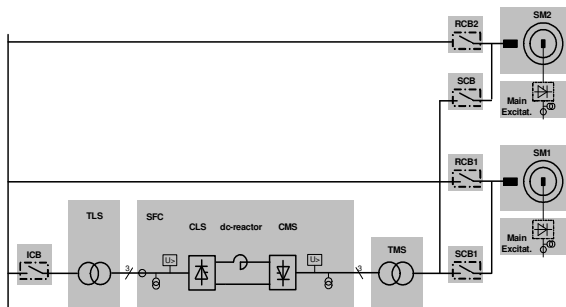


Figure 9: VFD soft starting of two motors with a 6/6-pulse LCI-converter.

After the installation of the soft-starter, an immediate benefit to the refinery was their profitability increase.

6 Conclusion

VFD starters can be used in new and existing MW applications. A pre-condition for using a VFD soft-starter is to have an AC type brushless excitation. A brief check will indicate if it's possible and what items eventually need to be modified. Depending upon the plant configuration the VFD can be used to soft-start one or more machines.

Compared to other starting methods, the VFD eliminates starting current peaks, reducing the stress on machines. This also results in reduced maintenance cost and increased lifetime of equipment. The number of starts can be selected as necessary. VFD for soft-starters has well proven design with documented reliability.

VFD soft-starters enables to accelerate the driven equipment safely to operation speed, limit the voltage drop in supply system and limit thermal and mechanical stresses in the equipment. A direct benefit of their utilization is the maximization of the distribution system capability. Taking all this aspects into consideration, VFD are an attractive solution for soft-starting compressors driven by electric machines in the petrochemical industry.

7 Acknowledgements

The authors express their thanks to the support and collaboration from colleagues from ABB Machines Sweden and Finland.

References

- ¹ Technical Notes, "Starting methods for AC motors", ABB Motors Oy
- ² H. N. Hickok, "Adjustable Speed – a tool for saving energy losses in pumps, fans, blowers and compressors", IEEE Transactions on Industry Applications, Vol. IA-21, No. 1, pp 124-136, Jan/Feb 1985.
- ³ B. K. Bose, "Power Electronics and Variable Frequency Drives – Technology and Applications", IEEE Press, 1997, pp 332 – 361.
- ⁴ L. Terens, W. Neudörfler, "Application aspects of the static frequency converter system in pumped storage power plants", Waterpower Conference, ASCE, 1995, San Francisco, CA, USA.